UNIONE EUROPEA
Fondo Sociale Europeo

Ministero dell'Istruzione, dell'Università e della Ricerca

PON RICERCA E INNOVAZIONE 2014 - 2020

UNIVERSITÀ DEGLI STUDI DI NAPOLI

"FEDERICO II"

Dottorato di ricerca in Biologia

XXXIII Ciclo

Tesi di Dottorato

Heterotrophic cultivation of microalgae: metabolism and biotechnological applications

Coordinatore
Prof. Salvatore Cozzolino

Tutors
Prof. Angelo Fontana
Dott.ssa Giuliana d'Ippolito

Candidato
dott.ssa Adelaide Cupo

Tutor universitario
Prof. Sergio Esposito

Table of Contents

UNIONE EUROPEA
Fondo Sociale Europeo
Ministero dell'Istruzione, dell'Università e della Ricerca
PON RICERCA E INNOVAZIONE 2014 - 2020

Abstract

This PhD thesis aims to explore the biotechnological potential of the marine diatom *Cyclotella cryptica* grown under heterotrophic growth conditions.

Diatoms are microorganisms generally cultivated in autotrophy, representing an important green source of valuable bio-products, like vitamins, pigments, omega-3 fatty acids and biofuels. However, there are significant limitations associated with autotrophic cultivation of microalgae on large scale, such as light supply and seasonal fluctuations, that affects overall costs.

On these grounds, we decided to explore the heterotrophic growth condition that appears to be interesting for the development of commercial products of interest. In this way, all the light dependence constraints would be completely eliminated, by using the fermenter technology already consolidated in the pharmaceutical field at industrial scale. The process could be well controlled in terms of pH, temperature, addition and consumption of nutrients and maintenance of axenicity.

The identification of candidate species and strains that have a high potential to grow in heterotrophy, as well as the improvement of culture conditions, represent a major challenge for biotechnology research.

We chose *Cyclotella cryptica* as a model, due to its metabolic plasticity, robustness and the potential of obtainable products as reported in the Aquatic Species Program (ASP) funded by the US Department of Energy.

The thesis is developed on several levels, conceptually grouped into three parts: the first one described the assessment of heterotrophic culture conditions and the behavior of *C. cryptica* grown in dark, the second part explores the potential products obtainable from the

heterotrophic growth of *C. cryptica* and the last one give insights into the lipid pathway, through -omics analysis.

Chapter 2 is focused on the development and optimization of *C. cryptica* growth conditions. We evaluated the cell growth both on medium prepared with different sources of salts and organic substrates. Glucose was used as model substrate for an adequate cell growth. We tested different glucose concentrations and developed a protocol by ^{1}H-NMR to estimate its consumption along the cultivation.

In **Chapter 3** we evaluated the sustainability of the heterotrophic process, through three cycles of fed-batch cultivation sets, analyzing the biomass' chemical composition obtained at different time point of the experiment. The result was well-balanced biomass, in terms of proteins (25.5-32.6%), carbohydrates (16.6-29.6%) and lipids (17.0-26.6%), potentially useful for food and feed sector.

The interesting fatty acids distribution inspired the experiments and the results described in the successive chapters.

Chapter 4 reported the data of our published paper, which highlights how *C. cryptica* could be considered a potential producer of eicosapentaenoic acid (EPA), with a yield of 18.0±0.7 mgL^{-1} after 14 days of dark growth.

The PhD funded by PON (2014-2020) funds also included an experimental phase of the project both within an industry and in a foreign Research Institute, each lasting 6 months.

In **Chapter 5** I reported the data acquired during the industrial period at I.GI., a vegetable oil refinery, located in Palomonte (SA). I scaled up the cultivation process by increasing culture volumes in 10 L of polypropylene carboys. Then we evaluated the potential of *C. cryptica* as a source of biofuel. Data presented in the chapter are the subject of a manuscript in preparation.

To give further insights in the phenotypic differences in some classes of glycerolipids and fatty acids, we used transcriptomics (RNAseq) and lipidomics (LC-MS) approaches to better understand the lipid pathway and its rearrangement in the dark; the results are presented in **Chapter 6**, in the form of a manuscript in preparation.

Data reported in chapter 6 directed our attention on the study of key genes involved in lipid biosynthetic pathway. **Chapter 7** describes the strategy to implement gene knockout using CRISPR-Cas-9 technology with the aim of uniquely attributing a function to a selected gene in *C. cryptica*.

This interesting experimental part of the PhD project took place last year in Paris at the "Institut de Biologie Physico- Chimique", under the supervision of Dr. Angela Falciatore.

Unfortunately, the spread of SARS-CoV-2 virus has not allowed the full development of the project that now we are planning to complete on-site thanks to the acquired knowledge, equipping the laboratory of ICB-CNR for molecular biology experiments.

This PhD thesis reports encouraging results obtained from the heterotrophic growth of *C. cryptica* in terms of yields and biochemical composition of biomass, products of commercial interest, acting also as a milestone to give further insights into diatom physiology and biotechnological exploitation of diatom-based bioprocesses.

List of Abbreviations

C. Cohnii = Crypthecodinium cohnii

C. cryptica = Cyclotella cryptica

C. protothecoides = Chlorella protothecoides

C. reinhardtii = Chlamydomonas reinhardtii

F. cylindrus = Fragilariopsis cylindrus

F. solaris = Fistulifera solaris

G. sulphuraria = Galdieria sulphuraria

H. pluvialis = Haematococcus pluvialis

N. alba= Nitzschia alba

N. gaditana = Nannochloropsis gaditana

N. laevis = Nitzschia laevis

N. oleoabundans = Neochloris oleoabundans

P. multiseries = Pseudo-nitzschia multiseries

P. multistriata = Pseudo-nitzschia multistriata

P. tricornutum = Phaeodactylum tricornutum

S. costatum = Skeletonema costatum

T. oceanica = Thalassiosira oceanica

T. pseudonana = Thalassiosira pseudonana

ARA = arachidonic acid

DGDG = digalactosyldiacylglycerol

DHA = docohexaenoic acid

DPA = docosapentaenoic acid

EPA = eicosapentaenoic acid

FA = fatty acid

FAME = methyl esters

FFA = free fatty acids

GL = glycolipid

GLA = linolenic acid

MGDG = monogalactosyldiacylglycerol

MUFA = monounsaturated fatty acid

NL = neutral lipid

PL = phospholipid

PUFA = polyunsaturated fatty acid

SQDG = sulfoquinovosyldiacylglyceride

TAG = triacylglycerol

LC-PUFA = Long chain polyunsaturated fatty acids

CFPP = cold filter plugging point

CN = cetane number

HHV = high Heating Value

IV = iodine value

LCSF = long Chain Saturation Factor

OS = oxidation stability

SV = saponification value

DGAT = diacylglycerol-acyltransferase

FAS = fatty acid synthase

GPAT = glycerol-3-phosphate acyltransferase

GPDH = glycerol-3-phosphate dehydrogenase

LAH = secretory phospholipase A2

LPAAT = lysophosphatidic acid acyltransferase

LPCAT = lysophosphatidylcholine acyltransferase

PDAT = phospholipid diacylglycerol acyltransferase

SQD1 = UDP-sulfoquinovose synthase

SULT = sulfotransferase

TGL4 = triacylglycerol-lipase

ASP = Aquatic Species Program

CFDA = China Food and Drug Administration

CFIA = Canadian Food Inspection Agency

EFSA = European Food Safety Authority

FDA = Food and Drug Administration

FDA = Food and Drug Administration

FSANZ = Food Standards Australia New Zealand

FSCJ = Food Safety Commission of Japan

GRAS = Generally Regarded as Safe

1. Introduction

1.1 Microalgae

Microalgae are microscopic unicellular organisms that can be found in a wide range of environments (like fresh water, seawater, salt lakes, soil, rocks, trees, even wastewater) and habitats: from the polar regions to the equator [1].

Therefore, they can tolerate different temperatures, salinities, and pH values, different light intensities and can grow alone or in symbiosis with other organisms [2].

Up to date, between 36000 - 45 000 single algae species have been described [3]. However, some studies estimate the total number of species (including still undiscovered strains) much higher, even up to ten million.

Microalgae are generally photosynthetic organisms, harvesting light energy via chloroplast and using CO_2 as carbon source to produce organic forms of carbon [4]. There are microalgae capable to adapt their metabolism on different illumination conditions and are classified as mixotrophic or heterotrophic microorganisms. [5].

Mixotrophic cultivation is the growth mode where microalgae simultaneously perform photosynthesis and catabolise exogenous organic nutrients [6]. Heterotrophic microalgae are able to grow in the absence of light and required organic substrates for growth [7].

The algal taxonomy in general is quite complex, due to complicated evolutionary history and it remains a challenging puzzle for applied phycologist.

However, the mayor phyla of commercial microalgal genera are: *Chlorophyta*, *Rhodophyta*, *Haptophyta*, *Stramenopiles* (which major classes are represented by *Eustigmatophyceae*, *Bacillariophyceae*, *Labyrinthulomycetes*) and *Dinophyta* [8].

Although cyanobacteria belong to the domain of bacteria, being photosynthetic prokaryotes, often they are considered microalgae [9]. Microalgae, and especially cyanobacteria, have extremely long geological history, the most archaic cyanobacteria species (the first photoautotrophic organisms) have been found within rocks older than 3.5 billion years. First eukaryotic algae have been found in fossils 1.2 billion years old [10] with chloroplasts having origin in cyanobacteria ancestors [11]. History of these organisms is significantly longer than of higher plants with “only” 400 million years of evolution [12]. Since cyanobacteria have been

occupying the Earth habitats for billions of years, and during most of this time the oxygenic photosynthesis was successfully operational, cyanobacteria have had enough time to produce enormous amounts of oxygen. The oxygen production over more than billion years changed the chemical properties of prehistoric, anoxic atmosphere to the current oxygenic state (the "Great Oxidation Event" was taking place approximately 2.4 billion years ago [13]) which was the basis for the evolution of aerobic eukaryotic organisms.

1.2 Biotechnological applications of microalgae

1.2.1 History

Man has been using algae for ages. The first known usage of microalgae dates back 2000 years, when the cyanobacteria strain *Nostoc* was utilized as a food source during a famine in China [14]. Also other cyanobacteria, including *Spirulina* and *Aphanizomenon* have been serving as a food source for more than thousand years [15]. Until 20th century, reports of algae biotechnology are fragmental. Microalgae usage as a food source has been followed back to the 4th century in Japan and the 6th century in China. First collection of algae "nori" as a food supplement is dated to the 6th century, although its first mass cultivation took place in the 17th century [16]. The first agar production is dated to the middle of 17th century, yet the controlled cultivation of agar producing strains started few centuries later. Brown algae were processed for iodine and soda production in the 18th century, and first cultivation of diatoms is dated back to the 19th century [16]. The industrial, wide spread algae biotechnology truly boomed in the 20th century, especially in its second half [14,16].

Although specific processing procedures for macrocystis or certain diatoms were known before the Second World War, industrial algae use was not developed to a large level. During the Second World War, Germans experimented with large cultivation of diatoms for liquid fuel generation. The first wide spread interest in algae mass cultivation took place in the early 1950´s with exploring possibilities of new protein sources, mainly in anticipation of world population increasing and predicted future insufficient protein supplies. At the same time, studying of production of biologically active substances by algae raised [17] and also less traditional applications were tested, including e.g. CO_2 / O_2 exchange during space travels [18].

Microalgae utilization as a renewable energy source was accelerated in 1970´s during the energy crisis; at first by studying the options of biomass conversion into methane or biodiesel [19].

The first commercial-scale microalgae cultivation plant was established in 1961 in Japan for *Chlorella* production. However, the first pilot plants were developed already in 1950´s in USA, Israel, Germany, and Japan. The Japanese plant was followed by establishment of Spirulina cultivation and harvesting facility in Mexico in 1970´s [14,17].

After *Chlorella* and *Spirulina*, *Dunaliella salina* was discovered to be a rich source of beta-carotene, and the first production facility was established in Australia in 1986, followed by commercial plants in Israel and the United States [14]. About the same time, commercial cultivation of cyanobacteria started in India. More recently, astaxanthin production by *Haematococcus pluvialis* was established in USA, India and Israel. During last decades, hundreds of new companies have been set up, focusing on production of various compounds described in following text. The algae industry is spread in 30 countries around the globe (with its majority in Asia and USA), and it is supported by hundreds, if not thousands of research laboratories worldwide.

1.2.2 Current algae industry overview

Nowadays most cultivated microalgae strains include *Spirulina*, *Chlorella*, *Dunaliella salina*, *Aphanizomenon flos-aquae* or *Haematococcus pluvialus*. There are many different ways of algae biotechnological applications, ranging from the simplest usage as food or feed to advanced utilization such as production of specific compounds with unique properties and high prices.

According to available data, algal biomass output increased globally in 2016, reaching 32.67 Mt [Fresh weight (FW)], with 0.57 percent of the amount generated in Europe (EU 27 + United Kingdom + Iceland + Norway). Aquaculture provides the majority of algal biomass (96.5 percent in 2016), while wild stock collection provided 98 percent of total algae output volume in Europe over the same year [20].

This trend reflects the political context worldwide: in Europe for example The new Green Deal from the European Commission focuses on priority areas where algae production could make

a significant contribution. For example, the EU's aims of being carbon neutral by 2050, biodiversity conservation, the creation of a circular economy, and participation in the farm to fork strategy for sustainable food are all examples. The Commissioner for Environment and Oceans' top goals are to expand the EU's blue economy while also ensuring the long-term viability of fisheries and aquaculture production, as well as their contribution to global food security and sustainability [20].

1.3 Products from microalgae

Microalgae are important sources of commercially produced high-value products (**Figure 1.1**). In this section we will report the major products obtainable from both microalgal biomass and extracts.

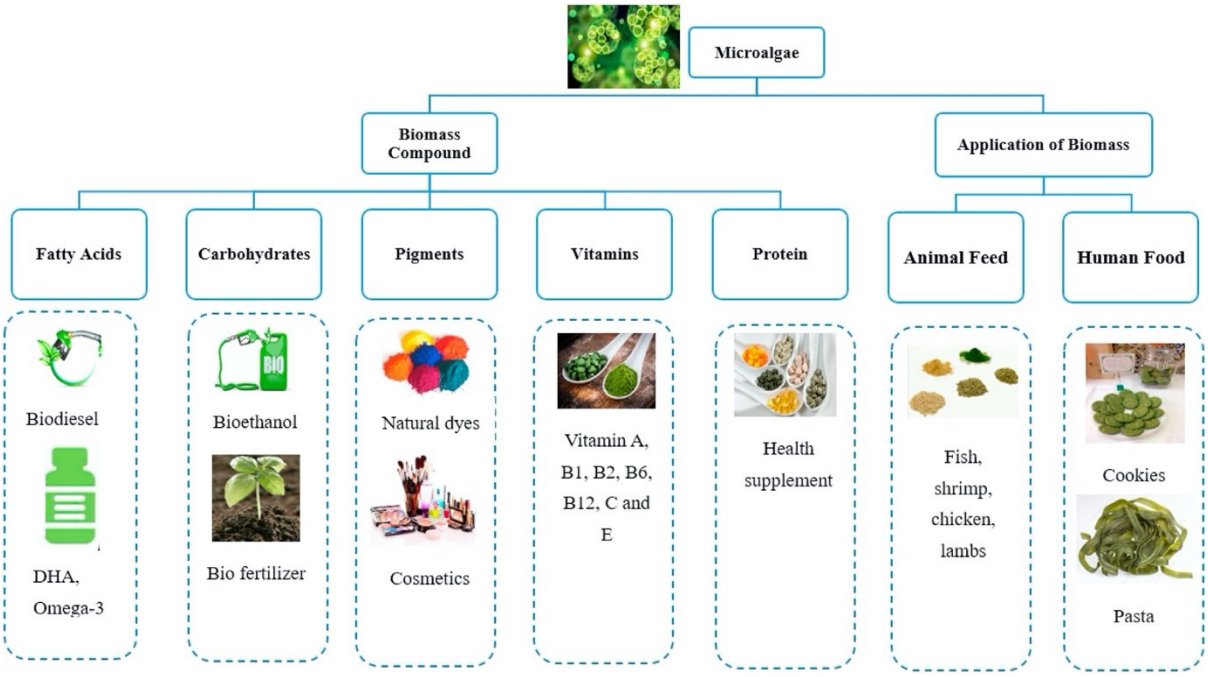

Figure 1.1 Bioproducts from algal biomass and their applications [21].

1.3.1 Fatty acids

Many animals, including human, lack enzymes for synthesis of essential Omega-3 and 6 fatty acids polyunsaturated fatty acids (PUFA), and therefore rely on external sources for their supply, which must be included in the daily diet [21]. Long-chain hydrocarbons, PUFAs have an average of more than 18 carbons in their structure. Arachidonic acid (ARA), docosahexaenoic

acid (DHA), linolenic acid (GLA), and eicosapentaenoic acid (EPA) are the most well-known PUFAs. PUFAs have a variety of health benefits, including cardiovascular and anti-inflammatory actions. There have also been indications of anti-carcinogenic, anti-atherogenic, anti-lipogenic, and immunosuppressive effects [22]. Arachidonic acid (ARA) is a 20-carbon chain fatty acid containing four methylene-interrupted cis double bonds, the first of which is situated between carbon 6 and 7 relative to the methyl end. As a result, ARA is classified as an omega-6 (n-6) polyunsaturated fatty acid (PUFA). It's a key component of biological cell membranes, giving them the fluidity and flexibility they need to operate properly, notably in the neurological, skeletal, and immunological systems [23]. DHA (omega-3) together with GLA (omega-3) and ARA (omega-6) are required for baby brain growth and development. Adults require DHA to maintain proper brain function. Adequate DHA in the diet increases cognitive ability, while DHA deficiency is linked to learning impairments. DHA deficiency in the brain has been linked to cognitive impairment as people age and the beginning of sporadic Alzheimer's disease [24]. The biggest source of PUFA are fish and other marine animals, including lobsters, shrimps, oysters, crabs, clams or scallops [14,24]. Many microalgae strains, such as *Porphyridium*, *Crypthecodinium*, *Arthrospira*, *Isochrysis*, *Nannochloropsis*, *Phaeodactylum*, and *Nitzschia*, generate PUFA. Phytoplankton is the foundation of ocean and freshwater food chains, and it is generally the primary source of PUFAs [14,16]. Microalgae-derived PUFAs have numerous benefits over fish oils, including a lack of unpleasant odor, a lower danger of chemical contamination, and a higher purifying capability [16].

The lipid content of cells may be changed in both quantitative and qualitative ways by manipulating external variables, such as nutrients availability. Deprivation of nitrogen and other nutrients is a common technique for increasing lipid content. Lipid content, on the other hand, increases when CO_2 input concentration rises [25,26].

The market for Omega 3 polyunsaturated fatty acids was valued at $2188.87 million and is estimated to reach by $3229.99 million by 2023. North America held the largest share in the market with a share of 46.3% followed by the APAC region. EPA has been the largest ingredient type in the Omega-3 polyunsaturated fatty acids holding a share value of 64.7% [27].

1.3.2 Biofuels

The approaches towards identification of sustainable energy sources were changing significantly during last decades. The "first generation" of biofuels used food crops directly for oil extraction or ethanol production during fermentation. This was linked to a number of issues, the most significant of which were the negative carbon balance and the occupancy of land that was previously used for food cultivation (the “fuel vs. food” dilemma). By using non-food crops or processing organic waste, including food crop waste, the “second generation” biofuels aimed to overcome the limitations of the first generation [28] . Although the carbon balance was predicted to be positive, both the first and second generations were unable to meet human energy demands. It was predicted that more than 10 million square miles of farmland would be required to replace global fossil fuel usage with agricultural biofuel; however, on Earth, only around 6 million square miles of farmland are available [29]. Microalgae can produce far more biodiesel than conventional oilseed crops while using significantly less water and area. The “third generation” biofuels are often referred to as microalgae biomass utilization for biofuels production, while the “fourth generation” biofuels are usually described as the use of metabolic engineering tools for specific compound formation or yield improvement of oxygenic photosynthetic microorganisms [30].

Microalgae, as a third-generation feedstock, offer enormous biofuel potential due to their rapid growth, high biomass output, and high lipid and carbohydrate content. Microalgae yield significant biofuels such as biodiesel, biogas, bioethanol, and biomethane. Algal carbohydrates are used to make bioethanol, while algal oils are utilized to make biodiesel. The remaining biomass is converted into methane or fuel oil [31].

1.3.3 Polysaccharides

Microalgae is also a great source of carbohydrates. They present in both the cytosol and inside the chloroplast of microalgae in the form of cellulose, sugars, starch, and other polysaccharides. Aside from their use in business, particularly the food sector, as gel-forming, emulsifying, or thickening agents [32], polysaccharides are also important in medicine, having stimulating effects on the human immune system, proper intestinal function, and cancer cell death. Furthermore, certain polysaccharides have been shown to have antiviral action [33,34].

Polysaccharides are generally produced as energy reserve molecules in microalgal cells, and they also play a significant role in intracellular homeostasis during drying, temperature, and pH changes. The culture system and environmental factors, such as light availability, salt stress, temperature, and nutrients, can be used to modify algal production and carbohydrate content. In addition, the kinds of carbon sources and the metabolic process are the primary factors that influence the sugar content in microalgae.

Because light is the primary source of energy for the photosynthetic process, the amount of light available during algal cultivation has a significant impact on both algal growth and biomass composition [21].

1.3.4 Biofertilizers

Algae are often utilized in agriculture as biofertilizers. The presence of cyanobacteria in soil (or in water reservoirs in rice fields) can result in not only increased nitrogen levels, but also increased carbon content, vitamins, and plant hormones, as well as improvements in soil pH and electrical conductivity [35,36].

Microalgae (mainly cyanobacteria) are commonly employed in agriculture because of their capacity to fix atmospheric nitrogen, allowing higher plants to overcome nitrogen restriction, which is frequently cited as a productivity limiting issue [37].

Apart from rice, cyanobacterial inoculation has been shown to have beneficial effects on barley, wheat, oats, tomato, radish, cotton, sugarcane, maize, chili, or lettuce [35,38–40]. The most common agricultural cyanobacteria genera are *Nostoc*, *Scytonema*, *Leptolyngbya*, *Phormidium*, *Microcoleus*, *Spirulina,* *Chroococcidiopsis*, *Synechococcus*, *Cyanothece*, *Chamaesiphon*, *Synechosystis* [41], *Tolypothrix*, *Aulosira*, *Anabaena* [36], and some others [42]. The relationship between plant and cyanobacteria can be often classified as symbiosis [43].

1.3.5 Pigments

The three main groups of microalgal photosynthetic pigments are carotenoids (fat-soluble), chlorophylls (fat-soluble), and phycobilin (water-soluble) [21].

The most commercially manufactured carotenoids are astaxanthin (made by *Haematococcus pluvialis*) and beta-carotene (*Dunaliella salina*) [14]. Total carotenoids market has been reported

to increase annually by 2% at least until 2018. Carotenoid concentration varies substantially across microalgae species, and it is influenced not only by environmental factors but also by cell cycle stage [18].

Carotenoids are used as food additives to improve the colour of fish (such as salmon), chicken skin, egg yolks, and even fruit juices. They're also utilized to help grain-fed animals become healthier and more fertile. Cosmetic applications have also been reported [36,44]. β-carotene is thought to be a superior anticancer and anti-heart-disease agent, with additional advantages such as protection against age-related illnesses including cataracts, macular degeneration, and multiple sclerosis [45]. Phycobilisomes are another biotechnologically produced pigment. They act as light-harvesting pigments in cells, complementing chlorophyll. Phycobilisomes are pigment-protein complexes that contain phycocyanin, allophycocyanin, and phycoerythrin subunits. Food colours (ice cream, chewing gums, sweets, non-alcoholic drinks, dietary delicacies, or wasabi, for example) are commonly used [18,34], in cosmetics (eye shadows, eyeliners or lipsticks), and as powerful fluorescent reagents in clinical or research laboratories [14,46].

Phycobilins are employed in immunolabelling studies, fluorescence microscopy, and diagnostics as labels for antibodies and receptors for fluorescence-activated cell sorting. Phycobiliproteins exhibit antioxidant properties (much as carotenoids) and hence have therapeutic potential [47–49].

1.3.6 Cosmetics

Microalgae, or rather microalgal extracts, are utilized in cosmetics for face, skin, and hair care, as well as sunscreens and peelers with emollient and anti-irritant properties [14,50]. They often act as thickening agents, water-binding agents, or antioxidants. The most utilized species used in cosmetics include *Chondrus crispus*, *Mastocarpus stellatus*, *Ascophyllum nodosum*, *Alaria esculenta*, *Spirulina platensis*, *Nannochloropsis oculata*, *Chlorella vulgaris* and *Dunaliella salina* [36].

1.3.7 Vitamins

Both macronutrients (carbohydrates, proteins, and fats) and micronutrients are required for human life. Vitamins are one of the most important micronutrients for energy metabolism, immunity, cellular damage repair, antioxidants, bone health, and other activities. Scurvy, beriberi, and rickets are all illnesses that can be caused by a vitamin deficiency. Microalgae are regarded as an excellent source of vitamins [21].

Mammals, including humans cannot synthesize all the required vitamins, and thus some vitamins must be taken up from external sources. The molecules produced by microalgae include several vitamins from group B (B1, B2, B6, B12), vitamins A, C, E, nicotinate, biotin, folic acid or pantothenic acid [51]. The production yields are comparable with yields achieved by some bacteria or yeasts [52].

1.3.8 Pharmaceutical Products

Microalgae have a wealth of physiologically active secondary metabolites, several of which are being investigated as novel medicines and biomolecules. When compared to laboratory synthesis, biomolecules produced in natural systems have numerous advantages: the molecules are more diverse, soluble in water, permeable through membranes, and in many cases bioavailable without further treatment [53].

Biologically active molecules possess high variability of effects and structures. Up to date, the bioactive compounds found in algae or cyanobacteria have been studied for their anthelmintic [54], antibacterial, antifungal, antiprotozoal, antiviral, anticancer [54,55], anticoagulant [56,57], antiplatelet [58,59], or antioxidant [60] properties. Besides these studies, several reviews are summarizing the state-of the art of discovery and advances of bioactive molecules production and utilization throughout the last decades [61].

1.3.9 Human food and animal feed

Algae have been utilized as a protein and carbohydrate source for over 2000 years.

Microalgae strains often used for the consumption of humans, namely *Chlorella*, *Dunaliella*, *Haematococcus*, *Schizochytrium*, and *Spirulina* are categorized as Generally Regarded as Safe (GRAS) by the US Food and Drug Administration [21].

Microalgal products are now often offered as dietary supplements in the form of pills, capsules, or suspensions, and microalgae-derived products are used in a variety of end goods, including pasta, snacks, gums, and drinks, not only as nutritional additions but also as colorants [62]. Because they contain large levels of proteins (typically over 50% of total volume), 3/6 PUFA, antioxidants, vitamins, and other useful compounds as stated above, microalgae have excellent nutritional characteristics. Furthermore, the quality of the proteins and fatty acids is equivalent to that of eggs and milk [63]. Microalgae also possess prebiotic activity [16], and they are involved in the alleviation of hyperlipidemia, hypertension suppression, or suppression of elevated serum glucose level [14]. The main species of algae cultivated commercially for food are *Spirulina*, *Chlorella* and *Dunaliella*, with worldwide annual production exceeding 6 000 tones in 2006 [14].

Since the 1950s, scientists have been researching algae as an animal feed. There are numerous advantages of using microalgae biomass as feed, particularly for animal physiology, such as improving immune response, disease resistance, and antibacterial and antiviral activity [21].

Microalgae are also frequently utilized in aquaculture as a feedstock for larval and juvenile finfish, certain molluscs, shrimps, prawns, salmonid fish, and ornamental fish, as well as for producing zooplankton for feeding juvenile animals [36]. In fact, 30% of the world algal production was used as animal feed at the end of the last century (Becker, 2004). Diversity of species for aquaculture is higher than that are used for human diets since genera such as *Phaeodactylum*, *Chaetoceros*, *Skeletonema*, *Thalassiosira*, *Chlorella*, *Tetraselmis*, *Isochrysis*, and *Nannochloropsis* are all easily digestible by cultivable organisms [62]. Apart from aquaculture, algae has also been successfully tried as a feedstock for cats, dogs, decorative birds, horses, poultry, rats, mice, sheep, cows, breeding bulls, pigs, and rudimentary animals [14,16,63,64].

1.4 Cultivation systems

Microalgal cultivation systems can be classified as open systems or enclosed systems, where enclosed systems include photobioreactors and fermenters. Microalgal culture systems are frequently defined also on the base of microalgal growth: photoautotrophic, heterotrophic

and mixotrophic. While open systems are generally only used to cultivate photoautotrophic microalgae and enclosed photobioreactors may be used to cultivate photoautotrophic and mixotrophic microalgae, fermenters enable the cultivation of heterotrophic microalgae.

1.4.1 Open systems

Open systems are generally the least sophisticated growing systems and often rely on the sun as the only source of light. The most common open systems for microalgae production are ponds. In open ponds, the oldest and simplest systems for algae culture, the algae are cultivated in conditions identical to those of the external environment. There are many different designs for open pond systems, but three main types have prevailed and are still operated on a commercial scale: raceway ponds, round ponds, and unstirred ponds (**Figure 1.2**).

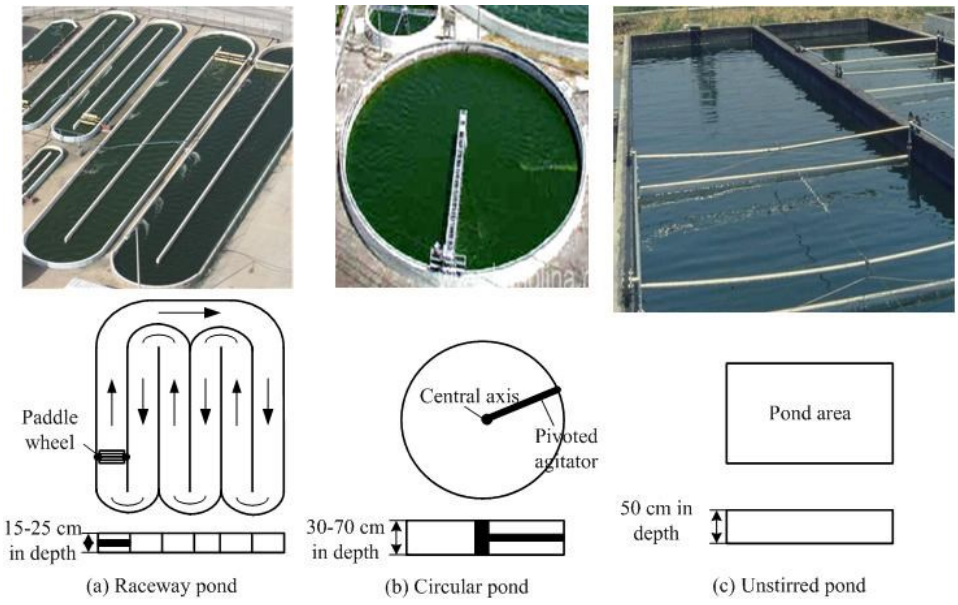

Figure 1.2 Three different designs of open-pond systems: raceway ponds (a), circular ponds (b) and unstirred pond (c) [65].

For mixing and circulation, a paddle wheel is used in rraceway ponds, and a swivel agitator in circular ponds. These agitation systems operate continuously to prevent sedimentation, avoid the formation of a temperature gradient, distribute nutrients and carbon dioxide, remove produced oxygen, and transport algae to and from the surface, which improves the overall light output [66].

The temperature in an open raceway fluctuates within a daily cycle and seasonally. Temperature is very difficult to control. Cooling can occur through evaporation. Water loss through evaporation can be significant and causes an increase in the concentration of salt and other compounds [67].

This could be countered by replenishing water with sufficiently low salinity, although this may be problematic in some geographic locations. While saline groundwater is unsuitable for agriculture, it could be used in some seaweed crops. The major advantages for using open systems are that they are often cheap to build and relatively easy to operate [68,69].

However, only a limited number of microalgae species, including *Dunaliella sp.*, *Spirulina sp.* and *Chlorella sp.* are commercially grown in open systems [18,68,70].

These species have an advantage over other microalgae in that they are able to grow rapidly or in hostile or highly selective environments. For example, *Dunaliella sp.* has adapted to tolerate very high salinity, while *Spirulina sp.* can tolerate high alkalinity.

Open systems tend to have high contaminations risks from other predator microorganisms and low biomass concentrations [71,72].

Biomass productivities can also be quite low and are often subject to high variability. This variability is often due to limited control of cultural and environmental conditions. Inadequate mixing, poor gas transfer, low light yield, and fouling are common characteristics of open systems [68]. The low biomass concentrations achieved in open systems require large culture volumes and extensive land areas to achieve a given biomass quantity. The low biomass concentrations can also result in significant harvesting costs if required, as a large volume of culture would need to be processed and harvesting a dilute culture containing small microorganisms presents technical difficulties [73].

1.4.2 Closed systems: photobioreactors

Many microalgal species that are unable to grow long-term in open systems must be grown in a closed system. Closed systems can reduce the risk of contamination of the culture and subsequent culture collapse. One of the advantages of closed systems is that growth conditions can be closely monitored and controlled [18,68,69].

A number of enclosed photobioreactors have been developed and include a range of tubular (glass, plastic, bags), flat plate and air- lift systems. **Figure 1.3** showed different shapes of photobioreactors: tubular (A), plate (B), column (C) and annular (D).

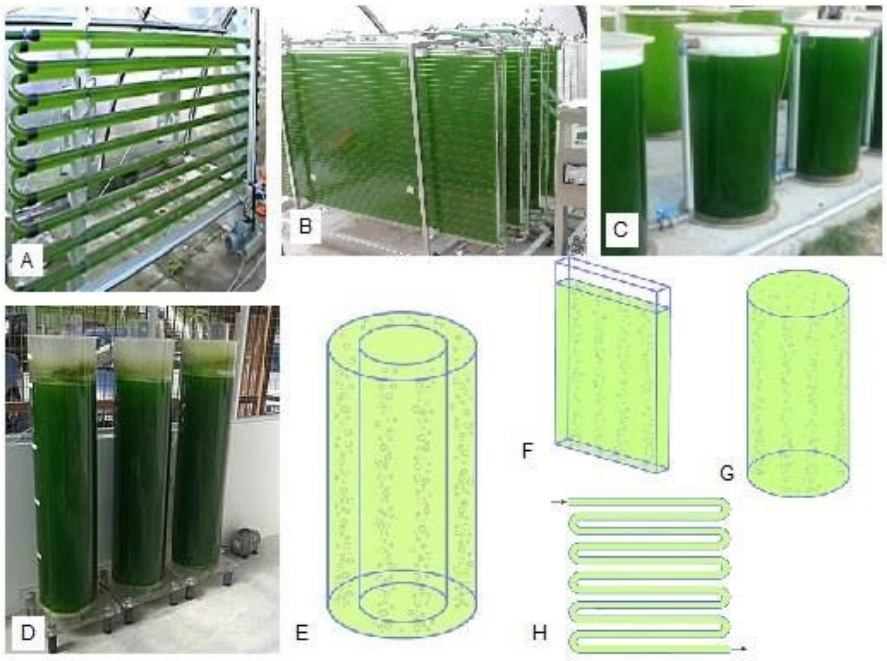

Figure 1.3 Showing different type of Photobioreactors for algal cultivation, A. Tubular (Source- Chempure Technologies Pvt. Ltd.), B. Plate (Source- IGV Biotech, Wikipedia), C. Column (Source-Oilgae), D. Annular (Source-Tan, Gallery), E-H. Diagrammatic representation of photobioreactors (Source- Hallmann, 2015), E. Annular, F. Plate, G. Column, H. Tubular [74].

Many closed photobioreactor systems have been developed to improve light-cell interactions by increasing the surface-to-volume ratio and reducing the path length of incident light [18,75]. The use of closed photobioreactors can generally lead to an increase in biomass productivity by increasing biomass concentration. Unfortunately, many closed photobioreactors are designed on a small scale and are technically and economically difficult to scale up. Furthermore, closed photobioreactors are not exempt from the technical and economic problems associated with biomass harvesting.

All materials used in the manufacture of closed photobioreactors reduce light penetration [71]. In addition, light penetration can be further reduced by material wear and contamination on the inner and outer surfaces. Closed photobioreactor systems may also suffer from high capital and operating costs, excessive oxygenation, overheating, and cell damage due to shear. To improve biomass productivity, fluorescent tubes or other artificial light sources are

routinely used in the design of closed photobioreactors. However, the use of artificial light sources increases the overall operating costs. The light requirement ultimately depends on the microalgae species and biomass concentration. If the biomass concentration changes, then the light requirement also changes. As biomass concentration increases, the distance of light penetration decreases, and light limitation may occur in the center of the culture. Furthermore, if the intensity of the incident light is too high, the biomass at the surface of the photobioreactor may receive too much light and suffer from photoinhibition. This photoinhibition hinders the growth rate and reduces the productivity of the biomass. Process optimization is often technically difficult due to the multitude of culture and environmental factors. All cultivation systems require circulation of the culture medium to prevent biomass sedimentation and to minimize light, gas, and nutrient gradients. Circulation mechanisms (agitators, pumps, etc.) can result in high shear conditions that can cause cell lysis and loss of cultures. Relative sensitivities to shear and turbulence have been categorized by microalgal class. [76]. In summary, the optimal design, development, and operation of closed photobioreactors can be difficult to achieve and also quite expensive. Furthermore, no photobioreactor system will be suitable for all microalgae or all microalgae applications. While the use of closed photobioreactors can increase biomass productivity, they generally require a large capital outlay and a high level of expertise to operate. In addition, the optimal design, development, and operation of photobioreactors is often difficult and expensive.

Several companies are using or developing closed systems for microalgae growth, in Europe. The scale is still small (the largest system has a total area of 1 ha), but in recent years many developments have taken place aimed at increasing the scale of production and industrialising the field.

Examples of these companies are: Ecoduna in Austria with rigid flat panels (www.ecoduna.com); Phytolutions in Germany (www. phytolutions.com), Archimede Ricerche in Italy (www. archimedericerche.com) and Proviron in Belgium (www. proviron.com). All these companies use thin plastic films flat panels. Tubular photobioreactors are used by the Spanish companies AlgaEnergy (www.algaenergy.es), Algasol (www. algasol.com) and Fitoplancton Marino (www.easyalgae.com), by Roquette in Germany (www.roquette.com) and A4F in Portugal (www.a4f.pt). The last two companies

represent the largest production plants in Europe, ca 1 hectare (the plant from Roquette is inside a greenhouse while the plant from A4F is outdoor)[77].

Southern Europe and Northern Africa are the best sites for microalgal biomass production due to solar conditions, but only with adequate fertilization and near CO_2 sources. Wastewater from urban or industrial activities can be used as a source of nutrients (nitrogen and phosphorus) for microalgae production. Flue and fermentation gases can be used as a source of CO_2. Now, it can be seen that technology development in this area is taking place throughout Europe, but sustainable large-scale production is likely to occur mainly in South Europe [77].

1.4.3 Closed systems: fermenters

Fermentation systems are used for the heterotrophic cultivation of microalgae (**Figure 1.4**). These systems, originally developed for use in bacterial and yeast cultures, already exist, are highly developed, and are used worldwide at various scales [78]. A major advantage of fermentation systems is that the technology is generally well understood and can be easily applied to heterotrophic cultivation of microalgae. Heterotrophic cultivation relies on the ability of organisms to assimilate organic carbon and eliminates the need for light. This elimination of light can be beneficial as it eliminates the need to maintain light-cell interactions and the problems associated with light limitation and/or photoinhibition commonly observed in photoautotrophic systems. However, not all organisms are able to assimilate organic carbon and consequently heterotrophic growth has only been demonstrated in a limited number of microalgal species. While glucose and acetate are the most commonly assimilated organic carbon compounds, other organic carbon compounds that are assimilated include acetic acid, asparagine, aspartate, galactose, glutamate, and lactate. The addition of the organic carbon (which is essential for heterotrophic growth) to the culture media results in an increase in the potential for bacterial contamination and strict sterilization procedures must be followed thereafter. Fermentation techniques allow for easy control and/or manipulation of culture and environmental conditions. This inherent control and elimination of light, as seen in fermentation systems, can be especially beneficial for

larger operations. Heterotrophic cultivation offers the possibility of achieving high cell densities and maintaining constant, year-round production.

Heterotrophic biomass concentrations of typically 50 – 100 g L-1 are at least 10-fold higher than those achieved in photoautotrophic systems [78] and more recently biomass concentrations as high as 120 g L-1 were reported [79].

Figure 1.4 Commercial fermentation plant for microalgae production.

1.5 Heterotrophy: a challenging opportunity

In general, microalgae are considered photoautotrophic organisms that is the energy used for their growth and maintenance originates from photosynthesis [80]. However, some microalgae are able to grow heterotrophically in dark environments. There is evidence that these microorganisms possess a 'dark metabolism', which is essentially the same as the non-photosynthetic metabolism of organisms like yeasts. Therefore, it would be expected that the carbon sources used by microalgae under dark conditions are transformed into carbon intermediates in the main metabolic pathways, replacing photosynthetically produced molecules [81,82]. A theory to why some microalgae are obligate photoautotrophs is the deficiency of an efficient cellular consumption of vital substrates, particularly sugars and other carbon sources [81,83]; as an example, *Phaeodactylum tricornutum* is a phototrophic microalga that was able to grow heterotrophically following the insertion of a single gene (glut1 or hup1), which encodes a transporter for glucose [80].

Benefits of heterotrophic microalgae cultivation have been described in [84], and can be summarized as follows: lighting requirements are eliminated; cell mass, growth rates and protein and lipid productivities can be significantly increased; bioreactors are easily operated

and maintained and they can also be operated under axenic conditions; high cell masses are obtained as a result of the high energy density of carbon sources when compared to CO_2; fed-batch culture strategies can be used to increase cell densities, ultimately leading to a reduction in costs for biomass harvesting; common air can be employed instead of previously treated flue gas since O_2 is consumed and CO_2 generated; and the same media components as those needed in phototrophic cultures are used.

1.5.1 Heterotrophic microalgae and commercial products

Commercially successful production in fermenters, to date, has focused on the use of strains from a limited number of microalgal groups: the green algae, the dinoflagellates, and the thraustochytrids [85].

Chlorella is the most diffused microalgae species belonging to the macro group of green algae. In Japan, over 2000 tons of dry *Chlorella* are produced each year and heterotrophic processes yield about half of this amount. A glucose-limited, fed-batch culture with a fermentation duration of roughly 40 hours is used in the fermentation process. The final cellular dry weight density is around 80 g L^{-1} [25,86].

The final stage of processing for certain companies takes place in outdoor ponds to green up the biomass for the production of the so-called "*Chlorella* growth factor," which is a key component of *Chlorella* extract products. In this way, the heterotrophic phase acts as a boost for the cellular growth. Spray dried whole cell algae are supplied as a powder or as tablets in the nutritional supplement industry. Digestibility and bioavailability are concerns for humans since *Chlorella spp.* have cellulose cell walls. Company that use a heterotrophic cultivation step to create *Chlorella* solve these concerns by employing strains with thin cell walls in the manufacturing process or by partially breaking the cell walls after harvest [85].

For the nutritional supplement and cosmetic industries, this substance is available in liquid, powder, or tablet form. Some of the heterotrophically produced *Chlorella* is also offered in paste form as an aquaculture feeding for the aquaculture industry to grow rotifers.

Solazyme Roquette Nutritionals (a joint venture between Solazyme and Roquette) stated in the beginning of 2012 that they would be launching a *Chlorella*-based algal flour to the

European food market. The flour will be offered in high protein and high fat variants, with use levels ranging from 3.5 to 50% in foods [87,88].

This ingredient form is claimed to make it easier to make lower-fat foods with better lipid profiles. *C. protothecoides* produces algal flours through heterotrophic fermentation with glucose and/or sucrose as the carbon source. It is claimed that the cells can be produced with a high lipid content (40–70 percent dry weight) or a high protein content (40–70 percent dry weight) depending on the fermentation procedure.

Solazyme and Solazyme Roquette Nutritionals have both recently filed patent applications for the synthesis and use of these sorts of algal flours in food [87,88].

Solazyme has also filed a patent application for the use of molecular engineering approaches to improve lipid synthesis and adjust the fatty acid profile of oleaginous bacteria, such as Chlorella generated through fermentation. The modified lipids detailed in the patent application are recommended as substitutes for a variety of food-grade oils that are typically obtained from palm oil, for example, or from other vegetable and animal sources [88].

As described in two papers of Wynn et al. [89], because of its capacity to develop heterotrophically and its unusual fatty acid profile, which contains only one PUFA, DHA, *Crypthecodinium cohnii* was chosen as a fermentation organism. Fermentation is a two-stage, fed-batch (carbon fed) process that takes place in huge commercial fermenters [89,90].

The fermentation process is divided into two stages: cell growth and lipid generation.

To control cell development, nitrogen is given at a set rate during the cell growth phase, and completely depleted during the lipid production phase.

A similar process, divided into a phase of cell growth and a phase of nutrient deprivation with the aim of increasing the lipid component, was used by d'Ippolito et al. [91] to explore the potential of the *Thalassiosira weissflogii* diatom grown under autotrophic conditions [91].

Nevertheless, for optimal cell growth and oil production of *Crypthecodinium*, dissolved oxygen, pH, temperature, and glucose concentration are all kept at predetermined levels.

The cells are centrifuged, pasteurized, and dried at the end of the fermentation, and then extracted using hexane in a technique virtually identical to that used to extract vegetable oils from seeds. The oil is subsequently refined, bleached, and deodorized in order to improve its purity and quality. The triglyceride-rich algal oil contains 50–65 percent DHA, which is standardized to 40% DHA by diluting it with high-oleic sunflower oil.

This oil is used in infant formula to support proper brain and eye development; it is widely accepted and now it is present in more than 95 percent of infant formula sold in the United States and more than 25 percent of infant formula sold worldwide. The oil is also sold as a dietary supplement for moms who are pregnant or breastfeeding.

The use of a unique strain with a very simple fatty acid profile made the oil easy to formulate into infant formula; the development of a strong patent strategy based on both the composition of the oil and its use in infant formula; and the implementation of an effective marketing effort around the emerging evidence of the DHA w-3 fatty acid in the growth of both the fetus and the child, made the oil easy to formulate into infant formula and drive efforts in the development of this technology and its continued success [85].

C. Cohnii oil is actually sold under several different brands products, as Neuromins © and DHASCO©.

Over the course of several years, technology for the development and commercialization of the *Schizochytrium*-based products was developed in three key steps: (1) strain isolation and preliminary fermentation optimization; (2) creation of a low-chloride fermentation process; and (3) development of a low-dissolved oxygen, high-cell-density fermentation process. Because *Schizochytrium sp.* is a marine organism that lives in saltwater, it was important to create a low-chloride fermentation method because seawater is too corrosive for use in traditional stainless-steel fermenters, especially at the high temperatures required in sterilizing culture medium.

The low-chloride fermentation technique lowered chloride levels in the medium from 19 g L^{-1} in seawater to less than 0.7 g L^{-1} in the media, resulting in excellent growth and, interestingly, increased DHA synthesis [92].

The presence of the unique PUFA–synthase system in this organism, which does not require oxygen for the desaturation stages in the synthesis of a highly unsaturated fatty acid such as DHA, aided the low-dissolved oxygen and the high-cell-density process. This method allowed the technology to achieve cell densities of over 200 g L^{-1} and DHA productivities of over 12 g L^{-1} day^{-1}. The technique was scaled up through a collaboration between OmegaTech Inc. and Kelco (San Diego, California).

Following the receipt of the necessary regulatory licenses for the items, the technology was commercialized in four steps: 1) entrance into the aquaculture market with a spray-dried,

whole cell product for use as an aquaculture feed (Barclay & Zeller, 1996); (2) entrance into the animal feed market as a drum-dried, whole cell product for feeding to laying hens to produce DHA-enriched eggs (Abril & Barclay, 1998); (3) entrance into the nutritional supplement market via production of capsules containing DHA-rich oil [93]; and (4) entrance into the food market via use of the extracted DHA-rich oil as a food ingredient [94].The use of the derived DHA-rich oil as a food component allows the oil to enter the food market [85].

The DHA-rich oil is now available worldwide as a branded ingredient (life's DHA ©) in a very wide variety of foods and nutritional supplements.

1.5.2 Future directions

While strains of green, dinoflagellate, or golden microalgae have proven commercially successful in the production of microalgae in fermenters, future heterotrophic technologies may use a broader range of algae species: inducing genes encoding glucose transport, typical photosynthetic strains may be genetically modified to import glucose and thrive in the dark [95]. These approaches might allow for a considerably larger spectrum of microalgae to be grown in fermenters than is now achievable.

The major limitations and problems raised to the heterotrophic growth of microalgae concern the sustainability of the process on the basis of available resources. The cost of simple sugars used in heterotrophic growths is substantial and tends to increase over the years, Over the last 30 years, sugar prices have ranged from about $0.11 to $0.77 per kg [96].

The future challenge is to use agricultural waste products as a source of organic material for microalgal growth. Research in this regard is providing interesting results.

On the other hand, in the future, the challenge remains open for the optimization of strain through genetic engineering so that they can use complex waste substrates associated with a refinement of technologies related to fermentation processes.

Finally, microalgal fermentations do not give the carbon dioxide emissions advantages that microalgal photosynthetic production does. However, because the cheapest carbon sources used in fermentations are obtained from photosynthetic sources, they constitute a step toward a more climate friendly approach to food and chemical production. Heterotrophic production will continue to be a key technique for the production of microalgae for the

foreseeable future, with substantial output from large-scale photosynthetic production methods remaining more than a decade away [85,97].

1.6 Diatoms

1.6.1 General characteristics

Diatoms are a group of unicellular algae, members of the algal class *Bacillariophycae* and *Stramenopile* phyla. They are unicellular photosynthetic microalgae existing ubiquitously in marine and freshwater environments [98], with about 16.000 living species.

One of the most important characteristics of these organisms is the ability to generate a silica cell wall, known as frustule. The cell wall is composed of two parts like a box: an upper part, the epitheca, that overlaps with a bottom half, the hypotheca (**Figure 1.5**). The hypotheca is slightly smaller than epitheca. The joint between the two thecae is guaranteed by bands of silica (girdle bands) that hold them together [99].

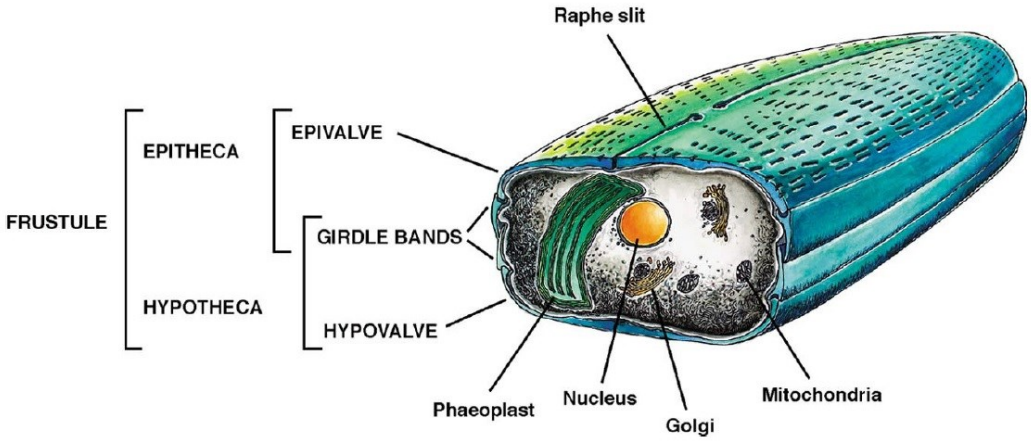

Figure 1.5 Representation of a diatom cell structure.

This has the important consequence that a cell can appear quite different if viewed from the side ("girdle view") than if it is viewed from above ("valve view").

The cytoplasm is completely shielded as a result, and any material exchange with the environment must take place through suitable pores or cracks. Diatoms are classified as centric or pennate based on the form of the frustule.

Centric diatoms have radial symmetry, while pennate diatoms have an extended form with bilateral symmetry in comparison to the plane of the valves (**Figure 1.6**).

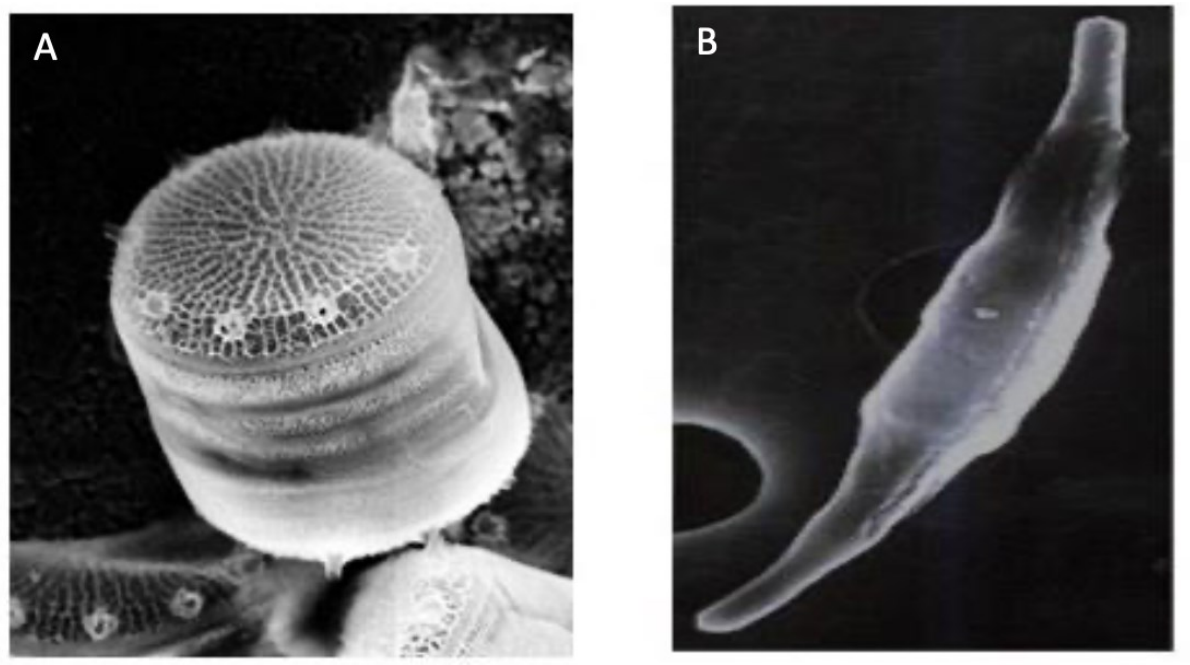

Figure 1.6 Pictures of the centric diatom *Thalassiosira pseudonana* (A) and the pennate diatom *Phaeodactylum tricornutum* (B).

Among the pennate, there is a further distinction based on the presence or lack of raphe, a polysaccharide structure that is likely employed for cell mobility on solid surfaces.

In reality, raphe species are frequently benthic, whereas planktonic species, both centric and pennate, retain just a residual residue of this structure (araphidinae) [100].

Like other eukaryotic organisms capable of carrying out photosynthesis, diatoms are equipped with plastids inside of which there are complexes of proteins and pigments important for the capture of light [101]. The presence of the supplementary carotenoid pigment fucoxanthin, which covers the green of chlorophyll a and c, gives diatoms their golden-brown hue. Fucoxanthin and chlorophyll are bound together inside the antenna complex to collect light from Fcp proteins (fucoxanthin chlorophyll a/c-binding proteins).

Phylogenetic analyses have clearly shown that the chloroplasts of most algae and higher plants are derived from a process of primary endosymbiosis that occurred at least 1.5 billion years ago between a photosynthetic bacterium (very similar to current cyanobacteria) and a eukaryotic unicellular heterotroph. Instead, diatom chloroplasts may be the product of a

second endosymbiotic event that happened around 1 billion years later, in which a eukaryotic alga, most likely a red alga, was absorbed into a second eukaryotic heterotrophic cell [102]. According to phylogenetic analyses, diatoms diverged early from the branch that gave birth to green algae and higher plants. According to this, the recent genome sequencing of two diatom species revealed that these creatures had distinct features. The most remarkable feature is that half of their genes encode proteins that are similar to those found in mammals rather than plants (**Figure 1.7**)[103,104].

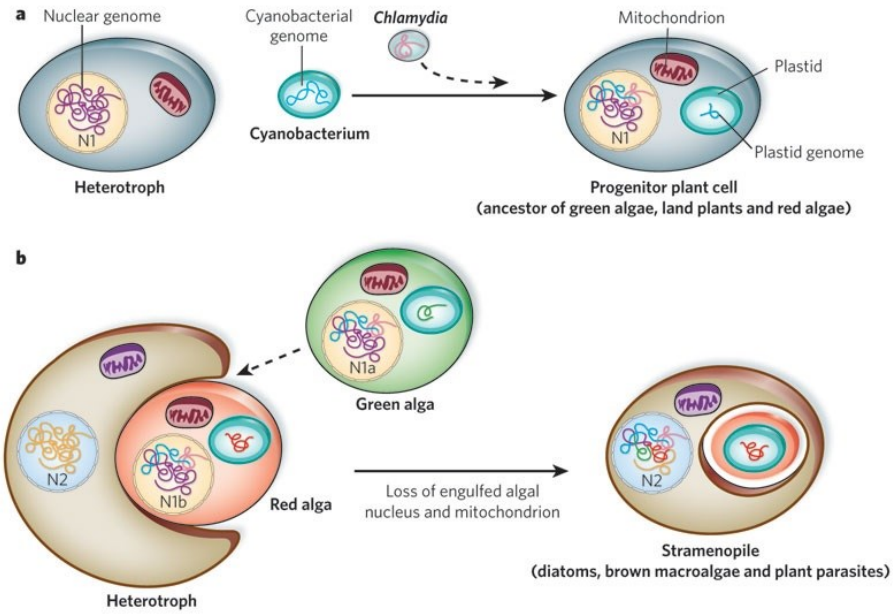

Figure 1.7 Representation of the origin of diatom plastids through sequential primary (a) and secondary (b) endosymbiosis and their potential effects on genome evolution [103].

Vegetative cells of diatoms are diploid. In a normal cycle of asexual division two daughter cells originates from a mother cell. Each valve of the parental cell becomes the epitheca of the daughter cell [105] and each daughter cell will generate a new hypotheca. Before the division, the cell elongates, pushing the epitheca away by the hypotheca, and the nucleus divides through a mitosis "open"(**Figure 1.8**). After the protoplast was divided by the invagination of the plasma membrane, each daughter cell generates a new hypotheca. This structure, which covers one half of the cell, is commonly generated through the production of polarized vesicles known as silica deposition vesicle (SDV). The construction of the hypotheca provides that the pattern of silica is wrapped by an organic matrix which prevents the dissolution. Once

the entire structure is generated, the organic structure is poured out, after which the two daughter cells can be separated. The design of the wall is reproduced from one generation to another, implying the presence of a strong genetic control.

In most of the diatoms, the process of wall formation causes, for each mitotic division, the reduction in the size of one of the two daughter cells. The regeneration of the size takes place through sexual reproduction, followed by the formation of auxospore. Gametogenesis normally occurs when the size of the cells was reduced by 30-40%. This is considered the threshold value. The resulting male and female gametes unite to create a diploid auxospore that is larger than the parents. Then, the new cell goes against processes of asexual division until an appropriate signal does not induce again gametogenesis.

When cells are exposed to unfavourable growth conditions can sometimes be induced to reproduce sexually. It has been reported that changes in the conditions of light, temperature, nutrient availability and salt concentration can induce a change in the mode of reproduction by asexual to sexual [106].

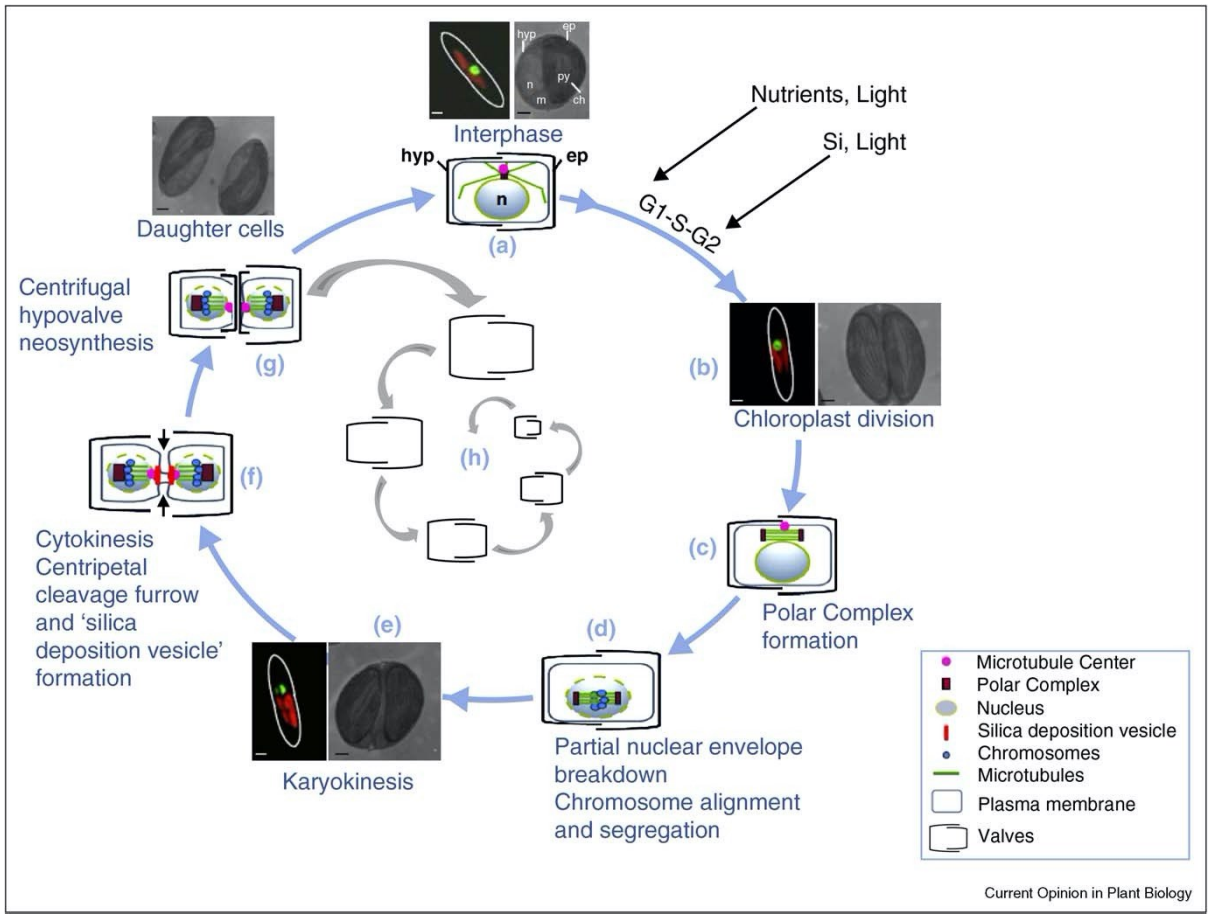

Figure 1.8 Overview of the diatom cell cycle [107].

1.6.2 Ecological importance

Diatoms play a number of critical roles in the ecosystem. The ecological importance of diatoms in studies on the quality of both marine and fresh water is essential, as this class is a fundamental component of the phytoplankton population.

In reality, diatoms are the most common group of marine eukaryotic phytoplankton, accounting for 40% of total photosynthetic activity and hence playing a critical role in primary oceanic production. They support many of the higher trophic levels and low-energy food chains that sustain large-scale coastal fishing, such as anchovies in the Peruvian rise. They support many of the higher trophic levels and low-energy food chains that sustain large-scale coastal fishing, such as anchovies in the Peruvian rise. Their presence in the oceans becomes observable also macroscopically in particular during the flowering periods, defined as bloom (**Figure 1.9**), in which these organisms increase their cell concentrations passing from hundreds to millions of cells per milliliter [108].

This important characteristic that confers ecological success, can be exploited for biological purpose as microorganisms capable of reaching high cell densities, while producing useful products. Since diatoms require silicon for the construction of the frustule, their growth greatly influences the silicon cycle at sea.

During the bloom phenomena of diatoms, silica dissolved in the oceans reaches very high levels. The subsequent "rain" of frustules from dead diatoms at the end of blooms forms organic silica deposits on the ocean floor. Given the stability of their siliceous shells, diatoms in a fossil state are very abundant: the first centric diatoms appear in the fossil deposits of the late Cretaceous, while the pinnate with raphe in the Eocene [109].

Figure 1.9 Phytoplankton bloom along the edge of the continental shelf southwest of Cornwall in the UK.

Furthermore, diatoms also play an important role in the biogeochemical cycle of carbon, as, due to their heavy silica wall, dead and dying organisms contribute to the transport of organic carbon to the seabed. This process transfers energy, electrons and carbon into the depths of the sea and is essential for the survival of all living organisms below the photic zone of the water column [108]. The process also helps sequester carbon in the deepest areas of the sea where it is stored for periods ranging from centuries to millennia. A large part of the oil fields, in fact, derives from diatoms that have sunk in the different geological temporal eras [110,111].
The high ability of diatoms to perform an important link in the process of CO_2 exchange between the atmosphere and the ocean is very complex and in part still little known to the scientific community today.

1.6.3 Diatoms and heterotrophy

There is apparently no previous record before 1953 that any chlorophyllous diatom has been cultivated successfully in the dark.
Certain species of diatoms acquired in pure culture did not develop in the dark or in semi-darkness on organic nutrient solutions, according to Miquel (1892), yet they kept their proliferative ability when reintroduced to the light after many months in darkness. In polluted coloured diatom cultures kept in the dark, either in hanging drop cultures or in mass cultures

with a rich organic nutrient, Benecke (1900) found no increase in numbers. Karsten (1901), who worked with impure diatom cultures, measured growth by making daily cell counts. Thirteen isolates of pennate diatoms cultures proved capable of growth under dark conditions by Lewin et al. [112]: they comprised seven isolates of *Navicula pelliculosa*, five of other different species of *Navicula*, and one of *Nitzschia* [112].

Active transport of carbon sources has been documented in several species of diatoms [113], and is likely the most common mechanism for sequestering these compounds. Despite the subsequent efforts of the scientific community on the identification and understanding of the adaptation mechanisms of microalgal species in the darkness, to date, only a small number of microalgal species have been cultured heterotrophically in conventional bioreactors [4,69,114], as reported also in the paragraph 1.5.1 of this Chapter.

Few diatoms are capable of adapting to heterotrophic conditions: *N. laevis*, *Navicula incerta*, *Navicula pelliculosa*, and *C. cryptica* have been tested for their ability to produce EPA but have not yet been optimized for large-scale production.

1.7 *C.cryptica* as a model to investigate heterotrophy

C. cryptica is a centric marine diatom and planktonic species, firstly isolated in 1956 from a brackish pond (West Tisbury Great Pond) on Martha's Vineyard, Massachusetts [115].

Like all diatoms, whose general characteristics have been described in paragraph 1.6.1., *C. cryptica* has a siliceous wall and an asexual cell division; the reduced cellular size resultant from divisions events is restored via sexual reproduction. *C. cryptica* exhibits interesting metabolic plasticity. Algal species from across the tree of life were evaluated for their ability to accumulate abundant triacylglycerol (a precursor to biofuel), to grow under variable environmental conditions such as pH, salinity, and temperature, and to grow at a productive and sustainable rate in outdoor raceway ponds during the Aquatic Species Program (ASP), which was funded by the US Department of Energy. *C. cryptica* was identified in the ASP as a top species for large-scale biofuel production [116]. *C. cryptica* has been found to be a good lipid producer (**Figure 1.10**), is euryhaline, allowing for greater flexibility in culture circumstances [115,117,118], and can grow outside at 20.0 and 29.7 g Ash Free Dry Weight m^2/day in a 2.8 and 48 m^2 pond, respectively [119,120].

This species is typically characterized as photoautotrophic, even if there are some evidences of heterotrophic growth [113,121,122],not deeply addressed by scientific community.

Several strains of *C. cryptica* have been isolated: T13L, O3A, SIMOB and WT18. The strain we used in this thesis is SIMOB, the culture ID from Provasoli-Guillard National Center for Culture of Marine Phytoplankton is CCCMP331.

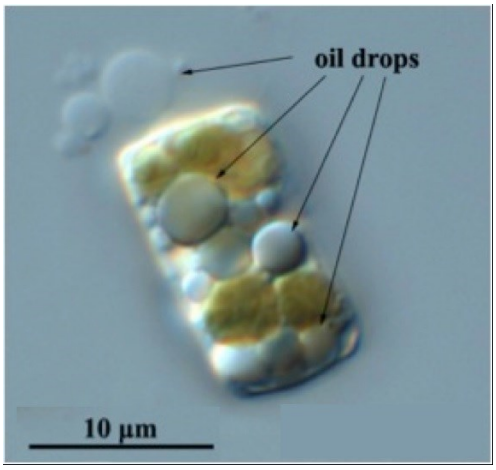

Figure 1.10 Image of *C. cryptica* [115].

1.8 Aim of the project

My PhD project has evolved with the objective of investigating the perspectives of heterotrophic growth, an uncommon growth modality among photosynthetic microalgae.

Infact, microalgae are mainly phototrophic organisms, and few species are reported being capable to switch their metabolism.

Given its promising metabolic plasticity, as underlined in the preceding paragraph, *C. cryptica* was chosen as a model diatom to evaluate the biotechnological potential and adaptation mechanisms to the dark.

As a result, the thesis addressed a variety of topics, including the optimization of *C. cryptica*'s growth conditions in the dark and the biochemical investigation of the biomasses obtained, in order to evaluate the products of interest achievable and consider the true applicability of the production process on a large scale.

The group of Dr. Fontana and Dr. d' Ippolito, with whom I conducted my doctorate study, has been working for years to shed light on the biosynthesis, biochemical features and biological activity of diatom lipids. [123–126]

Heterotrophy is a growth condition that also allows to address the physiological response of the cells to the switch-off of photosynthetic apparatus, and its impact on lipid remodeling and lipid biosynthesis. On these grounds, lipidomic (LC-MS, NMR) and transcriptomic (RNAseq) techniques were very useful during PhD.

These approaches led us to the selection of potential genes to be used as a model study for testing genetic manipulation (CRISPR-Cas-9) with the goal of unambiguously determining their function.

1.9. References

(1) Borowitzka, M. A. Microalgae in Health and Disease Prevention. In *Biology of Microalgae*; In I. A. Levine & J. B. T. Fleurence, Ed.; Levine & J. B. T. Fleurence, **2018**; pp 23–72. https://doi.org/https://doi.org/10.1016/B978-0-12-811405-6.00003-7.

(2) Barsanti, L.; Coltelli, P.; Evangelista, V.; Frassanito, A. M.; Passarelli, V.; Vesentini, N.; Gualtieri, P. Algal Toxins: Nature, Occurrence, Effect and Detection. In *Oddities and curiosities in the algal world*; Evangelista V, Barsanti L, Frassanito AM, Passarelli V, G. P., Ed.; Dordrecht: Springer, **2008**; pp 353–391.

(3) Sharma, N. K.; Rai, A. K. Biodiversity and Biogeography of Microalgae: Progress and Pitfalls. *Environ. Rev.* **2011**, *19* (1). https://doi.org/10.1139/A10-020.

(4) Perez-Garcia, O.; Escalante, F. M. E.; de-Bashan, L. E.; Bashan, Y. Heterotrophic Cultures of Microalgae: Metabolism and Potential Products. *Water Res.* **2011**, *45* (1), 11–36. https://doi.org/10.1016/j.watres.2010.08.037.

(5) Shen, X.-F.; Hu, H.; Ma, L.-L.; Lam, P. K. S.; Yan, S.-K.; Zhou, S.-B.; Zeng, R. J. FAMEs Production from *Scenedesmus Obliquus* in Autotrophic, Heterotrophic and Mixotrophic Cultures under Different Nitrogen Conditions. *Environ. Sci. Water Res. Technol.* **2018**, *4* (3), 461–468. https://doi.org/10.1039/C7EW00470B.

(6) Wijffels, R. H.; Kruse, O.; Hellingwerf, K. J. Potential of Industrial Biotechnology with Cyanobacteria and Eukaryotic Microalgae. *Curr. Opin. Biotechnol.* **2013**, *24* (3), 405–413. https://doi.org/10.1016/j.copbio.2013.04.004.

(7) Droop, M. R. Heterotrophy of Carbon. In *Algal Physiology and Biochemistry*; Stewart, W. D. ., Ed.; Blackwell Scientific, Oxford, UK, **1974**; pp 530–559.

(8) Heimann, K.; Huerlimann, R. Major Classes and Genera of Commercial Microalgal Species. In *Handbook of Marine Microalgae*; Se-Kwon, K., Ed.; **2015**; pp 25–41.

(9) Brodie, J.; Lewis, J. *Unravelling the Algae the Past, Present, and Future of Algal Systematics*; Brodie, J., Lewis, J., Eds.; CRC press, **2007**.

(10) Buick, R. When Did Oxygenic Photosynthesis Evolve? In *Philosophical Transactions of the Royal Society B: Biological Sciences*; **2008**; Vol. 363. https://doi.org/10.1098/rstb.2008.0041.

(11) Kopp, R. E.; Kirschvink, J. L.; Hilburn, I. A.; Nash, C. Z. The Paleoproterozoic Snowball Earth: A Climate Disaster Triggered by the Evolution of Oxygenic Photosynthesis. *Proceedings of the National Academy of Sciences of the United States of America*. **2005**. https://doi.org/10.1073/pnas.0504878102.

(12) Field, C. B.; Behrenfeld, M. J.; Randerson, J. T.; Falkowski, P. Primary Production of the Biosphere: Integrating Terrestrial and Oceanic Components. *Science.* **1998**, *281* (5374). https://doi.org/10.1126/science.281.5374.237.

(13) Capone, D. G. The Marine Nitrogen Cycle. *Microbe*. **2008**. https://doi.org/10.1128/microbe.3.186.1.

(14) Spolaore, P.; Joannis-Cassan, C.; Duran, E.; Isambert, A. Commercial Applications of Microalgae. *J. Biosci. Bioeng.* **2006**, *101* (2), 87–96. https://doi.org/10.1263/jbb.101.87.

(15) Jensen, G. S. Blue-Green Algae as an Immuno-Enhancer and Biomodulator. *JANA* **2001**, *3* (4).

(16) Pulz, O.; Gross, W. Valuable Products from Biotechnology of Microalgae. *Applied Microbiology and Biotechnology*. **2004**. https://doi.org/10.1007/s00253-004-1647-x.

(17) Borowitzka, M. A. Microalgae as Sources of Pharmaceuticals and Other Biologically Active Compounds. *J. Appl. Phycol.* **1995**, *7* (1). https://doi.org/10.1007/BF00003544.
(18) Borowitzka, M. A. Commercial Production of Microalgae : Ponds , Tanks , Tubes and Fermenters. **1999**, *70*, 313–321.
(19) Sheehan John; Terri, D.; John, B.; Paul, R. A Look Back at the U.S. Department of Energy's Aquatic Species. *Eur. Phys. J. C* **2012**, *72* (6), 14.
(20) Araújo, R.; Vázquez Calderón, F.; Sánchez López, J.; Azevedo, I. C.; Bruhn, A.; Fluch, S.; Garcia Tasende, M.; Ghaderiardakani, F.; Ilmjärv, T.; Laurans, M.; Mac Monagail, M.; Mangini, S.; Peteiro, C.; Rebours, C.; Stefansson, T.; Ullmann, J. Current Status of the Algae Production Industry in Europe: An Emerging Sector of the Blue Bioeconomy. *Front. Mar. Sci.* **2021**, *7* (January), 1–24. https://doi.org/10.3389/fmars.2020.626389.
(21) Kusmayadi, A.; Leong, Y. K.; Yen, H. W.; Huang, C. Y.; Chang, J. S. Microalgae as Sustainable Food and Feed Sources for Animals and Humans – Biotechnological and Environmental Aspects. *Chemosphere* **2021**, *271*, 129800. https://doi.org/10.1016/j.chemosphere.2021.129800.
(22) Williams, C. M. Dietary Fatty Acids and Human Health. *Anim. Res.* **2000**, *49* (3). https://doi.org/10.1051/animres:2000116.
(23) Tallima, H.; El Ridi, R. Arachidonic Acid: Physiological Roles and Potential Health Benefits – A Review. *J. Adv. Res.* **2018**, *11*, 33–41. https://doi.org/10.1016/j.jare.2017.11.004.
(24) Ward, O. P.; Singh, A. Omega-3/6 Fatty Acids: Alternative Sources of Production. *Process Biochem.* **2005**, *40* (12). https://doi.org/10.1016/j.procbio.2005.02.020.
(25) Iwamoto, H. Part III Economic Applications of Microalgae. In *Handbook of Microalgal Culture: Applied Phycology and Biotechnology*; Richmond, A., Ed.; 2004; pp 255–353.
(26) Solovchenko, A.; Khozin-Goldberg, I. High-CO2 Tolerance in Microalgae: Possible Mechanisms and Implications for Biotechnology and Bioremediation. *Biotechnology Letters*. **2013**. https://doi.org/10.1007/s10529-013-1274-7.
(27) *Omega 3 PUFA Market - Forecast (2020 - 2025)*; **2020**.
(28) Inderwildi, O. R.; King, D. A. Quo Vadis Biofuels? *Energy Environ. Sci.* **2009**, *2* (4). https://doi.org/10.1039/b822951c.
(29) Ratha, S. K.; Prasanna, R. Bioprospecting Microalgae as Potential Sources of "Green Energy"-Challenges and Perspectives (Review). *Applied Biochemistry and Microbiology*. **2012**. https://doi.org/10.1134/S000368381202010X.
(30) Lü, J.; Sheahan, C.; Fu, P. Metabolic Engineering of Algae for Fourth Generation Biofuels Production. *Energy and Environmental Science*. **2011**. https://doi.org/10.1039/c0ee00593b.
(31) Saad, M. G.; Dosoky, N. S.; Zoromba, M. S.; Shafik, H. M. Algal Biofuels: Current Status and Key Challenges. *Energies* **2019**, *12* (10). https://doi.org/10.3390/en12101920.
(32) Ioannou, E.; Roussis, V. Natural Products from Seaweeds BT - Plant-Derived Natural Products: Synthesis, Function, and Application; Osbourn, A. E., Lanzotti, V., Eds.; Springer US: New York, NY, **2009**; pp 51–81. https://doi.org/10.1007/978-0-387-85498-4_2.
(33) Kumar, V.; Sinha, A. K.; Makkar, H. P. S.; de Boeck, G.; Becker, K. Dietary Roles of Non-Starch Polysachharides in Human Nutrition: A Review. *Critical Reviews in Food Science and Nutrition*. **2012**. https://doi.org/10.1080/10408398.2010.512671.
(34) Varfolomeev, S. D.; Wasserman, L. A. Microalgae as Source of Biofuel, Food, Fodder,

and Medicines. *Applied Biochemistry and Microbiology*. **2011**. https://doi.org/10.1134/S0003683811090079.

(35) Gupta, V.; Ratha, S. K.; Sood, A.; Chaudhary, V.; Prasanna, R. New Insights into the Biodiversity and Applications of Cyanobacteria (Blue-Green Algae)-Prospects and Challenges. *Algal Research*. **2013**. https://doi.org/10.1016/j.algal.2013.01.006.

(36) Priyadarshani, I.; Rath, B. Commercial and Industrial Applications of Micro Algae – A Review. **2012**, *3* (4), 89–100.

(37) Malik, F. R.; Ahmed, S.; Yazdana, M. R. Utilization of Lignocellulosic Waste for the Preparation of Nitrogenous Biofertilizer. *Pakistan J. Biol. Sci.* **2001**, *4* (10). https://doi.org/10.3923/pjbs.2001.1217.1220.

(38) Thajuddin, N.; Subramanian, G. Cyanobacterial Biodiversity and Potential Applications in Biotechnology. *Current Science*. **2005**.

(39) Dadhich, K. S.; Varma, A. K.; Venkataraman, G. S. The Effect of Calothrix Inoculation on Vegetable Crops. *Plant Soil* **1969**, *31* (2). https://doi.org/10.1007/BF01373582.

(40) Kaushik, B. D.; Venkataraman, G. S. Effect of Algal Inoculation on the Yield and Vitamin C Content of Two Varieties of Tomato. *Plant Soil* **1979**, *52* (1). https://doi.org/10.1007/BF02197740.

(41) Song, T.; Mårtensson, L.; Eriksson, T.; Zheng, W.; Rasmussen, U. Biodiversity and Seasonal Variation of the Cyanobacterial Assemblage in a Rice Paddy Field in Fujian, China. *FEMS Microbiol. Ecol.* **2005**, *54* (1). https://doi.org/10.1016/j.femsec.2005.03.008.

(42) Vaishampayan, A.; Sinha, R. P.; Häder, D. P.; Dey, T.; Gupta, A. K.; Bhan, U.; Rao, A. L. Cyanobacterial Biofertilizers in Rice Agriculture. *Botanical Review*. **2001**. https://doi.org/10.1007/BF02857893.

(43) Adams, D. G.; Bergman, B.; Nierzwicki-Bauer, S. A.; Duggan, P. S.; Rai, A. N.; Schüßler, A. Cyanobacterial-Plant Symbioses. In *The Prokaryotes: Prokaryotic Biology and Symbiotic Associations*; **2013**. https://doi.org/10.1007/978-3-642-30194-0_17.

(44) Del Campo, J. A.; Moreno, J.; Rodríguez, H.; Angeles Vargas, M.; Rivas, J.; Guerrero, M. G. Carotenoid Content of Chlorophycean Microalgae: Factors Determining Lutein Accumulation in *Muriellopsis Sp. (Chlorophyta)*. *J. Biotechnol.* **2000**, *76* (1). https://doi.org/10.1016/S0168-1656(99)00178-9.

(45) Larsson, S. C.; Bergkvist, L.; Näslund, I.; Rutegård, J.; Wolk, A. Vitamin A, Retinol, and Carotenoids and the Risk of Gastric Cancer: A Prospective Cohort Study. *Am. J. Clin. Nutr.* **2007**, *85* (2), 497–503. https://doi.org/10.1093/ajcn/85.2.497.

(46) Parmar, A.; Singh, N. K.; Pandey, A.; Gnansounou, E.; Madamwar, D. Cyanobacteria and Microalgae: A Positive Prospect for Biofuels. *Bioresource Technology*. **2011**. https://doi.org/10.1016/j.biortech.2011.08.030.

(47) Román, R. B.; Alvárez-Pez, J. M.; Fernández, F. G. A.; Grima, E. M. Recovery of Pure B-Phycoerythrin from the Microalga *Porphyridium Cruentum*. *J. Biotechnol.* **2002**, *93* (1). https://doi.org/10.1016/S0168-1656(01)00385-6.

(48) Pandey, V. D.; Pandey, A.; Sharma, V. Review Article Biotechnological Applications of Cyanobacterial Phycobiliproteins. *Int. J. Curr. Microbiol. Appl. Sci.* **2013**, *2* (9).

(49) Hirata, T.; Tanaka, M.; Ooike, M.; Tsunomura, T.; Sakaguchi, M. Antioxidant Activities of Phycocyanobilin Prepared from Spirulina Platensis. In *Journal of Applied Phycology*; **2000**; Vol. 12. https://doi.org/10.1023/a:1008175217194.

(50) Stolz, P.; Obermayer, B. Manufacturing Microalgae for Skin Care. *Cosmet. Toilet.* **2005**,

120 (3).

(51) Tang, G.; Suter, P. M. Vitamin A, Nutrition, and Health Values of Algae: *Spirulina, Chlorella, and Dunaliella*. *J. Pharm. Nutr. Sci.* **2011**, *1* (2). https://doi.org/10.6000/1927-5951.2011.01.02.04.

(52) Nakamura, K.; Gowans, C. S. Nicotinic Acid-Excreting Mutants in *Chlamydomonas* [44]. *Nature*. 1964. https://doi.org/10.1038/202826a0.

(53) Cragg, G. M.; Newman, D. J.; Snader, K. M. Natural Products in Drug Discovery and Development. *Journal of Natural Products*. **1997**. https://doi.org/10.1021/np9604893.

(54) Awad, N. E. Bioactive Brominated Diterpenes from the Marine Red Alga Jania Rubens (L.) Lamx. *Phyther. Res.* **2004**, *18* (4). https://doi.org/10.1002/ptr.1273.

(55) Tan, L. T. Filamentous Tropical Marine Cyanobacteria: A Rich Source of Natural Products for Anticancer Drug Discovery. *Journal of Applied Phycology*. **2010**. https://doi.org/10.1007/s10811-010-9506-x.

(56) Athukorala, Y.; Lee, K. W.; Kim, S. K.; Jeon, Y. J. Anticoagulant Activity of Marine Green and Brown Algae Collected from Jeju Island in Korea. *Bioresour. Technol.* **2007**, *98* (9). https://doi.org/10.1016/j.biortech.2006.07.034.

(57) Kim, S. K.; Wijesekara, I. Anticoagulant Effect of Marine Algae. In *Advances in Food and Nutrition Research*; **2011**; Vol. 64. https://doi.org/10.1016/B978-0-12-387669-0.00018-1.

(58) Giiven, K. C.; Ozsoy, Y.; Ulutin, O. N. Anticoagulant, Fibrinolytic and Antiaggregant Activity of Carrageenans and Alginic Acid. *Bot. Mar.* **1991**, *34* (5). https://doi.org/10.1515/botm.1991.34.5.429.

(59) Han, F.; Yao, W.; Yang, X.; Liu, X.; Gao, X. Experimental Study on Anticoagulant and Antiplatelet Aggregation Activity of a Chemically Sulfated Marine Polysaccharide YCP. *Int. J. Biol. Macromol.* **2005**, *36* (4). https://doi.org/10.1016/j.ijbiomac.2005.06.003.

(60) Matsukawa, R.; Dubinsky, Z.; Masaki, K.; Takeuchi, T.; Karube, I. Enzymatic Screening of Microalgae as a Potential Source of Natural Antioxidants. *Appl. Biochem. Biotechnol. - Part A Enzym. Eng. Biotechnol.* **1997**, *66* (3). https://doi.org/10.1007/BF02785590.

(61) Tabarzad, M.; Atabaki, V.; Hosseinabadi, T. Anti-Inflammatory Activity of Bioactive Compounds from Microalgae and Cyanobacteria by Focusing on the Mechanisms of Action. *Mol. Biol. Rep.* **2020**, *47* (8), 6193–6205. https://doi.org/10.1007/s11033-020-05562-9.

(62) Barra, L.; Chandrasekaran, R.; Corato, F.; Brunet, C. The Challenge of Ecophysiological Biodiversity for Biotechnological Applications of Marine Microalgae. *Marine Drugs*. **2014**, pp 1641–1675. https://doi.org/10.3390/md12031641.

(63) de la Noue, J.; de Pauw, N. The Potential of Microalgal Biotechnology: A Review of Production and Uses of Microalgae. *Biotechnology Advances*. **1988**. https://doi.org/10.1016/0734-9750(88)91921-0.

(64) Belay, A.; Kato, T.; Ota, Y. *Spirulina (Arthrospira)*: Potential Application as an Animal Feed Supplement. *J. Appl. Phycol.* **1996**, *8* (4–5). https://doi.org/10.1007/BF02178573.

(65) Y. Shen; W. Yuan; Z. J. Pei; Q. Wu; E. Mao. Microalgae Mass Production Methods. *Trans. ASABE* **2009**, *52* (4), 1275–1287. https://doi.org/10.13031/2013.27771.

(66) Terry, K. L.; Raymond, L. P. System Design for the Autotrophic Production of Microalgae. *Enzyme Microb. Technol.* **1985**, *7* (10), 474–487. https://doi.org/10.1016/0141-0229(85)90148-6.

(67) Chisti, Y. Biodiesel from Microalgae. *Biotechnol. Adv.* **2007**, *25* (3), 294–306.

https://doi.org/10.1016/j.biotechadv.2007.02.001.

(68) Tredici, M. R.; Materassi, R. From Open Ponds to Vertical Alveolar Panels: The Italian Experience in the Development of Reactors for the Mass Cultivation of Phototrophic Microorganisms. *J. Appl. Phycol.* **1992**, *4* (3), 221–231. https://doi.org/10.1007/BF02161208.

(69) Chen, F. High Cell Density Culture of Microalgae in Heterotrophic Growth. *Trends Biotechnol.* **1996**, *14* (11), 421–426. https://doi.org/10.1016/0167-7799(96)10060-3.

(70) Chen, F.; Johns, M. R. Relationship between Substrate Inhibition and Maintenance Energy of *Chlamydomonas Reinhardtii* in Heterotrophic Culture. *J. Appl. Phycol.* **1996**, *8* (1), 15–19. https://doi.org/10.1007/BF02186216.

(71) Chaumont, D. Biotechnology of Algal Biomass Production: A Review of Systems for Outdoor Mass Culture. *J. Appl. Phycol.* **1993**, *5* (6), 593–604. https://doi.org/10.1007/BF02184638.

(72) Richmond, A. Open Systems for the Mass Production of Photoautotrophic Microalgae Outdoors: Physiological Principles. *J. Appl. Phycol.* **1992**, *4* (3), 281–286. https://doi.org/10.1007/BF02161213.

(73) Molina Grima, E.; Belarbi, E. H.; Acién Fernández, F. G.; Robles Medina, A.; Chisti, Y. Recovery of Microalgal Biomass and Metabolites: Process Options and Economics. *Biotechnol. Adv.* **2003**, *20* (7–8), 491–515. https://doi.org/10.1016/S0734-9750(02)00050-2.

(74) Satpati, G. G.; Pal, R. Microalgae - Biomass to Biodiesel : A Review. *J. Algal Biomass Util.* **2018**, *9* (4), 11–37.

(75) Posten, C. Design Principles of Photo-Bioreactors for Cultivation of Microalgae. *Eng. Life Sci.* **2009**, *9* (3), 165–177. https://doi.org/10.1002/elsc.200900003.

(76) Thomas, W. H.; Gibson, C. H. Effects of Small-Scale Turbulence on Microalgae. *J. Appl. Phycol.* **1990**, *2* (1), 71–77. https://doi.org/10.1007/BF02179771.

(77) Enzing, C.; Ploeg, M.; Barbosa, M.; Sijtsma, L. *Microalgae-Based Products for the Food and Feed Sector: An Outlook for Europe*; **2014**. https://doi.org/10.2791/3339.

(78) Apt, K. E.; Behrens, P. W. Commercial Developments in Microalgal Biotechnology. *J. Phycol.* **1999**, *35* (2), 215–226. https://doi.org/10.1046/j.1529-8817.1999.3520215.x.

(79) Schmidt, R. A.; Wiebe, M. G.; Eriksen, N. T. Heterotrophic High Cell-Density Fed-Batch Cultures of the Phycocyanin-Producing Red Alga *Galdieria Sulphuraria*. *Biotechnol. Bioeng.* **2005**, *90* (1), 77–84. https://doi.org/10.1002/bit.20417.

(80) Zaslavskaia, L. A.; Lippmeier, J. C.; Shih, C.; Ehrhardt, D.; Grossman, A. R.; Apt, K. E. Trophic Conversion of an Obligate Photoautotrophic Organism through Metabolic Engineering. *Science (80-.).* **2001**, *292* (5524), 2073–2075. https://doi.org/10.1126/science.160015.

(81) Chen, G. Q.; Chen, F. Growing Phototrophic Cells without Light. *Biotechnol. Lett.* **2006**, *28* (9), 607–616. https://doi.org/10.1007/s10529-006-0025-4.

(82) Lewin J. C., R. A. Autotrophy and Heterotrophy in Marine Littoral Diatoms. *Can. J. Microbiol.* **1960**, *6* (2), 127–134.

(83) Zhang, C. C.; Jeanjean, R.; Joset, F. Obligate Phototrophy in Cyanobacteria: More than a Lack of Sugar Transport. *FEMS Microbiol. Lett.* **1998**, *161* (2), 285–292. https://doi.org/10.1016/S0378-1097(98)00084-6.

(84) Morales-Sánchez, D.; Tinoco-Valencia, R.; Kyndt, J.; Martinez, A. Heterotrophic Growth of *Neochloris Oleoabundans* Using Glucose as a Carbon Source. *Biotechnol. Biofuels*

2013, *6* (1), 100. https://doi.org/10.1186/1754-6834-6-100.

(85) Barclay, W.; Apt, K.; Dong, X. D. Commercial Production of Microalgae via Fermentation. *Handb. Microalgal Cult. Appl. Phycol. Biotechnol. Second Ed.* **2013**, 134–145. https://doi.org/10.1002/9781118567166.ch9.

(86) Lee, Y. K. Commercial Production of Microalgae in the Asia-Pacific Rim. *J. Appl. Phycol.* **1997**, *9* (5), 403–411. https://doi.org/10.1023/A:1007900423275.

(87) Franklin, S., Somanchi, A., Wee, J., Rudenko, G., Moseley, J.L. & Rakitsky, W. Food Compositions Comprising Tailored Oils. U.S. Patent Application 2011/0293785, **2011**.

(88) Piechocki, J., Zdanis, D., Morris, L.M., Ratitsky, W & Klamczynska, B. Lipid-Rich Microalgal Flour Food Compositions. U.S. Patent Application 2011/0256282, 2**011**.

(89) Wynn, J., Behrens, P., Sundararajan, A., Hansen, J. & Apt, K. Production of Single Cell Oils by Dinoflagellates. In *Single Cell Oils: Microbial and Algal Oils*; Z. Cohen & C. Ratledge, Ed.; Press, Champaign, IL., **2010**; pp 115–129.

(90) Kyle, D.J., Reeb, S.E. & Sicotte, V. J. Docosahexaenoic Acid, Methods for Its Production, and Compounds Containing the Same. European Patent 0515460, 1998.

(91) D'Ippolito, G.; Sardo, A.; Paris, D.; Vella, F. M.; Adelfi, M. G.; Botte, P.; Gallo, C.; Fontana, A. Potential of Lipid Metabolism in Marine Diatoms for Biofuel Production. *Biotechnol. Biofuels* **2015**, *8* (1), 1–10. https://doi.org/10.1186/s13068-015-0212-4.

(92) Barclay, W. R. Process for Growing *Thraustochytrium* and *Schizochytrium* Using Non-Chloride Salts to Produce a Microfloral Biomass Having Omega-3 Highly Unsaturated Fatty Acids. U.S. Patent 5,340,742, **1994**.

(93) Barclay, W. & Van Elswyk, M. Natural Enrichment of Foods with DHA Omega-3 from Golden Marine Algae. In *Functional Foods 2000 Conference Proceedings*; F. Angus & C. Miller, Ed.; Leatherhead Publishing, Surrey, UK., **2000**; pp 60–67.

(94) Stagnitti, G.; Barclay, B.; Elswyk, M. Fermented Fortification - OmegaTech's Patented Fermentation Technology Uses Micro-Algae to Produce a Vegetarian Source of DHA. *Dairy Ind. Int.* **2001**, *66*, 26–27.

(95) Apt, K.E., Allnutt, F.C.T., Kyle, D.J. & Lippmeier, J. C. Trophic Conversion of Obligate Phototrophic Algae through Metabolic Engineering. U.S. Patent 7,939,710, **2011**.

(96) U.S. Department of agriculture. USDA ERS https://www.ers.usda.gov/.

(97) Lundquist, T. J.; Woertz, I. C.; Quinn, N. W. T.; Benemann, J. R. A Realistic Technology and Engineering Assessment of Algae Biofue. **2010**.

(98) Yang, R.; Wei, D.; Xie, J. Diatoms as Cell Factories for High-Value Products: Chrysolaminarin, Eicosapentaenoic Acid, and Fucoxanthin. *Crit. Rev. Biotechnol.* **2020**, *40* (7), 993–1009. https://doi.org/10.1080/07388551.2020.1805402.

(99) Tesson, B.; Hildebrand, M. Characterization and Localization of Insoluble Organic Matrices Associated with Diatom Cell Walls: Insight into Their Roles during Cell Wall Formation. *PLoS One* **2013**, *8* (4). https://doi.org/10.1371/journal.pone.0061675.

(100) C. Van Den Hoek, D. G. M. and H. M. J. *Algae. An Introduction to Phycology.*; **1997**; Vol. 32. https://doi.org/10.1017/s096702629621100x.

(101) Falciatore, A.; Bowler, C. Revealing the Molecular Secrets of Marine Diatoms. *Annu. Rev. Plant Biol.* **2002**, *53* (29), 109–130. https://doi.org/10.1146/annurev.arplant.53.091701.153921.

(102) Bhattacharya, D.; Medlin, L. The Phylogeny of Plastids: A Review Based on Comparisons of Small-Subunit Ribosomal Rna Coding Regions. *J. Phycol.* **1995**, *31* (4), 489–498. https://doi.org/10.1111/j.1529-8817.1995.tb02542.x.

(103) Armbrust, E. V.; Berges, J. A.; Bowler, C.; Green, B. R.; Martinez, D.; Putnam, N. H.; Zhou, S.; Allen, A. E.; Apt, K. E.; Bechner, M.; Brzezinski, M. A.; Chaal, B. K.; Chiovitti, A.; Davis, A. K.; Demarest, M. S.; Detter, J. C.; Glavina, T.; Goodstein, D.; Hadi, M. Z.; Hellsten, U.; Hildebrand, M.; Jenkins, B. D.; Jurka, J.; Kapitonov, V. V.; Kröger, N.; Lau, W. W. Y.; Lane, T. W.; Larimer, F. W.; Lippmeier, J. C.; Lucas, S.; Medina, M.; Montsant, A.; Obornik, M.; Parker, M. S.; Palenik, B.; Pazour, G. J.; Richardson, P. M.; Rynearson, T. A.; Saito, M. A.; Schwartz, D. C.; Thamatrakoln, K.; Valentin, K.; Vardi, A.; Wilkerson, F. P.; Rokhsar, D. S. The Genome of the Diatom *Thalassiosira Pseudonana*: Ecology, Evolution, and Metabolism. *Science.* **2004**, *306* (5693), 79–86. https://doi.org/10.1126/science.1101156.

(104) Brownlee, C. Diatom Signalling: Deadly Messages. *Curr. Biol.* **2008**, *18* (12), 518–519. https://doi.org/10.1016/j.cub.**2008**.05.003.

(105) Pickett-Heaps J.D., S. A.-M. E. L. A. *The Cell Biology of Diatom Valve Formation*; 1990.

(106) Armbrust, EV, Chisholm, S. Role of Light and the Cell-Cycle on the Induction of Spermatogenesis in a Centric Diatom. *J. Phycol.* **1990**, *26*, 470–478.

(107) Bowler, C.; De Martino, A.; Falciatore, A. Diatom Cell Division in an Environmental Context. *Curr. Opin. Plant Biol.* **2010**, *13* (6), 623–630. https://doi.org/10.1016/j.pbi.2010.09.014.

(108) Bowler, C.; Vardi, A.; Allen, A. E. Oceanographic and Biogeochemical Insights from Diatom Genomes. *Ann. Rev. Mar. Sci.* **2010**, *2* (1), 333–365. https://doi.org/10.1146/annurev-marine-120308-081051.

(109) Round FE, Crawford RM, M. D. *The Diatoms: Biology and Morphology of the Genera*; Cambridge University Press, **1990**.

(110) Falkowski, P. G.; Katz, M. E.; Milligan, A. J.; Fennel, K.; Cramer, B. S.; Aubry, M. P.; Berner, R. A.; Novacek, M. J.; Zapol, W. M. Evolution: The Rise of Oxygen over the Past 205 Million Years and the Evolution of Large Placental Mammals. *Science.* **2005**, *309* (5744), 2202–2204. https://doi.org/10.1126/science.1116047.

(111) Falkowski, P. G.; Fenchel, T.; Delong, E. F. The Microbial Engines That Drive Earth's Biogeochemical Cycles. *Science.* **2008**, *320* (5879), 1034–1039. https://doi.org/10.1126/science.1153213.

(112) Lewin, J. C. Heterotrophy in Diatoms. *J. Gen. Microbiol.* **1953**, *9*, 305–313. https://doi.org/10.1099/00221287-9-2-305.

(113) Hellebust, J. A. Kinetics of Glucose Transport and Growth of *Cyclotella Cryptica*. *Journal of Phycology*. **1971**, pp 1–4. https://doi.org/10.1111/j.1529-8817.1971.tb01469.x.

(114) Bumbak, F.; Cook, S.; Zachleder, V.; Hauser, S.; Kovar, K. Best Practices in Heterotrophic High-Cell-Density Microalgal Processes: Achievements, Potential and Possible Limitations. *Appl. Microbiol. Biotechnol.* **2011**, *91* (1), 31–46. https://doi.org/10.1007/s00253-011-3311-6.

(115) Reimann, B.E.F., Lewin, J.M.C. & Guillard, R. R. L. *Cyclotella Cryptica*, a New Brackish-Water Diatom Species. *Phycologia* **1963**, *3* (2), 75–84.

(116) Traller, J. C.; Cokus, S. J.; Lopez, D. A.; Gaidarenko, O.; Smith, S. R.; McCrow, J. P.; Gallaher, S. D.; Podell, S.; Thompson, M.; Cook, O.; Morselli, M.; Jaroszewicz, A.; Allen, E. E.; Allen, A. E.; Merchant, S. S.; Pellegrini, M.; Hildebrand, M. Genome and Methylome of the Oleaginous Diatom *Cyclotella Cryptica* Reveal Genetic Flexibility toward a High Lipid Phenotype. *Biotechnol. Biofuels* **2016**, *9* (1), 1–20. https://doi.org/10.1186/s13068-016-0670-3.

(117) Slocombe, S. P.; Zhang, Q.; Ross, M.; Anderson, A.; Thomas, N. J.; Lapresa, Á.; Rad-Menéndez, C.; Campbell, C. N.; Black, K. D.; Stanley, M. S.; Day, J. G. Unlocking Nature's Treasure-Chest: Screening for Oleaginous Algae. *Sci. Rep.* **2015**, *5*, 1–17. https://doi.org/10.1038/srep09844.

(118) Roessler, P. G. Effects of Silicon Deficiency on Lipid Composition and Metabolism in the Diatom Cyclotella Cryptica. *J. Phycol.* **1988**, *24* (3), 394–400. https://doi.org/10.1111/j.1529-8817.1988.tb00189.x.

(119) Huesemann, M. H.; Hausmann, T. S.; Bartha, R.; Aksoy, M.; Weissman, J. C.; Benemann, J. R. Biomass Productivities in Wild Type and Pigment Mutant of *Cyclotella Sp.* (Diatom). *Appl. Biochem. Biotechnol.* **2009**, *157* (3), 507–526. https://doi.org/10.1007/s12010-008-8298-9.

(120) Laws, E. A.; Taguchi, S.; Hirata, J.; Pang, L. Optimization of Microalgal Production in a Shallow Outdoor Flume. *Biotechnol. Bioeng.* **1988**, *32* (2), 140–147. https://doi.org/10.1002/bit.260320204.

(121) White, A. W. Growth of the Two Facultatively Heterotrophic Marine Centric Diatoms. *J.Phycol.* **1974**, *10*, 292–300.

(122) Pahl, S. L.; Lewis, D. M.; King, K. D.; Chen, F. Heterotrophic Growth and Nutritional Aspects of the Diatom *Cyclotella Cryptica (Bacillariophyceae):* Effect of Nitrogen Source and Concentration. *J. Appl. Phycol.* **2012**, *24* (2), 301–307. https://doi.org/10.1007/s10811-011-9680-5.

(123) d'Ippolito, G.; Cutignano, A.; Briante, R.; Febbraio, F.; Cimino, G.; Fontana, A. New C16 Fatty-Acid-Based Oxylipin Pathway in the Marine Diatom *Thalassiosira Rotula*. *Org. Biomol. Chem.* **2005**, *3* (22), 4065–4070. https://doi.org/10.1039/B510640K.

(124) Fontana, A.; D'Ippolito, G.; Cutignano, A.; Romano, G.; Lamari, N.; Gallucci, A. M.; Cimino, G.; Miralto, A.; Lanora, A. LOX-Induced Lipid Peroxidation Mechanism Responsible for the Detrimental Effect of Marine Diatoms on Zooplankton Grazers. *ChemBioChem* **2007**, *8* (15), 1810–1818. https://doi.org/10.1002/cbic.200700269.

(125) Adelfi, M. G.; Vitale, R. M.; d'Ippolito, G.; Nuzzo, G.; Gallo, C.; Amodeo, P.; Manzo, E.; Pagano, D.; Landi, S.; Picariello, G.; Ferrante, M. I.; Fontana, A. Patatin-like Lipolytic Acyl Hydrolases and Galactolipid Metabolism in Marine Diatoms of the Genus *Pseudo-Nitzschia*. *Biochim. Biophys. Acta - Mol. Cell Biol. Lipids* **2019**, *1864* (2), 181–190. https://doi.org/10.1016/j.bbalip.**2018**.11.008.

(126) Gallo, C.; Nuzzo, G.; d'Ippolito, G.; Manzo, E.; Sardo, A.; Fontana, A. *Sterol Sulfates and Sulfotransferases in Marine Diatoms*, 1st ed.; Elsevier Inc., **2018**; Vol. 605. https://doi.org/10.1016/bs.mie.**2018**.03.003.

2. Assessment of heterotrophic growth conditions

2.1 Introduction

In order to pursue the challenging goals of this thesis, the first pivotal steps were the identification of a suitable diatom specie and the assessment of growth conditions.

As widely reported in literature, few species of microalgae are able to grow under heterotrophic conditions [1]. Therefore, the identification of candidate species and strains with a high potential to grow in heterotrophy, as well as the improvement of culture conditions, represent a major challenge for biotechnological research [2,3].

The marine diatom *C. cryptica* was chosen as a model specie to work up my PhD project, due to its adaptability to different growth conditions and valuable products obtainable for pharmaceutical, aquaculture and agricultural applications [4].

Moreover, only two papers published in 2010 by Pahl et al. [5,6] represented the first efforts to study the basic features of *C. cryptica* when grown under heterotrophic conditions [5,6].

Thus, the possibility to explore a promising yet still infant research field guided our choice on the specie and the development of optimal growth condition.

2.2 Results and discussion

2.2.1 Establishment and maintenance of axenic culture

During the first experiments conducted to verify the possibility of growing *C. cryptica* in heterotrophy, we dealt with the difficulty of maintaining axenic cultures. As a matter of fact, the first limiting issue to overcome was related to high grade of bacterial contaminations generally occurring during heterotrophic cultures.

It is widely reported in literature that a problem to be faced in heterotrophic cultures is the prevention of contamination due to the presence of organic source in the medium ; any minor contamination introduced with the inoculum could limit the growth of the desired microalgal species [7].

Thus, I decided to move forward through several steps. The first step consisted of ensuring a monocellular culture, so I isolated a single cell from the stub maintained in the laboratory's Collection of Microalgae, by the use of micro-pipettes. Micro-pipettes were prepared from simple Pasteur pipettes, as shown in the **Figure 2.1**. The Pasteur pipette is held on the flame of a Bunsen burner, firmly supported on the left by a hand and on the right by forceps. As soon as the pipette became soft it is required to rotate it to facilitate a homogeneous distribution of heat. When the glass is soft, the pipette is quickly removed from the flame with a gentle pull to produce a thin tube. Finally, the forceps are used to break the thinned extremity, forming a micropipette. Ideally, the diameter of the micropipette's tip should be larger than the cell diameter, thus reducing the probability of cell cut during the isolation. On the other hand, the diameter should be neither too large thus allowing the flowing of multiple cells.

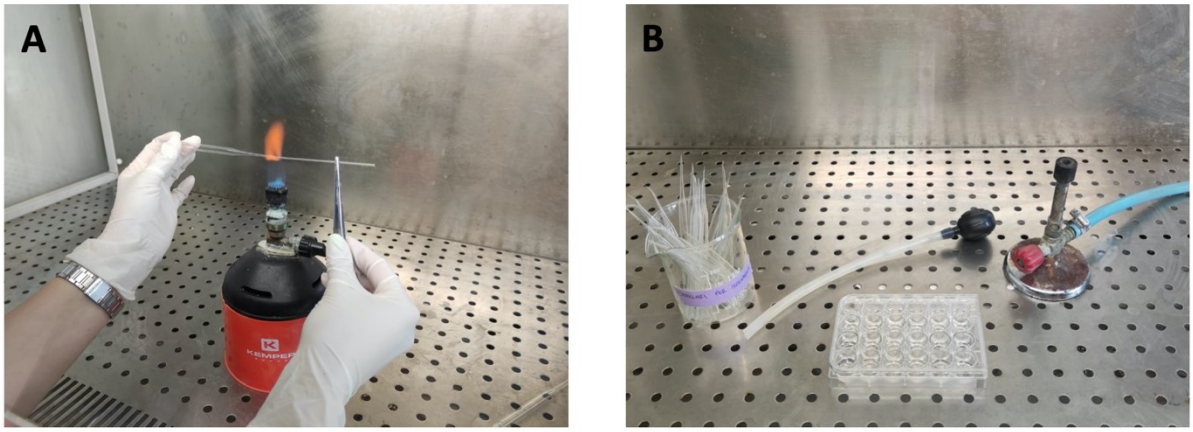

Figure 2.1 A) Preparation of micropipette from Pasteur pipette. B) Equipment required under biological hood to carry out cell isolation.

About 1 ml of exponential culture is placed in a petri dish with 15 ml of F/2 medium supplemented with 35 µg/ml of Penicillin G and 70 µg/ml of Streptomycin. Under the Microscope (Axio VertA1, Carl Zeiss, magnification of 10X) a single cell is collected with the micropipette linked to a pump to draw and transfer it into a well of a multiwell containing F/2 growth medium and antibiotics (Penicillin G and Streptomycin in the same concentration mentioned above). A particular attention is required when picking a single cell: It is recommended to position the micropipette at one end of the target cell in a way that when collected, the cell is not irreversibly damaged [8].

Isolated cells in the multiwell are placed in a cell room at 20°C ± 2°C, with a 14:10-h light:dark photoperiod.

After 3-4 weeks, cell density reached a concentration (value) of about 100.000 cells/ml-150.000 cells/ml. Cells then were transferred in increasingly larger volume: from 20 ml to 100 ml of F/2 medium in a couple of weeks.

Before using isolated cells as inoculum for new cultures, I considered useful the separating methods described by Vu et al [9]. Cells were gently centrifuged at 3750 rpm for 5 minutes. The supernatant was discarded, and cells were resuspended in a fresh medium before used as inoculum. This simple passage allows to move away contaminants, as bacteria, that settle at higher speed and time, due to their lower sedimentation coefficient.

Another approach described by Vu et al. [9], to maintain axenic cultures consists of "killing methods", namely the use of antibiotics. I used Penicillin-G 35 µg/ml and Streptomycin 70 µg/ml only in the initial phase of cell isolation and expansion. Then I successfully obtained axenic cultures without using antibiotics routinely, just adopting strict conditions of sterility.

Antibiotics, in general, are not only toxic to bacterial cells, but also to microalgal cells. They, in fact, can suppress algal cell growth and induce a change in genetic information [10,11].

Another issue associated to the reiterated use of antibiotics is the spread of antibiotic-resistant microbes. This mechanism occurs when microbes are continuously exposed to a non- lethal dose of an antibiotic and generally the spread of antibiotic resistance is faster than the time required to develop a new molecule to counteract it.

Anyway, to ensure the axenicity of culture and the effectiveness of the method described in this first paragraph, I usually tested cells with F/2 medium enriched of Peptone 1g/L.

In detail, before each experiment, I prepared F/2 medium with 1g/L of Peptone, under hood. Enriched media, as a matter of fact, in either liquid or solid form, are designed to favor contaminant growth and reveal their presence.

Then I put 0.5 ml of cells with a concentration of 100.000 cells/ml and 5ml of medium enriched in a sterile falcon, wrapped in aluminum foil and left in the dark over/night, to enable only bacteria growth. Subsequently I observed changes in turbidity, if present, measuring absorbance at 600 nm.

2.2.2 Natural and artificial seawater

The marine diatom *C. cryptica* was grown in heterotrophic conditions in F/2 medium prepared both with natural and artificial seawater, supplemented with 1 g/L of glucose and maintained under dark.

Natural seawater was collected from the Gulf of Naples (40°49'57.72"N 14°14'08.77"E) with a salinity of about 40 g / L, measured using an ATC 106 refractometer, and filtered through Millipore filters with pores of 1 µm diameter.

Artificial seawater was prepared as described in section 2.3.1.2. The aim of this experiment was to test the ability of *C. cryptica* to grow in the dark, comparing growth performances in F/2 medium prepared with a different salinity source.

I tried to design experiments with a special attention to the applicability of the process not only on a laboratory-scale, but also on a larger volume and for plants geographically located in different positions.

Cells were inoculated at a concentration of 10.000 cells/ml and as shown in **Figure 2.2**, after 4 days of adaptation, cells grown in F/2 medium prepared with laboratory salts reached $3.8x0^5$ cells/ml, $2.92x10^5$ cells/ml in F/2 with Tropic ©, $2.0x10^5$ cells/ml in F/2 with natural seawater and $2.0x10^4$ cells/ml in F/2 with Sardinia Sea salts. Thus, comparing the initial lag phase of the growth curves we can observe an advantage in cell density with laboratory salts; this trend is maintained until the 6^{th} day. Then cells in Natural Seawater and Tropic marin © went through a rapid recovery, reaching the same cell concentration of $1.5x10^6$ cells/ml at 14^{th} day.

C. cryptica kept in F/2 medium prepared with lisal salts got lower density, reaching a concentration of 850.000 cells/ml at 14^{th} day.

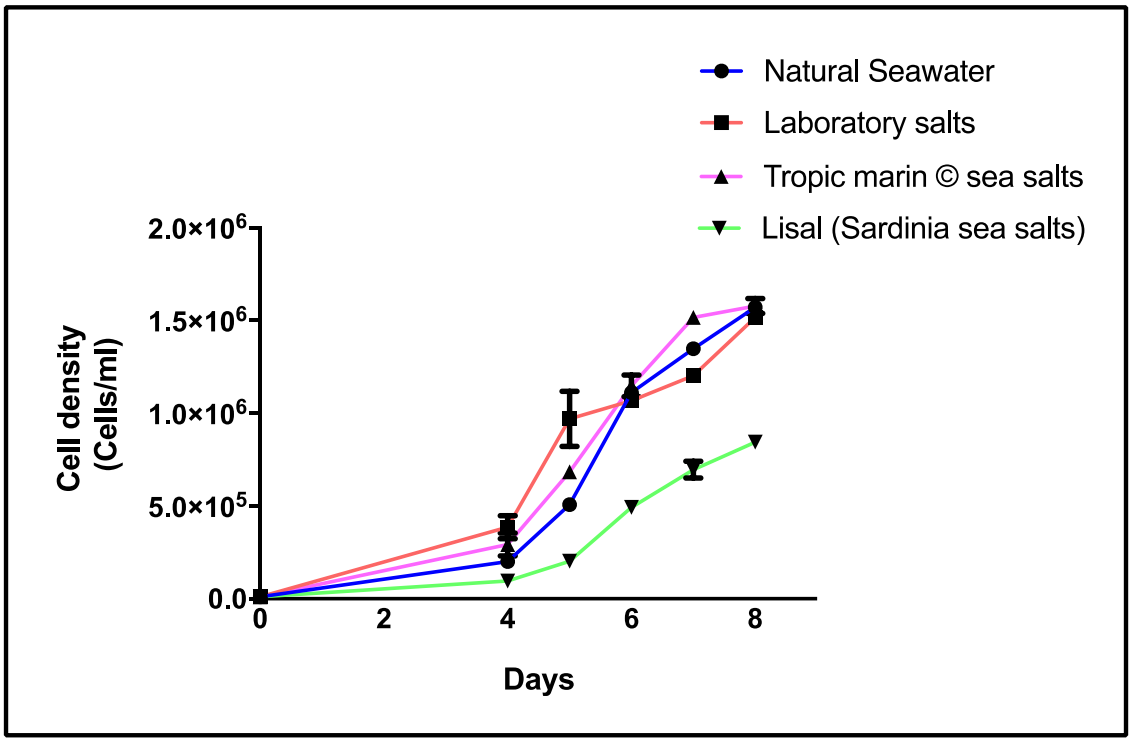

Figure 2.2 Growth curves of *C. cryptica* by using natural or artificial water to prepare F/2 medium.

In the end, laboratory Salts and Tropic marin © sea salts could be an effective alternative to natural seawater for the growth of *C. cryptica,* also in laboratory or plants distant from seaside areas.

2.2.3 Growth on different organic sources

The possibility to make use of food waste suitable for heterotrophic microalgae cultivation could represent a turning point to decrease process costs and help to overcome one of the major economic drawbacks for feasible large scale cultivation and food, feed, and biodiesel production [12].

For this experiment we tested the ability of *C. cryptica* to grow on different organic substrates, in particular: glucose, lactose, sucrose and wheat starch.

Glucose is the preferred carbon and energy source used for the heterotrophic cultivation of microalgae [13]. Lactose is a disaccharide consisting of galactose and glucose and it is found mostly in milk and dairy wastes. Lactose has been reported as a carbon source for *N. oleoabundans* under mixotrophic conditions [14].

Sucrose is a disaccharide formed by glucose and fructose. Heterotrophic cultivation of *Chlorella vulgaris* and *Scenedesmus Bijugus* were performed to test different substrate and among them also sucrose, by using the methodology of miniaturized growth [15].

Wheat starch could be considered a by-product in the manufacture of wheat gluten.

As shown in **Figure 2.3** a considerable growth was detected only with glucose as substrate.

This experiment conducted in triplicates, in flasks with a final volume of 300 ml, indicated that *C. cryptica* does not use lactose, sucrose and wheat starch under strict heterotrophic conditions, that is dark conditions and mineral media.

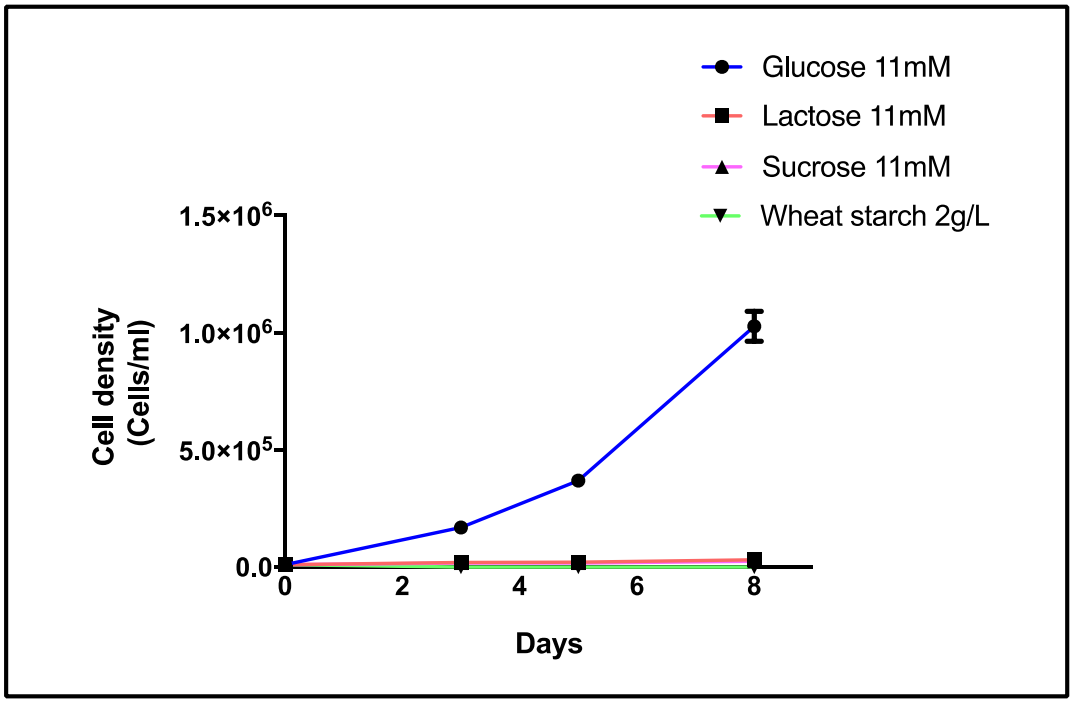

Figure 2.3 Growth curves of *C. cryptica* in F/2 medium supplemented with 11mM Glucose, 11mM Lactose, 11mM Sucrose or 2g/L of wheat starch.

We can assume that *C. cryptica* does not grow on substrates other than glucose, mainly due to: a lack or low activity of certain enzymes, the inability to simultaneously oxidize alternative carbon sources and supply the cell with reducing power for biosynthesis.

In this experiment we tested the rude possibility of use polysaccharides as organic substrate avoiding the passage of hydrolysis, since this pre-treatment phase complicates the culture process and increase the cost. Surely, one of the forthcoming experiments will perform the recovery of nutrients by the enzymatic or fungal hydrolysis of food waste.

2.2.4 Growth on different glucose concentrations

The aim of the following experiment was to find the best glucose concentration to obtain a good amount of biomass without occurring bacteria contamination.

The experiment was conducted in triplicates, in flasks with a volume of 300 ml, inoculating 10.000 cells/ml in F/2 medium enriched with 0.5 g/L, 1g/L, 2 g/L and 4 g/L of glucose, without replacing the organic substrate, and following the growth curves until the late stationary-early senescence phase.

As clearly shown in **Figure 2.4**, cells reached a cell density of $8.3x10^5$ cells/ml at 7^{th} day, under 0.5 g/L of glucose (grey curve), entering in a stationary phase. Cells enter in a stationary phase at day 10^{th} under 1g/L of glucose (red curve), reaching $2.0x10^6$ cells/ml. While cells under 2 g/L of glucose entered in early senescent phase at 14^{th}day with a concentration of $2.7x10^6$cells/ml, under 4 g/L of glucose at 14^{th} day cells started their stationary phase with a concentration of $3.1x10^6$ cells/ml.

The first 3 days from the starting point of the experiment showed an overlapping of the curves, indicating that this early phase is independent from the concentration of the organic substrate supplied. Likely, in this lag phase cells adapted to the new culture conditions, putting in place mechanisms as the expression of glucose transport and new enzymes necessary to sustain their switch versus a heterotrophic metabolism.

Growth rate (μ) and duplication time (T_d) calculated as indicated in the equations I-II, between day 3 and 10 reflect the trend analyzed with cell density.

I. $\mu = (\ln(N_2)-\ln(N_1))/t_2-t_1$

II. $T_d = \ln 2/\mu$

Growth rate μ expressed the number of cell division in a day, and in the first equation N_2 indicates the cell concentration at day 10 (t_2), while N_1 the cell concentration at day 3 (t_1). Duplication time (t_d), calculated as the base-2 logarithm of growth rate, expressed the time required to a cell to duplicate itself.

Growth rate for cells under 0.5 g/L of glucose is 0.29, while 0.37 for cells under 2 g/L and 4 g/L of glucose, respectively; 0.38 for cells under 4 g/L of glucose. A surplus of glucose in the range between 2 and 4 g/L of glucose does not sustain an increment in cell division.

As the cell density, also the growth rate reflects that in the time interval between day 3 and 10 cells are their maximum capacity of intake glucose and cell duplication, under an adequate carbon and energy support. Duplication time, obviously, is the same for cells under 2 and 4 g/L of glucose, which is 1.9, while is higher for cells under 0.5 g/L, accordingly with cell density and growth rate. At this limiting concentration cells required more time to duplicate themselves, contrary to what happens under a regime of 4 g/L of glucose with a lower duplication time of 1.8.

In the figure 2.4 are showed also the flasks with cultures at the end of growth time; which is the 14^{th} days for cells under 0.5 and 1 g/L of glucose and 16^{th} days for cells under 2 and 4 g/L. Cells maintained their characteristic brown color, due to the presence of pigments, in particular fucoxanthin [16]. Colour gradation reflected cell density.

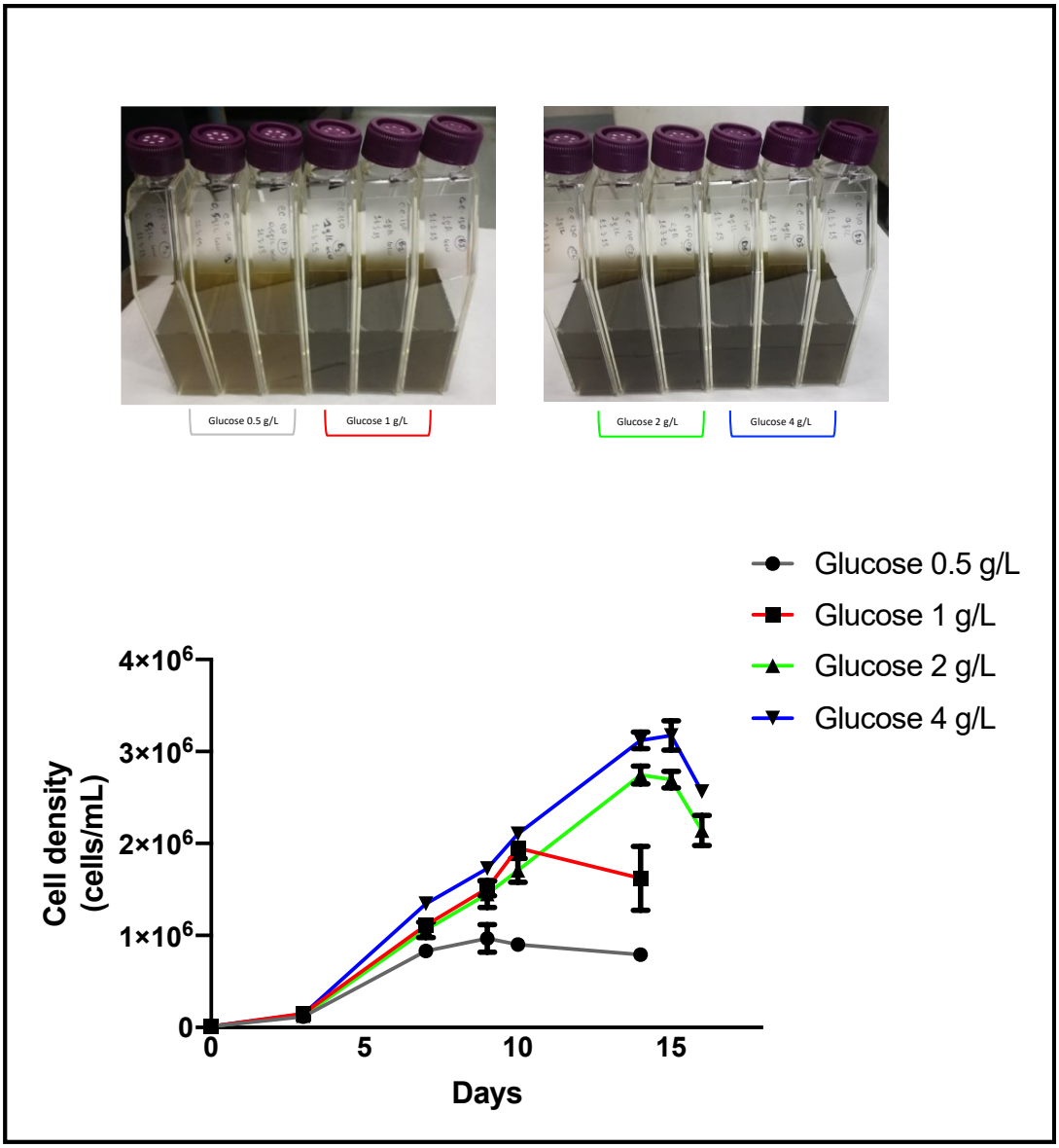

Figure 2.4 *C. cryptica* cultures in 300ml flasks and the relative growth curves, in F/2 medium enriched with 0.5g/L, 1g/L, 2g/L and 4g/L of glucose.

We set up a method to estimate glucose consumption, using ERETIC ^{1}H-NMR method.

Residual glucose in the medium (not internalized by cells) was estimated after culture's centrifugation at 3750 rpm (2100 g) for 10 min; then 50 µl of D_2O (deuterium oxide) and 650 µl of supernatant were mixed and analysed on Bruker DRX 600 spectrometer equipped with an inverse TCI CryoProbe.

The **Figure 2.5** showed a typical NMR spectrum of a standard glucose solution 1mg/ml. I defined the concentration of residual glucose, setting the micromoles present in the standard

solution and, using this file as reference, I calculated the µmol/ml of glucose in the sample analyzed by HERETIC method.

The diagnostic peak, centered at 3.24 ppm, refers to the signal of protons of ß-anomer of carbon in position 2 of glucose molecule.

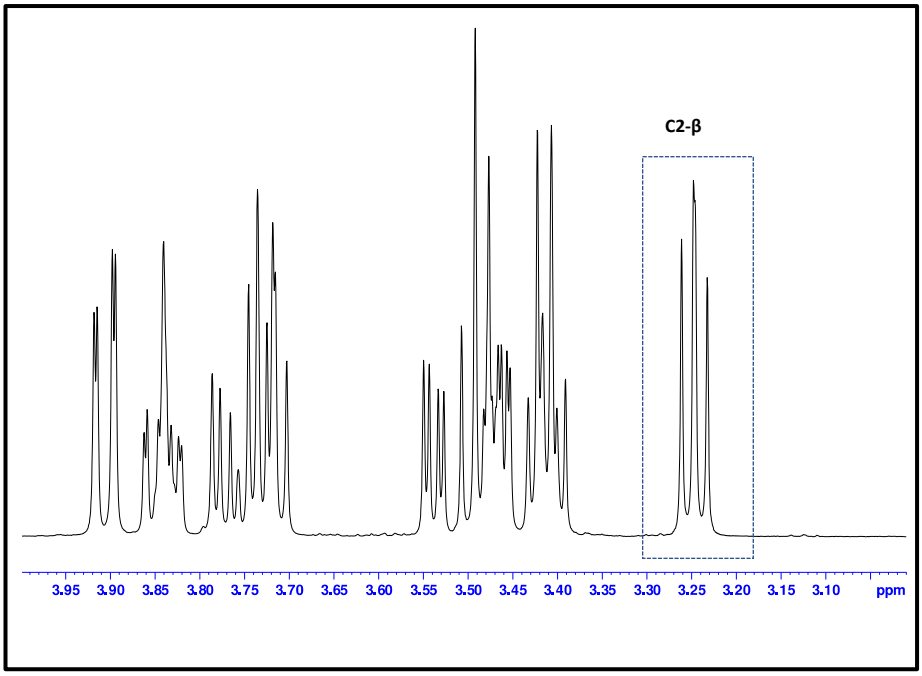

Figure 2.5 NMR spectrum of glucose standard solution 1mg/ml.

When α-d-glucose dissolves in water, the optical rotation of the solution slowly changes from the initial value of + 112.2° to an equilibrium value of + 54°. If α-d-glucose dissolves in water, the rotation of the solution slowly changes from the initial value of + 18.7° to the same equilibrium value of + 54°. This gradual change in rotation to an equilibrium point is known as mutarotation. Mutarotation results from the interconversion of the cyclic hemiacetals with the open-chain form in solution. Ring opening followed by recyclization can form either the α or β anomer. At equilibrium, the solution contains 36% of the α anomer and 64% of the β anomer of glucose, with less than 0.01% of the open-chain form [17]. This thermodynamic proportion is always preserved, thus considering the β anomeric form of glucose representative of the whole glucose molecules is a reasonable assumption.

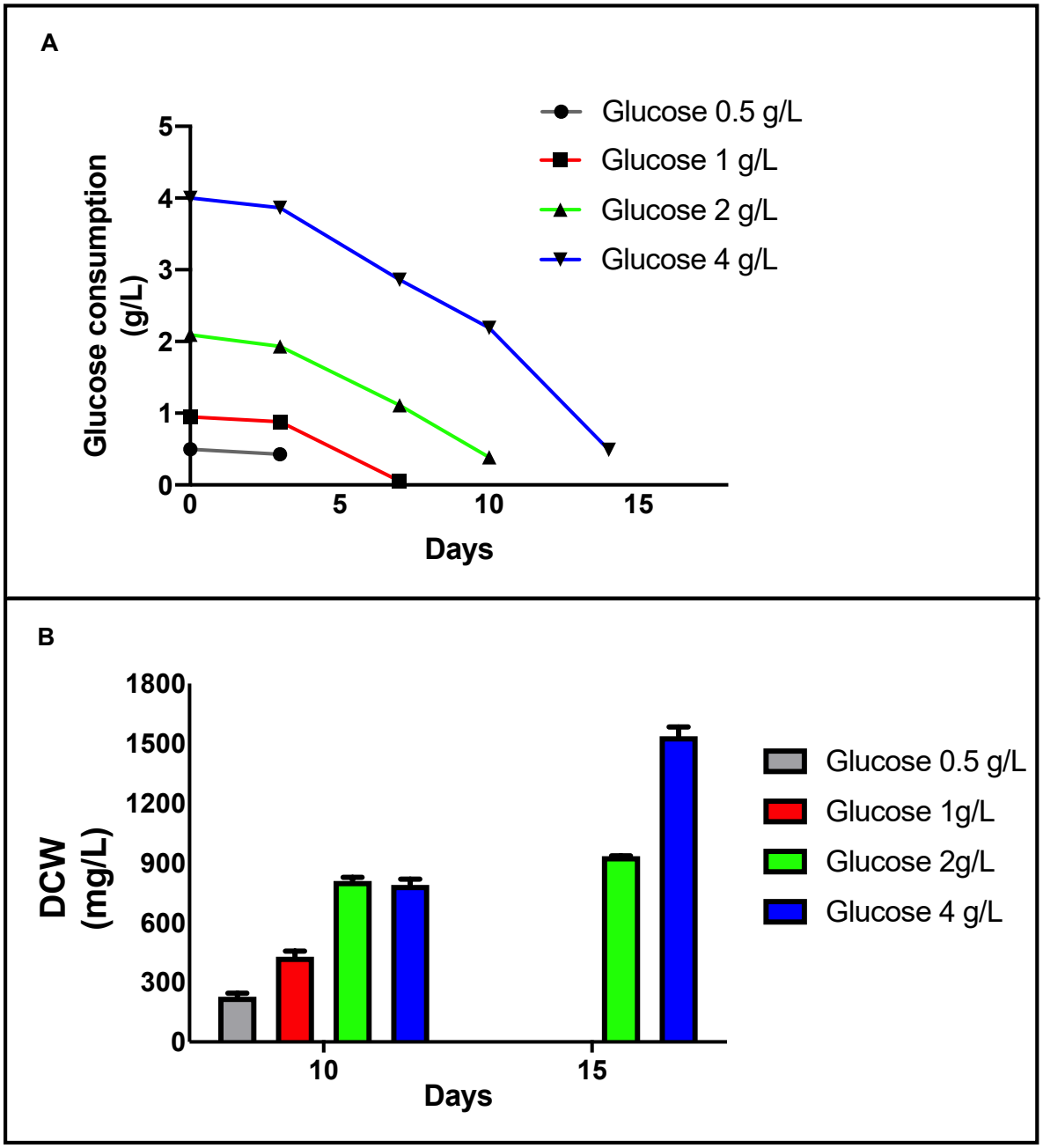

Figure 2.6 A) Glucose consumption by *C. cryptica* cultivated in F/2 medium enriched with 0.5g/L, 1g/L, 2g/L and 4g/L of glucose. B) Dry cell weight expressed as mg/L of *C. cryptica* cultivated in F/2 medium enriched with 0.5g/L, 1g/L, 2g/L and 4g/L of glucose.

Figure 2.6A represents the residual glucose in the medium during the cultivation period. Grey line indicates the glucose consumption of cells under 0.5 g/L. At 3th day the amount of residual glucose was 0.43 g/L ± 0.02, in the 7th day the signal of glucose was not detectable by ^{1}H-NMR. Accordingly with the cell density, cells entered in a stationary phase, stopping their duplication due to a lack of organic and energy source.

The biomass obtained at day 10th, during late stationary phase was 227 mg/L ± 14.35 (grey column), **Figure 2.6B**

Red line in **Figure 2.6A** indicates glucose consumption for cells under 1 g/L of glucose, at day 7th the amount of glucose was 0.05 g/L ± 0.04 and the relative biomass harvested at day 10th was 428 mg/L ± 23.37.

The amount of biomass was quite similar at day 10th for cells under 2 g/L of glucose (green column) and cells under 4 g/L (blue column): 809.33 mg/L ± 14.34 and 789 mg/L ± 23.76, respectively. The biomass yield is in agreement with glucose consumption since the residual glucose was 0.38 g/L ± 0.01 and 2.19 g/L ± 0.03 as shown in **Figure 2.6A** and thus, the net use of glucose of about 1.7 g/L in both conditions. The surplus of glucose available for cells under 4 g/L represents an advantage on biomass production at 14th day of culture, allowing the production of 1.536 g/L versus 933.33 mg/L ± 1.89 under 2 g/L.

In conclusion, 2 g/L seems to be the best glucose condition among those tested in this experiment, considering a growth period of 10 days in relation to the biomass obtained and nutrient costs.

If we compare our data in terms of biomass productivity and organic substrate supplied to other heterotrophic diatoms, our culture model seems to be promising.

The ratio between biomass (g/L) and glucose (g/L) supplied in our culture condition after 10 days of growth, considering 2 g/L of glucose, is 0.46.

Nitzschia laevis grown in heterotrophy displayed a ratio of 0.44 on a total of 5 g/L supplied [18]; *C. cryptica* grown by Pahl a ratio of 0.1 on a total of 10 g/L supplied [19].

2.3 Materials and methods

2.3.1 Growth media

2.3.1.1 Standard F/2 medium preparation

Natural seawater was collected from the Gulf of Naples (40°49'57.72"N 14°14'08.77"E) with a salinity of about 40 g/L, measured using an ATC 106 refractometer, filtered through

Millipore filters with pores of 1 µm diameter and autoclaved. Macronutrients, micronutrients and vitamins were added to prepare the complete F/2 [20], as reported below:

MACRONUTRIENTS

1 mL L^{-1} di Na_2SiO_3 x $9H_2O$ = 30 g L-1 (final concentration 106 µM);

1 mL L^{-1} di $NaNO_3$ = 75 g L^{-1} (final concentration 882 µM);

1 mL L^{-1} di NaH_2PO_4 x H2O = 5 g L^{-1} (final concentration 36.2 µM);

MICRONUTRIENTS

1 mL L^{-1} of stock solution made by:

Na_2EDTA x $2H_2O$ = 4.36 g L^{-1};

$FeCl_3$ x $6H_2O$ = 3.15 g L^{-1};

$MnCl_2$ x $4H_2O$ = 0.18 g L^{-1};

$CuSO_4$ x $5H_2O$ = 0.01 g L^{-1};

$ZnSO_4$ x $7H_2O$ = 0.022 g L^{-1};

$CoCl_2$ x $6H_2O$ = 0.01 g L^{-1};

$NaMoO_4$ x $2H_2O$ = 0.006 g L^{-1};

VITAMINS

0.5 mL L^{-1} of stock solution containing:

Biotin = 0.001 g L^{-1};

Cobalamin = 0.001 g L^{-1};

Thiamine-HCl = 0.2 g L^{-1}

The pH of medium was adjusted using Trizma® (TRIS base) 500 mM pH 7.8 (5 mL L^{-1}).

2.3.1.2 Artificial seawater

Artificial seawater for experiments reported in paragraph 2.2.2 was prepared with different salt sources as reported below:

Laboratory salts: salts reported in **Table 2.1** were added to 1 L of distilled water and then autoclaved.

Table 2.1 Artificial seawater recipe

Salt	Concentration (g kg^{-1})
NaCl	24.55
KCl	0.75
$MgCl_2 \times 6H_2O$	4.07
$CaCl_2 \times 2H_2O$	1.47
$MgSO_4 \times 7H_2O$	6.04
$NaHCO_3$	0.21

Tropic Marin ©: Tropic Marin © sea salts were purchased from specialized retailers in Naples. These salts contained all trace elements found in natural seawater, the exact composition is unknown, since this product is covered by patent.

40 g of salts, previously dried for 1 hour in the laboratory stove, were added to 1 Liter of distilled water and then autoclaved before adding other nutrients to prepare F/2 medium.

Lisal Salts: Lisal Salts are sold for food and industrial use. They are a natural product, coming from Sardinia saltworks. The same procedure adopted with Tropic Marin was repeated with Lisal Salts, thus 40 g of salts were added to 1 Liter of distilled water and then autoclaved before adding other nutrients to prepare F/2 medium. Also in this case, salts were previously well dried in the stove, since their hygroscopic nature properties.

2.3.1.3 Organic substrates

The culture media for the experiments described in paragraph 2.2.3 were supplemented with 11 mM of glucose, 11 mM of sucrose, 11 mM lactose and 2 g/L of wheat starch, previously filtered with a 0.22 µm filter by sterile syringe, in a standard F/2 medium (prepared as reported in paragraph 2.3.1.1).

All the substrates were purchased from Sigma Aldrich (Milan).

2.3.2 Strain and culture conditions

Stock cultures of the diatom *C. cryptica* (CCMP 331) purchased from Bigelow Laboratories, were maintained in F/2 medium [20] in batch culture using a week transfer cycle.

For experiments described in this chapter, diatoms were grown in 300ml flasks in prefiltered sterile (0.22 µm) F/2 medium at an initial concentration of $1x10^4$ cells mL^{-1}.

The cultures were maintained under autotrophic condition, in a growth chamber at 20 ± 2°C on a 14:10 light: dark cycle under a photon flux density of 200 µmol quanta m^{-2} sec^{-1}.

Cells were grown under heterotrophic conditions in a dark chamber 20 ± 2°C. F/2 medium was supplemented with organic substrates.

Macronutrients levels were maintained at high regimes, adding nitrates ($NaNO_3$, 882 µmoles L^{-1}) and phosphates ($NaH_2PO_4 \cdot H2O$, 36 µmoles L^{-1}) every 48 hours, and silicate ($Na_2SiO_3 \cdot 9H_2O$, 107 µmoles L^{-1}) every 24 hours.

2.3.3 Cell growth monitoring

The cells were counted and monitored every day by microscopic observation (AxioVertA1; Carl Zeiss; magnification of 20 and 40 X), counting by using a Bürker chamber. This chamber consists of nine squares delimited by three adjacent lines and has a total volume of 0.1 mm^3 (10^{-4} cm^3 = 1 mL); the concentration of cells per milliliter (cells / mL) was determined by the following calculation:

Cells/ mL = average count per square · dilution factor · 10^4

2.3.4 Biomass content

Cells were harvested by centrifugation at 3600 rpm for 10 minutes at 12 °C using a swing-out rotor (Allegra X12R - Beckman Coulter).

The supernatant is recovered, and an aliquot filtered with 0.22 µm Millipore filters for the quantitative glucose analysis. With the residual part of the supernatant, the cells are resuspended and concentrated in a single weighed falcon to estimate the amount of wet biomass. Pellets were frozen at −80°C and lyophilized with a MicroModulyo 230 (Thermo Electron Corporation, Milford, MA, USA). Dry weight was estimated on lyophilized biomass and expressed as mg L−1 culture. Biomass productivity was calculated in agreement with d'Ippolito et al. [21].

2.3.5 ^{1}H- NMR analysis of glucose consumption

C. cryptica culture (10 mL) were centrifuged at 3750 rpm for 10 minutes at 12 °C and glucose consumption was estimated on supernatant.

50 µl of D_2O (deuterium oxide) were added to 650 µl of supernatant in 5 mm NMR tube and analyzed on Bruker DRX 600 spectrometer equipped with an inverse TCI CryoProbe.

We used a standard glucose solution 1 mg/ml (5.5 µmol L^{-1}) as reference. Using this file as reference, we calculated the µmol/ml of glucose in the sample analyzed by ERETIC method.

The diagnostic peak, centered at 3.24 ppm, refers to the signal of protons of ß-anomer of carbon in position 2 of glucose molecule, as showed in **Figure 2.5**.

2.4 References

(1) Borowitzka, M. A. Commercial Production of Microalgae : Ponds , Tanks , Tubes and Fermenters. **1999**, *70*, 313–321.

(2) Sheehan John; Terri, D.; John, B.; Paul, R. A Look Back at the U.S. Department of Energy's Aquatic Species. *Eur. Phys. J. C* **2012**, *72* (6), 14.

(3) Pérez-López, P.; González-García, S.; Allewaert, C.; Verween, A.; Murray, P.; Feijoo, G.; Moreira, M. T. Environmental Evaluation of Eicosapentaenoic Acid Production by *Phaeodactylum Tricornutum*. *Sci. Total Environ.* **2014**, *466–467*, 991–1002. https://doi.org/10.1016/j.scitotenv.2013.07.105.

(4) Traller, J. C.; Cokus, S. J.; Lopez, D. A.; Gaidarenko, O.; Smith, S. R.; McCrow, J. P.; Gallaher, S. D.; Podell, S.; Thompson, M.; Cook, O.; Morselli, M.; Jaroszewicz, A.; Allen, E. E.; Allen, A. E.; Merchant, S. S.; Pellegrini, M.; Hildebrand, M. Genome and Methylome of the Oleaginous Diatom *Cyclotella Cryptica* Reveal Genetic Flexibility toward a High Lipid Phenotype. *Biotechnol. Biofuels* **2016**, *9* (1), 1–20. https://doi.org/10.1186/s13068-016-0670-3.

(5) Pahl, S. L.; Lewis, D. M.; King, K. D.; Chen, F. Heterotrophic Production of the Microalgae *Cyclotella Cryptica* ; Fed for Aquaculture. *PhD Thesis Univ. Adelaide* **2010**, *24* (May), 235–239. https://doi.org/10.1016/j.jbiosc.2009.08.480.

(6) Pahl, S. L.; Lewis, D. M.; Chen, F.; King, K. D. Heterotrophic Growth and Nutritional Aspects of the Diatom *Cyclotella Cryptica (Bacillariophyceae)*: Effect of Some Environmental Factors. *J. Biosci. Bioeng.* **2010**, *109* (3). https://doi.org/10.1016/j.jbiosc.2009.08.480.

(7) Bumbak, F.; Cook, S.; Zachleder, V.; Hauser, S.; Kovar, K. Best Practices in Heterotrophic High-Cell-Density Microalgal Processes: Achievements, Potential and Possible Limitations. *Appl. Microbiol. Biotechnol.* **2011**, *91* (1), 31–46. https://doi.org/10.1007/s00253-011-3311-6.

(8) Šulčius, S.; Slavuckytė, K.; Januškaitė, M.; Paškauskas, R. Establishment of Axenic Cultures from Cyanobacterium Aphanizomenon Flos-Aquae Akinetes by Micromanipulation and Chemical Treatment. *Algal Res.* **2017**, *23*, 43–50. https://doi.org/10.1016/j.algal.2017.01.006.

(9) Vu, C. H. T.; Lee, H. G.; Chang, Y. K.; Oh, H. M. Axenic Cultures for Microalgal Biotechnology: Establishment, Assessment, Maintenance, and Applications. *Biotechnol. Adv.* **2018**, *36* (2), 380–396. https://doi.org/10.1016/j.biotechadv.2017.12.018.

(10) Cattolico, R. A. Fragile Algae: Axenic Culture of Field-Collected Samples of Heterosigma Carterae. *Mar. Biol.* **1996**, *125* (2), 421–426. https://doi.org/10.1007/bf00346322.

(11) Scholz, B. Purification and Culture Characteristics of 36 Benthic Marine Diatoms Isolated from the Solthörn Tidal Flat (Southern North Sea). *J. Phycol.* **2014**, *50* (4), 685–697. https://doi.org/10.1111/jpy.12193.

(12) Pleissner, D.; Lam, W. C.; Sun, Z.; Lin, C. S. K. Food Waste as Nutrient Source in Heterotrophic Microalgae Cultivation. *Bioresour. Technol.* **2013**, *137*, 139–146. https://doi.org/10.1016/j.biortech.2013.03.088.

(13) Perez-Garcia, O.; Escalante, F. M. E.; de-Bashan, L. E.; Bashan, Y. Heterotrophic Cultures of Microalgae: Metabolism and Potential Products. *Water Res.* **2011**, *45* (1), 11–36. https://doi.org/10.1016/j.watres.2010.08.037.

(14) Morales-Sánchez, D.; Tinoco-Valencia, R.; Kyndt, J.; Martinez, A. Heterotrophic Growth of *Neochloris Oleoabundans* Using Glucose as a Carbon Source. *Biotechnol. Biofuels* **2013**, *6* (1), 100. https://doi.org/10.1186/1754-6834-6-100.

(15) Vidotti, A. D. S.; Coelho, R. S.; Franco, L. M.; Franco, T. T. Miniaturized Culture for Heterotrophic Microalgae Using Low Cost Carbon Sources as a Tool to Isolate Fast and Economical Strains. *Chem. Eng. Trans.* **2014**, *38*, 325–330. https://doi.org/10.3303/CET1438055.

(16) Guo, B.; Liu, B.; Yang, B.; Sun, P.; Lu, X.; Liu, J.; Chen, F. Screening of Diatom Strains and Characterization of *Cyclotella Cryptica* as a Potential Fucoxanthin Producer. *Mar. Drugs* **2016**, *14* (7). https://doi.org/10.3390/md14070125.

(17) Ouellette, Robert J., R. J. D. Carbohydrates. In *Organic Chemistry: Structure, Mechanism, Synthesis*; 2018; pp 889–928. https://doi.org/https://doi.org/10.1016/B978-0-12-812838-1.50028-1.

(18) Wen, Z.-Y.; Chen, F. Production Potential of Eicosapentaenoic Acid by the Diatom *Nitzschia Laevis*; **2000**; Vol. 22.

(19) Pahl, S. L.; Lewis, D. M.; Chen, F.; King, K. D. Growth Dynamics and the Proximate Biochemical Composition and Fatty Acid Profile of the Heterotrophically Grown Diatom *Cyclotella Cryptica*. *J. Appl. Phycol.* **2010**, *22* (2), 165–171. https://doi.org/10.1007/s10811-009-9436-7.

(20) Guillard, R. R. L.; Ryther, J. H. Studies of Marine Planktonic Diatoms. I. *Cyclotella Nana Hustedt, and Detonula Confervacea* (CLEVE) . Canadian Journal of Microbiology 8:229-239. *Can. J. Microbiol.* **1962**, *8* (1140), 229–239.

(21) D'Ippolito, G.; Sardo, A.; Paris, D.; Vella, F. M.; Adelfi, M. G.; Botte, P.; Gallo, C.; Fontana, A. Potential of Lipid Metabolism in Marine Diatoms for Biofuel Production. *Biotechnol. Biofuels* **2015**, *8* (1), 1–10. https://doi.org/10.1186/s13068-015-0212-4.

3. Cyclotella cryptica: biochemical characterization and preliminary results for development of sustainable products

3.1 Introduction

United Nations estimates that the current world population is actually 7.8 billion and it is expected to increase by 2 billion persons in the next 30 years, reaching thus 9.7 billion in 2050 (United Nations, https://www.un.org/en). The resulting changes in population size has a huge impact on the achievement of Sustainable Development Goals: a set of 17 goals have been signed in September 2015 by the government of ONU member countries, in order to reach social well-being while protecting the planet [1].

The expansion and intensive exploitation of cropland have severe impact on the environment, such as CO_2 emission, chemical pollution and degradation of quality water due to fertilizers use [2].

Steffen at al. defined the land system a critical factor, a zone of increasing risk inside the "planetary bound framework" that provides an analysis of anthropic impact and defines environmental boundaries [3].

Moreover, the effort to find effective strategies to meet the nutritional needs of the world population without depriving the planet of its biodiversity is a strategic way to avoid spill-over effects. The whole world is now experiencing the heavy economic and social impact of a spill-over effect because of SARS-CoV-2 spread.

Microalgae could represent a sustainable food and feed resource by owning the capacity to grow in salty or wastewater, using atmospheric CO_2 without mining of arable land [4]. It is reported that obtaining protein from animals like beef requires 144-258 m^2 for Kg of protein in comparison with 2.5 m^2 necessary for microalgae [5]. Consequently, microalgal biotechnology is emerging due to the great potential of bioactive compound that can be obtained from biomass [6].

Currently many species of microalgae were cultivated on a commercial scale and 75% of production is related to healthier supplements for human consumption [7], either in the form of dry algae powders or as extracts [8]. *Chlorella* and *Spirulina* are widely used for food

application: 70 companies in the world produce 3000 tons dry weight of *Chlorella* with an overall income of US$38 billion [7,9], while *Spirulina* market has been estimated around US$ 348 million in 2018 and a global amount of 2000 tons dry weight [9].

The critical points still to be resolved are linked to the public acceptance in consuming microalgae and their products, process scalability and the search of other nutritionally interesting strains.

In this chapter we want to show the nutritional profile of the marine diatom *C. cryptica* grown in dark in comparison to light condition. The possibility to grow massively *C. cryptica* heterotrophically opens to new attractive industrial food and feed application.

3.2 Results and discussion

3.2.1 Sustainability of heterotrophic process

The marine diatom *C. cryptica* was grown in autotrophic and heterotrophic conditions in order to evaluate differences in growth performances, biomass production and biochemical composition. Autotrophic cultivation was guaranteed by an illumination at 200 µmol (photons) $m^{-2}s^{-1}$ with 14:10 h (light/dark) photoperiod, whereas heterotrophic growth was carried out by cultivating cells completely in the dark and by supplementing the medium with glucose as organic carbon source.

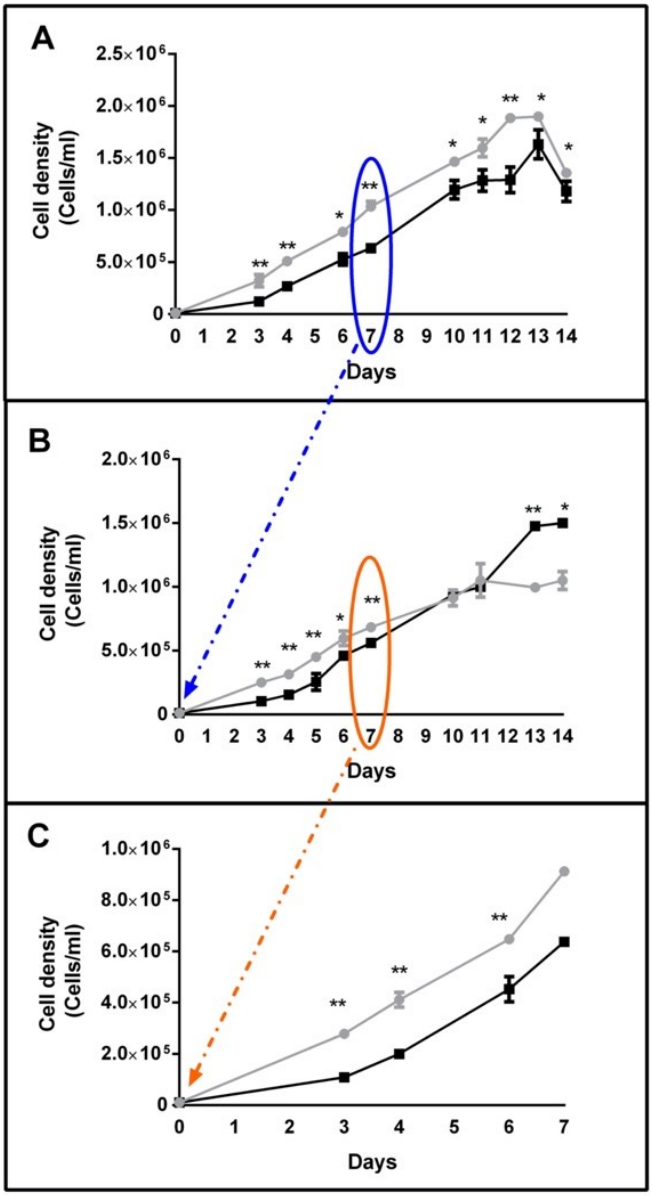

Figure 3.1 Growth curves of *C. cryptica* under autotrophic (grey line) and heterotrophic conditions (black line) in 1st cycle (A), 2nd cycle (B) and 3rd cycle of growth (C). Asterisks indicate significantly different values in autotrophic and heterotrophic samples at p≤ 0.05 (*) and p ≤ 0.005 (**).

As illustrated in **Figure 3.1**, we performed an experiment to test the sustainability of the heterotrophic process, maintaining cells in batch systems via three cycles.

Then we evaluated the nutritional profile of biomasses, harvested in different times to perform the best productive strategy.

In the first cycle (**Figure 3.1A**) growth curves in autotrophic and heterotrophic conditions displayed a similar trend under a sufficient nutrient regime, albeit cellular density was slightly smaller in the dark. After an adaptation phase of 3-4 days, the growth rate reflected a rapid

increase of cell division. In fact, during the exponential phase, that is between day 3 and 10, doubling time was 2 ± 0.05 day in heterotrophy in comparison with a value of 3.3 ± 0.2 day in autotrophy, supporting a minor amount of time to double cell number under heterotrophic conditions.

At day 7th and 14th an amount of 500 ml was harvested and centrifugated for biochemical analysis. Furthermore, at 7th day of growth, in exponential phase, a volume of both autotrophic and heterotrophic cultures was utilized as inoculum for the second cycle in order to re-start from 10.000 cells/ml (**Figure 3.1B**).

Similarly with first cycle, we observed an initial phase of adaptation, followed by a rapid increase in growth rate, decrease in doubling time with the final result of a significant boost in cell density at 14th day, under heterotrophic conditions.

In details, growth rate, namely cell divisions day $^{-1}$, during exponential phase, between 3rd and 10th day was 0.2 ± 0.01 in autotrophy and 0.3 ± 0.009 in heterotrophy. The doubling time, time required to achieve a doubling of the number of viable cells, was 3.8±0.2 in autotrophy and 2.2±0.06 in heterotrophy in the same temporal interval mentioned above.

Consequently, in the second cycle we can assume that heterotrophic cells spent less time to duplicate, so in the same time unit they made more cell divisions, reaching at day 14th 1.5x10^{6} cells/ml versus 1.03x10^{6} cells/ml in autotrophy.

Again, a volume of both autotrophic and heterotrophic cultures, at 7th day of the second cycle was picked up to kick-start the 3rd and final cycle of cell growth (**Figure 3.1C**).

After 7 days of cultivation, we detected bacteria contamination as described in the chapter 2 paragraph 2.2.1.: the absorbance at 600 nm was about 0.9 OD for heterotrophic cultures, thus we decided to arrest the cell cycle.

It is important to underline that no antibiotic was used during these three cycles of growth, both in autotrophy and in heterotrophy.

3.2.2 Biomass production

As shown in **Table 3.1**, biomass production was evaluated at 7th day (exponential phase) and 14th day (first point of senescent phase).

Table3.1 Dry cell weight expressed as mg/L in autotrophy and heterotrophy. Data are expressed as means of three replicates ± SD. Asterisks indicate significantly different values in autotrophic and heterotrophic samples at p≤ 0.05 (*).

	Autotrophy			Heterotrophy	
	Days	Biomass (mg/L)	Biomass (mg/L/d)	Biomass (mg/L)	Biomass (mg/L/d)
1°cycle	7 (A)	246.4 ± 15.9	35.2 ± 2.3	285.5 ± 21.3*	40.8 ± 3.0*
	14 (B)	584.8 ± 38.9	41.8 ± 2.8	584.0 ± 45.1	41.7 ± 3.2
2°cycle	7 (C)	200.0 ± 7.3	28.6 ± 1.0	217.7± 6.4*	31.1 ± 0.9*
	14 (D)	404.5 ± 21.6	28.9 ± 1.5	467.2 ± 2.2*	33.4 ± 0.2
3°cycle	7 (E)	193.2 ± 21.7	27.6 ± 3.1	228.4 ± 6.7*	32.6 ± 1.0*
A+C	7+7	446.4 ± 15.1	64 ± 2.2	503,2 ± 14.8	72 ± 5.6
A+D	7+14	650.9 ± 23.2	64 ± 2.4	752.7 ± 19.4	74 ± 6.1
A+C+E	7+7+7	639.6 ± 19.7	91 ± 2.8	731.6 ± 16.4	104 ± 2.3

After 7 days, dry biomass was 246.4 ±15.9 mg L^{-1} in autotrophy and 285.5 ±21.3 mg L^{-1} in heterotrophy while a similar value of about 584 mg L^{-1} was reached after 14 days in both conditions.

In the 2nd and 3rd cycles, we recorded a significant increase in biomass amount under heterotrophic condition towards autotrophic one. This increase is also reflected in cell number at 14th day of the second cycle.

At the bottom of the table, in the blue bordered area, data extrapolated by our calculations are reported.

We hypothesized alternative batch schemes and harvesting time to evaluate which approach could be more advantageous.

In terms of daily biomass productivity, it was evident that keeping cells in weekly refreshed medium could guarantee better yield.

The best result was obtained by hypothesizing to keep the cells in fed-batch, collect them at the 7th day of growth and resuspend them entirely in new medium three times (A+C+E), thus mimicking a continuous process in the final phase, thereby achieving 104 ± 2.3 mg $L^{-1}d^{-1}$ in heterotrophy, towards 91±2.8 mg $L^{-1}d^{-1}$in autotrophy.

These data are explainable if we think that the cells are kept constantly in an exponential phase, without ever reaching the maximum peak of cell density.

The punctual, daily yield is therefore greater than the cumulative yield per unit of culture volume. As a matter of fact, we obtained 639.6±19.7 mg/L of biomass in autotrophy versus 731.6±16.4 mg/L, after three hypothetical cycles of 7 days each one (A+C+E).

On the contrary, no significant variations seem to be noticeable in terms of daily biomass productivity, whether considering two cycles each one of 7 days (A+C), or two cycles one 7-days and another 14-days (A+D).

On the other hand, there is an increase on cumulative biomass in the cycle composed by 7 and 14 days (A+D), justified by the achievement of a greater number of cells made possible by the presumed achievement of the late exponential phase compared to 7 days+ 7 days+ 7 days (A+C+E) along with a longer growth time than (A + B).

It is therefore evident that depending on the destination of heterotrophic biomass, it could be advantageous to opt for one scheme or another.

For example, If the goal is to obtain the maximum in terms of biomass yield in heterotrophy, on the basis of our study, it could be useful maintaining a starter culture for 7 days, and then sustaining a growth cycle for other 14 days, under sufficient nutrient regime.

3.2.3 Biochemical composition of *C. cryptica* biomass

The organic fraction of each microalga is essentially made up of lipids, proteins and carbohydrates. The remaining part of the dry weight consists of inorganic matter [10], silica for diatoms, insoluble carbohydrates, such as cellulose and nitrogen of non-protein origin. In **Table 3.2** and **Table 3.3** is reported the biochemical composition of biomasses under autotrophic and heterotrophic conditions, expressed respectively as percentage on dry weight and as mg/L of culture. The representation of biochemical composition in % of dry weight and as mg/L of culture offers two different perspectives: the first is useful for understanding the partition of biomass into different classes of macromolecules, and the second is useful for evaluating the system's productivity, as it is correlated to the quantity of biomass produced.

We obtained balanced flour in nutrients composition, with a major contribution of the protein component: 30% ± 3.0 and 32.6% ± 1.6 of dry cell weight after 7 days under light and dark conditions, that means 96.1 mg/L ± 14.2 and 106.1 mg/L ± 10.7.

Biomass composition in percentage remained almost constant in all cycles for each culture condition, considering the same harvesting time (7 or 14 days), without a dramatic rearrangement of the organic fractions. These data demonstrated the robustness and reproducibility of *C. cryptica* to maintain a constant response to the same experimental conditions. It's interesting to note that carbohydrate's percentage is always higher in heterotrophy than in autotrophy, a similar trend also occurs in the filamentous microalgae *Tribonema minus* [11] , in *Scenedesmus sp*. and in *Chlorella sp*.[12]. Keeping cells in culture for prolonged periods of time does not appear to be a stressful situation that induces the cell to change the biochemical structure of the biomass for each culture condition.

Instead, the periods of culture and inocula replenishment have an influence on the system's production, which represents the cumulative growth stages mentioned in the preceding paragraph.

Table 3.2 Dry cell weight expressed as mg/L and biomass composition in percentage in autotrophy and heterotrophy. Data are expressed as means of three replicates ± SD. Asterisks indicate significantly different values in autotrophic and heterotrophic samples at p≤ 0.05 (*) and p ≤ 0.005 (**).

		Autotrophy				**Heterotrophy**			
	Days	Biomass (mg/L)	% Lipid	% Protein	% Carbohydrates	Biomass (mg/L)	% Lipid	% Protein	% Carbohydrates
1°cycle	7	246.4 ± 15.9	24.7 ± 1.0	30.0 ± 3.0	4.2 ± 0.9	285.5 ± 21.3*	21.7 ± 0.7**	32.6 ± 1.6	18.0 ± 2.7**
	14	584.8 ± 38.9	20.9 ± 1.7	27.4 ± 3.4	2.9 ± 0.5	584.0 ± 45.1	18.8 ± 1.4	25.5 ± 2.3	16.6 ± 2.8
2°cycle	7	200.0 ± 7.3	17.5 ± 0.7	28.3 ± 1.4	5.4 ± 1.1	217.7± 6.4*	17.0 ± 1.3	28.5 ± 0.4	22.8 ± 2.7**
	14	404.5 ± 21.6	23.0 ± 3.9	33.3 ± 1.9	3.5 ± 0.3	467.2 ± 2.2*	26.6 ± 1.4	25.9 ± 2.5	21.1 ± 0.5**
3°cycle	7	193.2 ± 21.7	21.6 ± 3.4	31.8 ± 6.5	7.0 ± 1.3	228.4 ± 6.7*	17.4 ± 0.6	30.9 ± 4.0	29.6 ± 2.7**

Table 3.3 Dry cell weight and biomass composition expressed as mg/L in autotrophy and heterotrophy. Data are expressed as means of three replicates ± SD. Asterisks indicate significantly different values in autotrophic and heterotrophic samples at p≤ 0.05 (*) and p ≤ 0.005 (**).

		Autotrophy				**Heterotrophy**			
	Days	Biomass (mg/L)	Lipid (mg/L)	Protein (mg/L)	Carbohydrates(mg/L)	Biomass (mg/L)	Lipid (mg/L)	Protein (mg/L)	Carbohydrates (mg/L)
1°cycle	7 (A)	246.4 ± 15.9	69.3 ± 5.6	96.1 ± 14.2	11.8 ± 1.9	285.5 ± 21.3*	70.4 ± 4.9	106.1 ± 10.7	58.4 ± 9.9**
	14 (B)	584.8 ± 38.9	138.0 ± 2.0	206.3 ± 28.8	19.1 ± 3.4	584.0 ± 45.1	124.9±14.7	174.7 ± 30.9	109.2 ± 10.8**
2°cycle	7 (C)	200.0 ± 7.3	39.8 ± 2.8	56.6 ± 4.9	12.1 ± 2.2	217.7 ± 6.4*	42.1 ± 3.9	62.1 ± 1.6	56.3 ± 6.5**
	14 (D)	404.5 ± 21.6	105.5 ± 15.3	135.0 ± 14.5	16.4 ± 2.0	467.2 ± 2.2*	141.0 ± 6.7*	120.9 ± 11.1	111.9 ± 3.3**
3°cycle	7 (E)	193.2 ± 21.7	48.4 ± 12.3	68.3 ± 6.2	15.7 ± 4.2	228.4 ± 6.7*	45.3 ± 2.6	80.0 ± 8.2	76.7 ± 4.8**

In order to better contextualize our data, we reported in **Table 3.4** and **Table 3.5** the main species of microalgae marketed and recognized by European and American regulatory bodies both in the food and feed sectors.

Generally Recognized As Safe (GRAS) is a status given by the Food and Drug Administration (U. S. Food and Drug Administration, 2018) to any substance or chemical, including sometimes whole organisms, that is considered safe for human consumption.

There are only a few microalgae that have GRAS status as re-cognized by the FDA. These algae include: *Arthrospira platensis, Chlamydomonas reinhardtii, Auxenochlorella protothecoides, Chlorella vulgaris, Dunaliella bardawil*, and *Euglena gracilis*. The GRAS designation, on the other hand, solely pertains to US jurisdiction and may differ from rules in other nations. The European Food Safety Authority (EFSA) is in charge of overseeing the laws governing human food and animal feed in the European Union (EU). Using the "precautionary principle," foods that were widely consumed in the EU before to May 1997 are judged safe to eat, but any new food, except Genetically Modified Organisms (GMOs), is labeled as "novel food" and must pass an EFSA safety evaluation before being sold. For algae to be considered as potential new food sources, one crucial factor is their composition and nutritional content. The nutritional composition varies tremendously among algal and microalgal species, and even within the same species nutritional content can vary significantly based on the growth environment. Important nutritional components to consider are protein and lipid content, as well as vitamins and mineral content, all of which are known to positively impact human health.

Microalgae may be integrated into the feed of a wide range of species, from fish (aquaculture) to pets and agricultural animals, in addition to human nutrition. In reality, 30% of current global algal output is sold for animal feed applications, while over 50% of current global *Arthrospira* production is used as a feed additive [13].

In these tables we reported the known composition in terms of percentage on dry cell weight of the microalgae recognized and placed on the market, for a comparison with our data.

Table3.4 Chemical profile of microalgae present on the worldwide market for food. Carbohydrates, protein, and lipid content are reported as percentage of dried biomass. Abbreviations: Food and Drug Administration (FDA), Canadian Food Inspection Agency (CFIA), China Food and Drug Administration (CFDA), European Food Safety Authority (EFSA), Food Standards Australia New Zealand (FSANZ), Food Safety Commission of Japan (FSCJ).

		Autotrophy			Heterotrophy					
Species	**Country/Certificate Authority**	**Carbohydrates**	**Protein**	**Lipid**	**Carbohydrates**	**Protein**	**Lipid**	**Commercial form**	**Company**	**References**
Arthrospira platensis	U.S.A./ FDA; Canada/CFIA; China/CFDA; EU/EFSA; Japan/FSCJ	8-14%	46-68%	4-14%	-	-	-	Whole dried biomass, extract	Earthrise Nutraceuticals (USA) Cyanotech Corporation (USA) Hainan DIC Microalgae (China) Japan Algae Co., Ltd. Parry Nutraceuticals (India) FEMICO (Taiwan) Nan Pao International (Taiwan) Biotechnology Co. Ltd. Biorigin (USA) TAAU Australia Pty Ltd	9,14–16
Chlamydomonas reinhardtii	U.S.A./FDA	17-50%	26%	19-21%	45%	22-48%	29%	Whole dried biomass	Triton Algae Innovations (USA)	9
Auxochlorella protothechoides	U.S.A./FDA	11%	53%	13-23%	15-25%	10-63%	15-46%	Whole dried biomass	Corbion-AlgaVia (the Neatherlands)	9,16
Chlorella vulgaris	U.S.A./FDA, Canada/CFIA, EU/EFSA, Japan/FSCJ	24-26%	24-44%	22-46%	23-44%	30-45%	22-36%	Whole dried biomass, extract	Roquette Klötze (Germany) Blue Biotech (Germany) Earthrise Nutritionals (USA) Cognis (Germany)	9,14
Dunaliella bardawil	U.S.A./FDA	11%	29%	10-19%	-	-	-	Biomass	NBT Ltd. (Israel) Nikken Sohonsha Co, (Japan)	9
Dunaliella salina	China/CFDA, Canada/CFIA	32%	57%	6%	-	-	-	Whole dried biomass	Cognis Australia; Tianjin Lantai (China)	14
Haematococcus pluvialis	U.S.A./FDA	27%	48%	15%	-	-	-	Extracts	Pro Algen (India) Algatech (India) Bue Biotech (Germany) Mera Pharma (USA) BioReal (Sweden) Fuji Chemicals (Japan) AlgaTech (Israel) AstraReal Co. (Japan) E.I.D Parry (India) Solix Inc. (USA)	14,16

Euglena gracilis	U.S.A./FDA; Canada/CFIA; China/CFDA; Japan/FSCJ	30%	30-47%	20-35%	60-90%	25%	10%	Biomass	Algatech (USA)	9
Tetraselmis chuii	EU/FDA	25%	31-46%	12%	-	-	-	Biomass	Fitoplancton Marino S.L. (Spain)	17,18
Schizochytrium sp.	EU/EFSA Australia/FSANZ	-	-	-	38.9%	12.5%	38.9%	Extracts	Xiamen Huison Biotech Co. (China)	16,19

Table 3.5 Chemical profile of microalgae present on the worldwide market for feed. Carbohydrates, protein, and lipid content are reported as percentage of dried biomass. Abbreviations: Food and Drug Administration (FDA), Canadian Food Inspection Agency (CFIA), China Food and Drug Administration (CFDA), European Food Safety Authority (EFSA), Food Standards Australia New Zealand (FSANZ), Food Safety Commission of Japan (FSCJ).

FEED		**Autotrophy**			**Heterotrophy**					
Species	**Country/Certificate Authority**	**Carbohydrates**	**Protein**	**Lipid**	**Carbohydrates**	**Protein**	**Lipid**	**Products**	**Company**	**References**
Chlorella	EU/EFSA U.S.A /FDA	24-26%	24-44%	22-46%	23-44%	30-45%	22-36%	Biomass	Blue-Biotech (Germany) Necton (Portugal)	16,19,20
Haematococcus pluvialis	EU/EFSA U.S.A. /FDA	27%	48%	15%	-	-	-	Biomass, extracts	Blue-Biotech (Germany)	16,20,21
Arthospira platensis	EU/EFSA U.S.A/FDA	8-14%	46-68%	4-14%	-	-	-	Biomass	Blue-Biotech (Germany) Ocean Nutrition (Canada)	16,20,21
Nannochloropsis granulate (CCMP-535)	EU/EFSA	36.2%	33.5%	23.6%	-	-	-	Living algae as feed -for fish in aquariums	Blue-Biotech (Germany)	16,20,21

Phaodactylum tricornutum (CCMP-1327)	EU/EFSA	25.2%	39.6%	18.2%	-	-	-	Living algae as feed for fish in aquariums	Necton (Portugal)	16,20,21
Tetraselmis sp.	EU/EFSA	45.4%	27.2%	14%	-	-	-	Living algae as feed for fish in aquariums	Necton (Portugal)	16,20,21

Few microalgal species recognized by regulatory authorities and commercialized have grown under heterotrophy, as shown in the two tables. These microalgae's nutritional composition is pushed toward a certain macromolecule. *Auxochlorella protheicodes*, for example, is sold as a lyophilic biomass with an high protein (max 63 % on DCW) and high lipid content (max 48 % on DCW) composition, while *Euglena gracilis*, recently approved by EFSA with a high carbohydrate content, is being considered for the production of 1,3-glucan paramylon, which is only found in euglenoids and is marketed as an immunostimulatory agent in nutraceuticals [22].

The only diatom of the listed species that is also cultivated in autotrophic conditions and utilized as fish feed in aquaculture, *P. tricornutum*, has a composition similar to our *C. cryptica* grown in heterotrophy. Nutritional profile of *C. cryptica* biomass under heterotrophic circumstances, which is balanced in composition with a boost towards the protein portion (32%), might be a useful starting point for further aquaculture research, if we consider that Crustaceans and fishes in their early larval stages require a nutritionally balanced diet [23].

We plan to do more experiments in which we modulate the supply of nutrients in order to enhance the protein component on the one hand and the lipid component on the other, with the goal of using whole biomass, potentially in the food industry.

The effects of nitrate and phosphate concentrations on marine diatom development, extracellular polysaccharide synthesis, and fatty acid profile have been studied [23].

For diatoms growing in autotrophy, it is known, for example, that under phosphate deficient circumstances, more CO_2 is fixed than is used by the Calvin cycle due to a decrease in the needs for carbon structures for the synthesis of proteins and phospholipids. To deal with this surplus, diatoms divert carbon flow to storage molecules such triacylglycerides and carbohydrates, which are expelled as extracellular polymeric polymers [24].

Organic carbon sources are employed in heterotrophic cultures, and the carbon/nitrogen (C/N) ratio governs the transition between protein and lipid synthesis [25].

Microalgae can be induced to consume more nutrients than are required for survival. For example, excess nitrogen is absorbed and stored in the form of proteins in this way.

The excess storage of a specific substrate is caused by two processes. The storing that occurs when microalgae are depleted of an element and then re-exposed to it is known as "over-compensation." The other process is known as "luxury intake," which is described as the

continuous absorption of a resource beyond what is necessary for immediate development without going through a starvation stage [26].

For optimal lipid synthesis by oleaginous microorganism in heterotrophic cultures, the starting C/N ratio must be higher than 20. Lipid accumulation was found in the oleaginous yeast *Rhodosporidium toruloides* at a C/N ratio of 30 and increased with a C/N ratio of up to 120 utilizing glucose as the carbon source. It was discovered that a C/N ratio of around 20 indicated a shift from carbon to nitrogen limitation in *Chlorella sorokiniana*, and that lipid content increased at C/N ratios greater or lower than the crucial value. The C/N ratio is affected not only by the microorganism strain, but also by the kind of carbon and nitrogen in the culture medium [25].

Based on these considerations, we intend to develop experiments based both on mechanisms of "over-compensation" and "luxury- uptake" that allow us to determine the right C/N ratio to push towards a higher protein or lipid percentage.

In conclusion we can reassume that *C. cryptica* biomass can be an important product as nutritional supplement of high value.

The potential of the heterotrophic system and the balanced biomass composition assessed in our experiments, give us sufficient elements to suppose that the optimization of the system could lead to the use of *C. cryptica* biomasses in the near future for food and feed sector [27].

3.2.4 Lipid profile of *C. cryptica*

The main polyunsaturated fatty acids present as component of glycerolipids in *C. cryptica* grown in autotrophic conditions are: C20:5 ω-3, C22:6 ω-3 , C16:3 ω-4 and C16:4 ω-1 [28–30].

The analysis of fatty acids by GC-MS showed a simplified framework in heterotrophy (**Table 3.6**). Similar results were obtained after 7 and 14 days of cultivation supporting the concept that the establishment of dark lipid-phenotype occurs early and stably along growth curve, independently from cycles number. It is worth to point out a significant reduction in heterotrophy of the main representative unsaturated fatty acid species except for 16:1 which showed the higher percentage among the fatty acid species. Similar profile was reported by Pahl et al. [31] in analogous cultivation of *C. cryptica* [31]. Interestingly, after 14 days of cultivation, the main plastidial polyunsaturated diatom markers 16:2 ω-4, 16:3 ω-4 and 16:4 ω-1

completely disappeared under heterotrophy, in favour of monounsaturated 16:1 ω-7. In particular, we observed an increase of 1.12 fold change in 16:1 ω-7 in the first cycle and 0.90 fold change in the second cycle. EPA and DHA, which remain the most abundant fatty acids among the ω-3 pool, slightly decreased in dark growth, representing 15% and 1.6% acids (TFA), 17.9% and 2.0% (TFA) in the first and second cycle, respectively. Interestingly, 18:0 completely disappeared. The pool of polyunsaturated fatty acids with 18 carbon atoms tends to increase in heterotrophy, particularly the monounsaturated 18: 1 ω -9 which represents 1.0% (TFA) in the first cycle, 1.4% (TFA) in the second cycle compared to 0.5% (TFA) and 0.4% (TFA) in autotrophy.

As a general trend, we observed a significant increase in the monounsatured fatty acids composition under heterotrophic condition, which represent 61.7% and 82.4% of total fatty acids in the first and second cycle, respectively. The polyunsaturated fatty acids, on the other hand, undergoes a reduction of 0.6 fold change both in the first and second cycle.

Similar results were obtained after 7 days of cultivation, supporting the concept that the establishment of dark lipid-phenotype occurs early and is maintained along the growth curve. This pattern of fatty acid distribution was similar with cultivations of *N. gaditana*, *C. protothecoides* and *G. sulphuraria* [32–34], where polyunsaturated fatty acids component was favorite autotrophically.

In C. reinhardtii, polyunsaturated fatty acids (PUFA) including C16:2, C16:3, C18:2, and C18:3 increase, compared to photoautotrophic and mixotrophic cultures [35].

A specific regulation of the unsaturated species was also reported by Yang et al. [36], in *P. tricornutum* subjected to nitrogen starvation [36]. This condition induced a reduction of total polyunsaturated fatty acid (PUFA), in C20:5 and C22:6, but an increase in the C16 unsaturated/C16:0 and the C18 unsaturated/C18:0 ratios. Particularly, the plastidial marker 16:4-ω1 and 16:3-4 reduced their content from 1.13% to 0% and from 21% to 1%, respectively. This evidence suggests a general dark-induced molecular and biochemical regulations of the fatty acid desaturase genes and a probable reduction of the chloroplastic glycolipids content. Similarly, *P. tricornutum* cells growth in nitrogen depletion/repletion conditions showed a reduction in 16:3 content upon lower N presence [37]. This suggests a critical role of 16:3 in perturbing diatoms conditions such as dark or starvation.

Curiously, the modification of the unsaturated fatty acid profile is a common behavior of transgenic diatoms modified to increase the amount of TAGs. Yao et al. [38] reported a reduction of 16:3 and 18:2 in *P. tricornutum* overexpressing GPDH (glycerol-3-phosphate dehydrogenase) while Cui et al. [37] reported similar behavior for 16:3, 18:1 and 20:3 in *P. tricornutum* overexpressing a DGAT isoform (diacylglycerol-acyltransferase)[37,38]. Furthermore, a different regulation of unsaturated fatty acid content and position in TGA were reported in *P. tricornutum* overexpressing GPAT and LPAT [39]. This genotype showed a specific reorganization of 16:1 and 18:1 which inverts their preferred sn^2/sn^{1-3} positions comparing wild type and transgenic genotypes. These evidences highlight the importance of unsaturated fatty acid along the entire lipid biosynthesis pathways.

In chapter 4 we present our published paper that proposes *C. cryptica* as a good candidate for the production of omega-3 fatty acid, C20: 5 ω3 (EPA).

Table3.6 Fatty acid composition of *C. cryptica* biomass grown under autotrophic and heterotrophic condition after 7 and 14 days in 1st cycle, 2nd cycle and 3rd cycle. Asterisks indicate significantly different values in autotrophic and heterotrophic samples at p ≤ 0.05 (*) and p≤ 0.005 (**).

	1°cycle				2°cycle				3°cycle	
	Day 7		Day 14		Day 7		Day 14		Day 7	
Fatty Acids	Autotrophy	Heterotrophy	Autotrophy	Heterotrophy	Autotrophy	Heterotrophy	Autotrophy	Heterotrophy	Autotrophy	Heterotrophy
14:0	5.3 ± 0.1	2.9 ± 0.5*	5.5 ± 0.03	2.5 ± 0.3**	4.0 ± 0.3	3.4 ±0.5	4.2 ± 0.6	2.9 ± 0.2	5.7 ± 0.9	4.8 ± 0.7
16:4 ω-1	0.3 ± 0.01	0*	1.1 ± 0.2	0**	0.4 ± 0.01	0**	1.4 ± 0.2	0**	0	0**
16:3 ω-4	22.5 ± 1.9	1.0 ± 0.01**	21.0 ± 2.3	1.1 ± 0.2**	22.1 ± 0.2	2.1 ± 0.1**	19.7 ± 0.5	1.8 ± 0.01**	17.6 ± 5.6	0**
16:2 ω-4	7.9 ± 0.1	0**	6.4 ± 0.9	0**	7.8 ± 0.5	0**	8.3 ± 0.7	0**	8.5 ± 1.2	0**
16:1 ω-7	23.5 ± 2.7	52.0 ± 0.1**	28.6 ± 2.6	60.7 ± 2.3**	24.0 ± 1.0	49.1 ± 3.0**	28.6 ± 1.8	54.5 ± 0.7**	29.9 ± 5.6	47.0 ± 0.8**
16:0	12.2 ± 0.7	17.2 ± 0.3**	11.4 ± 1.2	16.6 ± 0.3*	12.5 ± 0.1	15.3 ± 0.3**	11 .± 0.4	16.6 ± 0.2**	14.0 ± 1.6	19.6 ± 0.5**
18:4 ω-3	1.4 ± 0.1	1.2 ± 0.2	0.8 ± 0.1	0.9 ± 0.1	1.3 ± 0.2	2.1 ± 0.2*	0.9 ± 0.03	1.6 ± 0.4	0	0
18:3 ω-3	0.1 ± 0.01	0.3 ± 0.01**	0.1 ± 0.01	0.1 ± 0.001*	0.1 ± 0.01	0.3 ± 0.2	0.1 ± 0	0.1 ± 0**	0.7 ± 0.3	1.6 ± 0.1**
18:2 ω-6	0.2 ± 0.03	1.0 ± 0.1**	0.2 ± 0.003	0.4 ± 0.1	0.6 ± 0.1	1.0 ± 0.5	0.4 ± 0.1	0.5 ± 0.1	0.6 ± 0.1	0.9 ± 0.1*
18:1 ω-9	0.4 ± 0.03	1.0 ± 0.05**	0.5 ± 0.05	1.0 ± 0.1*	0.4 ± 0.03	1.7 ± 0.01**	0.4 ± 0.1	1.41 ± 0.2*	0	0
18:0	0.8 ± 0.6	0.3 ± 0.03	0.19 ± 0.03	0*	0.1 ± 0	0.2 ± 0.01*	0.1 ± 0.01	0.7 ± 0.1**	0.3 ± 0.0	0.4 ± 0.0*
20:5 ω-3	23.3 ± 0.6	21.2 ± 0.2*	19.4 ± 1.0	15.1 ± 1.7*	23.6 ± 1.5	22.52 ± 1.3	18.3 ± 0.1	17.9 ± 0.3	19.4 ± 1.9	22.8 ± 0.5*
22:6 ω-3	2.5 ± 0.3	1.9 ± 0.03	4.8 ± 0.3	1.6 ± 0.2**	3.1 ± 0.3	2.3 ± 0.6	6.2 ± 0.1	2.0 ± 0.4**	3.2 ± 0.1	2.0 ± 0.3**
SFA (%TFA)	18.3±0.03	20.4±0.2**	17.1 ± 1.3	19.2 ± 0.1	16.6 ± 0.4	18.9 ± 0.7	15.7 ± 0.2	20.1 ± 0.3**	19.9 ± 2.4	24.8 ± 0.2*
MUFA (%TFA)	23.9±2.6	53.0±0.2**	29.1 ± 2.7	61.7 ± 0.2**	24.4 ± 1.0	50.8 ± 3.1**	55.6 ± 4.3	82.4 ± 3.1**	29.9 ± 5.6	47.9 ± 0.8**
PUFA (%TFA)	58.4±3.2	26.6±0.03**	53.8 ± 3.9	19.2 ± 2.3**	59.0 ± 1.4	30.3 ± 2.3**	55.3 ± 1.5	23.9 ± 0.2**	50.1 ± 7.9	27.3 ± 0.6**

Distribution of glycerolipids was assessed by ERETIC ^{1}H-NMR method applied on organic extracts [40]. Data are reported in **Table 3.7**. A more detailed description of the method and quantitave analysis to determine the lipidic classed is reported in paragraph 3.3.5.

Galactolipids are the predominant lipids in thylakoid membranes and indispensable for photosynthesis. Diatoms biosynthesize three major types of glycolipids: monogalactosyldiacylglycerides (MGDGs), digalactosyldiacylglycerides (DGDGs), and sulfoquinovosyldiacylglycerides (SQDGs).

As shown in **Table 3.7**, the glycolipid component tends to decrease in heterotrophy. Data ere expressed as µmol per liter of culture, thus we intending to describe the productivity of our system in the two growth conditions; a description of the distribution in percentage on the biomass with the respective fatty acid composition is provided in Chapter 6, where we present the data from a paper under submission which clarifies the lipid metabolism using transcriptomic (RNA seq) and lipidomic (LCMS) approaches.

As reported **in Table 3.7**, we observed a decrease in DGDG content of 0.3 fold change both after 7 days of the first cycle and 14 days of the second one. SQDG is the molecular glycolipid species which mostly undergoes to a dramatic reduction in all three cycles: after 14 days of cultivation the whole content was reduced of 0.9 fold change in both first and second cycle.

PL pool slightly increases the content after 7 days of cultivation in all three cycles, while a content reduction is observed at 14th day of cultivation. Triacylglycerols, like SQDG, keep a constant trend, independently from harvesting time and cycle. This lipid pool is the most abundant under heterotrophic conditions and these preliminary results inspired the study presented in Chapter 5 where we propose *C. cryptica* a good potential biofuel producer.

The heterotrophic culture conditions decreased the content of GL also of *N. laevis* and *N. alba*, whereas the contents of GLs were normally much higher in phototrophic conditions [41].

The glycolipid content in *Chlorella zoofingiensis* is lower when grown in heterotrophy: in photoautotrophic cells, membrane lipids, namely glycolipids and phospholipids, were the major lipid classes which altogether accounted for 70.6% of total lipids, while the storage lipids neutal lipids (NL) accounted for only 29.4% of the total lipids. In contrast, heterotrophic cells produced predominantly NL which represented 80.9% of total lipids [42].

This might be because MGDG, DGDG and SQDG were highly associated with photosynthetic membranes of microalgae [41].

Interestingly, membrane lipid composition was similar between phototrophic and heterotrophic cultures of heterotrophically grown red alga *Cyanidioschyzon merolae*, except that the levels of monogalactosyl diacylglycerol (MGDG) and sulfoquinovosyl diacylglycerol (SQDG) were slightly higher in heterotrophic cells, contrary to our data [35].

Photoautotrophic cells of *O. danica* contained 5 to 6 times as much sulfolipid, sulfoquinovosyldiglyceride, as did cells grown under heterotrophic conditions [43].

Surprisingly, the effects of extended darkness on lipid metabolism in the benthic diatom *Navicula perminuta* result in a progressive decrease in glycolypides from week 0 to week 2 of darkness, followed by a gradual increase until week 8 of dark [44].

TAG was also the most abundant lipid fraction of *N. laevis* grown in heterotrophy, which represented 69.1% of the total lipids. Triacylglycerols are reported to be the predominant lipid class in heterotrophic microalgae, such as *N. alba* (about 87.0%) and *Crypthecodinium cohnii* (about 55.0%) [41] and are the major lipid pool suitable for biofuel production.

Table3.7 Lipid classes in *C. cryptica* grown under autotrophic and heterotrophic condition after 7 and 14 days in 1st cycle, 2nd cycle and 3rd cycle, expresses as µmol L^{-1}. Asterisks indicate significantly different values in autotrophic and heterotrophic samples at $p \leq 0.05$ (*) and $p \leq 0.005$ (**).

	1°cycle				2°cycle				3°cycle	
	Day 7		Day 14		Day 7		Day 14		Day 7	
	Autotrophy	Heterotrophy	Autotrophy	Heterotrophy	Autotrophy	Heterotrophy	Autotrophy	Heterotrophy	Autotrophy	Heterotrophy
MGDG	13.0 ± 2.7	13.6 ± 1.6	28.1 ± 5.1	26.5 ± 2.3	10.4 ± 0.7	10.2 ± 0.7	22.5 ± 2.2	13.2 ± 9.3	9.5 ± 1.7	10.4 ± 0.4
DGDG	7.6 ± 0.9	5.6 ± 0.6*	15.4 ± 2.2	11.9 ± 1.9	5.3 ± 0.4	3.7 ± 0.3**	10.6 ± 1.3	5.5 ± 4.0	4.7 ± 0.3	4.4 ± 0.3
SQDG	1.6 ± 0.4	0.9 ± 0.3	5.8 ± 2.1	0.5 ± 0.6**	1.3 ± 0.3	0.3 ± 0.2*	2.8 ± 0.7	0.3 ± 0.4*	1.3 ± 0.2	0.8 ± 0.1*
PL	18.2 ± 5.3	19.7 ± 2.1	45.7 ± 13.4	28.7 ± 2.5	15.0 ± 2.7	16.1 ± 1.5	32.7 ± 5.8	19.0 ± 13.5	11.6 ± 1.1	15.3 ± 1.1*
TAG	6.0 ± 2.4	14.9 ± 2.1**	10.9 ± 4.3	89.2 ± 23.4**	4.1 ± 0.4	18.3 ± 10.9*	7.0 ± 1.4	48.5 ± 34.3**	14.2 ± 9.3	11.7 ± 1.7
FFA	1.9 ± 0.3	0.8 ± 1.2	1.9 ± 0.3	0.8 ± 1.2	1.9 ± 0.3	0.8 ± 1.2	1.9 ± 0.3	0.8 ± 1.2	0.0	0.0

3.3 Materials and methods

3.3.1 Strain and culture conditions

Stock cultures of the diatom *C. cryptica* (CCMP 331) purchased from Bigelow Laboratories, were maintained in F/2 medium [45] in batch culture using a week transfer cycle.

For experiments described in this chapter, diatoms were grown in 2L sterile carboy in prefiltered sterile (0.22 µm) F/2 medium at an initial concentration of $1x10^4$ cells/mL.

The cultures were maintained under autotrophic condition, in a growth chamber at 20 ± 2°C on a 14:10 light:dark cycle under a photon flux density of 200 µmol quanta m^{-2} sec^{-1}.

Cells were grown under heterotrophic conditions in a dark chamber 20 ± 2°C. F/2 medium was supplemented with 1 g/L of glucose at day 0 and 7, previously dissolved in natural seawater and filtered with 0.22 µm filter by sterile syringe.

Macronutrients levels were maintained at high regimes, adding nitrates ($NaNO_3$, 882 µmoles L^{-1}) and phosphates ($NaH_2PO_4 \cdot H2O$, 36 µmoles L^{-1}) every 48 hours, and silicate ($Na_2SiO_3 \cdot 9H_2O$, 107 µmoles L^{-1}) every 24 hours.

3.3.2 Batch cultures

In this chapter we reported an experiment conducted in three cycles of growth, both under autotrophic and heterotrophic conditions.

The first cycle started with an inoculum of 10.000 cells/mL in standard F/2 medium. The experiment was conducted in triplicates, in 2L of polypropylene carboys.

At 7^{th} day of culture an aliquot of the cells was collected from each carboy to start a second cycle of growth from 10.000 cells/ml in 2L of final volume, in triplicates, in both conditions.

500 ml of culture were centrifuged for analysis on biomass and the remaining cells were left growing for another 7 days, at 14^{th} day 500 ml of culture were centrifuged again. The same scheme was repeated for the second cycle. The third cycles stopped completely after 7 days.

3.3.3 Biomass content

Cells were harvested after 7 and 14 days of culture, by centrifugation at 3600 rpm for 10 minutes at 12 °C using a swing-out rotor (Allegra X12R - Beckman Coulter).

500 mL of culture were taken from carboys, aliquoted inside a 50 mL falcon and centrifuged. Cells are resuspended and concentrated in a single weighed falcon. The set of concentrated cells is then divided into three parts (1 falcon of 50 mL and 2 of 15 mL):

- 44 mL for the quantification of biomass production, according with d'Ippolito et al. [46] and lipids extraction (MTBE method);
- 5 mL for carbohydrates analysis (DuBois method);
- 1 mL for protein analysis (Lowry method).

These three falcons were centrifuged at 3750 rpm for 10 minutes at 4 ° C, the supernatant removed and re-centrifuged at 3750 rpm for 1 minute at 4 ° C to remove the residual water. All pellets for quantitative analysis were stored at -80° C until analysis. Supernatants filtered with 0.22 µm filter were stored at -20°C.

3.3.3.1 Carbohydrates content measurement (DuBois Method)

The determination of intracellular carbohydrates was performed on the pellet obtained from 5 ml of culture, by the phenol / sulfuric acid assay [47], derived from a method of spectrophotometric analysis of total carbohydrates. Calibration curves were performed with D- glucose as standard (1mg/L). Cells from 50 mL of culture were dissolved in 400 µL of distilled water and hydrolyzed in 1.6 mL of H_2SO_4 (98%) for 20 hours. After diluting with distilled water (1:3; v/v) samples were centrifuged 4°C 5 minutes at 10000 rpm (Thermo ALC PK131R) and supernatants were assayed. In test tubes were added 100 µL of sample, 400 µL of distilled water, 250 µL phenol 5% and 1.25 mL of H_2SO_4 (98%). The samples were shaken and incubated 30 minutes at room temperature. Absorbance readings were performed at λ = 490 nm with a spectrophotometer Jasco (V-650).

3.3.3.2 Protein content measurement (Lowry Method)

The protein content was determined by using the Lowry protein assay following the manufacturer's instructions (Bio-Rad). Calibration curves were performed with bovin serin albumin (BSA) as standard (1mg/L) [48].

The pellet from 1 mL of culture was lyophilized (MicroModulyo, Thermo Fisher Scientific) and dissolved in 100 µL of phosphate buffer 50 mM pH 7.0 and 20 µL of Triton X-100 25%. Samples were then sonicated on ice 5 minutes in an ultrasonic bath at 100 MHz (UltraSONIK NDI) and incubated 15 minutes at room temperature. 380 µL of phosphate buffer was added to each sample and they were centrifuged at 4°C 5 minutes at 10000 rpm (Thermo ALC PK131R). 10, 20 and 40 µL of supernatant were assayed with 50 µL of phosphate buffer 50mM pH 7.0, Triton X-100 1% (v / v) and the sample for a total volume of 50 µL, 100 µL of reagent A + S (20 µL of reagent S / 980 µL of reagent A; alkaline solution of copper tartrate) and 800 µL of reagent B (Folin's reagent).

All tubes were vortexed and incubated at room temperature for 15 minutes in the dark. Spectrophotometric readings were taken at λ = 740 nm (Jasco V-650) against a blank containing all the reagents listed above except the sample. The characteristic blue color is due to the presence of the amino acids tryptophan and tyrosine and, to a lesser extent, cysteine and histidine.

3.3.4 Lipid extraction

Lipid extraction was performed using Methyl tert-butyl ether (MTBE) method, in agreement with Cutignano et al. [49] as reported in the following protocol (solvent volumes are referred to 50 mg of dry weight):

- Transfer 50 mg of lyophilized biomass in a falcon
- Add 500 µL of 4,4'-Dihydroxybenzophenone (DHBP) (1mg/mL) as internal standard
- Add 400 µL of CH_3OH
- Homogenize samples by vortex
- Add 3 ml of Methyl tert-butyl ether (MTBE)
- Allow extraction at room temperature for 1 hour, at constant shaking
- Add 750 µL of distilled water
- Allow extraction at room temperature for 10 min, at constant shaking

- Centrifuge at 1000g, 10min at 4°C
- Transfer organic phase with a Pasteur pipette to a glass rotary evaporator flask
- Add 1 ml of MTBE at the aqueous phase
- Repeat steps 7, 8, 9
- Recover the organic phase in the same round-bottom flask used before
- Dry with rotavapor
- Resuspend the extract in as small volume as possible of a solution of methanol/MTBE 8:2 (v/v)
- Recover the extract in a volumetric vial
- Dry under nitrogen stream, then under vacuum at room temperature
- Weight the extract

3.3.5 ^{1}H-NMR of lipid extracts

The crude lipid extracts, obtained as reported in 3.3.4, were dissolved in 700 µL of $CDCl_3$ / CD_3OD 1: 1 (v / v) and transferred into 5 mm NMR tubes. NMR spectra were recorded on Bruker DRX 600 spectrometer equipped with an inverse TCI CryoProbe. Peak integration, ERETIC measurements and spectrum calibration were obtained by the specific subroutines of Bruker Top-Spin 3.1 program. Spectra were acquired with 14 ppm of spectral width (8417.5 Hz), 32 K of time domain data points, 90°pulse, 32 K spectrum size, and processed with 0.6 Hz of line broadening for the exponential decay function.

The calibration was carried out on the water signal of the deuterated methanol (signal δ 3.34). The quantitative evaluation was performed with the ERETIC method calibrated on the doublet signal at δ 6.90 of the 4,4'-Dihydroxybenzophenone (DHBP) 1 mg ml^{-1} (2.23 µmol in 700 µL of $CDCl_3$/CD_3OD 1:1) (**Figure 3.2**).

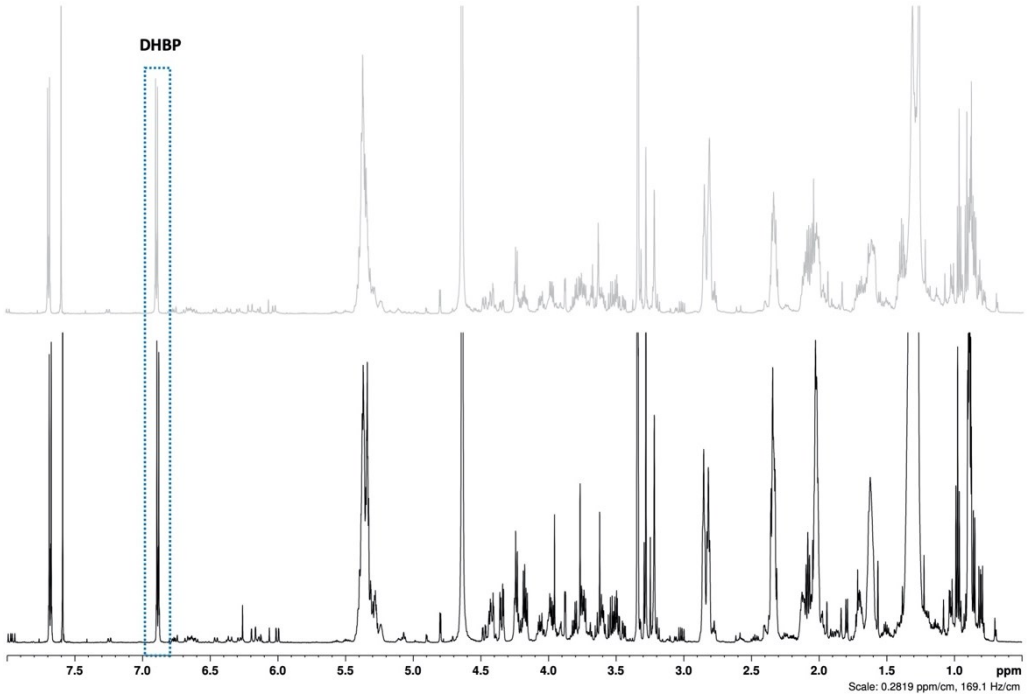

Figure 3.2 ^{1}H-NMR Full spectra in $CDCl_3$:CD_3OD (1:1 v/v) under autototrophic (grey line) and heterotrophic (black line) conditions.

Quantitative assessment of fatty acids was established by ERETIC method in agreement with Nuzzo et al.[40].

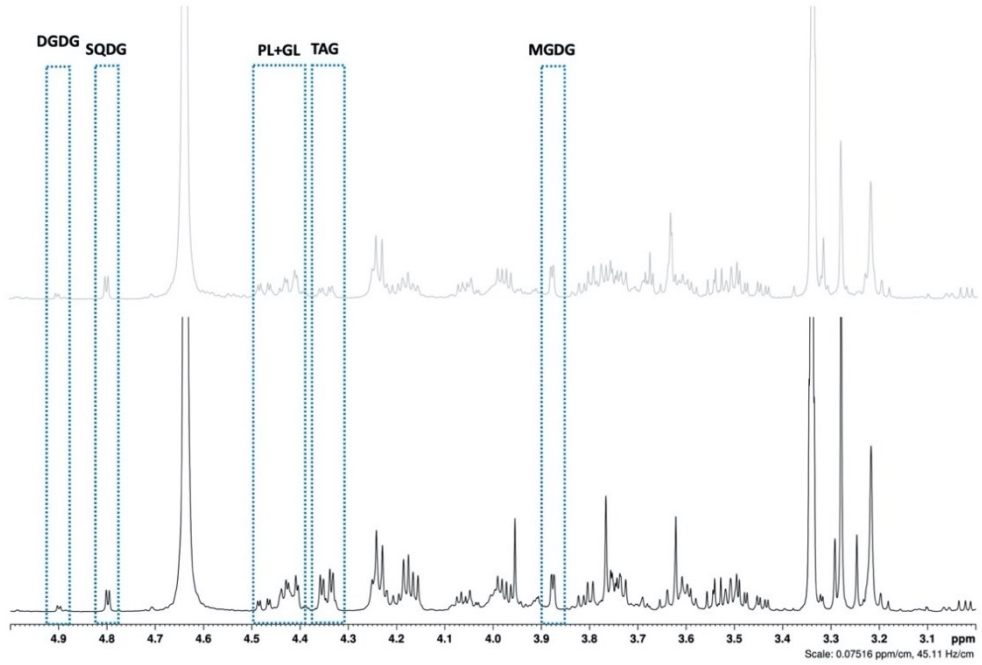

Figure 3.3 ^{1}H-NMR Full in $CDCl_3$:CD_3OD (1:1 v/v) under autototrophic (grey line) and heterotrophic (black line) conditions in the region between 5 and 3 ppm.

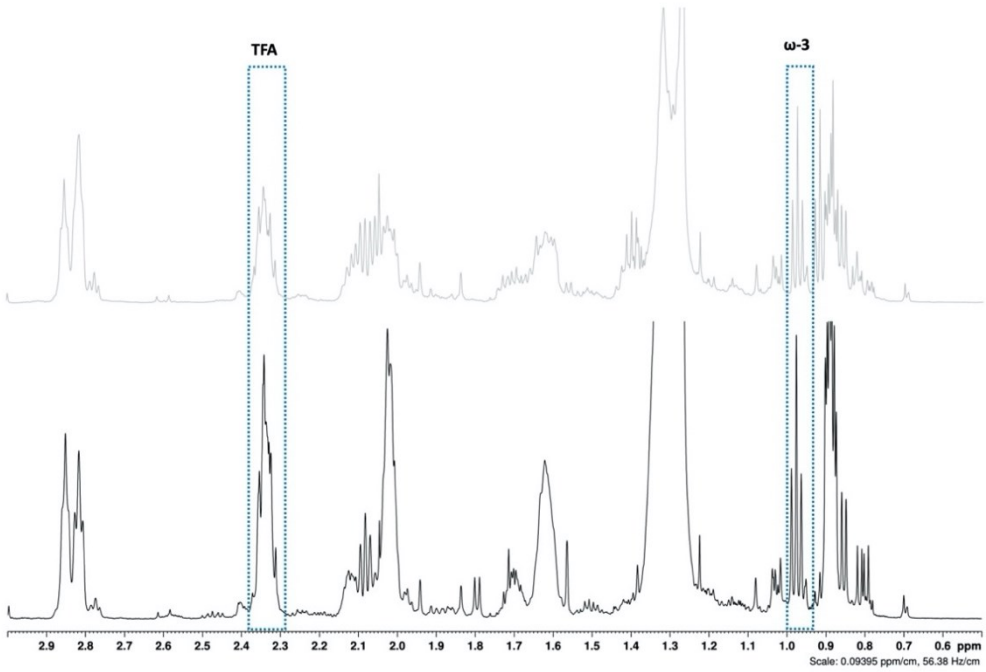

Figure 3.4 ^{1}H-NMR Full in $CDCl_3$:CD_3OD (1:1 v/v) under autototrophic (grey line) and heterotrophic (black line) conditions in the region between 3 and 1 ppm.

In particular, a pure sample of 4,4'-Dihydroxybenzophenone DHBP standard dissolved in $CDCl_3$: CD_3OD (1: 1v/v) was set as ERETIC reference file, assigning to the diagnostic signal at 6.90 ppm a concentration equal to 2.23 µmol in 700 µL of $CDCl_3$ /CD_3OD 1: 1.

Then, the diagnostic signals have been integrated into the spectra of the samples extracts at 4.90 ppm, correspondent to anomeric proton of galactose and assigned to digalactosyldiacylglycerols (DGDG), at 4.80 ppm correspondent to anomeric proton of sulfoquinovoside and assigned to sulfoquinovosyldiacylglycerols (SQDG), in the region comprises between 4.53-4.38 ppm correspondent to methylene proton of glycerol and assigned to phospholipids (PL) and glycolipids (GL) classes, at 4.34 ppm correspondent to methylene protons of glycerol and assigned to triacylglycerols (TAG), at 3.88 ppm correspondent to methine proton at C4 of galactose and assigned to monogalactosyldiacylglycerols (MGDG), (**Figure 3.3**).

Figure 3.4 shows the diagnostic signals centered at 2.34 ppm correspondent to methylene protons α to carboxyl group and assigned to total fatty acids (TFA), at 0.99 ppm correspondent to methyl protons of ω-3 fatty acids and thus assigned to ω-3 fatty acids class.

For each sample, the real number of moles contained in the analyzed extract is calculated based on the percentage of the standard's recovery.

3.3.6 GCMS analysis of lipid extracts

The total fatty acid composition of organic extracts and of lipid classes was determined by GC-MS on the corresponding fatty acid methyl esters (FAME) obtained after saponification of lipid extracts (1mg) with Na_2CO_3 in methanol at 42°C for 4 hours.

The reaction of transesterification was blocked by adding water (to dissolve completely Na_2CO_3) and adjusting to pH=7 with HCl. The extraction was conducted with diethyl ether and water (1:1), the organic phase recovered and dried under nitrogen stream. FAME mixtures were dissolved in methanol (1 µg μL^{-1}) and analyzed by GC-MS (Thermo ITQ 700 Mass spectrometer interfaced with Thermo Focus GC Polaris Q) equipped with an ion-trap on a 5% diphenyl column in EI (70 eV) and positive mode analyzer. Elution of free fatty acid methyl esters required an increasing gradient of temperature according to the following method: 160°C for 3 min then 3°C till 260°C followed by 7min at 310°C. FAME have been identified by

comparation of retention time and mass spectra with FAME standard mixture (Marine source analytical standards, Sigma Aldrich), (**Figure 3.5**).

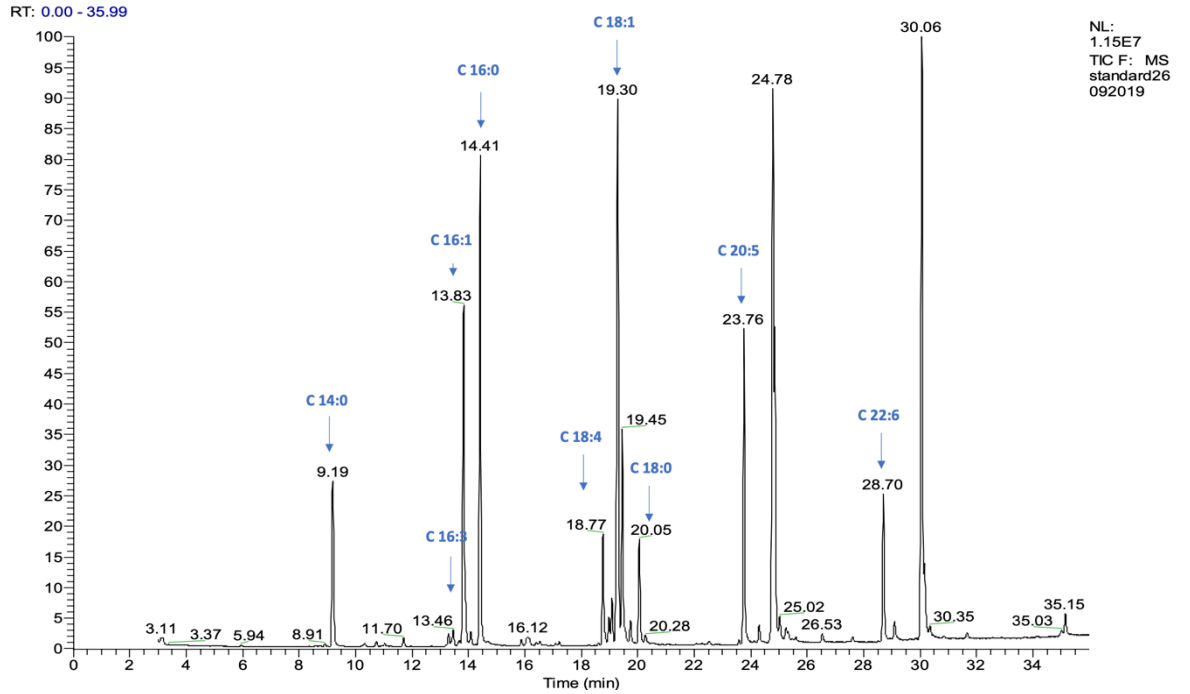

Figure 3.5 GC-MS Full chromatogram of a FAME standard mixture (Marine source analytical standards, Sigma Aldrich).

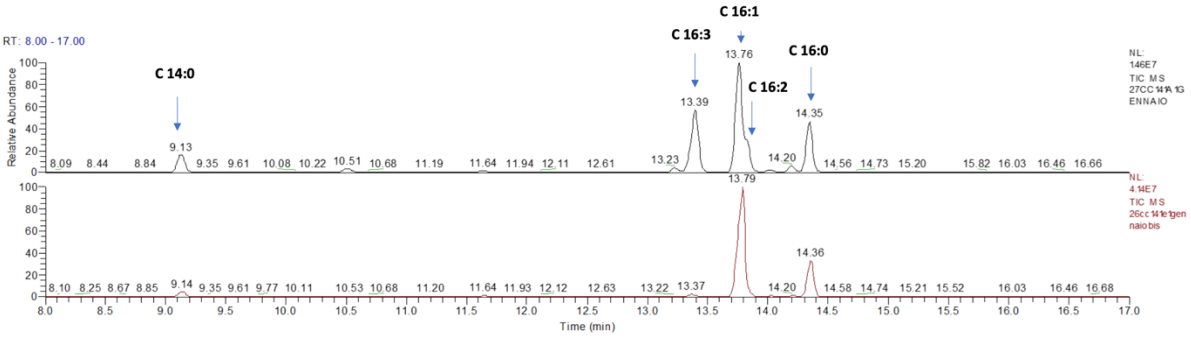

Figure 3.6 GC-MS Chromatogram of *C. cryptica* fatty acids under autotrophic (black line) and heterotrophic (red line) in the region between 8 and 17 min.

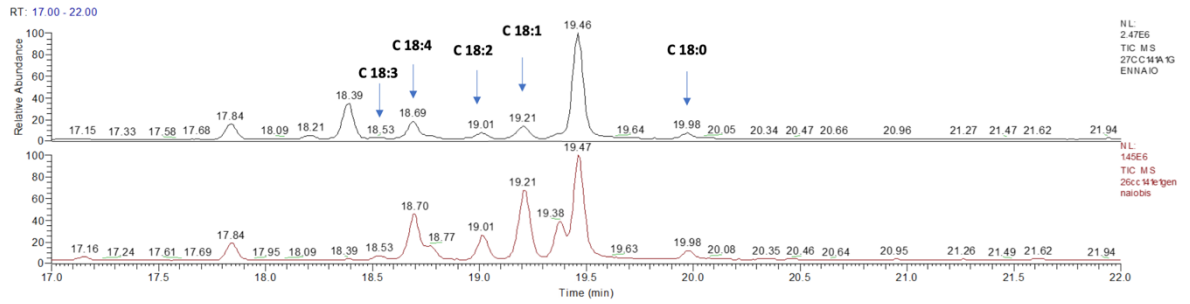

Figure 3.7 GC-MS Chromatogram of *C. cryptica* fatty acids under autotrophic (black line) and heterotrophic (red line) in the region between 17 and 22 min.

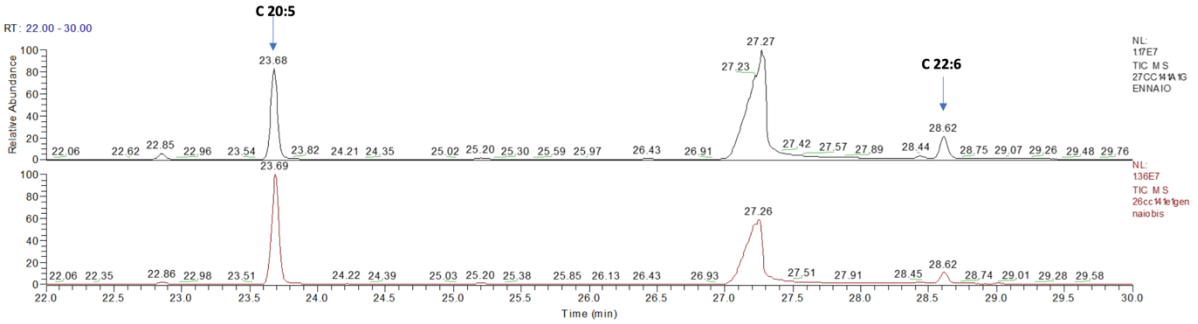

Figure 3.8 GC-MS Chromatogram of *C. cryptica* fatty acids under autotrophic (black line) and heterotrophic (red line) in the region between 22 and 30 min.

Figure 3.6, **Figure 3.7** and **Figure 3.8** showed typical chromatograms of *C. cryptic*a fatty acids under autotrophic condition (black line) and heterotrophic condition (red line) at different retention times.

Following verification of the retention times, mass spectra and thus the presence of molecular ion (**Table 3.8**) for each fatty acid in comparison to the FAME standard mixture, the area associated with each fatty acid in the sample is integrated.

Finally, the relative percentage of each specie is calculated on the total fatty acids.

Table 3.8 Fatty acids and molecular ion mass of correspondent methyl ester

Fatty acids	Molecular Ion Mass
C 22:6	342
C 20:5	316
C 18:4	290
C 18:3	292
C 18:2	294
C 18:1	296
C 18:0	298
C 16:4	262
C 16:3	264
C 16:2	266
C 16:1	268
C 16:0	270

3.4 References

(1) Henry, R. C.; Engström, K.; Olin, S.; Alexander, P.; Arneth, A.; Rounsevell, M. D. A. Food Supply and Bioenergy Production within the Global Cropland Planetary Boundary. *PLoS One* **2018**, *13* (3), 1–17. https://doi.org/10.1371/journal.pone.0194695.

(2) Foley, J. A.; DeFries, R.; Asner, G. P.; Barford, C.; Bonan, G.; Carpenter, S. R.; Chapin, F. S.; Coe, M. T.; Daily, G. C.; Gibbs, H. K.; Helkowski, J. H.; Holloway, T.; Howard, E. A.; Kucharik, C. J.; Monfreda, C.; Patz, J. A.; Prentice, I. C.; Ramankutty, N.; Snyder, P. K. Global Consequences of Land Use. *Science.* **2005**, *309* (5734), 570–574. https://doi.org/10.1126/science.1111772.

(3) Steffen, W.; Richardson, K.; Rockström, J.; Cornell, S. E.; Fetzer, I.; Bennett, E. M.; Biggs, R.; Carpenter, S. R.; De Vries, W.; De Wit, C. A.; Folke, C.; Gerten, D.; Heinke, J.; Mace, G. M.; Persson, L. M.; Ramanathan, V.; Reyers, B.; Sörlin, S. Planetary Boundaries: Guiding Human Development on a Changing Planet. *Science.* **2015**, *347* (6223). https://doi.org/10.1126/science.1259855.

(4) Suganya, T.; Varman, M.; Masjuki, H. H.; Renganathan, S. Macroalgae and Microalgae as a Potential Source for Commercial Applications along with Biofuels Production: A Biorefinery Approach. *Renew. Sustain. Energy Rev.* **2016**, *55* (C), 909–941.

(5) Caporgno, M. P.; Mathys, A. Trends in Microalgae Incorporation Into Innovative Food Products With Potential Health Benefits. *Front. Nutr.* **2018**, *5*. https://doi.org/10.3389/fnut.2018.00058.

(6) Hamed, I. The Evolution and Versatility of Microalgal Biotechnology: A Review. *Compr. Rev. Food Sci. Food Saf.* **2016**, *15* (6), 1104–1123. https://doi.org/10.1111/1541-4337.12227.

(7) Hashemian, M.; Ahmadzadeh, H.; Hosseini, M.; Lyon, S.; Pourianfar, H. R. *Production of Microalgae-Derived High-Protein Biomass to Enhance Food for Animal Feedstock and Human Consumption*; Elsevier Inc., **2019**. https://doi.org/10.1016/B978-0-12-817941-3.00020-6.

(8) Raja, R.; Coelho, A.; Hemaiswarya, S.; Kumar, P.; Carvalho, I. S.; Alagarsamy, A. Applications of Microalgal Paste and Powder as Food and Feed: An Update Using Text Mining Tool. *Beni-Suef Univ. J. Basic Appl. Sci.* **2018**, *7* (4), 740–747.

https://doi.org/10.1016/j.bjbas.2018.10.004.

(9) Torres-Tiji, Y.; Fields, F. J.; Mayfield, S. P. Microalgae as a Future Food Source. *Biotechnol. Adv.* **2020**, *41* (August 2019). https://doi.org/10.1016/j.biotechadv.2020.107536.

(10) Zhu, C. J.; Lee, Y. K. Determination of Biomass Dry Weight of Marine Microalgae. *J. Appl. Phycol.* **1997**, *9* (2), 189–194. https://doi.org/10.1023/A:1007914806640.

(11) Wang, H.; Zhang, Y.; Zhou, W.; Noppol, L.; Liu, T. Mechanism and Enhancement of Lipid Accumulation in Filamentous Oleaginous Microalgae Tribonema Minus under Heterotrophic Condition. *Biotechnol. Biofuels* **2018**, *11* (1), 1–14. https://doi.org/10.1186/s13068-018-1329-z.

(12) Visca, A.; Di Caprio, F.; Spinelli, R.; Altimari, P.; Cicci, A.; Iaquaniello, G.; Toro, L.; Pagnanelli, F. Microalgae Cultivation for Lipids and Carbohydrates Production. *Chem. Eng. Trans.* **2017**, *57*, 127–132. https://doi.org/10.3303/CET1757022.

(13) Spolaore, P.; Joannis-Cassan, C.; Duran, E.; Isambert, A. Commercial Applications of Microalgae. *J. Biosci. Bioeng.* **2006**, *101* (2), 87–96. https://doi.org/10.1263/jbb.101.87.

(14) Camacho, F.; Macedo, A.; Malcata, F. Potential Industrial Applications and Commercialization of Microalgae in the Functional Food and Feed Industries: A Short Review. *Marine Drugs*. **2019**. https://doi.org/10.3390/md17060312.

(15) Vigani, M.; Parisi, C.; Rodríguez-Cerezo, E.; Barbosa, M. J.; Sijtsma, L.; Ploeg, M.; Enzing, C. Food and Feed Products from Micro-Algae: Market Opportunities and Challenges for the EU. *Trends in Food Science and Technology*. Elsevier Ltd March 1, **2015**, pp 81–92. https://doi.org/10.1016/j.tifs.2014.12.004.

(16) Enzing, C.; Ploeg, M.; Barbosa, M.; Sijtsma, L. *Microalgae-Based Products for the Food and Feed Sector: An Outlook for Europe*; **2014**. https://doi.org/10.2791/3339.

(17) Barat, M.; Ferrús, M. A.; Font, G.; Hardisson, A.; Herrera, A.; Lorente, F.; Marcos, A.; Martín, M. R.; Martínez, M. R.; Martínez, A.; Martínez, E.; Nerín, C.; Pérez, G.; Picó, C.; Pintó, R. M.; Pla, A.; Rios, J. L.; Salas, J.; Simal, J. Report of the Scientific Committee of the Spanish Agency for Food Safety and Nutrition on a Request for Initial Assessment for Marketing of the Marine Microalgae *Tetraselmis Chuii* under Regulation (EC) No 258/97 on Novel Foods and Novel Food Ingredients. *Rev. del Com. Científico la AESAN*

2013, *18* (258), 11–28.

(18) Nunes, M. C.; Fernandes, I.; Vasco, I.; Sousa, I.; Raymundo, A. *Tetraselmis Chuii* as a Sustainable and Healthy Ingredient to Produce Gluten-Free Bread: Impact on Structure, Colour and Bioactivity. *Foods* **2020**, *9* (5), 1–15. https://doi.org/10.3390/foods9050579.

(19) Sidari, R.; Tofalo, R. A Comprehensive Overview on Microalgal-Fortified/Based Food and Beverages. *Food Rev. Int.* **2019**, *35* (8), 778–805. https://doi.org/10.1080/87559129.2019.1608557.

(20) Molina Grima, E.; Sánchez Pérez, J. A.; García Camacho, F.; Fernández Sevilla, J. M.; Acién Fernández, F. G.; Urda Cardona, J. Biomass and Icosapentaenoic Acid Productivities from an Outdoor Batch Culture of *Phaeodactylum Tricornutum UTEX 640* in an Airlift Tubular Photobioreactor. *Appl. Microbiol. Biotechnol.* **1995**, *42* (5), 658–663. https://doi.org/10.1007/BF00171940.

(21) Sidari, R.; Tofalo, R. A Comprehensive Overview on Microalgal-Fortified/Based Food and Beverages. *Food Rev. Int.* **2019**, 1–28. https://doi.org/10.1080/87559129.2019.1608557.

(22) Gissibl, A.; Sun, A.; Care, A.; Nevalainen, H.; Sunna, A. Bioproducts From *Euglena Gracilis*: Synthesis and Applications. *Front. Bioeng. Biotechnol.* **2019**, *7* (May), 1–16. https://doi.org/10.3389/fbioe.2019.00108.

(23) Girija, K.; Hemalatha, A.; Karthikeyan, P.; Saranya, C.; Anantharaman, P.; Sampathkumar, P. Effect of Nutrients on the Growth and Biochemical Composition of the Marine Diatom, *Chaetoceros Simplex*. *Int. Res.* **2014**, *5* (1), 30–35.

(24) Lovio-Fragoso, J. P.; de Jesús-Campos, D.; López-Elías, J. A.; Medina-Juárez, L. Á.; Fimbres-Olivarría, D.; Hayano-Kanashiro, C. Biochemical and Molecular Aspects of Phosphorus Limitation in Diatoms and Their Relationship with Biomolecule Accumulation. *Biology (Basel).* **2021**, *10* (7), 565. https://doi.org/10.3390/biology10070565.

(25) Gao, B.; Wang, F.; Huang, L.; Liu, H.; Zhong, Y.; Zhang, C. Biomass, Lipid Accumulation Kinetics, and the Transcriptome of Heterotrophic Oleaginous Microalga *Tetradesmus Bernardii* under Different Carbon and Nitrogen Sources. *Biotechnol. Biofuels* **2021**, *14* (1), 1–16. https://doi.org/10.1186/s13068-020-01868-9.

(26) Xie, T.; Xia, Y.; Zeng, Y.; Li, X.; Zhang, Y. Nitrate Concentration-Shift Cultivation to Enhance Protein Content of Heterotrophic Microalga *Chlorella Vulgaris*: Over-Compensation Strategy. *Bioresour. Technol.* **2017**, *233*, 247–255. https://doi.org/10.1016/j.biortech.2017.02.099.

(27) Pahl, S. L.; Lewis, D. M.; Chen, F.; King, K. D. Heterotrophic Growth and Nutritional Aspects of the Diatom *Cyclotella Cryptica (Bacillariophyceae)*: Effect of Some Environmental Factors. *J. Biosci. Bioeng.* **2010**, *109* (3). https://doi.org/10.1016/j.jbiosc.2009.08.480.

(28) d'Ippolito, G.; Cutignano, A.; Briante, R.; Febbraio, F.; Cimino, G.; Fontana, A. New C16 Fatty-Acid-Based Oxylipin Pathway in the Marine Diatom *Thalassiosira Rotula*. *Org. Biomol. Chem.* **2005**, *3* (22), 4065–4070. https://doi.org/10.1039/B510640K.

(29) Fontana, A.; D'Ippolito, G.; Cutignano, A.; Romano, G.; Lamari, N.; Gallucci, A. M.; Cimino, G.; Miralto, A.; Lanora, A. LOX-Induced Lipid Peroxidation Mechanism Responsible for the Detrimental Effect of Marine Diatoms on Zooplankton Grazers. *ChemBioChem* **2007**, *8* (15), 1810–1818. https://doi.org/10.1002/cbic.200700269.

(30) Hu, Q.; Sommerfeld, M.; Jarvis, E.; Ghirardi, M.; Posewitz, M.; Seibert, M.; Darzins, A. Microalgal Triacylglycerols as Feedstocks for Biofuel Production: Perspectives and Advances. *Plant J.* **2008**, *54* (4), 621–639. https://doi.org/10.1111/j.1365-313X.2008.03492.x.

(31) Pahl, S. L.; Lewis, D. M.; Chen, F.; King, K. D. Growth Dynamics and the Proximate Biochemical Composition and Fatty Acid Profile of the Heterotrophically Grown Diatom *Cyclotella Cryptica*. *J. Appl. Phycol.* **2010**, *22* (2), 165–171. https://doi.org/10.1007/s10811-009-9436-7.

(32) Chen, H. H.; Jiang, J. G. Lipid Accumulation Mechanisms in Auto- and Heterotrophic Microalgae. *J. Agric. Food Chem.* **2017**, *65* (37), 8099–8110. https://doi.org/10.1021/acs.jafc.7b03495.

(33) Barone, R.; de Napoli, L.; Mayol, L.; Paolucci, M.; Volpe, M. G.; D'Elia, L.; Pollio, A.; Guida, M.; Gambino, E.; Carraturo, F.; Marra, R.; Vinale, F.; Woo, S. L.; Lorito, M. Autotrophic and Heterotrophic Growth Conditions Modify Biomolecole Production in the Microalga *Galdieria Sulphuraria (Cyanidiophyceae, Rhodophyta)*. *Mar. Drugs* **2020**, *18* (3). https://doi.org/10.3390/md18030169.

(34) Matos, Â. P.; Cavanholi, M. G.; Moecke, E. H. S.; Sant'Anna, E. S. Effects of Different Photoperiod and Trophic Conditions on Biomass, Protein and Lipid Production by the Marine Alga Nannochloropsis Gaditana at Optimal Concentration of Desalination Concentrate. *Bioresour. Technol.* **2017**, *224*, 490–497. https://doi.org/10.1016/j.biortech.2016.11.004.

(35) Moriyama, T.; Mori, N.; Nagata, N.; Sato, N. Selective Loss of Photosystem I and Formation of Tubular Thylakoids in Heterotrophically Grown Red Alga *Cyanidioschyzon Merolae*. *Photosynth. Res.* **2019**, *140* (3), 275–287. https://doi.org/10.1007/s11120-018-0603-z.

(36) Yang, Z.; Niu, Y.; Ma, Y.; Xue, J.; Zhang, M.; Yang, W.; Liu, J.; Lu, S.; Guan, Y.; Li, H. Molecular and Cellular Mechanisms of Neutral Lipid Accumulation in Diatom Following Nitrogen Deprivation. *Biotechnol. Biofuels* **2013**, *6* (1), 1. https://doi.org/10.1186/1754-6834-6-67.

(37) Cui, Y.; Zhao, J.; Wang, Y.; Qin, S.; Lu, Y. Characterization and Engineering of a Dual-Function Diacylglycerol Acyltransferase in the Oleaginous Marine Diatom *Phaeodactylum Tricornutum*. *Biotechnol. Biofuels* **2018**, *11* (1), 1–13. https://doi.org/10.1186/s13068-018-1029-8.

(38) Yao, Y.; Lu, Y.; Peng, K. T.; Huang, T.; Niu, Y. F.; Xie, W. H.; Yang, W. D.; Liu, J. S.; Li, H. Y. Glycerol and Neutral Lipid Production in the Oleaginous Marine Diatom *Phaeodactylum Tricornutum* Promoted by Overexpression of Glycerol-3-Phosphate Dehydrogenase. *Biotechnol. Biofuels* **2014**, *7* (1), 1–9. https://doi.org/10.1186/1754-6834-7-110.

(39) Wang, X.; Dong, H. P.; Wei, W.; Balamurugan, S.; Yang, W. D.; Liu, J. S.; Li, H. Y. Dual Expression of Plastidial GPAT1 and LPAT1 Regulates Triacylglycerol Production and the Fatty Acid Profile in *Phaeodactylum Tricornutum* 06 Biological Sciences 0601 Biochemistry and Cell Biology. *Biotechnol. Biofuels* **2018**, *11* (1), 1–14. https://doi.org/10.1186/s13068-018-1317-3.

(40) Nuzzo, G.; Gallo, C.; D'Ippolito, G.; Cutignano, A.; Sardo, A.; Fontana, A. Composition and Quantitation of Microalgal Lipids by ERETIC 1H NMR Method. *Mar. Drugs* **2013**, *11* (10), 3742–3753. https://doi.org/10.3390/md11103742.

(41) Chen, G. Q.; Jiang, Y.; Chen, F. Fatty Acid and Lipid Class Composition of the Eicosapentaenoic Acid-Producing Microalga, *Nitzschia Laevis*. *Food Chem.* **2007**, *104*

(4), 1580–1585. https://doi.org/10.1016/j.foodchem.2007.03.008.

(42) Liu, J.; Huang, J.; Sun, Z.; Zhong, Y.; Jiang, Y.; Chen, F. Differential Lipid and Fatty Acid Profiles of Photoautotrophic and Heterotrophic *Chlorella Zofingiensis*: Assessment of Algal Oils for Biodiesel Production. *Bioresour. Technol.* **2011**, *102* (1), 106–110. https://doi.org/10.1016/j.biortech.2010.06.017.

(43) Miyachi, S.; Miyachi, S. and B. A. A. Sulfolipid in *Ochromonas Danica*. *J. Protozool. Protozool.* **1963**, *13* (1), 76–78.

(44) Schaub, I.; Wagner, H.; Graeve, M.; Karsten, U. Effects of Prolonged Darkness and Temperature on the Lipid Metabolism in the Benthic Diatom *Navicula Perminuta* from the Arctic Adventfjorden, Svalbard. *Polar Biol.* **2017**, *40* (7), 1425–1439. https://doi.org/10.1007/s00300-016-2067-y.

(45) Guillard, R. R. L.; Ryther, J. H. Studies of Marine Planktonic Diatoms. I. *Cyclotella Nana Hustedt, and Detonula Confervacea* (CLEVE) . Canadian Journal of Microbiology 8:229-239. *Can. J. Microbiol.* **1962**, *8* (1140), 229–239.

(46) D'Ippolito, G.; Sardo, A.; Paris, D.; Vella, F. M.; Adelfi, M. G.; Botte, P.; Gallo, C.; Fontana, A. Potential of Lipid Metabolism in Marine Diatoms for Biofuel Production. *Biotechnol. Biofuels* **2015**, *8* (1), 1–10. https://doi.org/10.1186/s13068-015-0212-4.

(47) Dubois, M.; Gilles, K. A.; Hamilton, J. K.; Rebers, P. A.; Smith, F. Colorimetric Method for Determination of Sugars and Related Substances. *Anal. Chem.* **1956**, *28* (3), 350–356. https://doi.org/10.1021/ac60111a017.

(48) Lowry, O. H.; Rosenburgh, N. J.; Farr, A. L.; Randall, R. J. Protein Measurement with the Folin Phenol Reagent. *J. Biol. Chem.* **1951**, *193* (1), 265–275. https://doi.org/10.1016/s0021-9258(19)52451-6.

(49) Cutignano, A.; Luongo, E.; Nuzzo, G.; Pagano, D.; Manzo, E.; Sardo, A.; Fontana, A. Profiling of Complex Lipids in Marine Microalgae by UHPLC/Tandem Mass Spectrometry. *Algal Res.* **2016**, *17*, 348–358. https://doi.org/10.1016/j.algal.2016.05.016.

4. Paper published:

Autotrophic vs heterotrophic cultivation of the marine diatom *Cyclotella cryptica* for EPA production

Adelaide Cupo[1,2], Simone Landi[2], Salvatore Morra[1], Genoveffa Nuzzo[1], Carmela Gallo[1], Emiliano Manzo[1], Angelo Fontana[1,2] and Giuliana d'Ippolito[1,*]

[1] Institute of Biomolecular Chemistry CNR (CNR-ICB), Via Campi Flegrei 34, 80078 Pozzuoli, Naples, Italy.
[2] Department of Biology, University of Naples "Federico II", Via Cinthia, I-80126 Napoli, Italy.
* Correspondence: gdippolito@icb.cnr.it

UNIONE EUROPEA
Fondo Sociale Europeo
Ministero dell'Istruzione, dell'Università e della Ricerca
PON RICERCA E INNOVAZIONE 2014 - 2020

marine drugs

MDPI

Article

Autotrophic vs. Heterotrophic Cultivation of the Marine Diatom *Cyclotella cryptica* for EPA Production

Adelaide Cupo [1,2], Simone Landi [2], Salvatore Morra [1], Genoveffa Nuzzo [1], Carmela Gallo [1], Emiliano Manzo [1], Angelo Fontana [1,2] and Giuliana d'Ippolito [1,*]

[1] Institute of Biomolecular Chemistry ICB-CNR, Via Campi Flegrei 34, 80078 Naples, Italy; adelaide.cupo@gmail.com (A.C.); s.morra@icb.cnr.it (S.M.); nuzzo.genoveffa@icb.cnr.it (G.N.); carmen.gallo@icb.cnr.it (C.G.); emanzo@icb.cnr.it (E.M.); afontana@icb.cnr.it (A.F.)
[2] Department of Biology, University of Naples "Federico II", Via Cinthia, 80126 Napoli, Italy; simone.landi@unina.it
* Correspondence: gdippolito@icb.cnr.it

Abstract: Recently, the marketable value of ω-3 fatty acid, particularly eicosapentaenoic acid (EPA), increased considering their health effects for human consumption. Microalgae are considered a valuable and "green" source of EPA alternative to fish oils, but considerable efforts are necessary for their exploitation at an industrial level. Due to the high operation costs of photoautotrophic microalgae cultivation, heterotrophic growth represents a promising economic solution. Marine diatoms are the major ecological producers of ω-3 fatty acids. Few species of diatoms are capable to grow in the dark using organic carbon sources. The marine diatom *Cyclotella cryptica* was cultivated for 14 days under photoautotrophic and heterotrophic conditions to define the effects on growth parameters, lipid production, total fatty acids and EPA content. Photoautotrophic conditions led to a total EPA production of 1.6% of dry weight, 12.2 mg L^{-1} culture and productivity of 0.9 mg L^{-1} day^{-1}. The heterotrophy cultures reported a total EPA production of 2.7% of dry cell weight, 18 mg L^{-1} culture, a productivity of 1.3 mg L^{-1} day^{-1}, which are promising values in the prospective of improving culture parameters for the biotechnological exploitation of dark cultivation. *C. cryptica* could be a potential candidate for the heterotrophic production of EPA, also considering its robustness, capacity to resist to bacterial contaminations and plasticity of lipid metabolism.

Keywords: microalgae; omega-3 fatty acids; biomass; lipids

Citation: Cupo, A.; Landi, S.; Morra, S.; Nuzzo, G.; Gallo, C.; Manzo, E.; Fontana, A.; d'Ippolito, G. Autotrophic vs. Heterotrophic Cultivation of the Marine Diatom *Cyclotella cryptica* for EPA Production. *Mar. Drugs* **2021**, *19*, 355. https://doi.org/10.3390/md19070355

Academic Editors: Marialuisa Menna, Andrew P. Desbois and Óscar Monroig

Received: 19 May 2021
Accepted: 15 June 2021
Published: 23 June 2021

1. Introduction

Eicosapentaenoic acid (EPA) represents a central nutrient for human consumption to counteract cardiovascular disease, diabetes, different types of carcinoma, diabetes mellitus and brain disorders [1–3]. EPA is also a key nutritional requirement during childhood, improving cognitive and visual development. EPA, as well as docosahexaenoic acid (DHA), cannot be synthesized by human beings due to lack of some desaturases and elongases that take part in the synthesis of EPA and DHA from parent ω-3 fatty acids such as linolenic acid (C18:3 ω-3) [4]. To fulfill the daily intake requirement, these ω-3 fatty acids must be taken from outside diet sources [5]. Actually, ω-3 polyunsaturated fatty acids (PUFA) were mainly obtained from fatty fish species, such as herring, mackerel, sardine, menhaden and salmon [6]. However, the global fish stocks cannot be considered a sustainable source of ω-3 fatty acids to fulfill the ever-rising global demand. To eliminate the issues related with fish oils, the exploration of alternative resources of PUFA has been gaining interest in recent years. A total annual worldwide demand of PUFA was calculated at over 1.27 million tonnes [7]. In 2019, the global ω-3 market size was evaluated at USD 2.49 billion and a 7% increase is expected over the period 2020–2027 [8].

Many marine microalgae species naturally produce EPA and DHA as components of glycerolipids [9,10], thus resulting in a sustainable source of these fatty acids [11,12].

Microalgae were mainly cultivated in phototrophic conditions in different systems, namely, open ponds, flat panel or photobioreactors [13]. Although many attempts to develop biorefinery platforms to obtain multiple products from microalgae (oils, pigments, proteins and carbohydrates), the operation costs remain non-competitive in comparison to other technologies [14]. At present, algal oil represents less than 2% of human EPA/DHA consumption, but its contribution has been increasing due to several social attributes including its environmental friendliness, the absence of ocean borne contaminants, its vegetarian nature, as well as the possibility to be manufactured under kosher or halal conditions. A feasible alternative for phototrophic cultures is the use of their heterotrophic growth capacity in the absence of light. Heterotrophy requires an organic carbon source dissolved in the culture media to replace the fixation of atmospheric CO_2 [15]. Any fermenter or bioreactor can be employed for this purpose, such as those used for the industrial production of medicines, beverages, food additives and energy. This approach represents a major outcome in the reduction in microalgae cultivation costs.

A limited number of microalgae species can grow in heterotrophic conditions, especially *Chlorella protothecoides*, *Galdieria sulphuraria*, *Nitzchia laevis*, *Crypthecodinium cohnii* and *Neochloris oleoabundans* [16]. These species were mainly used for the biotechnological production of astaxanthin, biomass, DHA, EPA, hydrogen, lipids, lutein and phycocyanin [14]. The identification of candidate species and strains that have a high potential to grow in heterotroph, as well as the improvement of culture conditions, represent a major challenge for biotechnology research [17,18].

Among microalgae, diatoms represent a primary trophic source in the marine food chain, sustaining zooplankton and fish nutrition and therefore are the major ecological producers of ω-3 fatty acids [19]. Lipid accumulation in these microorganisms represent a carbon and energy storage mechanism, mainly occurring upon perturbing conditions or when photosynthesis exceeds the limitations of growth [9,20,21]. The lipid content can range from 10 to 60% of the diatom biomass and this value is influenced by the species and the metabolic status of the cells [22,23]. Despite the recognized role of diatoms as cell factories for high-value products, few studies have been explored their capacity to grow under heterotrophic conditions. *Nitzschia laevis* represents the most studied case for which impact of cultivation parameters on heterotrophic production of EPA has been assessed [24,25], suggesting that this diatom is a good heterotrophic EPA producer.

The marine diatom *Cyclotella cryptica* has been reported as a species capable of heterotrophic growth [26–28], that has been trialed as part of an artificial diet in the development of juvenile mollusks [29]. Subsequent works have analyzed biochemical composition and nutritional aspects of *C. cryptica* at the exponential growth phase (maximum of 4 days of cultivation), as continuous cultivations are frequently used in aquaculture facilities [30–32], or as fucoxanthin producers [33]. The aim of this study is the assessment of growth performances and EPA production in *C. cryptica* under photoautotrophic and heterotrophic conditions.

2. Results and Discussion

2.1. Growth Curves and Biomass Production by Cyclotella cryptica

The marine diatom *Cyclotella cryptica* was grown in autotrophic and heterotrophic conditions in order to compare the growth performances and EPA production among ω-3 polyunsaturated fatty acids. Autotrophic cultivation was guaranteed by an illumination at 200 µmol (photons) m^{-2} s^{-1} with a 14:10 h (light/dark) photoperiod, whereas heterotrophic growth was carried out by cultivating cells completely in the dark and by supplementing the medium with glucose as an organic carbon source. As showed in Figure 1a, growth curves under autotrophic and heterotrophic conditions displayed a similar trend under a sufficient nutrient regime, albeit the cellular density was slightly smaller in the dark. After a short adaptation phase to the heterotrophic conditions of 3–4 days, the growth rate reflected a rapid increase in cell division. In fact, the doubling time was 2 ± 0.05 days in heterotrophy in comparison with a value of 3.3 ± 0.2 days in

autotrophy, supporting the concept that a minor amount of time is necessary to double the cell number under heterotrophy. The cultures maintained the same intense brown color under photoautotrophic and heterotrophic conditions (Figure 1b,c), due to the persistent presence of fucoxanthin [33].

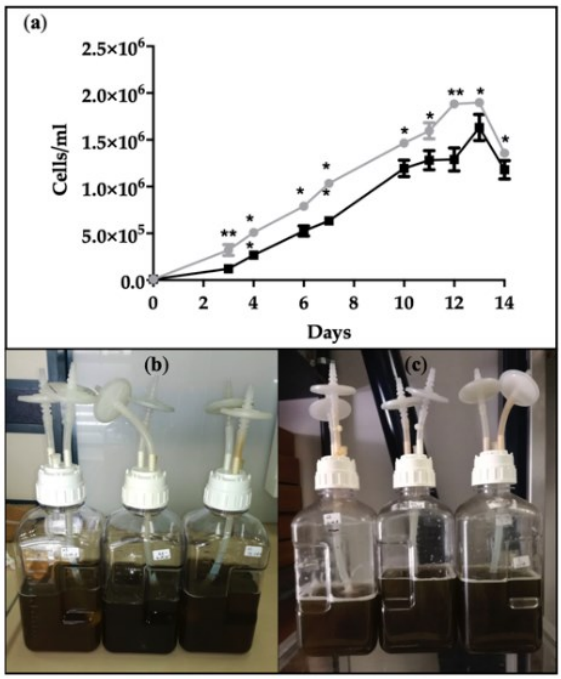

Figure 1. (**a**) Growth curves of *C. cryptica* cells cultivated in autotrophic (grey line) and heterotrophic (black line) conditions. Asterisks indicate significantly different values in autotrophic and heterotrophic samples at $p \leq 0.05$ (*) and $p \leq 0.001$ (**). Data are expressed as means ± SD, $n = 3$. *C. cryptica* cultures in 2 L propylene carboys under autotrophic (**b**) and heterotrophic (**c**) conditions.

2.2. Biomass and Lipid Production

Biomass production was evaluated on the 7th day (exponential phase) and 14th day (first point of senescent phase). After 7 days, the dry biomass was 246.4 ± 15.9 mg L^{-1} in autotrophy and 285.5 ± 21.3 mg L^{-1} in heterotrophy, and similar values of around 584 ± 39 mg L^{-1} were reached after 14 days in both conditions (Figure 2a). Although major cell densities were reached under autotrophic conditions, the comparable biomass level can be explained by considering the major dimension of heterotrophic cells, showing a medium area of about 110 ± 4 μm^2, in comparison with 64 ± 9 μm^2 in autotrophy (Figure 2a), according to the evidence that the glucose generally induced an increase in cell weight due to the higher energetic content of this carbon source. The data are in agreement with reports in other microalgae species such as *Galdiera sulphuraria*, in which a major biomass production and average cell size (10–30%) has been described in heterotrophic conditions [34]. Response in biomass production is strongly species dependent as demonstrated for *Chlorella protothecoides*, *C. vulgaris* and *C. sorokiniana* [35,36]. The marine diatom *Nitzschia laevis* produces major biomass under heterotrophic conditions [25], although the photoautotrophic performance depends on the illumination and photoperiod used for comparation, as well as whether inoculum was cultured in the dark or in the light [21,37].

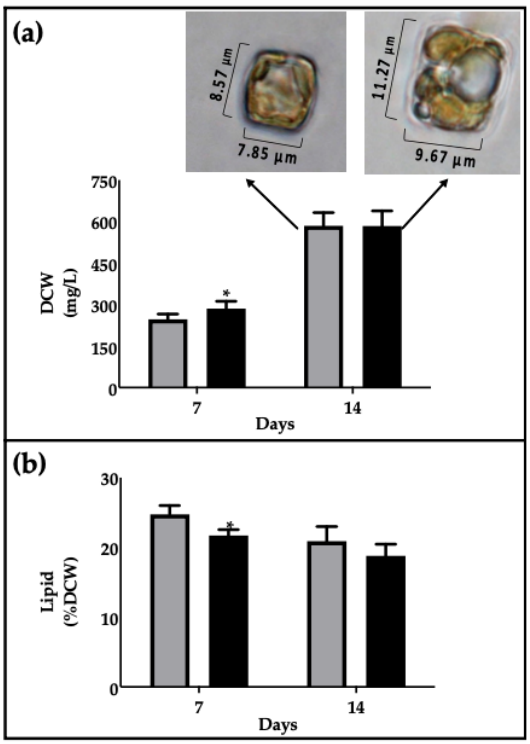

Figure 2. Biomass and lipid content in *C. cryptica* grown in autotrophic (grey bars) and heterotrophic (black bars) conditions. (**a**) Dry cell weight (DCW) expressed as mg/L; boxes contained microscopy images of cells. (**b**) Lipid content expressed as % of DCW. Data are expressed as means ± SD, n = 3. Asterisks indicate significantly different values in autotrophic and heterotrophic samples at $p \leq 0.05$ (*).

The lipid percentage was not significantly affected under two different culture conditions, being 22.2 and 18.8% of dry cell weight (DCW) in autotrophy and heterotrophy, respectively (Figure 2b). Cells were cultivated in both cases under a sufficient nutrient regime and were provided with adequate glucose input in the case of dark cultivation. The response in lipid accumulation by the microalgal cells under autotrophic, mixotrophic and heterotrophic conditions is dependent on the strain and on operational cultivation parameters, such as nutritional factors [38]. *Nannochloropsis gaditana* showed similar percentages of lipids on dry weight in autotrophic, mixotrophic and heterotrophic conditions (10.7–15.7%) [37]. *Chlorella* species showed a higher lipid content in heterotrophy, in comparison to autotrophic conditions [36].

2.3. Fatty Acid Composition

Fatty acid methyl ester (FAME) analysis using GC–MS showed a simplified framework in heterotrophy (Table 1), with a general reduction in some polyunsaturated fatty acid species. Interestingly, the main plastidial polyunsaturated diatom markers 16:2 ω-4, 16:3 ω-4 and 16:4 ω-1 were significantly reduced or disappeared under heterotrophic conditions, in favor of monounsaturated 16:1 ω-7, which is the most abundant fatty acid (around 60% of total fatty acids). EPA and DHA, which remain the most abundant fatty acids among the ω-3 pool, slightly decreased in dark growth, representing 15% and 1.6% of total fatty acids (TFA), respectively, at day 14. Interestingly, 18:0 completely disappeared under heterotrophic conditions.

Similar results were obtained after 7 days of cultivation, supporting the concept that the establishment of dark lipid-phenotype occurs early and is maintained along the growth curve. Data about the EPA% on TFA at the 14th day are in agreement with previous works on the diatoms *C. cryptica* and *N. laevis* grown in heterotrophy, reporting a range of 15–20%, depending on the salinity and silicate levels, glucose input and temperature [31,39]. Overall, the percentage of saturated fatty acids (SFA) did not significantly change, whereas monounsaturated fatty acids (MUFA) significantly increased at the expense of polyunsaturated fatty acids (PUFA), arising values around 60%. This massive mutual redistribution among MUFA and PUFA comparing autotrophy vs. heterotrophy has been rarely documented in marine diatoms, whereas some studies reported a similar, but less attenuated, effect in microalgae such as *Chlorella zofingiensis* and *Galdiera* sp. [40,41]. *Chlorella vulgaris* showed an opposite trend, with a decrease in MUFA in favor of PUFA in heterotrophy, suggesting that the response of fatty acid elongation and desaturation strictly depends on the microalgal species [42–44].

Table 1. Fatty acid composition of *C. cryptica* grown under autotrophic and heterotrophic condition for 7 and 14 days, expressed as a percentage of Total Fatty Acids (TFA). SFA = Saturated Fatty Acids; MUFA = MonoUnsaturated Fatty Acids; PUFA = PolyUnsaturated Fatty Acids, expressed as a percentage of TFA. Asterisks indicate significantly different values in autotrophic and heterotrophic samples at $p \leq 0.05$ (*) and $p \leq 0.001$ (**). Data are expressed as means ± SD, n = 3.

	Day 7		Day 14	
Fatty Acids	**Autotrophy**	**Heterotrophy**	**Autotrophy**	**Heterotrophy**
14:0	5.3 ± 0.1	2.9 ± 0.5 *	5.5 ± 0.03	2.5 ± 0.3 **
16:4 ω-1	0.3 ± 0.01	0 *	1.1 ± 0.2	0 **
16:3 ω-4	22.5 ± 1.9	1.0 ± 0.01 **	21.0 ± 2.3	1.1 ± 0.2 **
16:2 ω-4	7.9 ± 0.1	0 **	6.4 ± 0.9	0 **
16:1 ω-7	23.5 ± 2.7	52.0 ± 0.1 **	28.6 ± 2.6	60.7 ± 2.3 **
16:0	12.2 ± 0.7	17.2 ± 0.3 **	11.4 ± 1.2	16.6 ± 0.3 *
18:4 ω-3	1.4 ± 0.1	1.2 ± 0.2	0.8 ± 0.1	0.9 ± 0.1
18:3 ω-3	0.1 ± 0.01	0.3 ± 0.01 **	0.1 ± 0.01	0.1 ± 0.001 *
18:2 ω-6	0.2 ± 0.03	1.0 ± 0.1 **	0.2 ± 0.003	0.4 ± 0.1
18:1 ω-9	0.4 ± 0.03	1.0 ± 0.05 **	0.5 ± 0.05	1.0 ± 0.1 *
18:0	0.8 ± 0.6	0.3 ± 0.03	0.19 ± 0.03	0 *
20:5 ω-3	23.3 ± 0.6	21.2 ± 0.2 *	19.4 ± 1.0	15.1 ± 1.7 *
22:6 ω-3	2.5 ± 0.3	1.9 ± 0.03	4.8 ± 0.3	1.6 ± 0.2 **
SFA (%TFA)	18.3 ± 0.03	20.4 ± 0.2 **	17.1 ± 1.3	19.2 ± 0.1
MUFA (%TFA)	23.9 ± 2.6	53.0 ± 0.2 **	29.1 ± 2.7	61.7 ± 0.2 **
PUFA (%TFA)	58.4 ± 3.2	26.6 ± 0.03 **	53.8 ± 3.9	19.2 ± 2.3 **

2.4. EPA Production and Productivity

The ERETIC ^{1}H-NMR method was used for the quantitative assessment of Total Fatty Acids (TFA) and ω-3 fatty acids in organic extracts, by integrating the diagnostic peaks at 2.35 ppm (methylene protons in α to carbonyl group) and at 0.9 ppm (methyl protons of ω-3 fatty acids), respectively [45].

In heterotrophy TFA were not significantly different after 7 days of cultivation but were 3-fold higher in heterotrophy than autotrophy after 14 days, arising values of 630 µmol/g DCW (Figure 3a). This is in agreement with the morphology of the cells, which showed an increased presence of vacuolar structures in the dark, attributable to oil droplets (Figure 2a). The diatom *N. laevis* also showed an increase in TFA in the heterotrophic growth mode in comparison to photoautotrophic conditions [25]. The ω-3 fatty acid content is around 80 µmol/g DCW in all conditions, except in the dark at day 14, in which it arises values of 100 µmol/g DCW (Figure 3b).

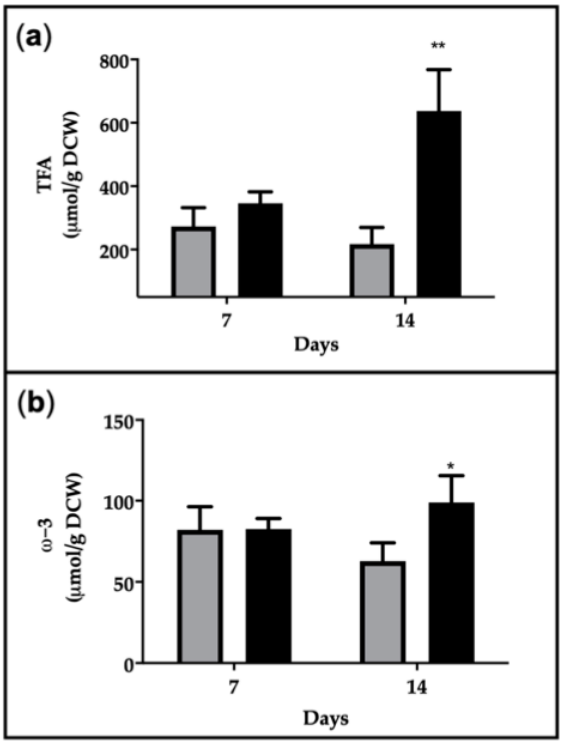

Figure 3. (**a**) TFA production and (**b**) ω-3 production assessed by ^{1}H-NMR in *C. cryptica* cultivated in autotrophic (grey bars) and heterotrophic (black bars) conditions. Data are expressed in µmol/g of Dry Cell Weight (DCW) as means ± SD. Asterisks indicate significantly different values in autotrophic and heterotrophic samples at $p \leq 0.05$ (*) and $p \leq 0.001$ (**).

Considering EPA contribution to ω-3 fatty acids determined by GC–MS, the quantitative assessment of EPA production is reported in Table 2. The results indicated no significant differences in the EPA production at day 7 between autotrophy and heterotrophy, but major values were reached at day 14 in heterotrophy, being 2.7% of DCW, 18 mg L^{-1} and productivity of 1.3 mg L^{-1} day^{-1}.

Table 2. EPA content, expressed as % DCW, production (mg L^{-1}) and productivity (mg L^{-1} day^{-1}), in a comparison between autotrophic and heterotrophic growth of *C. cryptica* at day 7 and day 14. Data are expressed as means ± SD, n = 3. Asterisks indicate significantly different values in autotrophic and heterotrophic conditions at $p \leq 0.05$ (*) and $p \leq 0.001$ (**).

	EPA			
	Day 7		Day 14	
	Autotrophy	Heterotrophy	Autotrophy	Heterotrophy
Content (% DCW)	2.2 ± 2.5	2.2 ± 1.2	1.6 ± 1.5	2.7 ± 1.9 **
Yield (mg L^{-1})	7.3 ± 1.4	7.1 ± 1.0	12.2 ± 1.3	18.0 ± 0.7 **
Productivity (mg L^{-1} day^{-1})	1.0 ± 0.2	1.0 ± 0.1	0.9 ± 0.1	1.3 ± 0.1 *

Despite the recognized role of diatoms as cell factories for high-value products, few studies have explored their capacity for growth under heterotrophic conditions. *Nitzschia laevis* represents the most studied case for which the impact of cultivation parameters on

the heterotrophic production of EPA has been assessed [25,38] suggesting that this diatom is a good heterotrophic EPA producer.

Among the numerous marine diatoms screened, few species were able to grow in heterotrophy and were investigated for heterotrophic EPA production, e.g., *N. laevis*, *Navicula incerta*, *Navicula pelliculosa* and *C. cryptica* (Table 3). Although culture volumes and duration are often limited, the EPA content was estimated between 0.5 and 2.7% of DCW, and EPA represents an abundant polyunsaturated fatty acid, with values from 4.6 to 23.2% of TFA.

Table 3. Comparison of biomass and EPA production of marine diatoms under heterotrophic conditions.

Algal Species	Volume (L)	Cultivation Period (days)	Glucose (g/L)	Biomass (g/L)	EPA (% DCW)	EPA (% in TFA)	Reference
Cyclotella cryptica	0.1	3	10	1	-	18–22	[30]
Nitzschia laevis	0.2	12	20	5.5	1.9	10.7	[41]
Nitzschia laevis	0.2	8	5	2.2	1.7	14.9	[24]
Nitzschia laevis	0.1	-	10	-	1.7	23.2	[23]
Navicula incerta	0.1	-	10	-	0.8	7.2	[23]
Navicula pelliculosa	0.1	-	10	-	0.5	4.6	[23]
Cyclotella cryptica	2	14	2	0.58	2.7	15.1	This study

Glucose and silicate input play a critical role in the production of EPA and TFA in marine diatoms. Although a sufficient amount of silicate appears necessary for an adequate carbon metabolism, the glucose concentration appeared to be mainly related to TFA amounts and, in minor part, to the EPA percentage. Major glucose concentrations (20–50 g/L) led to a major accumulation of TFA but did not change the EPA% on TFA. The nutritional factors to significantly burst EPA biosynthesis have not yet been determined under heterotrophic conditions. Some environmental factors (e.g., salinity, temperature, pH, nitrate sources, silicate concentration), which can modulate lipid metabolism in a massive way under autotrophic conditions, did not affect the fatty acid distribution under heterotrophic growth. Alternative cultivation strategies to improve the final yield of biomass and EPA have been developed. A combination of perfusion and bleeding systems enhance the ability of *N. laevis*, obtaining 6.75 g L^{-1} day^{-1} and 175 mg L^{-1} day^{-1} of biomass and EPA yield, respectively, which are among the highest values ever reported in microalgal cultures [46].

Due to the high biotechnological potential of marine diatoms, the comprehension of lipid metabolism and fatty acid biosynthesis under heterotrophic conditions is crucial to develop economically sustainable processes for the production of high-added value products.

3. Conclusions

Nowadays, the efficient heterotrophic cultivation of diatoms still remains an open challenge. The present work contributed to the expansion of the knowledge about the "dark phenotype" of *C. cryptica* obtained under heterotrophic conditions, in comparison with the classic profile of diatoms under autotrophic conditions. The results indicated comparable levels of EPA production, suggesting that light and CO_2 can be substituted by dark and an organic C source, with the view of reducing cultivation costs using fermentation technologies. This is a promising outcome to ulteriorly improve the heterotrophic cultivation of *C. cryptica* as a suitable method for EPA production to face the increasing global EPA demand. Further studies will be necessary to elucidate the biochemical and molecular network regulating the adaptation of marine diatoms to dark, the metabolic pathways for EPA biosynthesis and lipid remodeling.

4. Materials and Methods

4.1. General

All solvents and standards were purchased from Sigma-Aldrich (Milan, Italy).

^{1}H NMR spectra were recorded on a Bruker DRX 600 spectrometer (purchased from Bruker, Milan, Italy) equipped with an inverse TCI CryoProbe. Peak integration, ERETIC measurements and spectrum calibration were obtained by the specific subroutines of the Bruker Top-Spin 3.1 program. Spectra were acquired with 14 ppm of spectral width (8417.5 Hz), 32 K of time domain data points, 90° pulse, 32 K spectrum size and processed with 0.6 Hz of line broadening for the exponential decay function.

4.2. Strain and Culture Conditions

Cyclotella cryptica (CCMP 331) was purchased from National Center for Marine Algae and Microbiota (Bigelow Laboratory for Ocean Sciences, East Boothbay, ME, USA) and was maintained in an F/2 medium. *C. cryptica* was grown at 20 ± 2 °C in 2 L of polycarbonate carboy in 2 L of pre-filtered sterile (0.22 µm) f/2 medium [47] at an initial concentration of 1×10^4 cells mL^{-1}. Cultures were gently bubbled with sterile air. In autotrophic conditions, diatoms were grown under artificial light (200 µmol photons m^{-2} s^{-1}), provided by daylight fluorescent tubes (OSRAM 965, Germany) with a 14:10 h light:dark photoperiod. In heterotrophic conditions, cultures were incubated in the dark and f/2 medium was supplemented with two pulses of 1g/L glucose for each one, at day 0 and day 7. Macronutrient levels were maintained at high regimes, adding nitrates ($NaNO_3$, 882 µmol L^{-1}) and phosphates ($NaH_2PO_4 \cdot H_2O$, 36 µmol L^{-1}) every 48 h, and silicate ($Na_2SiO_3 \cdot 9H_2O$, 107 µmol L^{-1}) every 24 h. Cell growth was monitored using a microscope (Axio VertA1, Carl Zeiss, magnification of 20X, Milan, Italy) and a Bürker counting chamber (depth 0.100 mm, Merck, Leuven, Belgium).

4.3. Calculation

Growth rate of cultures µ, expressed as divisions day^{-1}, was calculated according to Equation (1), as follows:

$$\mu = (\ln(N_2) - \ln(N_1))/t_2 - t_1 \quad (1)$$

where N_1 and N_2 are cell numbers (cells/mL) at time 1 (t_1) and time 2 (t_2) at the extremes of the linear phase [48]. Doubling time t_d was calculated according to Equation (2), as follows:

$$t_d = \ln 2/\mu \quad (2)$$

Number of doublings (n) at a time interval t is determined by the relation t/t_d, where td is the doubling time or time required to achieve a doubling of the number of viable cells.

4.4. Biomass Content

Cells (500 mL) were harvested using centrifugation with a swing-out rotor at 2300 g for 10 min (Allegra X-12R, Beckman Coulter Inc., Palo Alto, CA, USA). Pellets were frozen at −80°C and lyophilized with a MicroModulyo 230 (Thermo Electron Corporation, Milford, MA, USA). Dry weight was estimated on lyophilized biomass and expressed as mg L^{-1} culture. Biomass productivity was calculated in agreement with d'Ippolito et al. [9].

4.5. Lipid Extraction

Lipid extraction was performed using the Methyl tert-butyl ether (MTBE) method, in agreement with Cutignano et al. [10], using 4,4′-Dihydroxybenzophenone (DHBP) (1 mg mL^{-1}) as the internal standard. In particular, dry cell pellet (50 mg) was suspended with 500 µL of DHBP and 400 µL of MeOH. After vortexing, 3 mL of MTBE were added to allow extraction at room temperature for 1 h, at constant shaking. Then, 750 µL of water were added and samples were left for another 10 min at room temperature, under shaking. Organic extracts were recovered (upper phase), after centrifugation at 1000× *g* for 10 min. The lower phase was re-extracted with 1 mL of MTBE and 750 µL of water, after centrifugation the upper phase was combined with the previous one. The extract was dried under nitrogen flow and weighed to gravimetrically estimate the lipid content (mg L^{-1} culture).

4.6. NMR Analysis of Lipid Extracts

Crude microalgal extracts were dissolved in 700 µL of $CDCl_3/CD_3OD$ 1:1 (*v*/*v*) and transferred to a 5-millimeter NMR tube. ^{1}H-NMR spectra were recorded on a Bruker DRX 600 spectrometer equipped with an inverse TCI CryoProbe. Chemical shift was referred to CHD_2OD signal at δ 3.34. Quantitative assessment of fatty acids was established using the ERETIC method in agreement with Nuzzo et al. [45]. The ERETIC signal was calibrated on the doublet signal at δ 6.90 of DHBP (2.23 µmol in 700 µL of CDCl3/CD3OD 1:1). Peak integration, ERETIC measurements and spectrum calibration were obtained by the specific subroutines of Bruker Top-Spin 3.1 program. Spectra were acquired with 14 ppm of spectral width (8417.5 Hz), 32 K of time domain data points, 90° pulse, 32 K spectrum size and processed with 0.6 Hz of line broadening for the exponential decay function.

The diagnostic peaks in the region between 2.38 and 2.28 ppm, centered at 2.35 ppm (methylene protons in α to carbonyl group), and between 0.99 and 0.95, centered at 0.97 ppm (methyl protons of ω-3 fatty acids) were integrated to assess the µmol of Total Fatty Acids (TFA) and ω-3 fatty acids, respectively [45].

4.7. GC–MS Analysis of Lipid Extracts

The total fatty acid composition of organic extracts was determined using GC–MS on the corresponding fatty acid methyl esters (FAMEs) obtained after saponification of lipid extracts with Na_2CO_3 in methanol at 40 °C for 4 h. The reaction mixture was diluted with milliQ water (to dissolve completely Na_2CO_3), neutralized with HCl 1M, and extracted with diethylether three times. Combined organic extracts were dried under a nitrogen stream, dissolved in MeOH at a final concentration of 1 µg μL^{-1} and analyzed using GC–MS (Thermo Focus GC Polaris Q) equipped with an ion-trap, EI (70 eV), a 5% diphenyl column, an injector temperature of 210 °C, a transfer line temperature of 280 °C. Elution of free fatty acid methyl esters required an increasing gradient of temperature according to the following method: 160 °C for 3 min, increase by 3 °C/min up to 260 °C, increase by 30 °C/min up to 310 °C, 7 min at 310 °C. FAMEs have been identified by the comparation of retention time and mass spectra with FAMEs' standard mixture (Marine source analytical standards, Sigma Aldrich, Milan, Italy). Fatty acid content was expressed as a percentage of total fatty acids, according to Equation (3), as follows:

$$\% \text{ FA} = (\text{Area}_{\text{FA}} * 100)/\text{Area}_{\text{sum of all FA}} \quad (3)$$

4.8. Assessment of EPA Productivity

EPA content on total ω-3 (X_{EPA}) was established using the GC–MS integrating area of all ω-3 fatty acids (EPA; DHA; 18:3 ω-3 and 18:4 ω-3), according to Equation (4). EPA (%DCW) was assessed according to Equation (5), considering the contribution of EPA fraction to ω-3 mmol assessed using ^{1}H-NMR on organic extract obtained from 50 mg of DCW of EPA. EPA production was calculated by considering EPA expressed as % DCW, according to Equation (6), as follows:

$$X_{\text{EPA}/\omega\text{-}3} = \text{Area}_{\text{EPA, GC-MS}}/\text{Area}_{\text{sum all } \omega\text{-}3, \text{ GC-MS}} \quad (4)$$

$$\text{EPA}_{(\%\text{DCW})} = (X_{\text{EPA}/\omega\text{-}3} \times \text{mmol } \omega\text{-}3_{\text{1H-NMR}} \times \text{PM}_{\text{EPA}})/50 \text{ mg DCW} \quad (5)$$

$$\text{EPA production}_{(\text{mg/L culture})} = (\text{Biomass}_{(\text{mg/L})} \times 100)/\text{EPA}_{(\%\text{DCW})} \quad (6)$$

4.9. Statistics

Each experiment was made in at least three replicates. Values were expressed as mean ± standard deviation (SD). The statistical significance was evaluated through Student's *t*-test ($p \leq 0.05$).

Author Contributions: G.d. conceived and planned the experiments; A.C. and S.M. carried out the experiments; A.C., S.L., G.d. and G.N. analyzed the data; C.G., E.M., A.F., reviewed and edited the manuscript. All authors have read and agreed to the published version of the manuscript.

Funding: This research was funded by ADRIAQUANET Project, funded thrugh ERDF, Interreg V-A Italy-Croatia 2014-2020 Program, Blue innovation, ERDF, ID10045161, under Grant Agreement No. 36008.

Institutional Review Board Statement: Not applicable.

Acknowledgments: All the authors acknowledge Lucio Caso for technical support.

Conflicts of Interest: The authors declare no conflict of interest.

References

1. Asgharpour, M.; Rodgers, B.; Hestekin, J.A. Eicosapentaenoic acid from Porphyridium cruentum: Increasing growth and productivity of microalgae for pharmaceutical products. *Energies* **2015**, *8*, 10487–10503. [CrossRef]
2. Dyerberg, J. Linolenate-derived Polyunsaturated Fatty Acids and Prevention of Atherosclerosis. *Nutr. Rev.* **1986**, *44*, 125–134. [CrossRef]
3. Nomura, S.; Kanazawa, S.; Fukuhara, S. Effects of eicosapentaenoic acid on platelet activation markers and cell adhesion molecules in hyperlipidemic patients with Type 2 diabetes mellitus. *J. Diabetes Complicat.* **2003**, *17*, 153–159. [CrossRef]
4. Lands, B. Historical perspectives on the impact of n-3 and n-6 nutrients on health. *Prog. Lipid Res.* **2014**, *55*, 17–29. [CrossRef]
5. Shahidi, F.; Wanasundara, U.N. Omega-3 fatty acid concentrates: Nutritional aspects and production technologies. *Trends Food Sci. Technol.* **1998**, *9*, 230–240. [CrossRef]
6. Leclercq, I.A.; Molendi-Coste, O.; Legry, V. Why and how meet n-3 PUFA dietary recommendations? *Gastroenterol. Res. Pract.* **2010**, *2011*. [CrossRef]
7. Tocher, D.R.; Betancor, M.B.; Sprague, M.; Olsen, R.E.; Napier, J.A. Omega-3 Long-Chain Polyunsaturated Fatty Acids, and Demand. *Nutrients* **2019**, *11*, 89. [CrossRef]
8. Oliver, L.; Dietrich, T.; Marañón, I.; Villarán, M.C.; Barrio, R.J. Producing omega-3 polyunsaturated fatty acids: A review of sustainable sources and future trends for the EPA and DHA market. *Resources* **2020**, *9*, 148. [CrossRef]
9. D'Ippolito, G.; Sardo, A.; Paris, D.; Vella, F.M.; Adelfi, M.G.; Botte, P.; Gallo, C.; Fontana, A. Potential of lipid metabolism in marine diatoms for biofuel production. *Biotechnol. Biofuels* **2015**, *8*, 1–10. [CrossRef]
10. Cutignano, A.; Luongo, E.; Nuzzo, G.; Pagano, D.; Manzo, E.; Sardo, A.; Fontana, A. Profiling of complex lipids in marine microalgae by UHPLC/tandem mass spectrometry. *Algal Res.* **2016**, *17*, 348–358. [CrossRef]
11. Sharma, J.; Sarmah, P.; Bishnoi, N.R. Market Perspective of EPA and DHA Production from Microalgae. In *Nutraceutical Fatty Acids from Oleaginous Microalgae: A Human Health Perspective*; Alok, K.P., Leonidas, M., Eds.; Wiley-Scrivener Publications, Scrivener Publishing LLC: Beverly, MA, USA, 2020; pp. 281–297. [CrossRef]
12. Patel, A.; Karageorgou, D.; Rova, E.; Katapodis, P.; Rova, U.; Christakopoulos, P.; Matsakas, L. An overview of potential oleaginous microorganisms and their role in biodiesel and omega-3 fatty acid-based industries. *Microorganisms* **2020**, *8*, 434. [CrossRef]
13. De Vree, J.H.; Bosma, R.; Janssen, M.; Barbosa, M.J.; Wijffels, R.H. Comparison of four outdoor pilot-scale photobioreactors. *Biotechnol. Biofuels* **2015**, *8*, 1–12. [CrossRef] [PubMed]
14. Wijffels, R.H.; Barbosa, M.J. An Outlook on Microalgal Biofuels. *Science* **2010**, *329*, 796–799. [CrossRef] [PubMed]
15. Perez-Garcia, O.; Escalante, F.M.E.; de-Bashan, L.E.; Bashan, Y. Heterotrophic cultures of microalgae: Metabolism and potential products. *Water Res.* **2011**, *45*, 11–36. [CrossRef] [PubMed]
16. Morales-Sánchez, D.; Martinez-Rodriguez, O.A.; Martinez, A. Heterotrophic cultivation of microalgae: Production of metabolites of commercial interest. *J. Chem. Technol. Biotechnol.* **2017**, *92*, 925–936. [CrossRef]
17. Sheehan, J.; Terri, D.; John, B.; Paul, R. A Look Back at the U.S. Department of Energy's Aquatic Species. *Eur. Phys. J. C* **2012**, *72*, 14.
18. Pérez-López, P.; González-García, S.; Allewaert, C.; Verween, A.; Murray, P.; Feijoo, G.; Moreira, M.T. Environmental evaluation of eicosapentaenoic acid production by Phaeodactylum tricornutum. *Sci. Total Environ.* **2014**, *466–467*, 991–1002. [CrossRef]
19. Jónasdóttir, S.H. Fatty acid profiles and production in marine phytoplankton. *Mar. Drugs* **2019**, *17*, 151. [CrossRef]
20. Chauton, M.S.; Winge, P.; Brembu, T.; Vadstein, O.; Bones, A.M. Gene regulation of carbon fixation, storage, and utilization in the diatom phaeodactylum tricornutum acclimated to light/dark cycles. *Plant Physiol.* **2013**, *161*, 1034–1048. [CrossRef]
21. Chiu, S.Y.; Kao, C.Y.; Tsai, M.T.; Ong, S.C.; Chen, C.H.; Lin, C.S. Lipid accumulation and CO_2 utilization of Nannochloropsis oculata in response to CO_2 aeration. *Bioresour. Technol.* **2009**, *100*, 833–838. [CrossRef]
22. Rodolfi, L.; Zittelli, G.C.; Bassi, N.; Padovani, G.; Biondi, N.; Bonini, G.; Tredici, M.R. Microalgae for oil: Strain selection, induction of lipid synthesis and outdoor mass cultivation in a low-cost photobioreactor. *Biotechnol. Bioeng.* **2009**, *102*, 100–112. [CrossRef] [PubMed]
23. Tan, C.K.; Johns, M.R. Screening of diatoms for heterotrophic eicosapentaenoic acid production. *J. Appl. Phycol.* **1996**, *8*, 59–64. [CrossRef]

24. Wen, Z.-Y.; Chen, F. Production Potential of Eicosapentaenoic Acid by the Diatom Nitzschia Laevis. *Biotechnol. Lett.* **2000**, *22*, 727–733. [CrossRef]
25. Hellebust, J.A. Kinetics of Glucose Transport and Growth of Cyclotella Cryptica Reimann, Lewin and Guillard. *J. Phycol.* **1971**, *7*, 1–4. [CrossRef]
26. White, A.W. Growth of the two facultatively heterotrophic marine centric diatoms. *J. Phycol.* **1974**, *10*, 292–300.
27. Gladue, R.M.; Maxey, J.E. Microalgal feeds for aquaculture. *J. Appl. Phycol.* **1994**, *6*, 131–141. [CrossRef]
28. Laing, I.; Millican, P.F. Indoor nursery cultivation of juvenile bivalve molluscs using diets of dried algae. *Aquaculture* **1992**, *102*, 231–243. [CrossRef]
29. Pahl, S.L.; Lewis, D.M.; King, K.D.; Chen, F. Heterotrophic Production of the Microalgae Cyclotella Cryptica: Fed for Aquaculture. Ph.D. Thesis, The University of Adelaide, Adelaide, Australia, 2010; Volume 24, pp. 235–239. [CrossRef]
30. Pahl, S.L.; Lewis, D.M.; Chen, F.; King, K.D. Growth dynamics and the proximate biochemical composition and fatty acid profile of the heterotrophically grown diatom Cyclotella cryptica. *J. Appl. Phycol.* **2010**, *22*, 165–171. [CrossRef]
31. Pahl, S.L.; Lewis, D.M.; King, K.D.; Chen, F. Heterotrophic growth and nutritional aspects of the diatom Cyclotella cryptica (Bacillariophyceae): Effect of nitrogen source and concentration. *J. Appl. Phycol.* **2012**, *24*, 301–307. [CrossRef]
32. Guo, B.; Liu, B.; Yang, B.; Sun, P.; Lu, X.; Liu, J.; Chen, F. Screening of diatom strains and characterization of Cyclotella cryptica as a potential fucoxanthin producer. *Mar. Drugs* **2016**, *14*, 125. [CrossRef]
33. Liang, Y.; Sarkany, N.; Cui, Y. Biomass and lipid productivities of Chlorella vulgaris under autotrophic, heterotrophic and mixotrophic growth conditions. *Biotechnol. Lett.* **2009**, *31*, 1043–1049. [CrossRef]
34. Rosenberg, J.N.; Kobayashi, N.; Barnes, A.; Noel, E.A.; Betenbaugh, M.J.; Oyler, G.A. Comparative analyses of three Chlorella species in response to light and sugar reveal distinctive lipid accumulation patterns in the microalga *C. sorokiniana*. *PLoS ONE* **2014**, *9*. [CrossRef]
35. Matos, Â.P. The Impact of Microalgae in Food Science and Technology. *J. Am. Oil Chem. Soc.* **2017**, *94*, 1333–1350. [CrossRef]
36. Stadnichuk, I.N.; Rakhimberdieva, M.G.; Bolychevtseva, Y.V.; Yurina, N.P.; Karapetyan, N.V.; Selyakh, I.O. Inhibition by glucose of chlorophyll a and phycocyanobilin biosynthesis in the unicellular red alga Galdieria partita at the stage of coproporphyrinogen III formation. *Plant Sci.* **1998**, *136*, 11–23. [CrossRef]
37. Barone, R.; de Napoli, L.; Mayol, L.; Paolucci, M.; Volpe, M.G.; D'Elia, L.; Pollio, A.; Guida, M.; Gambino, E.; Carraturo, F.; et al. Autotrophic and heterotrophic growth conditions modify biomolecole production in the microalga galdieria sulphuraria (cyanidiophyceae, rhodophyta). *Mar. Drugs* **2020**, *18*, 169. [CrossRef] [PubMed]
38. Sajadian, S.F.; Morowvat, M.H.; Ghasemi, Y. Investigation of autotrophic, heterotrophic, and mixotrophic modes of cultivation on lipid and biomass production in Chlorella vulgaris. *Natl. J. Physiol. Pharm. Pharmacol.* **2018**, *8*, 594–599. [CrossRef]
39. Matos, Â.P.; Cavanholi, M.G.; Moecke, E.H.S.; Sant'Anna, E.S. Effects of different photoperiod and trophic conditions on biomass, protein and lipid production by the marine alga Nannochloropsis gaditana at optimal concentration of desalination concentrate. *Bioresour. Technol.* **2017**, *224*, 490–497. [CrossRef] [PubMed]
40. Wen, Z.Y.; Chen, F. Heterotrophic production of eicosapentaenoic acid by microalgae. *Biotechnol. Adv.* **2003**, *21*, 273–294. [CrossRef]
41. Wen, Z.Y.; Chen, F. Heterotrophic production of eicosapentaenoid acid by the diatom Nitzschia laevis: Effects of silicate and glucose. *J. Ind. Microbiol. Biotechnol.* **2000**, *25*, 218–224. [CrossRef]
42. Liu, J.; Huang, J.; Sun, Z.; Zhong, Y.; Jiang, Y.; Chen, F. Differential lipid and fatty acid profiles of photoautotrophic and heterotrophic Chlorella zofingiensis: Assessment of algal oils for biodiesel production. *Bioresour. Technol.* **2011**, *102*, 106–110. [CrossRef]
43. López, G.; Yate, C.; Ramos, F.A.; Cala, M.P.; Restrepo, S.; Baena, S. Production of Polyunsaturated Fatty Acids and Lipids from Autotrophic, Mixotrophic and Heterotrophic cultivation of Galdieria sp. strain USBA-GBX-832. *Sci. Rep.* **2019**, *9*, 1–13. [CrossRef]
44. Couto, D.; Melo, T.; Conde, T.A.; Costa, M.; Silva, J.; Domingues, M.R.M.; Domingues, P. Chemoplasticity of the polar lipid profile of the microalgae Chlorella vulgaris grown under heterotrophic and autotrophic conditions. *Algal Res.* **2021**, *53*. [CrossRef]
45. Nuzzo, G.; Gallo, C.; D'Ippolito, G.; Cutignano, A.; Sardo, A.; Fontana, A. Composition and quantitation of microalgal lipids by ERETIC 1H NMR method. *Mar. Drugs* **2013**, *11*, 3742–3753. [CrossRef] [PubMed]
46. Wen, Z.Y.; Chen, F. Optimization of nitrogen sources for heterotrophic production of eicosapentaenoic acid by the diatom Nitzschia laevis. *Enzyme Microb. Technol.* **2001**, *29*, 341–347. [CrossRef]
47. Guillard, R.R.L.; Ryther, J.H. Studies of marine planktonic diatoms. I. Cyclotella nana hustedt, and Detonula confervacea (CLEVE). Canadian Journal of Microbiology. *Can. J. Microbiol.* **1962**, *8*, 229–239. [CrossRef] [PubMed]
48. Wood, A.M.; Everroad, R.C.; Wingard, L.M. Measuring growth rates in microalgal cultures. In *Algal Culturing Techniques*; Andersen, R.A., Ed.; Elsevier: Burlington, MA, USA, 2005; pp. 269–286.

5. Manuscript in preparation for submission:

Heterotrophic production of biofuels in the marine diatom *Cyclotella cryptica* by a repeated-batch process.

Salvatore Morra[a], Adelaide Cupo[a,b], Lucio Caso[a], Mariamichela Lanzilli[a], Simone Landi[b], Carmela Gallo[a], Genoveffa Nuzzo[a], Emiliano Manzo[a], Angelo Fontana[a,b] and Giuliana d'Ippolito[a],*

a Bio-Organic Chemistry Unit, Institute of Biomolecular Chemistry CNR (CNR-ICB), Via Campi Flegrei 34, Pozzuoli. Naples. 80078. Italy.
b Department of Biology, University of Naples "Federico II", Via Cinthia, I-80126 Napoli, Italy.
* Corresponding author: gdippolito@icb.cnr.it

This chapter contains part of the experimental activities carried out at I.GI., a vegetable oil refinery, located in Palomonte (SA).

5.1 Abstract

Among microalgae, diatoms are the main component of the phytoplankton and play a major role in the global cycling of carbon and silicon at sea. Diatoms are excellent lipid accumulators and have characteristics, both conceptual and proven, which make them amenable to large-scale biofuel production. Although many attempts to develop biorefinery platforms to obtain multiple products from microalgae (oils, pigments, proteins, and carbohydrates), the operation costs remained non-competitive in comparison to other technologies. Heterotrophic growth represents a sustainable alternative to overcome light and climatic/geographic dependency, and to reduce cultivation costs.

In this context, a repeated-batch process for heterotrophic cultivation of marine diatoms *C. cryptica* for biodiesel production will be described. The marine diatom is cultured under optimized heterotrophic conditions in 6 bioreactors of 10 L each, using glucose as carbon source, harvesting every 7 days 9/10 of the culture, and using 1/10 as seed culture for the next cycle. Results indicated that it's possible to sustain diatom growth in heterotrophic conditions for at least 6 cycles, without using antibiotics. The process led to an average dry biomass production of 1.5 ±0.12 g L^{-1} and a lipid production of 290 ± 36 mg L^{-1}. Lipid extracts contained about 60% triglycerides, 20% phospholipids and 20% glycolipids, as assessed by ^{1}H-NMR. Main fatty acids in biooil were C16:0 (55%), C16:1 ω-7 (25%) and C20:5 ω-3 (14%), distributed in specific modality as acyl chains in glycerolipids. On these bases, biodiesel properties were estimated in terms of main parameters (iodine value, cetane number, saponification value) to define the potentiality of diatom oil as biofuel.

Keywords

Biodiesel; triglycerides; heterotrophy; microalgae

5.2 Introduction

The increasing demand for biofuels, the forthcoming exhaustion of petroleum reservoirs and, the environmental implications of fossil-based diesel productions have attracted huge interest on alternative fuel materials [1–4]. Biodiesel is considered a form of clean, renewable and environmentally beneficial resource to replace or supplement the fossil fuel. Factors like the physicochemical properties of biodiesel, which are comparable to existing diesel, and the increase in the prices of petroleum, further enhance the exploiting of sustainable platforms to meet the worldwide biofuel demand [5,6]. In 2019, the output of biodiesel in European Union, the largest consumer of biodiesel in the global market, reached a record 15.7 billion L, and its demand is set to expand considerably up to reach 16.5 billion L over 2023-2025 [7]. Nowadays, a high percentage of the biodiesel produced comes from a wide range of feedstocks, including plant oils, non-edible oils, animal fats and other resources [3,8,9]. Although, these conventional biodiesel-sources partially satisfy the existing demand, they strongly depend on availability of cultivable lands that compete with areas necessary for the production assigned to human consumption [10]. In this context, microalgae have been proven to be a potent resource for next-generation renewable fuels due to their ability to produce oil [2,3,5]. Microalgae harvest light energy and use CO_2 as a carbon source, producing organic matter and biomass more efficiently and rapidly than terrestrial plants [3,11]. Emphasis on microalgae as biofuel feedstock originates from their capability to synthesize massive amounts of lipids that can be extracted and converted into biofuels, providing simultaneously other commercially compounds with applications in nutraceuticals, pharmaceuticals, and food and chemical industries [11–14]. Oil productivities of microalgae (121104 kg biodiesel/ha/year) greatly surpass those attained from the best producing oil crops (4747 kg biodiesel/ha/year), apart from land area requirements for microalgae cultivation are very low (4%) in comparison to that of crops (soya (330%), jatropha (75%), oil palm (23%) [15–17]. Moreover, microalgae promote a more sustainable biofuel production due to their: (1) contribute in reducing environmental impacts, caused by the use of non-renewable fuels, by capturing atmospheric CO_2; (2) adaptability to the fluctuating growing conditions that allows their cultivation in harsh environments not suitable for other existing biofuel feedstocks [18]. Traditional microalgae cultivation systems are based on autotrophic growth in outdoor open ponds or indoors ponds under artificial lights [19]. Despite many advantages, autotrophic growth can be limited in terms of achieving high

biomass yield and hence oil production as a result of the limitations imposed by lighting at high cell densities during large scale cultivation, and susceptibility to climate, nutrition, and temperature. Additionally, the mass production of algal biomass is generally expensive due to the low biomass productivity and the small cell size that makes costly downstream processes [20]. Challenges to commercial production of microalgae biodiesel could be overcome by maximizing their oil content and cell density and minimizing the cost by coupling residues valorisation, wastewater treatment and, not to mention the recovery of other valuable products [18,19,21–24]. To develop cost-effective algal oil production, a feasible alternative to autotrophic culture, but restricted to a few species, is to harness microalgal ability to grow under heterotrophic conditions. Heterotrophic cultivation is completely performed in a dark environment where the cell growth and the energy requirement are completely supported by organic carbons [25–31]. This approach can circumvent limitations of photoautotrophic cultivation, such as the dependence on light, low photosynthetic efficiencies, the seasonality of manufacturing and the not-economically biomass harvesting, and therefore offers the possibility to obtain high cell density and lipid productivity [19,32,33]. However, only a discrete number of microalgal species have the native capacity to grow heterotrophically, such as *Chlorella*, *Botryococcus*, *Dunaliella*, *Nannochloris*, *Neochloris* and *Parietochloris* species [22,25,34–37]. The average lipid content in different microalgal heterotrophic cultures ranges from 40% to 73% of dry cell weight, rather than 20-50% in autotrophic growth, and some species can reach even 50-100 g/L of dry biomass in heterotrophy, much higher than the maximum 30 g/L of dry cell biomass in autotrophy [3,14,22,38–41]. Notwithstanding this, microalgal-derived biofuel quality and the conversion reaction are affected by lipid class and fatty acid compositions that, in turn, are mostly dependent on multiple abiotic stress factors [13,42]. Lipids produced by microalgae can be classified in: (1) polar lipids (glycolipids and phospholipids) which have a structural function in the cell, and could be transformed in polyunsaturated fatty acids (PUFA) like eicosapentaenoic acid (EPA), docosapentaenoic acid (DPA) and docohexaenoic acid (DHA), and (2) neutral lipids, mainly responsible for energy storage within microalgal cells [2,43–45]. Among the different types of lipids, triacylglycerols (TAG) are the main targets, over glycolipids or phospholipids, for profitable biodiesel production due to their lower degree of unsaturation [2,14,46]. Moreover, TAG can be easily extracted from biomass and directly converted in biofuels by hydrotreating, transesterification, or pyrolysis [14,46,47]. During

heterotrophy, microalgae accumulate a large variety of lipid compounds as storage lipids, but especially triacylglycerols (TAGs) up to 30% of dry cell weight and 70% of total lipid content [31,48]. Alongside the clear benefits of heterotrophy, this mode of growth also has several disadvantages: (1) limited number of microalgae species that can grow heterotrophically, (2) susceptibility to bacterial contamination in a nutrient-rich media; (3) inability to synthetize light-induced metabolites, and (4) costs by adding an organic substrate which leads the nutrient supply to accounts more than 65% on the overall process costs [49,50]. However, high carbon cost can be overcome by integrating heterotrophic growth on inexpensive organic substrate [51–58].

Decades of research on biofuels from microalgae has hidden the attractive attributes of the most productive and environmentally flexible microalgae meaning diatoms. They are highly abundant, with of over 200000 species, and widely distributed in nature which makes them adapt to grow in different environmental conditions [59–63]. Due to their robust nature, the highest cellular density conferred by the naturally bloom formation, and the characteristic to accumulate lipids to greater extent compared to other microalgal classes, diatoms could be biological factories to develop a wide range of sustainable products [60,61,63,64]. On this note, detailed analyses of lipid content in autotrophic diatoms have been reported, while their heterotrophic cultivations have been rarely investigated [61,63,65–72]. Several reports are concentrated on the optimization of EPA, DPA, omega- 3 and DHA productions in heterotrophic diatom for different applications [73–82]. However, diatoms can rapidly tend to produce triacylglycerol, encouraging their application in the biofuel field [63,83]. As a matter of fact, TAG was the predominant lipid class in heterotrophic cultivation achieving, for example, 55.0 %, 69.1%, 87.0% of total lipids in *Crypthecodinium cohnii* [84], *Nitzschia laevis* and *Nitzschia alba* [85] respectively.

5.3 Results and discussion

5.3.1 Growth curves, biomass production and biochemical composition of *C. cryptica*

The marine diatom *C. cryptica* was grown in 10 L carboys under heterotrophic conditions by cultivating cells completely in the dark and by supplementing the medium with glucose as organic carbon source. Optimal glucose concentration for an initial cell density of $2.5x10^5$ cells

mL^{-1} was established as 4 g L^{-1}, under sufficient macronutrient regimes guaranteed by ratio of C/N=30, C/P =25 and Si/C=0.02. Glucose consumption was monitored by ^{1}H-NMR on the media, integrating the diagnostic peak of protons of ß-anomer at C-2 of glucose, centered at 3.24 ppm, considering that at equilibrium the solution contains 36% of the α-anomer and 64% of the β-anomer of glucose. Between day 1 and 5 cells undergo rapid growth, with a doubling time of 1.11 ± 0.1 day and a growth rate of 0.63, that is number of divisions per day. After 5 days of cultivation, glucose was completely consumed, and cell density was $2.7x10^{6}$ cells ml^{-1} (**Figure 5.1**).

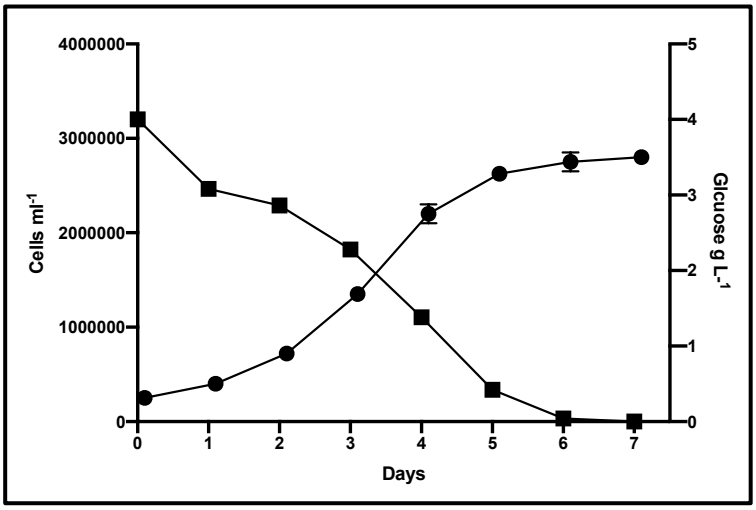

Figure 5.1 Growth curve (round, cells ml^{-1}) and glucose consumption (square, g L^{-1}) of *C. cryptica* cultivated in heterotrophic conditions with 4 g L^{-1} glucose, C/N=30, C/P =25 and Si/C=0.02. Data are expressed as means ± SD, n=3

Biomass increased along the growth curve, arising values around 2.2 g L^{-1} after 5 days of cultivation, and maintaining a stable value due to the shortage of organic source (**Figure 5.2A**). Lipids represent about 13-15% of total biomass and raised the maximum level of 20% ± 0.8 after 7 days, which corresponds to a productive yield of 435.53 mg L^{-1} (**Figure 5.2B**).

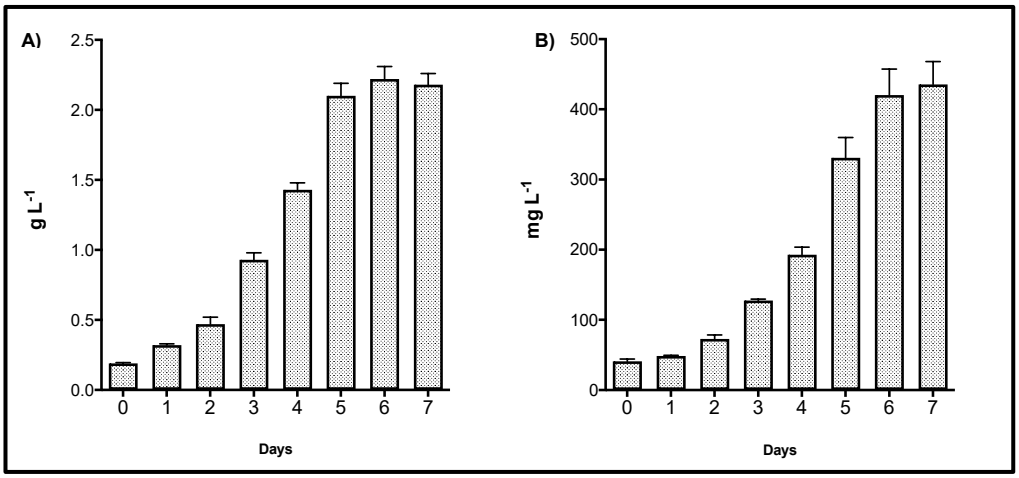

Figure 5.2 Biomass (A, g L^{-1}) and lipid content (B, mg L^{-1}) in *C. cryptica* grown in heterotrophic conditions with 4 g L^{-1} glucose, C/N=30, C/P =25 and Si/C=0.02. Data are expressed as means ± SD, n=3

Distribution of glycerolipids was assessed by ERETIC ^{1}H-NMR method. ^{1}H-NMR spectra of the microalgal extracts were featured by a complex profile showing severe peak overlapping of signals due to triacylglycerols (TAG), free fatty acids (FFA), phospholipids (PL) and glycolipids (GL). This last group was further composed of monogalactosyldiacylglycerols (MGDG), digalactosyldiacylglycerols (DGDG) and sulfoquinovosyldiacylglycerols (SQDG). Regardless of this complexity, the diagnostic signals of each group were clearly discernible and could be integrated by routine Bruker software.

In particular, concentration of TAG was ascertained on the signal at δ 4.34 (dd, J = 4.0, 12.0 Hz) of the primary glycerol protons, whereas the three classes of glycolipids were determined by the sugar resonances at δ 3.88 (d, J = 3.0 Hz) of H-4 of MGDG, and at δ 4.90 (d, J = 3.5 Hz) and 4.80 (d, J = 3.7 Hz) of the anomeric protons of DGDG and SQDG, respectively. Phospholipid percentage was simply inferred by difference between pooled concentrations of PL and GL, as assessed on the signal in the region between 4.53 and 4.38 ppm (sn-1 glycerol protons). Glycerolipids profile undergoes a rearrangement along the growth curve (**Figure 5.3**). Along growth curve TAG increase as percentual component of glycerolipids at the expense of chloroplastic lipids, such as MGDG, DGDG and SQDG. It's interesting to note that negligible level of FFA were detected, demonstrating that under this cultivation conditions and harvesting, cells didn't go to phenomena of lipid hydrolysis, being fatty acids present only as Acyl-CoA in glycerolipids. It's interesting to note that TAG level tends to increase starting from day 5, which coincide with the complete glucose consumption in the culture.

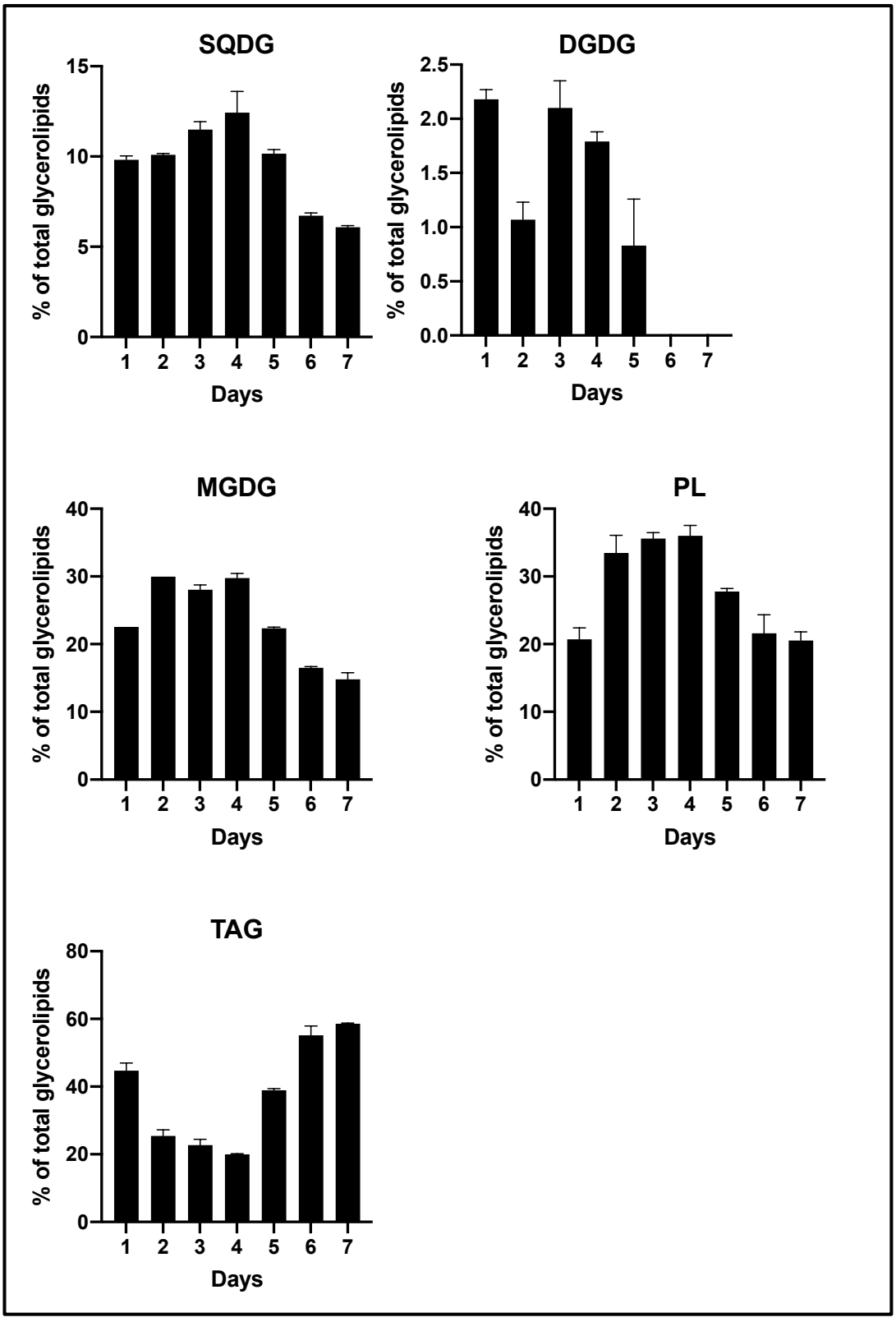

Figure 5.3 Glycerolipid distribution assessed by ^{1}H-NMR, expressed as percentage of total glycerolipids. TAG triacylglycerides, MGDG monogalactosyldiacylglycerol, DGDG digalactosyldiacylglycerol, SQDG sulfoquinovosyldiacylglycerol, PL phospholipids. Data are presented as means ± SD, n = 3

5.3.2 Repeated-batch process: constant cycle repetitions

Heterotrophic repeated batch culture of *C. cryptica* was carried out by continuously repeating different cycles of batch culture at same time interval. The first cycle of repeated batch culture was run by transferring 10% (v/v) of seed culture (1 L) into 9 L of fresh medium, to make a final volume of 10 L for each carboy, for a total of 6 carboy and a total cultivation volume of 60 L. The rest of repeated batch cycles were conducted in similar method to the first cycle. The time interval for the cycles of repeated batch culture, harvesting time, was established as 7 days for each cycle. At the end of this time, 9/10 of culture broth was harvested. And 1/10 was used as inoculum for the next cycle. The whole repeated batch cultures lasted 42 days, for a total of 6 cycles. Cells were harvested at the end of each cycle to assess biochemical parameters, such cell number, biomass, lipid content and glycerolipid distribution. The medium was composed by 4 g/L glucose, C:N 30, C:P 525 e Si:C 0.02. Biomass production along 6 cycles of cultivation tend to decrease from 1.7 g L^{-1} to 1.4 g L^{-1}, with a median value of 1.5 ± 0.1 g L^{-1} (**Figure 5.4A**). Lipid's production expressed as mg L^{-1} varied in a range comprised from 265 mg L^{-1} to 340.04 mg L^{-1} with a median value of 278.2 mg L^{-1} (**Figure 5.4B**).

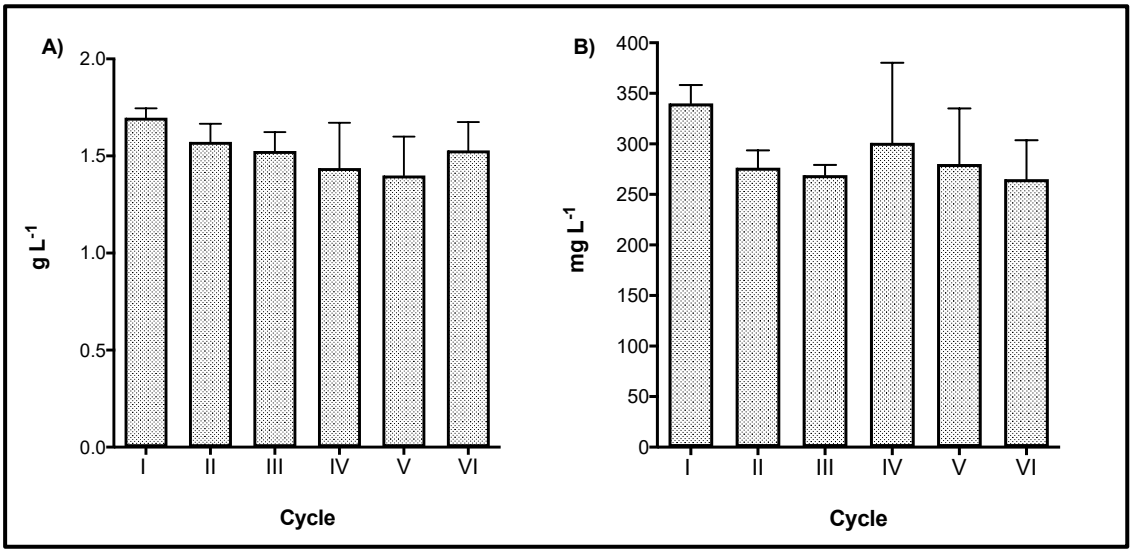

Figure 5.4 Biomass (A, g L^{-1}) and lipid content (B, mg L^{-1}) in *C. cryptica* grown in heterotrophic conditions by repeated batch process with 4 g L^{-1} glucose, C/N=30, C/P =25 and Si/C=0.02. Data are reported as content at the end of each cycle. Data are expressed as means ± SD, n=6

It's interesting to note that glycerolipid distribution remain constant along the cycle of the process, supporting the stability of the cellular phenotype, robustness and reproducibility of

the entire process. In fact, DGDG level varies from 1.7 to 2.3 %, SQDG from 5.1 to 6.4%, MGDG 10 to 14%, PL from 16 to 26% and TAG from 52 to 65% (**Figure 5.5**).

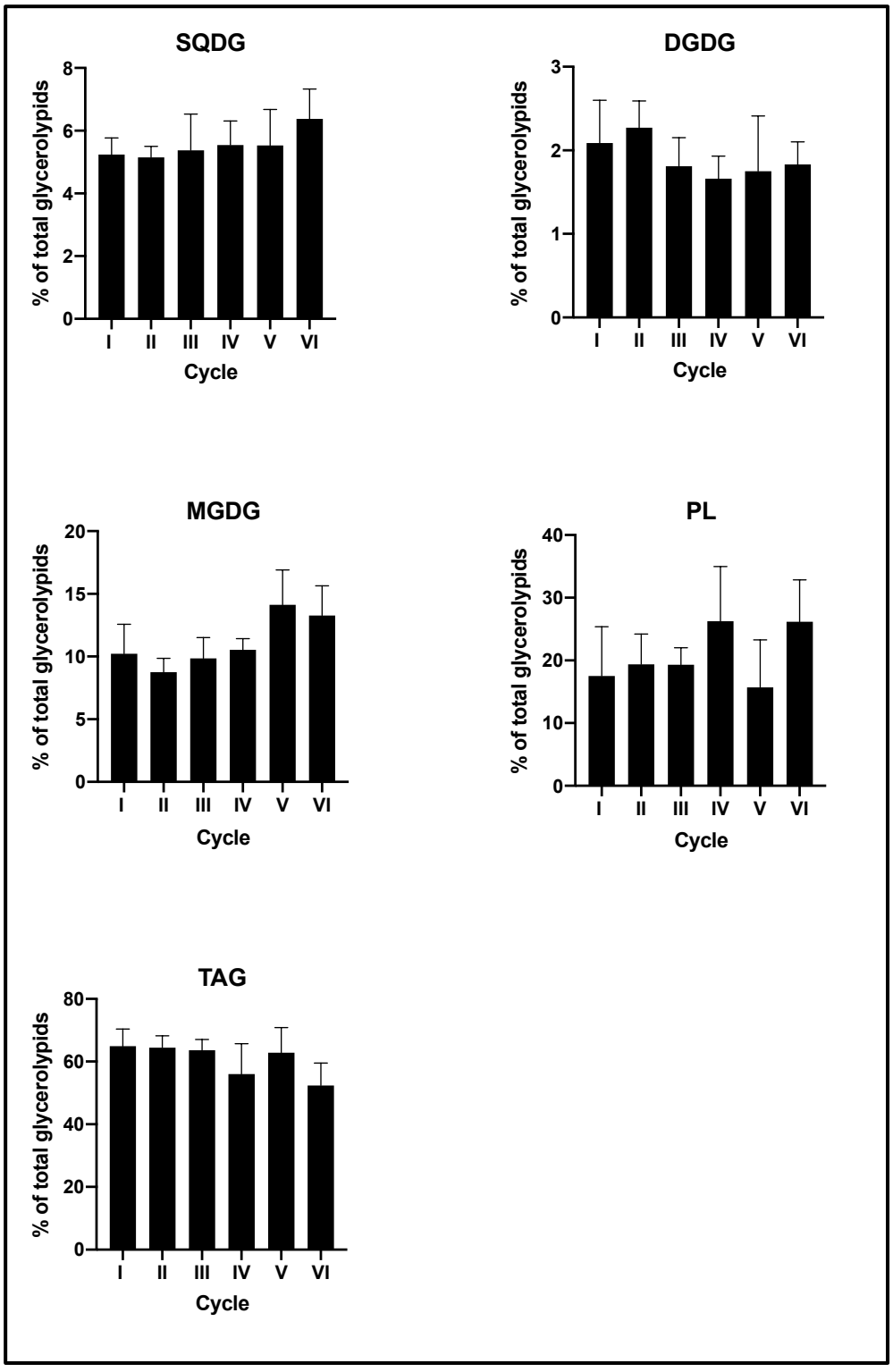

Figure 5.5 Glycerolipid distribution assessed by ^{1}H-NMR, expressed as percentage of total glycerolipids. TAG triacylglycerides, MGDG monogalactosyldiacylglycerol, DGDG digalactosyldiacylglycerol, SQDG sulfoquinovosyldiacylglycerol, PL phospholipids. Data are expressed as means ± SD, n=6.

It's interesting to note that negligible level of FFA were detected in the harvested biomass, demonstrating that under this cultivation conditions and harvesting, cells didn't go to phenomena of lipid hydrolysis, being fatty acids present only as Acyl-CoA in glycerolipids. This aspect is important to prevent soap formation due to high content of free fatty acids in biomass, that impact on the subsequent separation process and leads to partial consumption of the catalyst during saponification.

5.3.3 Biodiesel properties

The fatty acid profile of *C. cryptica* cells grown in heterotrophic conditions showed the presence of mainly C16:0 (55%), C16:1 ω-7 (25%) and C20:5 ω-3 (14%) (**Table 5.1**), that is reflected on the same ground in determination of Saturated Fatty acids (SFA), Mono Unsaturated Fatty Acid (MUFA) and PolyUnsaturated Fatty Acids (PUFA).

Table 5.1 Fatty acid composition of *C. cryptica* grown under heterotrophic conditions by repeated batch process with 4 g L-1 glucose, C/N=30, C/P =25 and Si/C=0.02. Data reported results of entire repeated-batch process, 6 cycles, 42 days of heterotrophic cultivation. Data are expressed as means ± SD, n=36. SFA=Saturated Fatty Acids; MUFA=MonoUnsaturated Fatty Acids; PUFA=PolyUnsaturated Fatty Acids, TFA= Total Fatty Acids.

Fatty Acids	% of TFA
14:0	2.1±0.3
16:1 ω-7	54.8±3.6
16:0	25.1±3.4
18:2 ω-6	0.3±0.1
18:1 ω-9	3.6±1.2
20:5 ω-3	14.1±2.4
22:6 ω-3	0.1±0.005
SFA	27.1±1.5
MUFA	58.4±1.2
PUFA	14.5±1.0

The quality of biodiesel obtained is directly influenced by the composition of the FAs produced by the algal species [86], this makes lipid composition an important parameter in species selection for commercial microalgae biodiesel production [87]. The structural properties of the fatty acids, such as level of saturation, chain length and branching, affects the chemical

and physical properties of biodiesel [88], and in turn, determine the main parameters of the biodiesel including cetane number, oxidative stability, kinematic viscosity, cold flow and lubricity [89].

Simple and reliable calculation methods can be used instead of experimental procedures to estimate biodiesel fuel properties. As a theoretical work, established reliable calculations (equations 1–9) for estimating fuel properties of biodiesel from the composition of FAME were used to estimate biodiesel properties in this study, reported in **Table 5.2**.

Table 5.2 Estimation of biodiesel properties based on the fatty acid profile of *C. cryptica* grown in heterotrophic conditions and comparison with the international standards.
–, not reported; min, minimum; max, maximum

Biodiesel properties	Unit	C.cryptica	ASTMD6751	EN14214
Long chain saturation factor LCSF	-	2.51	-	-
Oxidative stability, 110 °C	h	10.78	min 3	min 6
Density	g/cm^3	0.96	-	0,86-0,90
Cold filter plugging point	°C	-8.6	-	-
Cetane number	-	41.64	min 47	min 51
Kinematic viscosity	mm^2/s	3.42	1.6-6.0	3.5-5
Saponification value	mg KOH/g-oil	214.7	min 0.5	min 0.5
Iodine value	$g\ I_2/100g$	118.1	-	max 120
High heating value	MJ/kg	38.86	-	-

Cetane number (CN) is one of the most important properties of biodiesel, which defines the ignition features of the fuel and is, therefore, correlated to engine performance such as noise generation and CO emissions [90]. Generally, ignition properties get better with increasing CN [91]. The oil obtained from *C. cryptica* showed a CN value of 41.64 which is below the limits set by the mains legislations.

The Cold filter plugging point (CFPP) is the lowest temperature (°C) at which biodiesel easily passes through a standardized filtration device in a specific time [92–94] CFPP of a biodiesel determines its performance during the cold weather. The oil obtained from *C. cryptica* showed low amount of long chain saturated fatty acid, SFA are a small 5 of TFA. The main regulation does not establish a limit on the value of LCSF, but this factor influences the other parameters that determine the quality of the oil.

Long Chain Saturation Factor (LCSF) is one of the most important characteristics of microbe-derived oil; this includes fatty acids where all the carbons of the fatty acid chains are totally saturated with H atoms and this is directly correlated to the cetane number (CN), the CFPP, and the viscosity of biodiesel. A high LCSF number gives a high CN value, which in turn leads to reduced NOx emissions [95]. The value of LCSF influences the parameter CFPP (value: -8.58 °C) which is lower than the main vegetables oil, as shown in the table n° 2. The legislation does not provide limits for the value of CFPP, but certainly a low value of this parameter is a quality index for the oil and allows its use in countries where the climate conditions are more rigids.

Oxidation stability is one of the major issues affecting the use of biodiesel because of its content of polyunsaturated methyl esters[96]. A minimum Rancimat induction period of six hours is defined for biodiesel samples within UNE-EN 14214. This limit corresponds to the period of time passing before fatty acid methyl esters, aged at 110°C under a constant air stream, is degraded to such an extent that the formation of volatile acids can be recorded through a conductivity increase. It is well known that it is very difficult to meet this limit for biodiesel fuels derived from many common raw materials, unless antioxidants are added to the biodiesel.

Saponification value (SV) defines the amount of KOH in mg required to saponify one g of fat under a specific condition and use to measure the molecular weight or chain length of fatty acids. SV is usually low for long chain fatty acids due to a lesser number of carboxylic functional groups per unit fat mass than the short chain fatty acids [97,98].

SV depends on the molecular weight and concentration of fatty acids. There is no limitation above the SV values in the two main regulations. In general, a value between 200 and 250 mg KOH / g oil defines good oil quality. Beyond the upper limit, the oil has the characteristic of producing more glycerol and of being more foaming (foamability). Oil produced by *C. cryptica* has an SV of 214 mg KOH/g oil.

Iodine value (IV) is a measure of total unsaturation within a mixture of fatty acid. It is expressed in grams of iodine which react with 100 g of the respective sample when formally adding iodine to the double bonds. The iodine value of a vegetable oil or animal fat is almost identical to that of the corresponding methyl esters [89].

The IV shows the ability of the oil to undergo oxidation or polymerize; it depends on the number and type of double bonds, even if different compositions of fatty acids can give rise to the same IV.

Several tests on the engine carried out with oils that have different IVs do not justify the preferential use of oils with a low value of this parameter and it is for this reason that a limit for IV is not defined in some regulations. Oil produced by *C. cryptica* showed a value just above the limit for European legislation, and as in the case of the cetane number the reason is to be found in the high concentration of palmitoleic acid and eicosapentaenoic acid.

High Heating Value (HHV) is the amount of heat produced when 1 g of fuel is combusted to produce CO_2 and H_2O at its original temperature. Due to its high oxygen content, biodiesel has lower mass energy values than petroleum diesel. Therefore, increasing the B-level of biodiesel blends results in decreasing energy content. As the FA carbon chain increases (for a constant unsaturation level) the mass fraction of oxygen decreases, so the heating value increases [99]. Unsaturation level has a somewhat stronger influence upon heating values. Compared to saturated esters, unsaturated esters have lower mass energy content (MJ/kg), but higher volumetric energy content (MJ/gal) [100]. Optimal biodiesel has HHV of 39–41 MJ kg that is in the range of *C. cryptica* oil.

In the complex, biodiesel properties of *C. cryptica* respect the characteristics required by American and European regulations, making the oil produced by heterotrophic cultivation of *C. cryptica* a suitable candidate for exploiting low-cost technologies for microalgae-based biodiesel production.

5.4 Materials and Methods

5.4.1 Strain and culture conditions

C. cryptica (CCMP 331) was purchased from National Center for Marine Algae and Microbiota (Bigelow Laboratory for Ocean Sciences, USA) and was maintained in F/2 medium. In heterotrophic conditions, cultures were incubated in the dark and grown at 20± 2°C in 10 L

polycarbonate carboy in a modification of F/2 medium and inoculated with 10% (v/v) up to an initial concentration of 250.000 cells mL^{-1}. The modified medium used during the investigation consisted of (per liter) 0.377g $NaNO_3$ (C/N 30), 0.0345g $NaH_2PO_4*H_2O$, 0.379g $Na_2SiO_3*9H_2O$, 0.0127mg $CuSO_4*5H_2O$, 0.0286mg $ZnSO_4*7H_2O$, 0.013mg $CoCl_2*6H_2O$, 0.008m2g $Na_2MoO_4*2H_2O$, 0.013mg $MnCl_2*4H_2O$, 0.0567g $Na_2EDTA*2H2O$, 0.0409g $FeCl_3*6H_2O$ and was supplemented with 4g/L glucose and refilled with 0.379g $Na_2SiO_3 \cdot 9H_2O$ at day 3. Cultures were gently bubbled with sterile air. Cell growth was monitored by microscope (Axio VertA1, Carl Zeiss, magnification of 20X) and a Bürker counting chamber (depth 0.100 mm, Merck, Leuven, Belgium).

5.4.2 Repeated batch cultures

Repeated batch cultures were carried out by continuously repeating different cycles of batch culture at same time interval of 7 days. The first cycle of repeated batch culture was run by transferring 10% (v/v) of seed culture (1 L) into 9 L of fresh medium in each carboy, to make a final culture medium in the carboy of 10 L, for 6 carboy. The rest of repeated batch cycles were conducted in similar method to the first cycle. The time interval for the cycles of repeated batch culture was defined as harvesting time (7 days) since at the end of this time defined volumes of culture broth were harvested. The whole repeated batch cultures lasted 42 days, for a total of 6 cycles.

5.4.3 Biomass content

An aliquot of 500 ml of culture was taken from the carboy and harvested by centrifugation at 3600 rpm for 10 minutes at 4 °C using a swing- out rotor (Allegra X12R - Beckman Coulter) at the end of the “starter cycle” and of each repeated batch culture. The pellet obtained was resuspended with 50 ml of supernatant. Residual supernatant was recovered, and an aliquot filtered with 0.22µm Millipore filters for the quantitative glucose analysis. Set of concentrated cells is then divided in the following way:

- 44 mL for the quantification of biomass production and lipids extraction (MTBE method);

- 5 mL for carbohydrates analysis (DuBois method);
- 1 mL for protein analysis (Lowry method).

5.4.4 Lipid extraction

Lipid extraction was performed using Methyl tert-butyl ether (MTBE) method, in agreement with [101], using 4,4'-Dihydroxybenzophenone (DHBP) (1mg mL^{-1}) as internal standard. In particular, dry cell pellet (50 mg) was suspended with 500 µl of DHBP and 400 µl of MeOH. After vortexing, 3 mL of MTBE were added to allow extraction at room temperature for 1 hour, at constant shaking. Then, 750 µl of water were added and samples were left for another 10 minutes at room temperature, under shaking. Organic extracts were recovered (upper phase), after centrifugation at 1000g for 10 min.

The lower phase was re- extracted with 1 mL of MTBE and 750 µl of water, after centrifugation the upper phase was combined with the previous one. The extract was dried under nitrogen flow and weighed to estimate, gravimetrically, the lipid content (mg L^{-1} culture)[102].

5.4.5 NMR analysis of lipid extracts

Crude microalgal extracts were dissolved in 700 µL $CDCl_3/CD_3OD$ 1:1 (v/v) and transferred to the 5-mm NMR tube. ^{1}H-NMR spectra were recorded on Bruker DRX 600 spectrometer equipped with an inverse TCI CryoProbe. Chemical shift was referred to CHD_2OD signal at δ 3.34. Quantitative assessment of fatty acids was established by ERETIC method in agreement with Nuzzo et al., [103]. The ERETIC signal was calibrated on the doublet signal at δ 6.90 of DHBP (2.23 µmol in 700 µL $CDCl_3/CD_3OD$ 1:1). Peak integration, ERETIC measurements and spectrum calibration were obtained by the specific subroutines of Bruker Top-Spin 3.1 program. Spectra were acquired with 14 ppm of spectral width (8417.5 Hz), 32 K of time domain data points, 90°pulse, 32 K spectrum size, and processed with 0.6 Hz of line broadening for the exponential decay function.

The diagnostic peaks in the region between 2.38 and 2.28 ppm, centered at 2.35 ppm (methylene protons in α to carbonyl group) and between 0.99 and 0.95 centered at 0.97 ppm

(methyl protons of ω-3 fatty acids) were integrated to assess µmoles of Total Fatty Acids (TFA) and ω-3 fatty acids, respectively.

5.4.6 GCMS analysis of lipid extracts

The total fatty acid composition of organic extracts was determined by GC-MS on the corresponding fatty acid methyl esters (FAME) obtained after saponification of lipid extracts with Na_2CO_3 in methanol at 40°C for 4 hours. The reaction mixture was diluted with milliQ water (to dissolve completely Na_2CO_3), neutralized with HCl 1M, and extracted with diethyl ether for three times. Combined organic extracts were dried under a nitrogen stream, dissolved in MeOH at a final concentration of 1 µg μL^{-1} and analyzed by GC-MS (Thermo Focus GC Polaris Q) equipped with an ion-trap, EI (70 eV), 5% diphenyl column, injector 210°C, transfer line 280°C. Elution of free fatty acid methyl esters required an increasing gradient of temperature according to the following method: 160°C for 3 min, 3°C/min up to 260°C, 30°C/min up to 310°C, 7 min at 310°C. FAMEs have been identified by comparison of retention time and mass spectra with FAME standard mixture (Marine source analytical standards, Sigma Aldrich). Fatty acid content was expressed as % of total fatty acids, according to the formula:

FA= (Area FA x 100) /Area sum of all FA

5.4.7 Calculation of Fuel Properties from Fatty Acid Profiles

Estimation of biodiesel properties was done using the following derived empirical formula, as proposed by [88,104].

Long chain saturation factor (LCSF) is calculated based on equation n° 1

$$LCSF = (0.1 \times C16:0) + (0.5 \times C18:0) + (1 \times C20:0) + (2 \times C24:0) \quad (1)$$

The cold filter plugging point (CFPP) of a biodiesel determines its performance during the cold weather and is calculated on equation n°2

$$CFPP = (3.1417 \times LCSF) - 16.477 \quad (2)$$

The cetane number (CN) is among the most important parameters to define the quality of biodiesel, and is calculated based on equation n°3

$$CN = 46.3 + \left(\frac{5458}{SV}\right) - (0.255 \times IV) \quad (3)$$

Oxidation stability (OS) is one of the major issues affecting the use of biodiesel because of its content of polyunsaturated methyl esters [96]. Value is calculated based on equation n°4.

$$OS = \left(\frac{117.9295}{(C18:2 + C20:5)}\right) + 2.5905 \quad (4)$$

The saponification value (SV) and iodine value (IV) of fat are predicted by the following equation n° 5,6

$$SV = \sum\left(\frac{560 \times \%FA_i}{M_i}\right) \quad (5)$$

$$IV = \sum\left(\frac{254 \times \%FA_i \times DB_i}{M_i}\right) \quad (6)$$

High eating value is calculated based on equation n° 7

$$HHV = 49.43 - (0.041 \times (SV)) - (0.015 \times (IV)) \quad (7)$$

Kinetic viscosity (KV) is calculated based on equation n°8

$$KV = (-12.503 + 2.496) \times \ln M_i - (0.178 \times DB_i) \quad (8)$$

Density (ρ) is calculated based on equation n°9

$$(\rho) = 0.8463 + \left(\frac{4.9}{M_i}\right) + (0.0118 \times DB_i) \quad (9)$$

5.5 References

(1) Ma, F.; Hanna, M. A. Biodiesel Production: A Review. *Bioresour. Technol.* **1999**, *70* (1), 1–15. https://doi.org/10.1016/s0960-8524(99)00025-5.

(2) Hu, Q.; Sommerfeld, M.; Jarvis, E.; Ghirardi, M.; Posewitz, M.; Seibert, M.; Darzins, A. Microalgal Triacylglycerols as Feedstocks for Biofuel Production: Perspectives and Advances. *Plant J.* **2008**, *54* (4), 621–639. https://doi.org/10.1111/j.1365-313X.2008.03492.x.

(3) Chisti, Y. Biodiesel from Microalgae. *Biotechnol. Adv.* **2007**, *25* (3), 294–306. https://doi.org/10.1016/j.biotechadv.2007.02.001.

(4) Shafiee, S.; Topal, E. When Will Fossil Fuel Reserves Be Diminished? *Energy Policy* **2009**, *37* (1), 181–189. https://doi.org/10.1016/j.enpol.2008.08.016.

(5) Huang, G. H.; Chen, F.; Wei, D.; Zhang, X. W.; Chen, G. Biodiesel Production by Microalgal Biotechnology. *Appl. Energy* **2010**, *87* (1), 38–46. https://doi.org/10.1016/j.apenergy.2009.06.016.

(6) Mofijur, M.; Atabani, A. E.; Masjuki, H. H.; Kalam, M. A.; Masum, B. M. A Study on the Effects of Promising Edible and Non-Edible Biodiesel Feedstocks on Engine Performance and Emissions Production: A Comparative Evaluation. *Renew. Sustain. Energy Rev.* **2013**, *23*, 391–404. https://doi.org/10.1016/j.rser.2013.03.009.

(7) IEA. Renewables 2020, IEA, Paris https://www.iea.org/reports/renewables-2020.

(8) Knothe, G.; Dunn, R. O.; Bagby, M. O. Biodiesel: The Use of Vegetable Oils and Their Derivatives as Alternative Diesel Fuels. *ACS Symp. Ser.* **1997**, *666*, 172–208. https://doi.org/10.1021/bk-1997-0666.ch010.

(9) Singh, S. P.; Singh, D. Biodiesel Production through the Use of Different Sources and Characterization of Oils and Their Esters as the Substitute of Diesel: A Review. *Renew. Sustain. Energy Rev.* **2010**, *14* (1), 200–216. https://doi.org/10.1016/j.rser.2009.07.017.

(10) Hajjari, M.; Tabatabaei, M.; Aghbashlo, M.; Ghanavati, H. A Review on the Prospects of Sustainable Biodiesel Production: A Global Scenario with an Emphasis on Waste-Oil Biodiesel Utilization. *Renew. Sustain. Energy Rev.* **2017**, *72* (October 2015), 445–464. https://doi.org/10.1016/j.rser.2017.01.034.

(11) Becker, E. W.; Wolfgang, E. Microalgae: Biotechnology and Microbiology. *Cambridge Univ. Press. Cambridge* **1994**, *153–154*.

(12) Khan, M. I.; Shin, J. H.; Kim, J. D. The Promising Future of Microalgae: Current Status, Challenges, and Optimization of a Sustainable and Renewable Industry for Biofuels, Feed, and Other Products. *Microb. Cell Fact.* **2018**, *17* (1), 1–21. https://doi.org/10.1186/s12934-018-0879-x.

(13) Sajjadi, B.; Chen, W. Y.; Raman, A. A. A.; Ibrahim, S. Microalgae Lipid and Biomass for Biofuel Production: A Comprehensive Review on Lipid Enhancement Strategies and Their Effects on Fatty Acid Composition. *Renew. Sustain. Energy Rev.* **2018**, *97* (September), 200–232. https://doi.org/10.1016/j.rser.2018.07.050.

(14) Ferreira, G. F.; Ríos Pinto, L. F.; Maciel Filho, R.; Fregolente, L. V. A Review on Lipid Production from Microalgae: Association between Cultivation Using Waste Streams and Fatty Acid Profiles. *Renew. Sustain. Energy Rev.* **2019**, *109* (April), 448–466. https://doi.org/10.1016/j.rser.2019.04.052.

(15) Georgianna, D. R.; Mayfield, S. P. Exploiting Diversity and Synthetic Biology for the

Production of Algal Biofuels. *Nature* **2012**, *488* (7411), 329–335. https://doi.org/10.1038/nature11479.

(16) Medipally, S. R.; Yusoff, F. M.; Banerjee, S.; Shariff, M. Microalgae as Sustainable Renewable Energy Feedstock for Biofuel Production. *Biomed Res. Int.* **2015**, *2015*. https://doi.org/10.1155/2015/519513.

(17) Culaba, A. B.; Ubando, A. T.; Ching, P. M. L.; Chen, W. H.; Chang, J. S. Biofuel from Microalgae: Sustainable Pathways. *Sustain.* **2020**, *12* (19), 1–19. https://doi.org/10.3390/su12198009.

(18) Razzak, S. A.; Hossain, M. M.; Lucky, R. A.; Bassi, A. S.; De Lasa, H. Integrated CO2 Capture, Wastewater Treatment and Biofuel Production by Microalgae Culturing - A Review. *Renew. Sustain. Energy Rev.* **2013**, *27*, 622–653. https://doi.org/10.1016/j.rser.2013.05.063.

(19) Suali, E.; Sarbatly, R. Conversion of Microalgae to Biofuel. *Renew. Sustain. Energy Rev.* **2012**, *16* (6), 4316–4342. https://doi.org/10.1016/j.rser.2012.03.047.

(20) Acién, F. G.; Molina, E.; Fernández-Sevilla, J. M.; Barbosa, M.; Gouveia, L.; Sepúlveda, C.; Bazaes, J.; Arbib, Z. Economics of Microalgae Production. *Microalgae-Based Biofuels Bioprod. From Feed. Cultiv. to End-Products* **2017**, 485–503. https://doi.org/10.1016/B978-0-08-101023-5.00020-0.

(21) Zhou, W.; Min, M.; Li, Y.; Hu, B.; Ma, X.; Cheng, Y.; Liu, Y.; Chen, P.; Ruan, R. A Hetero-Photoautotrophic Two-Stage Cultivation Process to Improve Wastewater Nutrient Removal and Enhance Algal Lipid Accumulation. *Bioresour. Technol.* **2012**, *110*, 448–455. https://doi.org/10.1016/j.biortech.2012.01.063.

(22) Zhang, T. Y.; Wu, Y. H.; Zhu, S. F.; Li, F. M.; Hu, H. Y. Isolation and Heterotrophic Cultivation of Mixotrophic Microalgae Strains for Domestic Wastewater Treatment and Lipid Production under Dark Condition. *Bioresour. Technol.* **2013**, *149*, 586–589. https://doi.org/10.1016/j.biortech.2013.09.106.

(23) Ummalyma, S. B.; Sukumaran, R. K. Cultivation of Microalgae in Dairy Effluent for Oil Production and Removal of Organic Pollution Load. *Bioresour. Technol.* **2014**, *165* (C), 295–301. https://doi.org/10.1016/j.biortech.2014.03.028.

(24) Morales-Sánchez, D.; Martinez-Rodriguez, O. A.; Martinez, A. Heterotrophic Cultivation of Microalgae: Production of Metabolites of Commercial Interest. *J. Chem. Technol. Biotechnol.* **2017**, *92* (5), 925–936. https://doi.org/10.1002/jctb.5115.

(25) Miao, X.; Wu, Q. Biodiesel Production from Heterotrophic Microalgal Oil. *Bioresour. Technol.* **2006**, *97* (6), 841–846. https://doi.org/10.1016/j.biortech.2005.04.008.

(26) Xu, H.; Miao, X.; Wu, Q. High Quality Biodiesel Production from a Microalga Chlorella Protothecoides by Heterotrophic Growth in Fermenters. *J. Biotechnol.* **2006**, *126* (4), 499–507. https://doi.org/10.1016/j.jbiotec.2006.05.002.

(27) Li, X.; Xu, H.; Wu, Q. Large-Scale Biodiesel Production from Microalga Chlorella Protothecoides through Heterotrophic Cultivation in Bioreactors. *Biotechnol. Bioeng.* **2007**, *98* (4), 764–771. https://doi.org/10.1002/bit.21489.

(28) Chen, G. Q.; Chen, F. Growing Phototrophic Cells without Light. *Biotechnol. Lett.* **2006**, *28* (9), 607–616. https://doi.org/10.1007/s10529-006-0025-4.

(29) Gao, C.; Zhai, Y.; Ding, Y.; Wu, Q. Application of Sweet Sorghum for Biodiesel Production by Heterotrophic Microalga Chlorella Protothecoides. *Appl. Energy* **2010**, *87* (3), 756–761. https://doi.org/10.1016/j.apenergy.2009.09.006.

(30) Perez-Garcia, O.; Escalante, F. M. E.; de-Bashan, L. E.; Bashan, Y. Heterotrophic Cultures

of Microalgae: Metabolism and Potential Products. *Water Res.* **2011**, *45* (1), 11–36. https://doi.org/10.1016/j.watres.2010.08.037.

(31) Chen, H. H.; Jiang, J. G. Lipid Accumulation Mechanisms in Auto- and Heterotrophic Microalgae. *J. Agric. Food Chem.* **2017**, *65* (37), 8099–8110. https://doi.org/10.1021/acs.jafc.7b03495.

(32) Zhu, X, G.; Long, S. R.; Ort, D. R. What Is the Maximum Efficiency with Which Photosynthesis Can Convert Solar Energy into Biomass? *Curr. Opin. Biotechnol.* **2008**, *19* (2), 153–159. https://doi.org/10.1016/j.copbio.2008.02.004.

(33) Bumbak, F.; Cook, S.; Zachleder, V.; Hauser, S.; Kovar, K. Best Practices in Heterotrophic High-Cell-Density Microalgal Processes: Achievements, Potential and Possible Limitations. *Appl. Microbiol. Biotechnol.* **2011**, *91* (1), 31–46. https://doi.org/10.1007/s00253-011-3311-6.

(34) Vazhappilly, R.; Chen, F. Eicosapentaenoic Acid and Docosahexaenoic Acid Production Potential of Microalgae and Their Heterotrophic Growth. *JAOCS, J. Am. Oil Chem. Soc.* **1998**, *75* (3), 393–397. https://doi.org/10.1007/s11746-998-0057-0.

(35) Pahl, S. L.; Lewis, D. M.; Chen, F.; King, K. D. Growth Dynamics and the Proximate Biochemical Composition and Fatty Acid Profile of the Heterotrophically Grown Diatom Cyclotella Cryptica. *J. Appl. Phycol.* **2010**, *22* (2), 165–171. https://doi.org/10.1007/s10811-009-9436-7.

(36) Xiong, W.; Li, X.; Xiang, J.; Wu, Q. High-Density Fermentation of Microalga Chlorella Protothecoides in Bioreactor for Microbio-Diesel Production. *Appl. Microbiol. Biotechnol.* **2008**, *78* (1), 29–36. https://doi.org/10.1007/s00253-007-1285-1.

(37) Alkhamis, Y.; Qin, J. G. Cultivation of Isochrysis Galbana in Phototrophic, Heterotrophic, and Mixotrophic Conditions. *Biomed Res. Int.* **2013**, *2013*. https://doi.org/10.1155/2013/983465.

(38) Yoo, C.; Jun, S. Y.; Lee, J. Y.; Ahn, C. Y.; Oh, H. M. Selection of Microalgae for Lipid Production under High Levels Carbon Dioxide. *Bioresour. Technol.* **2010**, *101* (1 SUPPL.), S71–S74. https://doi.org/10.1016/j.biortech.2009.03.030.

(39) Liang, Y.; Sarkany, N.; Cui, Y. Biomass and Lipid Productivities of Chlorella Vulgaris under Autotrophic, Heterotrophic and Mixotrophic Growth Conditions. *Biotechnol. Lett.* **2009**, *31* (7), 1043–1049. https://doi.org/10.1007/s10529-009-9975-7.

(40) Nascimento, I.; Andrade, M.; Sheyla, S. I.; Cabanelas, I. T.; Dominguez; Pereira, S. A.; Druzian, J. I.; de Souza, C. O.; Vich, D. V.; de Carvalho, G. C.; Nascimento, M. A. Screening Microalgae Strains for Biodiesel Production: Lipid Productivity and Estimation of Fuel Quality Based on Fatty Acids Profiles as Selective Criteria. *Bioenergy Res.* **2013**, *6* (1), 1–13. https://doi.org/10.1007/s12155-012-9222-2.

(41) Pal, P.; Chew, K. W.; Yen, H. W.; Lim, J. W.; Lam, M. K.; Show, P. L. Cultivation of Oily Microalgae for the Production of Third-Generation Biofuels. *Sustain.* **2019**, *11* (19), 1–16. https://doi.org/10.3390/su11195424.

(42) Aratboni, H. A.; Rafiei, N.; Garcia-Granados, R.; Alemzadeh, A.; Morones-Ramírez, J. R. Biomass and Lipid Induction Strategies in Microalgae for Biofuel Production and Other Applications. *Microb. Cell Fact.* **2019**, *18* (1), 1–17. https://doi.org/10.1186/s12934-019-1228-4.

(43) Harwood, J. L.; Guschina, I. A. The Versatility of Algae and Their Lipid Metabolism. *Biochimie* **2009**, *91* (6), 679–684. https://doi.org/10.1016/j.biochi.2008.11.004.

(44) Bellou, S.; Baeshen, M. N.; Elazzazy, A. M.; Aggeli, D.; Sayegh, F.; Aggelis, G. Microalgal

Lipids Biochemistry and Biotechnological Perspectives. *Biotechnol. Adv.* **2014**, *32* (8), 1476–1493. https://doi.org/10.1016/j.biotechadv.2014.10.003.

(45) Dong, T.; Knoshaug, E. P.; Pienkos, P. T.; Laurens, L. M. L. Lipid Recovery from Wet Oleaginous Microbial Biomass for Biofuel Production: A Critical Review. *Appl. Energy* **2016**, *177*, 879–895. https://doi.org/10.1016/j.apenergy.2016.06.002.

(46) Singh, A.; Nigam, P. S.; Murphy, J. D. Mechanism and Challenges in Commercialisation of Algal Biofuels. *Bioresour. Technol.* **2011**, *102* (1), 26–34. https://doi.org/10.1016/j.biortech.2010.06.057.

(47) Rosenberg, J. N.; Kobayashi, N.; Barnes, A.; Noel, E. A.; Betenbaugh, M. J.; Oyler, G. A. Comparative Analyses of Three Chlorella Species in Response to Light and Sugar Reveal Distinctive Lipid Accumulation Patterns in the Microalga C. Sorokiniana. *PLoS One* **2014**, *9* (4). https://doi.org/10.1371/journal.pone.0092460.

(48) Liu, J.; Huang, J.; Sun, Z.; Zhong, Y.; Jiang, Y.; Chen, F. Differential Lipid and Fatty Acid Profiles of Photoautotrophic and Heterotrophic Chlorella Zofingiensis: Assessment of Algal Oils for Biodiesel Production. *Bioresour. Technol.* **2011**, *102* (1), 106–110. https://doi.org/10.1016/j.biortech.2010.06.017.

(49) Amer, L.; Adhikari, B.; Pellegrino, J. Technoeconomic Analysis of Five Microalgae-to-Biofuels Processes of Varying Complexity. *Bioresour. Technol.* **2011**, *102* (20), 9350–9359. https://doi.org/10.1016/j.biortech.2011.08.010.

(50) Harun, R.; Davidson, M.; Doyle, M.; Gopiraj, R.; Danquah, M.; Forde, G. Technoeconomic Analysis of an Integrated Microalgae Photobioreactor, Biodiesel and Biogas Production Facility. *Biomass and Bioenergy* **2011**, *35* (1), 741–747. https://doi.org/10.1016/j.biombioe.2010.10.007.

(51) Cheng, Y.; Zhou, W.; Gao, C.; Lan, K.; Gao, Y.; Wu, Q. Biodiesel Production from Jerusalem Artichoke (Helianthus Tuberosus L.) Tuber by Heterotrophic Microalgae Chlorella Protothecoides. *J. Chem. Technol. Biotechnol.* **2009**, *84* (5), 777–781. https://doi.org/10.1002/jctb.2111.

(52) Wei, A.; Zhang, X.; Wei, D.; Chen, G.; Wu, Q.; Yang, S. T. Effects of Cassava Starch Hydrolysate on Cell Growth and Lipid Accumulation of the Heterotrophic Microalgae Chlorella Protothecoides. *J. Ind. Microbiol. Biotechnol.* **2009**, *36* (11), 1383–1389. https://doi.org/10.1007/s10295-009-0624-x.

(53) Yan, D.; Lu, Y.; Chen, Y. F.; Wu, Q. Waste Molasses Alone Displaces Glucose-Based Medium for Microalgal Fermentation towards Cost-Saving Biodiesel Production. *Bioresour. Technol.* **2011**, *102* (11), 6487–6493. https://doi.org/10.1016/j.biortech.2011.03.036.

(54) Mitra, D.; van Leeuwen, J. (Hans); Lamsal, B. Heterotrophic/Mixotrophic Cultivation of Oleaginous Chlorella Vulgaris on Industrial Co-Products. *Algal Res.* **2012**, *1* (1), 40–48. https://doi.org/10.1016/j.algal.2012.03.002.

(55) Dubey, K. K.; Kumar, S.; Dixit, D.; Kumar, P.; Kumar, D.; Jawed, A.; Haque, S. Implication of Industrial Waste for Biomass and Lipid Production in Chlorella Minutissima Under Autotrophic, Heterotrophic, and Mixotrophic Grown Conditions. *Appl. Biochem. Biotechnol.* **2015**, *176* (6), 1581–1595. https://doi.org/10.1007/s12010-015-1663-6.

(56) Venkata Mohan, S.; Rohit, M. V.; Chiranjeevi, P.; Chandra, R.; Navaneeth, B. Heterotrophic Microalgae Cultivation to Synergize Biodiesel Production with Waste Remediation: Progress and Perspectives. *Bioresour. Technol.* **2015**, *184*, 169–178. https://doi.org/10.1016/j.biortech.2014.10.056.

(57) Zheng, H.; Ma, X.; Gao, Z.; Wan, Y.; Min, M.; Zhou, W.; Li, Y.; Liu, Y.; Huang, H.; Chen, P.; Ruan, R. Lipid Production of Heterotrophic Chlorella Sp. from Hydrolysate Mixtures of Lipid-Extracted Microalgal Biomass Residues and Molasses. *Appl. Biochem. Biotechnol.* **2015**, *177* (3), 662–674. https://doi.org/10.1007/s12010-015-1770-4.

(58) Pleissner, D.; Rumpold, B. A. Utilization of Organic Residues Using Heterotrophic Microalgae and Insects. *Waste Manag.* **2018**, *72*, 227–239. https://doi.org/10.1016/j.wasman.2017.11.020.

(59) Field, C. B.; Behrenfeld, M. J.; Randerson, J. T.; Falkowski, P. Primary Production of the Biosphere: Integrating Terrestrial and Oceanic Components. *Science (80-.).* **1998**, *281* (5374), 237–240. https://doi.org/10.1126/science.281.5374.237.

(60) Hildebrand, M.; Davis, A. K.; Smith, S. R.; Traller, J. C.; Abbriano, R. The Place of Diatoms in the Biofuels Industry. *Biofuels* **2012**, *3* (2), 221–240. https://doi.org/10.4155/BFS.11.157.

(61) D'Ippolito, G.; Sardo, A.; Paris, D.; Vella, F. M.; Adelfi, M. G.; Botte, P.; Gallo, C.; Fontana, A. Potential of Lipid Metabolism in Marine Diatoms for Biofuel Production. *Biotechnol. Biofuels* **2015**, *8* (1), 1–10. https://doi.org/10.1186/s13068-015-0212-4.

(62) Jin, P.; Agustí, S. Fast Adaptation of Tropical Diatoms to Increased Warming with Trade-Offs. *Sci. Rep.* **2018**, *8* (1), 1–11. https://doi.org/10.1038/s41598-018-36091-y.

(63) Sharma, N.; Simon, D. P.; Diaz-Garza, A. M.; Fantino, E.; Messaabi, A.; Meddeb-Mouelhi, F.; Germain, H.; Desgagné-Penix, I. Diatoms Biotechnology: Various Industrial Applications for a Greener Tomorrow. *Front. Mar. Sci.* **2021**, *8* (February). https://doi.org/10.3389/fmars.2021.636613.

(64) Wang, X. W.; Huang, L.; Ji, P. Y.; Chen, C. P.; Li, X. S.; Gao, Y. H.; Liang, J. R. Using a Mixture of Wastewater and Seawater as the Growth Medium for Wastewater Treatment and Lipid Production by the Marine Diatom Phaeodactylum Tricornutum. *Bioresour. Technol.* **2019**, *289* (June), 121681. https://doi.org/10.1016/j.biortech.2019.121681.

(65) Orcutt, D. M.; Patterson, G. W. Sterol, Fatty Acid and Elemental Composition of Diatoms. *Comp. Biochem. Physiol.* **1975**, *50b* (685), 579–583.

(66) Ying, L.; Kang-sen, M.; Shi-chun, S.; Dao-zhan, Y. Effect of Light Intensity on the Total Lipid and Fatty Acid Composition of Six Strains of Marine Diatoms. *Chinese J. Oceanol. Limnol.* **2001**, *19* (3), 249–254. https://doi.org/10.1007/bf02850662.

(67) Tuchman, N. C.; Schollett, M. A.; Rier, S. T.; Geddes, P. Differential Heterotrophic Utilization of Organic Compounds by Diatoms and Bacteria under Light and Dark Conditions. *Hydrobiologia* **2006**, *561* (1), 167–177. https://doi.org/10.1007/s10750-005-1612-4.

(68) Chen, Y. C. The Biomass and Total Lipid Content and Composition of Twelve Species of Marine Diatoms Cultured under Various Environments. *Food Chem.* **2012**, *131* (1), 211–219. https://doi.org/10.1016/j.foodchem.2011.08.062.

(69) Li, X. L.; Marella, T. K.; Tao, L.; Li, R.; Tiwari, A.; Li, G. Optimization of Growth Conditions and Fatty Acid Analysis for Three Freshwater Diatom Isolates. *Phycol. Res.* **2017**, *65* (3), 177–187. https://doi.org/10.1111/pre.12174.

(70) Maeda, Y.; Nojima, D.; Yoshino, T.; Tanaka, T. Structure and Properties of Oil Bodies in Diatoms. *Philos. Trans. R. Soc. B Biol. Sci.* **2017**, *372* (1728). https://doi.org/10.1098/rstb.2016.0408.

(71) Sayanova, O.; Mimouni, V.; Ulmann, L.; Morant-Manceau, A.; Pasquet, V.; Schoefs, B.;

Napier, J. A. Modulation of Lipid Biosynthesis by Stress in Diatoms. *Philos. Trans. R. Soc. B Biol. Sci.* **2017**, *372* (1728). https://doi.org/10.1098/rstb.2016.0407.

(72) Govindan, N.; Maniam, G. P.; Ab. Rahim, M.; Sulaiman, A. Z.; Ajit, A.; Chatsungnoen, T.; Chisti, Y. Production of Renewable Lipids by the Diatom Amphora Copulata. *Fermentation* **2021**, *7* (1), 37. https://doi.org/10.3390/fermentation7010037.

(73) Tan, C. K.; Johns, M. R. Screening of Diatoms for Heterotrophic Eicosapentaenoic Acid Production. *J. Appl. Phycol.* **1996**, *8* (1), 59–64. https://doi.org/10.1007/BF02186223.

(74) Wen, Z. Y.; Chen, F. Production Potential of Eicosapentaenoic Acid by the Diatom Nitzschia Laevis. *Biotechnol. Lett.* **2000**, *22* (9), 727–733. https://doi.org/10.1023/A:1005666219163.

(75) Wen, Z. Y.; Chen, F. Optimization of Nitrogen Sources for Heterotrophic Production of Eicosapentaenoic Acid by the Diatom Nitzschia Laevis. *Enzyme Microb. Technol.* **2001**, *29* (6–7), 341–347. https://doi.org/10.1016/S0141-0229(01)00385-4.

(76) Wen, Z. Y.; Chen, F. A Perfusion-Cell Bleeding Culture Strategy for Enhancing the Productivity of Eicosapentaenoic Acid by Nitzschia Laevis. *Appl. Microbiol. Biotechnol.* **2001**, *57* (3), 316–322. https://doi.org/10.1007/s002530100786.

(77) Wen, Z. Y.; Jiang, Y.; Chen, F. High Cell Density Culture of the Diatom Nitzschia Laevis for Eicosapentaenoic Acid Production: Fed-Batch Development. *Process Biochem.* **2002**, *37* (12), 1447–1453. https://doi.org/10.1016/S0032-9592(02)00034-1.

(78) Wen, Z. Y.; Chen, F. Continuous Cultivation of the Diatom Nitzschia Laevis for Eicosapentaenoic Acid Production: Physiological Study and Process Optimization. *Biotechnol. Prog.* **2002**, *18* (1), 21–28. https://doi.org/10.1021/bp010125n.

(79) Chen, G. Q.; Jiang, Y.; Chen, F. Fatty Acid and Lipid Class Composition of the Eicosapentaenoic Acid-Producing Microalga, Nitzschia Laevis. *Food Chem.* **2007**, *104* (4), 1580–1585. https://doi.org/10.1016/j.foodchem.2007.03.008.

(80) Chen, G. Q.; Jiang, Y.; Chen, F. Salt-Induced Alterations in Lipid Composition of Diatom Nitzschia Laevis (Bacillariophyceae) under Heterotrophic Culture Condition. *J. Phycol.* **2008**, *44* (5), 1309–1314. https://doi.org/10.1111/j.1529-8817.2008.00565.x.

(81) Chen, G. Q.; Jiang, Y.; Chen, F. Variation of Lipid Class Composition in Nitzschia Laevis as a Response to Growth Temperature Change. *Food Chem.* **2008**, *109* (1), 88–94. https://doi.org/10.1016/j.foodchem.2007.12.022.

(82) Hamilton, M. L.; Powers, S.; Napier, J. A.; Sayanova, O. Heterotrophic Production of Omega-3 Long-Chain Polyunsaturated Fatty Acids by Trophically Converted Marine Diatom Phaeodactylum Tricornutum. *Mar. Drugs* **2016**, *14* (3). https://doi.org/10.3390/md14030053.

(83) Leyland, B.; Boussiba, S.; Khozin-Goldberg, I. A Review of Diatom Lipid Droplets. *Biology (Basel).* **2020**, *9* (2), 38. https://doi.org/10.3390/biology9020038.

(84) Henderson, R. J.; Leftley, J. W.; Sargent, J. R. Lipid Composition and Biosynthesis in the Marine Dinoflagellate Crypthecodinium Cohnii. *Phytochemistry* **1988**, *27* (6), 1679–1683. https://doi.org/10.1016/0031-9422(88)80425-4.

(85) Anderson, R.; Livermore, B. P.; Kates, M.; Volcani, B. E. The Lipid Composition of the Non-Photosynthetic Marine Diatom , Nitzschia Alba. *Biochim. Biophys. Acta* **1978**, *528*, 77–88.

(86) Talebi, A. F.; Mohtashami, S. K.; Tabatabaei, M.; Tohidfar, M.; Bagheri, A.; Zeinalabedini, M.; Hadavand Mirzaei, H.; Mirzajanzadeh, M.; Malekzadeh Shafaroudi, S.; Bakhtiari, S. Fatty Acids Profiling: A Selective Criterion for Screening Microalgae

Strains for Biodiesel Production. *Algal Res.* **2013**, *2* (3), 258–267. https://doi.org/10.1016/j.algal.2013.04.003.

(87) Huerlimann, R.; de Nys, R.; Heimann, K. Growth, Lipid Content, Productivity, and Fatty Acid Composition of Tropical Microalgae for Scale-up Production. *Biotechnol. Bioeng.* **2010**, *107* (2), 245–257. https://doi.org/10.1002/bit.22809.

(88) Islam, M. A.; Magnusson, M.; Brown, R. J.; Ayoko, G. A.; Nabi, M. N.; Heimann, K. Microalgal Species Selection for Biodiesel Production Based on Fuel Properties Derived from Fatty Acid Profiles. *Energies* **2013**, *6* (11), 5676–5702. https://doi.org/10.3390/en6115676.

(89) Knothe, G. Dependence of Biodiesel Fuel Properties on the Structure of Fatty Acid Alkyl Esters. *Fuel Process. Technol.* **2005**, *86* (10), 1059–1070. https://doi.org/10.1016/j.fuproc.2004.11.002.

(90) Knothe, G.; Razon, L. F. Biodiesel Fuels. *Prog. Energy Combust. Sci.* **2017**, *58*, 36–59. https://doi.org/10.1016/j.pecs.2016.08.001.

(91) Meher, L. C.; Vidya Sagar, D.; Naik, S. N. Technical Aspects of Biodiesel Production by Transesterification - A Review. *Renew. Sustain. Energy Rev.* **2006**, *10* (3), 248–268. https://doi.org/10.1016/j.rser.2004.09.002.

(92) Yuan, M. H.; Chen, Y. H.; Chen, J. H.; Luo, Y. M. Dependence of Cold Filter Plugging Point on Saturated Fatty Acid Profile of Biodiesel Blends Derived from Different Feedstocks. *Fuel* **2017**, *195*, 59–68. https://doi.org/10.1016/j.fuel.2017.01.054.

(93) Sierra-Cantor, J. F.; Guerrero-Fajardo, C. A. Methods for Improving the Cold Flow Properties of Biodiesel with High Saturated Fatty Acids Content: A Review. *Renew. Sustain. Energy Rev.* **2017**, *72* (December 2016), 774–790. https://doi.org/10.1016/j.rser.2017.01.077.

(94) Dwivedi, G.; Sharma, M. P. Impact of Cold Flow Properties of Biodiesel on Engine Performance. *Renew. Sustain. Energy Rev.* **2014**, *31*, 650–656. https://doi.org/10.1016/j.rser.2013.12.035.

(95) He, B. Q. Advances in Emission Characteristics of Diesel Engines Using Different Biodiesel Fuels. *Renew. Sustain. Energy Rev.* **2016**, *60*, 570–586. https://doi.org/10.1016/j.rser.2016.01.093.

(96) Knothe, G. Analyzing Biodiesel: Standards and Other Methods. *JAOCS, J. Am. Oil Chem. Soc.* **2006**, *83* (10), 823–833. https://doi.org/10.1007/s11746-006-5033-y.

(97) Toscano, G.; Riva, G.; Foppa Pedretti, E.; Duca, D. Vegetable Oil and Fat Viscosity Forecast Models Based on Iodine Number and Saponification Number. *Biomass and Bioenergy* **2012**, *46*, 511–516. https://doi.org/10.1016/j.biombioe.2012.07.009.

(98) Datta, A.; Mandal, B. K. A Comprehensive Review of Biodiesel as an Alternative Fuel for Compression Ignition Engine. *Renew. Sustain. Energy Rev.* **2016**, *57*, 799–821. https://doi.org/10.1016/j.rser.2015.12.170.

(99) Demirbas, A. Relationships Derived from Physical Properties of Vegetable Oil and Biodiesel Fuels. *Fuel* **2008**, *87* (8–9), 1743–1748. https://doi.org/10.1016/j.fuel.2007.08.007.

(100) Refaat, A. A. Correlation between the Chemical Structure of Biodiesel and Its Physical Properties. *Int. J. Environ. Sci. Technol.* **2009**, *6* (4), 677–694. https://doi.org/10.1007/BF03326109.

(101) Cutignano, A.; Luongo, E.; Nuzzo, G.; Pagano, D.; Manzo, E.; Sardo, A.; Fontana, A. Profiling of Complex Lipids in Marine Microalgae by UHPLC/Tandem Mass

Spectrometry. *Algal Res.* **2016**, *17*, 348–358. https://doi.org/10.1016/j.algal.2016.05.016.

(102) Cupo, A.; Landi, S.; Morra, S.; Nuzzo, G.; Gallo, C.; Manzo, E.; Fontana, A.; Ippolito, G. Autotrophic vs . Heterotrophic Cultivation of the Marine Diatom Cyclotella Cryptica for EPA Production. **2021**, 1–11.

(103) Nuzzo, G.; Gallo, C.; D'Ippolito, G.; Cutignano, A.; Sardo, A.; Fontana, A. Composition and Quantitation of Microalgal Lipids by ERETIC 1H NMR Method. *Mar. Drugs* **2013**, *11* (10), 3742–3753. https://doi.org/10.3390/md11103742.

(104) Patel, A.; Arora, N.; Mehtani, J.; Pruthi, V.; Pruthi, P. A. Assessment of Fuel Properties on the Basis of Fatty Acid Profiles of Oleaginous Yeast for Potential Biodiesel Production. *Renew. Sustain. Energy Rev.* **2017**, *77* (September), 604–616. https://doi.org/10.1016/j.rser.2017.04.016.

6. Manuscript in preparation for submission:

Heterotrophy regulates lipid metabolism in the marine diatom *C. cryptica*

Adelaide Cupo[1,2,a], Simone Landi[2,a,*], Salvatore Morra[1], Genoveffa Nuzzo[1], Carmela Gallo[1], Emiliano Manzo[1], Angelo Fontana[1,2] and Giuliana d'Ippolito[1,*]

[1] Institute of Biomolecular Chemistry CNR (CNR-ICB), Via Campi Flegrei 34, 80078 Pozzuoli, Naples, Italy.
[2] Department of Biology, University of Naples "Federico II", Via Cinthia, I-80126 Napoli, Italy.
[*] Correspondence: gdippolito@icb.cnr.it; simone.landi@unina.it

[a]These authors contributed equally to this work

6.1 Abstract

Diatoms cultivation upon heterotrophic condition is a desirable benefit for biotechnology application on industrial large-scale system. Dark cultivation represents a suitable technology to overcome the limitations of phototrophic cultivation namely, light dependency, seasonality, climatic conditions dependence, need of arable lands and the excessive cost to avoid these constrains. Usually, diatoms are prototroph, using photosynthesis for their energy production but few natural and engineering species are able to grow in heterotrophy and mixotrophy. In these conditions, diatoms exhibited their natural metabolic flexibility showing, in some case, the possibility to increase biomass accumulation and the production of compounds with biological activities. Particularly, among the marketable products of diatoms, lipids are one of the most desirable for a wide range of commercial applications such as nutraceutical, pharmaceutical and biofuels. Up to now, no exhaustive overview about transcriptomic and lipidomic fingerprinting of heterotrophic cultivation have been reported. In this manuscript we investigated the effects of heterotrophy on *C. cryptica*, one of the best diatom specie for large-scale biofuel production. Dark cultivation slightly reduced the cell number of *C. cryptica* but increase biomass, lipids, protein and particularly carbohydrates content. Among lipid species triacylglycerol (TAG) showed up-regulation while sulfoquinovosyldiacylglycerol (SQDG) showed a drastic reduction. Transcriptomic sequencing and differential expression analysis were used to reconstruct the entire set of genes related to fatty acids and lipids biosynthesis and to identify the complex network regulating the metabolic switch induced by the heterotrophy. Our data highlighted significant regulation of key enzymes of the fatty acid and lipid biosynthetic pathways namely up-regulation of GPDH, GPAT, LPAAT (chloroplastic and no), DGAT and PDAT and down-regulation of SQD1, MGDGS and DGDGS.

Keywords

Diatoms; heterotrophy; triacylglycerol; lipids; RNA-seq; fatty acids; desaturases; gluconeogenesis; cell division.

6.2 Introduction

In recent years marine organisms highlighted a renewed commercial interests for the production of natural compounds suitable for nutraceutical, pharmaceutical, and energetic industries [1–4]. Diatoms constitute the primary group of marine phytoplankton, playing a critical role for oceanic and worldwide ecology [5–9]. It has been estimated the existence of at least 10^5 - 10^7 different species of diatoms contributing for the 20% of terrestrial global fixation and for the 40% of primary productivity in oceans [10,11]. The fixed carbon is specifically stored into carbohydrates such as chrysolaminarin or lipids, mostly represented by triacylglycerols (TAGs) [12]. These organisms also play a central role in silica, nitrogen and carbon marine cycles by the organization of short-term big populations called blooms able to export and move carbon and silica from the ocean's bottom [7].

Diatoms showed limitless biotechnology applications addressing for sustainable industrial applications [1,13]. Particularly, the opportunity to obtain fatty acids and lipids growing diatoms in photo-bioreactors represents an attractive industrial interest [14–17]. In their fatty acid profiles, diatoms are enriched with medium-chain fatty acids as well as with very long chain-polyunsaturated fatty acids (VLC-PUFAs). This represent an important added value considering the appreciate value of medium-chain fatty acids for biofuel production application [12,18].

Upon physiological condition, diatom glycerolipids are grouped in neutral lipids (triglycerides, TAG), phospholipids (PL) and glycolipids (GL) as monogalactosyldiacylglycerol (MGDG), digalactosyldiacylglycerol (DGDG) and sulfoquinovosyldiacylglycerol (SQDG)[16]. Part of these species were physiologically involved in complex metabolic pathways in order to product signal molecules [19]. Upon specific environmental conditions namely nutritional deprivations and/or CO_2 insufflation, diatoms showed remodeling process of the lipid species [20–24]. Particularly, upon nitrate, phosphate and silicate starvations diatoms significantly increased the lipid content, especially of triacylglycerols (TAG) [19,20,25]. Artificial starvation strategies have been reported as functional approach to induce remodeling and obtain TAG, [26,27]. Particularly, *Thalassiosira weissflogii* and *C. cryptica* were recently reported as best diatom species for biofuel application and by the imposition of artificial starvation, these species showed an increased TAG production up to 80% [25].

On the other hands, alternative cultivation conditions are desirable to expand the use of diatoms and microalgae in commercial applications. Generally, diatoms are cultivated in phototrophic condition in photobioreactors, open ponds or flat panel but light dependency represents a costly and restrictive factor [17,28,29]. In native environment diatoms are prototroph, using photosynthesis for their energy production but few natural and engineering species are able to grow in heterotrophic conditions [4,9,30–32]. Diatoms showed a natural metabolic flexibility, which make possible a nutritional switch depending by substrate and light availabilities [29]. Dark cultivation represents an alternative system to overcome the limitations of phototrophic cultivation because using heterotrophic condition it is possible increase biomass accumulation, lipid yield and use the well-known fermenter technology, commonly used for biotechnological production of drugs, food additives and beverages [4,28,29,32–34]. Large-scale dark cultivation of diatoms requires a number of technical issues namely good survival of the strain, low cultivation costs and the ability of metabolize inexpensive carbon sources. The achievements of these issues generate economical value in the use of heterotrophic growth [33]. Recently, a number of works focused on transcriptomic and metabolomic effects of starvation and CO_2 in diatoms and a large collection[35] of related genes were identified [20,21,23]. Up to now, no exhaustive overview about transcriptomic and lipidomic fingerprinting of heterotrophic cultivation have been reported. Two papers reported similar analysis. The proteomics effects of dark cultivation in *Fragilariopsis cylindrus* and the transcriptomic effects in a cryptochrome knockout *Phaeodactylum tricornutum* strain [9,36].

In this manuscript, *C. cryptica* was selected as model specie. The Aquatic Species Program of the US Department of Energy indicated *C. cryptica* as top microalgae specie for large-scale biofuel production [35]. *C. cryptica* showed an interesting high-lipid accumulation and flexibility in cultivation conditions and the unconventional ability among diatoms to growth upon heterotrophic conditions [16,31]. The purpose of this manuscript is to investigate biochemical and molecular basis of *C. cryptica in* adapting its metabolism to the absence of light and to internalization and metabolization of organic sources. RNA-sequencing, mass spectrometry and NMR strategies were selected to analyze the physiological ability of *C. cryptica* to growth upon dark, addressing the molecular and metabolic networks involved in lipid production and reorganization induced by heterotrophy.

6.3 Results and Discussion

6.3.1 Light and dark-induced phenotypes

In the present study *C. cryptica* was cultivated upon autotrophic and heterotrophic conditions for 7 days. Dark cultivated diatoms were supplemented with 1 g/L of glucose to sustain the growth. No contaminations were reported during the entire cultivation period upon heterotrophy. As showed in **Figure 6.1A,** the heterotrophy showed negative effects in terms of number of cells from day 3 to day 7 compared with autotrophy. Particularly, heterotrophic cultivation showed a reduction of cells number about 58.6% after 3 days, 43.3% after 5 days and 18.1% after 7 days. These differences reflected an adaptation phase in the first days of heterotrophy followed by a rapid increase of cell division until day 7. In fact, doubling time was 2.9±0.13 day in heterotrophy and 4.8±0.13 day in autotrophy. On the other hand, heterotrophic cultures showed a significant increase of biomass compared with control (**Figure 6.1B**). In detail, after 7 days *C. cryptica* biomass showed values of about 0.29 and 0.38 ng cell^{-1} for autotrophy and heterotrophy, respectively. The imposed heterotrophy conditions also changed lipid, protein and carbohydrate content (**Figure 6.1C**). Particularly after 7 days lipids showed a significant increase of 1.29 fold change (fc), proteins showed a significant increase of 1.34 fc and carbohydrates showed a huge and significant increase of 5.69 fc comparing heterotrophy *vs* autotrophy. Particularly, *C. cryptica* cells cultured upon heterotrophic condition showed lipid, protein and carbohydrate amounts of about 0.075, 0.111 and 0.101 µg cell^{-1}, respectively. These data certainly demonstrated the ability of efficiently grown upon dark conditions. This heterotrophic adaptation is guided by a substantial transcriptomic re-organization. Using RNA sequencing, we identified 12327 differential expressed genes (DEGs), comparing heterotrophic *vs* autotrophic conditions. In detail, 5195 DEGs were up regulated (≥ 1.5 fc) upon heterotrophy while 7132 DEGs were down regulated (≤ -1.5 fc).

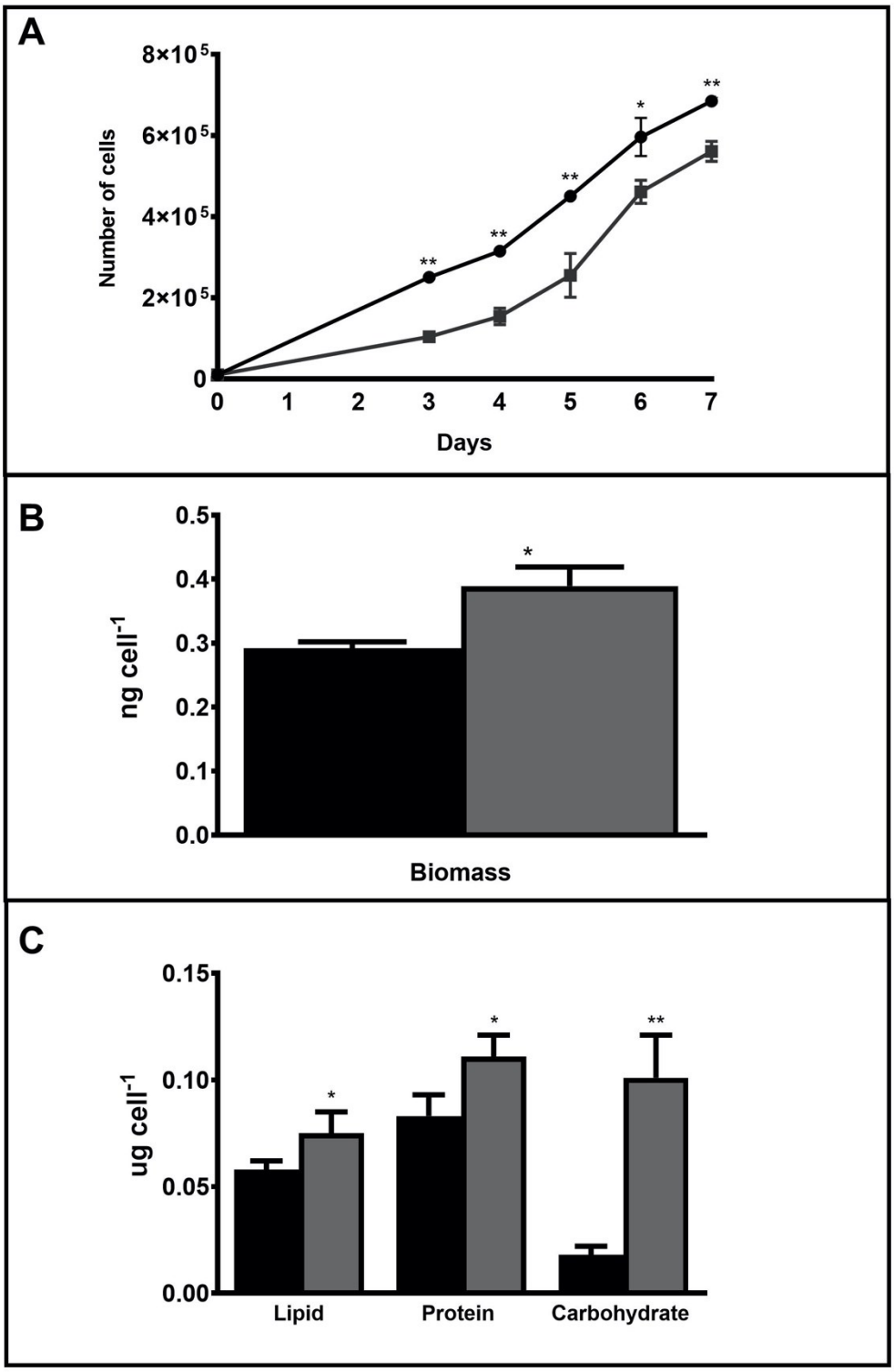

Figure 6.1 Growth curves (A), biomass (ng cell^{-1}) (B) and lipid, protein and carbohydrates content (C) of *C. cryptica* cells cultivated in autotrophic (black line) and heterotrophic (gray line) conditions after 7 days. Asterisks indicate significantly different values in autotrophic and heterotrophic samples at $p \leq 0.05$ (*) and $p \leq 0.005$ (**).

6.3.2 Reconstruction of lipid biosynthesis in *C. cryptica* upon heterotrophy

C. cryptica cultivated upon heterotrophic conditions, showed a specific fatty acid profile and characteristic lipid fingerprinting (**Table 6.1** and **Figure 6.2**).

Table 6.1 Fatty acid composition of *C. cryptica* grown under autotrophic and heterotrophic condition for 7 days. SFA=Saturated Fatty acids; MUFA=MonoUnsaturated Fatty acids; PUFA=PolyUnsaturated fatty Acids, expressed as percentage of Total Fatty Acids. Asterisks indicate significantly different values in autotrophic and heterotrophic samples at $p \leq 0.05$ (*) and $p \leq 0.01$ (**). Data are expressed as means ± SD, n=3.

Fatty Acid	Autotrophy	Heterotrophy
14:0	3.99 ± 0.30	3.38 ± 0.47
16:4	0.40 ± 0.01	0.00 **
16:3	22.1 ± 0.2	2.17 ± 0.12 **
16:2	7.83 ± 0.50	0.00 **
16:1	23.96 ± 1	49.1 ± 3 **
16:0	12.5 ± 0.1	15.3 ± 0.3 **
18:4	1.31 ± 0.15	2.13 ± 0.16
18:3	0.11 ± 0.01	0.25 ± 0.15 **
18:2	0.59 ± 0.11	0.99 ± 0.52 *
18:1	0.40 ± 0.03	1.70 ± 0.01 **
18:0	0.11 ± 0.01	0.18 ± 0.01 *
20:5	23.6 ± 1.5	22.5 ± 1.3
22:6	3.13 ± 0.34	2.29 ± 0.62
SFA	16.6 ± 0.6	18.9 ± 1
MUFA	23.4 ± 1.4	50.1 ± 4 **
PUFA	59.03 ± 2	30.3 ± 3 **

SQDG significantly decreased and a slight increase of MGDG was reported (**Figure 6.2**).

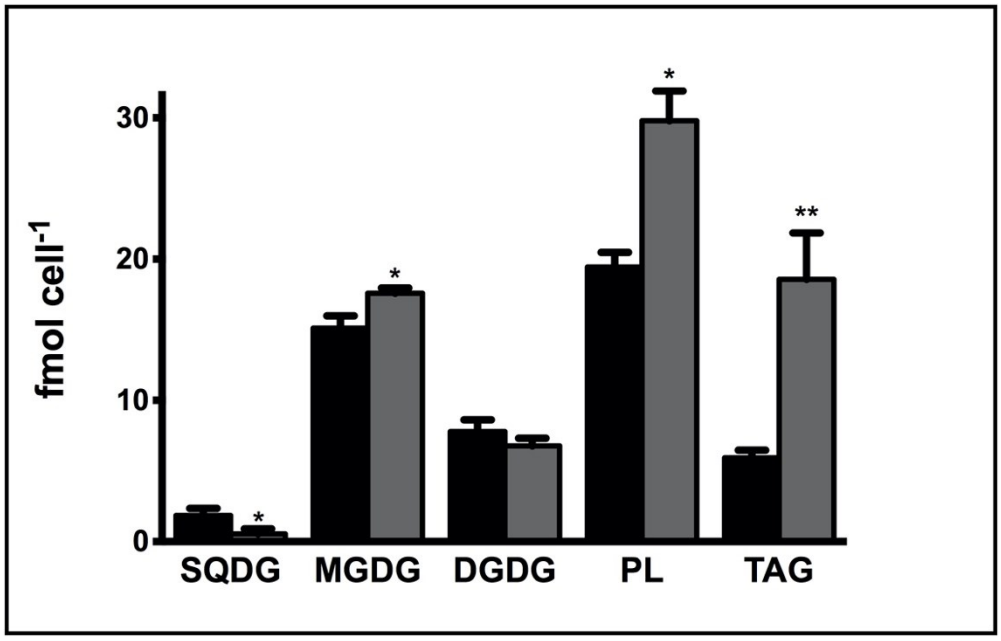

Figure 6.2 SQDG, MGDG, DGDG, PL and TAG content (fmol cell^{-1}) of *C. cryptica* cells cultivated upon autotrophic (black bars) and heterotrophic (grey bars) conditions after 7 days (B). Asterisks indicate significantly different values in autotrophic and heterotrophic samples at $p \leq 0.05$ (*) and $p \leq 0.005$ (**).

The valuable effects of heterotrophy were observed about the increased content of PL and TAG. These lipid species showed an increase of about 1.53 and 3.13 fold change comparing heterotrophy *vs* autotrophy. In order to analyze the complete lipid biosynthetic pathway of *C. cryptica,* we used the well-known *Arabidopsis thaliana* and diatoms notions about the enzymes sequences and pathways [12,37,38] to mine the *C. cryptica* transcriptome assembled in this work. Using this approach, we identified putative orthologous related to fatty acid, SQDG, MQDG, DGDG, PL and TAG biosynthetic pathways (**Table 6.2**) and for the related fatty acid desaturases (FAD - **Table 6.3**). A total of 100 lipid related transcripts were identified. Among these, 36 were up regulated and 20 were down regulated comparing heterotrophy *vs* autotrophy. Using these transcripts we reconstructed lipid pathways models for fatty acid, chloroplastic PL and GL biosynthesis and PL and TAG non-plastidial biosynthesis. Accordingly, with lipidomics, transcriptomics data clearly showed that heterotrophy trigger an increased fatty acid synthesis by the up-regulation of the enzymes constituting the fatty acid synthase (FAS) complex. GL synthesis was reduced by the down-regulation of nodes genes (MGDGS, DGDGS and SQD2), channeling a major amount of fatty acids and diacylglycerol (DAG) to PL and TAG synthesis.

Table 6.2 List of transcripts *C. cryptica* related to fatty acid, GL, PL and TAG biosynthesis. Expression analysis was performed using RNA-sequencing comparing heterotrophy (HE) vs autotrophy (AU).

Genes	Identified Transcripts	HE vs AU	Descriptions	EC numbers
Fatty Acid Biosynthesis				
PDH	*TRINITY_DN19306*	1.75	Pyruvate dehydrogenase	1.2.4.1
PDH	*TRINITY_DN18471*	83.28	Pyruvate dehydrogenase	1.2.4.1
PDH	*TRINITY_DN8372*	-3.15	Pyruvate dehydrogenase	1.2.4.1
PDH	*TRINITY_DN9125*	2.04	Pyruvate dehydrogenase	1.2.4.1
ACAC/BC	*TRINITY_DN20242*	NDE	Biotin carboxylase/acetyl-CoA carboxylase	6.4.1.2; 6.3.4.14
ACAC/BC	*TRINITY_DN20117*	2.66	Biotin carboxylase/acetyl-CoA carboxylase	6.4.1.2; 6.3.4.14
ACAC/BC	*TRINITY_DN17120*	-148.66	Biotin carboxylase/acetyl-CoA carboxylase	6.4.1.2; 6.3.4.14
MCMT (fabD)	*TRINITY_DN14933*	NDE	Malonyl-CoA: ACP malonyltransferase	2.3.1.39
KAS I (fabB)	*TRINITY_DN12300*	NDE	Ketoacyl-ACP synthase	2.3.1.41
KAS II (fabF)	*TRINITY_DN11432*	4.74	Ketoacyl-ACP synthase	2.3.1.179
KAS III (fabH)	*TRINITY_DN13597*	NDE	Ketoacyl-ACP synthase	2.3.1.180
KAR (fabG)	*TRINITY_DN17343*	-5.65	Ketoacyl-ACP reductase	1.1.1.100
KAR (fabG)	*TRINITY_DN18786*	NDE	Ketoacyl-ACP reductase	1.1.1.100
KAR (fabG)	*TRINITY_DN13438*	2.28	Ketoacyl-ACP reductase	1.1.1.100
KAR (fabG)	*TRINITY_DN11303*	NDE	Ketoacyl-ACP reductase	1.1.1.100
KAR (fabG)	*TRINITY_DN19074*	NDE	Ketoacyl-ACP reductase	1.1.1.100
KAR (fabG)	*TRINITY_DN11720*	-1.67	Ketoacyl-ACP reductase	1.1.1.100
KAR (fabG)	*TRINITY_DN12894*	NDE	Ketoacyl-ACP reductase	1.1.1.100
KAR (fabG)	*TRINITY_DN8850*	NDE	Ketoacyl-ACP reductase	1.1.1.100
KAR (fabG)	*TRINITY_DN17780*	-1.93	Ketoacyl-ACP reductase	1.1.1.100
KAR (fabG)	*TRINITY_DN8746*	NDE	Ketoacyl-ACP reductase	1.1.1.100
HAD (fabZ)	*TRINITY_DN10930*	NDE	Hydroxyacyl-ACP dehydrogenase	4.2.1.59
ENR (fabI)	*TRINITY_DN15942*	2.29	Enoyl-ACP reductase	1.3.1.9/ 1.3.1.10
SAD	*TRINITY_DN18100*	32.45	Stearoyl-ACP desaturase	1.14.19.2
LACS (fadD)	*TRINITY_DN19543*	NDE	Long-chain acyl-CoA synthetase	6.2.1.3
ELOVL	*TRINITY_DN13721*	1.79	Very long-chain acyl-CoA synthetase	2.3.1.199
ELOVL	*TRINITY_DN16245*	2.62	Very long-chain acyl-CoA synthetase	2.3.1.199
ELOVL	*TRINITY_DN15010*	NDE	Very long-chain acyl-CoA synthetase	2.3.1.199
ABCAT	*TRINITY_DN18575*	NDE	ABC acyl transporter	
GL and PL chloroplastic biosynthesis				
GPDH	*TRINITY_DN16495*	17.77	Glycerol-3-phosphate dehydrogenase	1.1.1.94
GPDH	*TRINITY_DN14467*	NDE	Glycerol-3-phosphate dehydrogenase	1.1.1.94
GPAT	*TRINITY_DN12213*	1.89	Glycerol-3-phosphate acyltransferase	2.3.1.51
GPAT	*TRINITY_DN16298*	3.49	Glycerol-3-phosphate acyltransferase	2.3.1.51
LPAAT	*TRINITY_DN20187*	9.24	2-lysophosphatidic acid acyltransferase	2.3.1.51
CDP-DAGS	*TRINITY_DN19904*	-79.70	CDP-diacylglycerol synthetase	2.7.7.41
PGPS	*TRINITY_DN10499*	NDE	Phosphatidylglycerophosphate synthase	2.7.8.5

PGPS	*TRINITY_DN18595*	-34.71	Phosphatidylglycerophosphate synthase	2.7.8.5
PGPP	*TRINITY_DN17300*	NDE	Phosphatidylglycerophosphate phosphatase	3.1.3.27
PP	*TRINITY_DN17590*	NDE	Phosphatidic acid phosphatase	3.1.3.4
PP	*TRINITY_DN16759*	NDE	Phosphatidic acid phosphatase	3.1.3.4
SQD1	*TRINITY_DN17430*	-1.78	UDP-sulfoquinovose synthase	3.13.1.1
SQD2	*TRINITY_DN18927*	NDE	UDP-sulfoquinovose:DAG sulfoquinovosyltransferase	2.4.1.-
MGDGS	*TRINITY_DN16328*	NDE	Monogalactosyldiacylglycerol Synthase	2.4.1.46
MGDGS	*TRINITY_DN19797*	NDE	Monogalactosyldiacylglycerol Synthase	2.4.1.46
MGDGS	*TRINITY_DN8064*	-2.27	Monogalactosyldiacylglycerol Synthase	2.4.1.46
MGDGS	*TRINITY_DN1596*	-3.65	Monogalactosyldiacylglycerol Synthase	2.4.1.46
MGDGS	*TRINITY_DN6203*	-2.98	Monogalactosyldiacylglycerol Synthase	2.4.1.46
DGDGS	*TRINITY_DN14334*	NDE	Digalactosyldiacylglycerol Synthase	2.4.1.241
DGDGS	*TRINITY_DN15718*	-2.97	Digalactosyldiacylglycerol Synthase	2.4.1.241
DGDGS	*TRINITY_DN16929*	NDE	Digalactosyldiacylglycerol Synthase	2.4.1.241
PL and TAG biosynthesis				
GPDH	*TRINITY_DN13269*	NDE	Glycerol-3-phosphate dehydrogenase	1.1.1.94
GPAT	*TRINITY_DN13184*	3.33	Glycerol-3-phosphate acyltransferase	2.3.1.51
LPAAT	*TRINITY_DN13209*	92.60	2-lysophosphatidic acid acyltransferase	2.3.1.51
CDP-DAGS	*TRINITY_DN16033*	NDE	CDP-diacylglycerol synthetase	2.7.7.41
CDP-DAGS	*TRINITY_DN15382*	NDE	CDP-diacylglycerol synthetase	2.7.7.41
CDP-DAGS	*TRINITY_DN19365*	NDE	CDP-diacylglycerol synthetase	2.7.7.41
PGPS	*TRINITY_DN9779*	NDE	Phosphatidylglycerophosphate synthase	2.7.8.5
PIS	*TRINITY_DN15756*	1.40	Phosphatidylinositol synthase	2.7.8.11
PIS	*TRINITY_DN20212*	1.74	Phosphatidylinositol synthase	2.7.8.11
PSD	*TRINITY_DN18157*	NDE	phosphatidylserine decarboxylase	4.1.1.65
DAG-cpt/ept	*TRINITY_DN15926*	4.29	Diacylglycerol choline(ethanolammine)phosphotransferase	2.7.8.1
DAG-cpt/ept	*TRINITY_DN11924*	3.23	Diacylglycerol choline(ethanolammine)phosphotransferase	2.7.8.1
PDCT/ROD	*TRINITY_DN15143*	19.27	Phosphatidylcholine:diacylglycerol cholinephosphotransferase	2.7.8.2
LPCAT	*TRINITY_DN14564*	NDE	2-lysophosphatidylcholine acyltransferase	2.3.1.51/ 2.3.1.-
DGK	*TRINITY_DN13952*	1.77	Diacylglycerol kinase (ATP dependent)	2.7.1.107
DGK	*TRINITY_DN16873*	-13.87	Diacylglycerol kinase (ATP dependent)	2.7.1.107
DGK	*TRINITY_DN10575*	NDE	Diacylglycerol kinase (ATP dependent)	2.7.1.107
MOGAT	*TRINITY_DN11700*	42.95	2-acylglycerol O-acyltransferase 2	2.3.1.22
MOGAT	*TRINITY_DN15448*	1.92	2-acylglycerol O-acyltransferase 2	2.3.1.22
MOGAT	*TRINITY_DN13615*	NDE	2-acylglycerol O-acyltransferase 2	2.3.1.22
MOGAT	*TRINITY_DN17271*	-3.24	2-acylglycerol O-acyltransferase 2	2.3.1.22
DGAT	*TRINITY_DN6303*	2.75	Acyl-CoA: diacylglycerol acyltransferase	2.3.1.20/ 2.3.1.75/ 2.3.1.76
DGAT	*TRINITY_DN20217*	1.92	Acyl-CoA: diacylglycerol acyltransferase	2.3.1.20 /2.3.1.75 /2.3.1.76
DGAT	*TRINITY_DN18843*	4.41	Acyl-CoA: diacylglycerol acyltransferase	2.3.1.20/ 2.3.1.75/ 2.3.1.76

DGAT	*TRINITY_DN12378*	NDE	Acyl-CoA: diacylglycerol acyltransferase	2.3.1.20/ 2.3.1.75/ 2.3.1.76
DGAT	*TRINITY_DN11708*	NDE	Acyl-CoA: diacylglycerol acyltransferase	2.3.1.20
PDAT	*TRINITY_DN17341*	33.78	Phospholipid:diacylglycerol acyltransferase	2.3.1.158
PDAT	*TRINITY_DN19832*	6.25	Phospholipid:diacylglycerol acyltransferase	2.3.1.158
PDAT	*TRINITY_DN18130*	-163.5	Phospholipid:diacylglycerol acyltransferase	2.3.1.158
Choline and ethanolamine pathway				
CK	*TRINITY_DN29815*	NDE	Choline kinase	2.7.1.82
CCT	*TRINITY_DN17134*	-2.57	Choline-phosphate cytidylyltransferase	2.7.7.14
EK	*TRINITY_DN18645*	-3.98	Ethanolamine kinase	2.7.1.82
PEMT	*TRINITY_DN11436*	NDE	Phosphoethanolamine N-methyltransferase	2.1.1.17
PEMT	*TRINITY_DN14375*	NDE	Phosphoethanolamine N-methyltransferase	2.1.1.17
PEMT	*TRINITY_DN11833*	2.33	Phosphoethanolamine N-methyltransferase	2.1.1.17
PECT	*TRINITY_DN19707*	NDE	CTP:phosphorylethanolamine cytidyltransferase	2.7.7.14
LPEAT	*TRINITY_DN14753*	-1.89	lysophosphatidylethanolamine acyltransferase	2.3.1.23

Table 6.3 List of transcripts of *C. cryptica* codifying for fatty acid desaturase (FAD). Expression analysis was performed using RNA-sequencing comparing heterotrophy (HE) vs autotrophy (AU). FAD features were inferred by phylogenetic similarities with *P. tricornutum* FADs reported by Dolch and Marechal (2015). * = TRINITY_DN17462 and TRINITY_DN16698 were both near with Phatr2|50443, in the phylogenetic tree.

Cyclotella FAD	**ET vs AU**	**Double bonds**	**Location**	**Lipid C number**	**Acyl liked to**	**P. tricornutum**	**NCBI ID**
TRINITY_DN20022	14.81	Δ12 or ω6	ER	18	Phospho and betaine lipid	Phatr2|25769	XP_002186139
TRINITY_DN11256	3.60	Δ5	ER	20	Phospho and betaine lipid	Phatr2|48830	XP_002185732
TRINITY_DN15101	5.70	Δ6	ER	18	Phospho and betaine lipid	Phatr2|29488	XP_002182901
TRINITY_DN13156	NDE	Δ12	Chl membrane	16	MGDG-DGDG-SQDG	Phatr2|48423	XP_002182832
TRINITY_DN18226	4.20	Δ5	ER	20	Phospho and betaine lipid	Phatr2|22459	XP_002182858
TRINITY_DN17462 *	NDE	Δ6	Chl membrane	16	MGDG-DGDG-SQDG	Phatr2|50443	XP_002185374
TRINITY_DN19657	-1.62	-	-	-	-	-	-
TRINITY_DN18100	32.45	Δ9	Chl stroma	16 - 18	ACP	Phatr2|9316	XP_002177417
TRINITY_DN19760	3.21	-	-	-	-	-	-
TRINITY_DN11467	NDE	Δ5	ER	22	Phospho and betaine lipid	Phatr2|22510	XP_002183026
TRINITY_DN10520	NDE	-	-	-	-	-	-
TRINITY_DN16698 *	NDE	Δ6	Chl membrane	16	MGDG-DGDG-SQDG	Phatr2|50443	XP_002185374
TRINITY_DN31394	NDE	Δ9	Endomembrane	18	CoA	Phatr2|28797	XP_002181794
TRINITY_DN18895	-2.20	-	-	-	-	-	-

6.3.3 Fatty acid synthase complex regulation

Diatoms and plants showed similar FA synthesis pathways using acetyl-CoA as precursor [12] (**Figure 6.3**). This originated from different subcellular compartments, including mitochondria, cytoplasm and plastids, by different routes. Our differential expression analysis, indicated up-regulations of transcripts codifying for pyruvate dehydrogenase complex (PDC) which represents the conventional major route for chloroplastic fatty acid biosynthesis and for acetyl-CoA synthetase (ACS), which represents a specific algal additional acetyl-CoA source for FA biosynthesis upon heterotrophy and mixotrophy [38]. The activity of PDC is repressed by pyruvate dehydrogenase kinase (PDK), thus make this enzyme a negative regulator of FA biosynthesis [39]. Our results did not display a regulation of PDK induced by heterotrophy, suggesting a different regulation of PDC upon dark cultivation. On the other hand, our results indicated a down-regulation of transcripts codifying for ATP: citrate lyase, which represents a different source of acetyl-CoA. Anyway, no evidences were reported about the role of this enzyme as FA precursor [38]. FA biosynthesis is a multistep process involving several enzymatic complexes both in plants and diatoms [37,38]. Our results reported an activation of key genes of this process namely acetyl-CoA carboxylase (ACC), Ketoacyl-ACP synthase II (KCSII), Enoyl-ACP reductase (ENR). Particularly, ACC is a key regulator of the flux of acetyl-CoA through the FA biosynthesis pathway in plants and microalgae (e.g. *Chlorella vulgaris*) but this role was not previous confirmed in *C. cryptica* [40]. In diatoms, these reactions lead to the biosynthesis of 16:0-ACP while plastidial 18:0-ACP were scarcely represented suggesting that FA biosynthesis pathway is partially different from higher plants [12,41]. The biosynthesis of very long fatty acid was catalyzed by a specific group of elongase (ELOVL). Usually, the maximum length of long acyl-chains generated in diatom plastids is 18 carbon atoms, while production of VLC-PUFAs (20 and more carbons atoms) occurs in the ER [12]. Our transcriptomic analysis identified three expressed transcripts codifying for very long fatty acid elongase (ELOVL). Using prediction software, the non-differentially expressed was assigned to chloroplastic localization while two up-regulated transcripts were assigned to ER. The transport process involved in VLC-PUFA import to plastids still remain unknown but in green algae it was proposed that this class of FA could be exported from ER through betaine lipids and then incorporated into galactolipids in plastids [42].

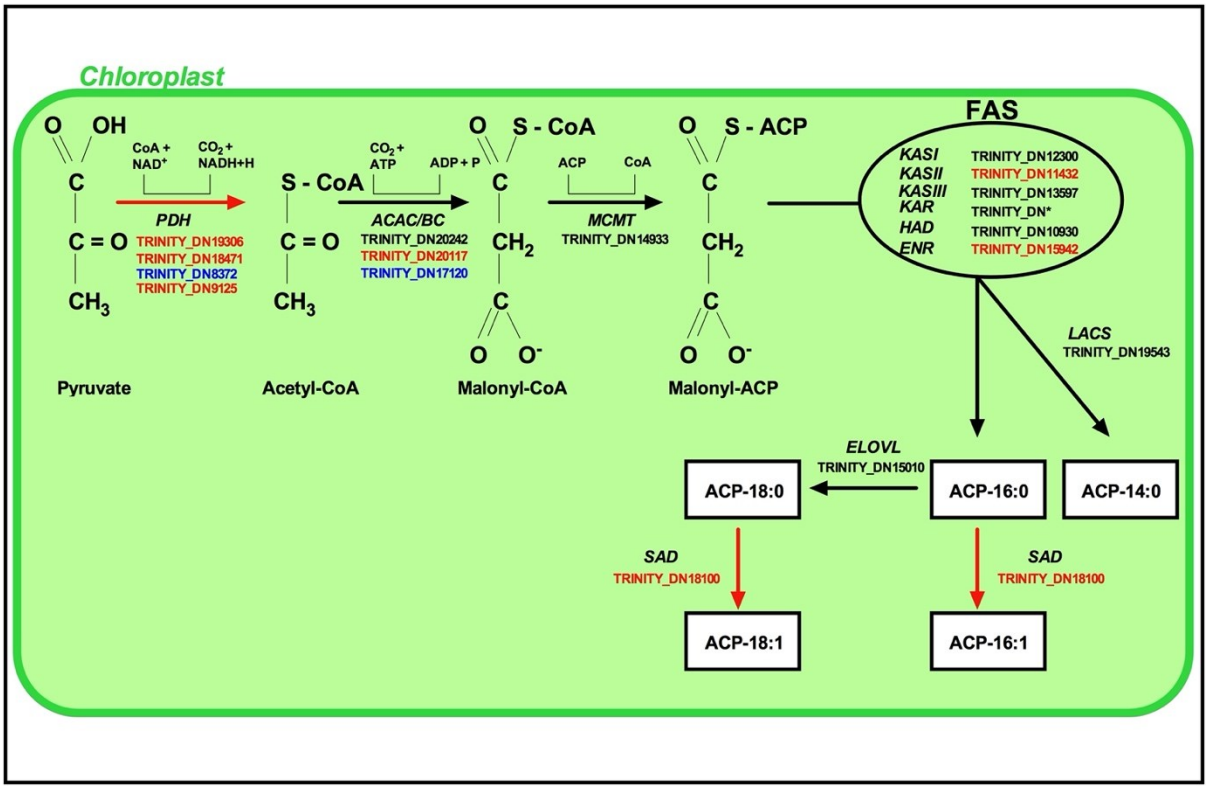

Figure 6.3 Reconstructed model pathway and expression analysis for FA biosynthesis in *C. cryptica*. Genes up- and down-regulation are highlighted in red and blue, respectively; NDE genes or ≤ 1.5/- 1.5 fc are in black. Expression details and abbreviation legends for enzymes are in table 3. * = Ketoacyl-ACP reductase (KAR) displayed 10 different coding transcripts. Detailed informations are in table 6.3.

Using GC- MS approach we identified the major fatty acid species biosynthesized by *Cyclotella* and the regulation induced by the auto/heterotrophy switch (**Table 6.1**). This diatom is able to synthesize FA starting from 14:0. This specie showed no significant difference comparing autotrophy and heterotrophy. The major FAs synthetized upon both conditions are palmitic acid (16:0), palmitoleic acid (16:1) and EPA (20:5). Interestingly, after 7 days upon dark cultivation 16:1 and 18:1 showed an increased content. This is probably related to the up-regulation upon dark condition of the SAD desaturase (TRINITY_DN18100 – **Table 6.3**) which catalyze the Δ9 desaturation on ACP-16:0 and ACP-18:0. It is worth to point out that this specie showed a scarce representation in both analyzed conditions. Interestingly, heterotrophy appeared a critical condition to manipulate the composition of monounsaturated fatty acid (MUFA) and polyunsaturated fatty acid (PUFA). Upon heterotrophy MUFA showed a significant increase of about 2.19 fc while PUFA showed a significant decrease of about 1.96 fc (**Table 6.1**). With the exception of 16:1 ω-7, multiple desaturated 16 C species reduced their content (16:3 ω-4 and 16:4 ω-1) or completely

disappeared (16:2 ω-7) upon heterotrophy. Particularly, 16:3 and 16:4 were commonly considered the main plastidial diatom FA markers, and this regulation would play a specific adaptation role of *Cyclotella* during persisting dark period, significantly affecting the composition of GL and PL species.

6.3.4 Glycolipids and phospholipids chloroplastic routes

The conclusive plastidial step in the formation of active FAs is the connection of acyl group from ACP to glycerol-3-phosphate (G3P). This process is considered the terminal step of FA synthesis and the initial step of GL biosynthesis [12]. Upon heterotrophy we identified a number of chloroplastic and non-plastidial transcripts codifying for GPAT (Glycerol-3-phosphate acyltransferase). These are up regulated upon heterotrophy. Analogously, transcripts codifying for the second enzyme (LPAT - lysophosphatidic acid acyltransferase) involved in the acylation of lysophosphatidic acid (LPA) were up regulated upon heterotrophy. The acyl-CoA pool used for the acylation of G3P can either originate from chloroplastic FAs namely 16:0, 16:1, 18:1 or by the deacylation of complex phospholipids (e.g., 18:2, 18:3 molecular species)[43].

al., 2009). Using ^{1}H-NMR and GC-MS approaches, we reported a drastically reduction of the total amount of SQDG upon dark cultivation. The percentages of SQDG species showed minor differences comparing heterotrophy and autotrophy (**Figure 6.4A**). With the exception of SQDG (14:0/14:0) and SQDG (16:0/16:3) SQDG species reported no significant differences, showing SQDG (16:1/16:0) as most abundant specie (≈ 70%). On the other hand, the other two class of GL showed diversified profiles in heterotrophy and autotrophy cultivations (**Figure 6.4B-C**). As showed in **Figure 6.4B**, the most representative MGDG species upon autotrophy are MGDG (16:2/16:3), MGDG (16:3/16:3) MGDG (16:3/20:5). These species were practically absent in heterotrophy. Dark cultivated *C. cryptica* reported different representative MGDG species namely MGDG (16:1/16:1) MGDG (16:1/20:5). These MGDG species showed an increase of about 5.9 and 6.5 fold change comparing heterotrophy *vs* autotrophy, respectively. Similar DGDG species (16:1/16:1) and (16:1/20:5) were equally overrepresented upon heterotrophy showing an increase about 2.2 and 2.3 fold change, respectively.

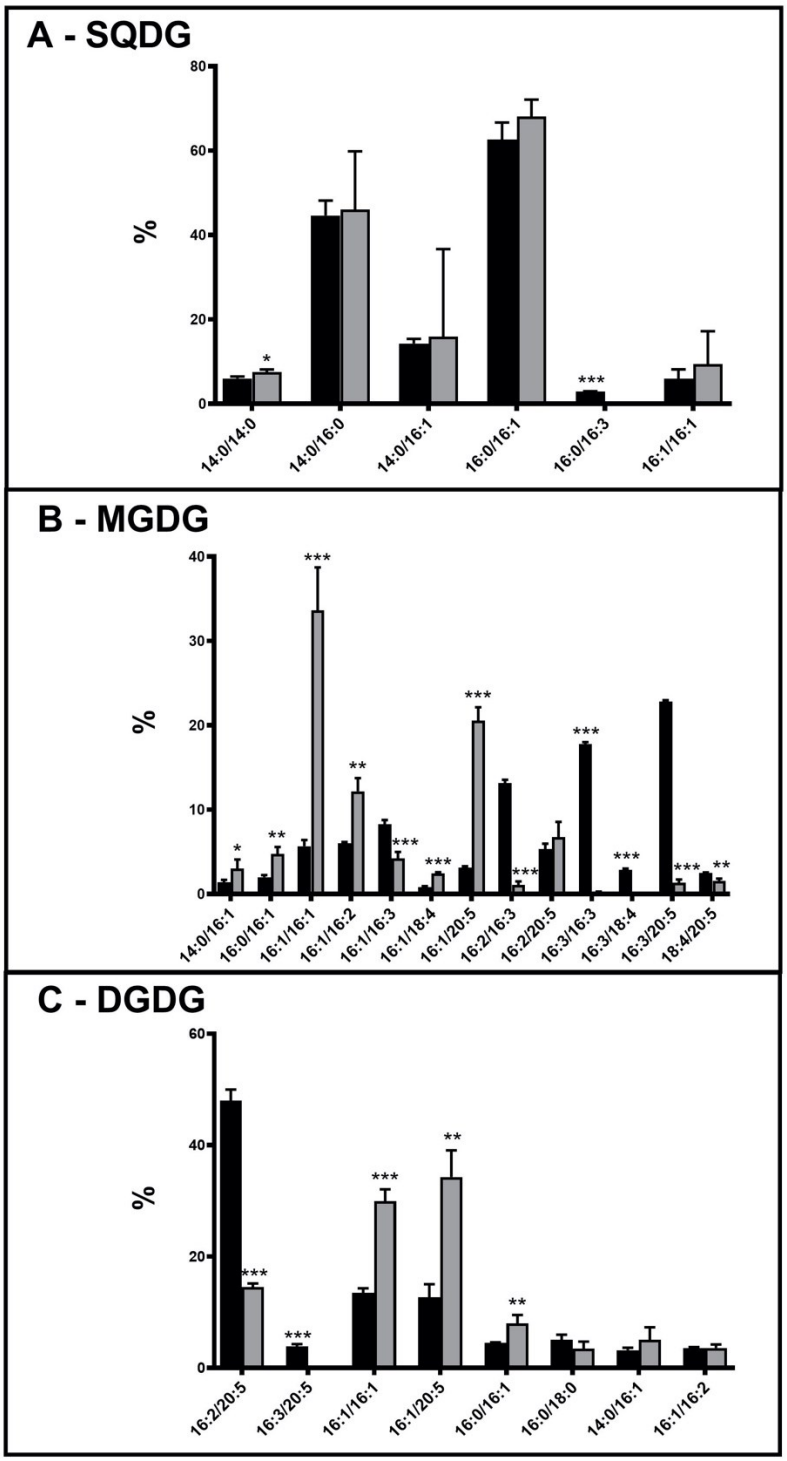

Figure 6.4 Profile of SQDG (A), MGDG (B) and DGDG (C) species percentages from *C. cryptica* lipids/biomass cultivated upon autotrophic (black bars) and heterotrophic (grey bars) conditions after 7 days. Species included in the figures showed a percentage ≥ 2.5%. Asterisks indicate significantly different values in autotrophic and heterotrophic samples at $p \leq 0.05$ (*), $p \leq 0.005$ (**) and $p \leq 0.0005$ (***).

As showed in **Figure 6.5,** PL showed diversified behaviors depending by the species. Upon heterotrophy, the most represented phosphoglycerids (PG) were 16:0/16:1 and 16:0/20:5.

The first showed an increase about 2.37 fc while the second was practically absent upon autotrophy. On the other hand, 16:1/20:5 was drastically reduced upon heterotrophy. Phosphatidylcholine (PC) 16:1/16:1 and 20:5/20:5 showed significant and contrasting differences. The first increased upon autotrophy while the second upon heterotrophy. Phosphatidylethanolamine (PE) showed minor differences.

Different authors reported diversified length of FAs in GL diatoms from 14 to 24 [44,45]. Particularly, the exposition to abiotic stresses, such as nutrients starvation or low temperatures induced modified composition of long chain of polyunsaturated fatty acids PUFAs (LC-PUFAs) [12,46]. Plants, microalgae and diatoms share the enzymes responsible for the biosynthesis of glycerolipids namely UDP-sulfoquinovose synthase (SQD1), UDP-sulfoquinovose:DAG sulfoquinovosyltransferase (SQD2), monogalactosyldiacylglycerol Synthase (MGDGS) and digalactosyldiacylglycerol synthase (DGDGS) [12,38].

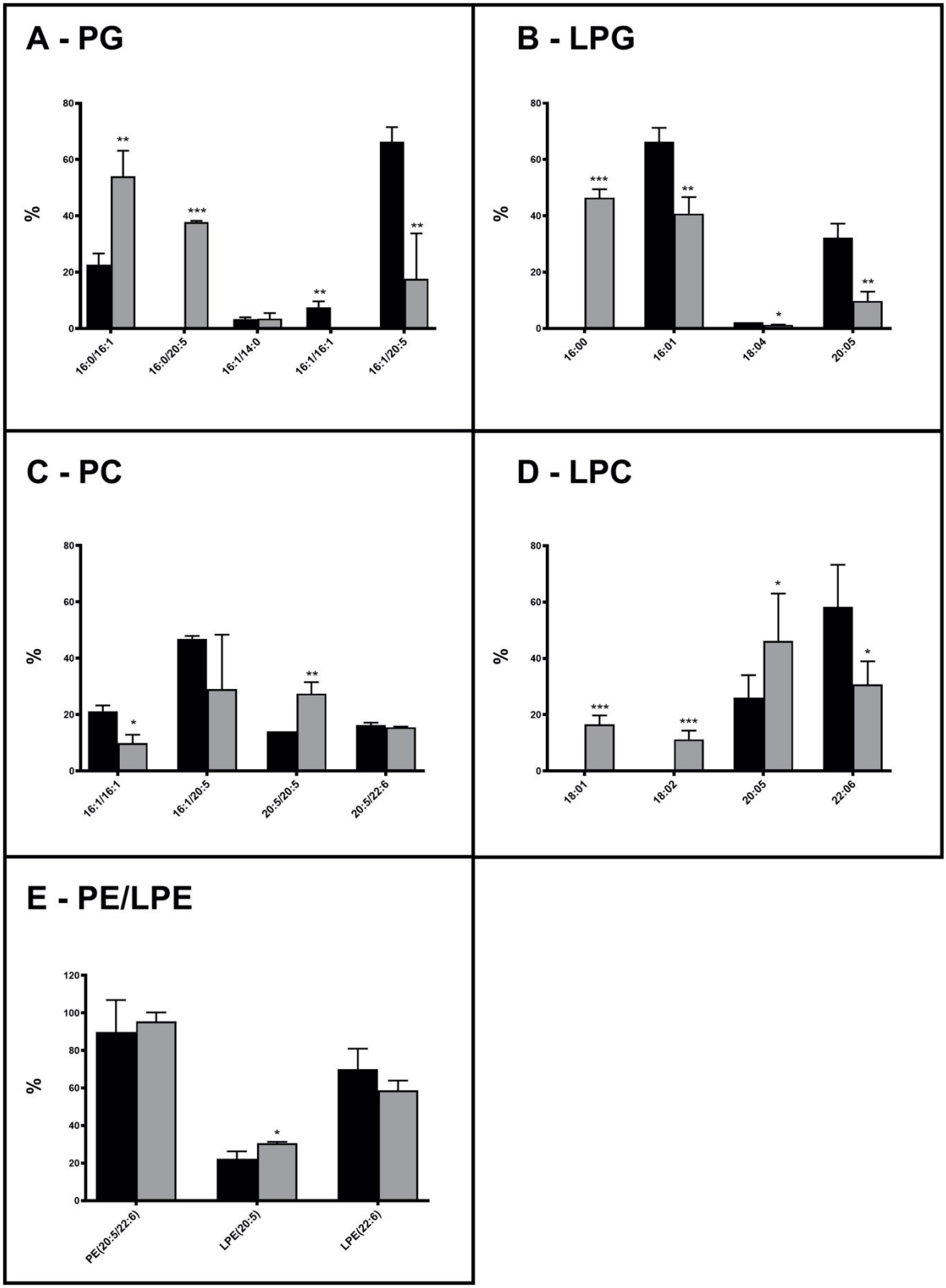

Figure 6.5 Profile of PG (A), LPG (B), PC (C), LPC (D) and PE/LPE (E) species percentages from *C. cryptica* lipids/biomass cultivated upon autotrophic (black bars) and heterotrophic (grey bars) conditions after 7 days. Species included in the figures showed a percentage ≥ 2.5%. Asterisks indicate significantly different values in autotrophic and heterotrophic samples at $p \leq 0.05$ (*), $p \leq 0.005$ (**) and $p \leq 0.0005$ (***).

A number of transcripts codifying for SQD1, SQD2, DGDGS and MGDGS were identified (**Figure 6.6**). With the exception of SQD2, these genes generally showed a decrease of expression upon heterotrophy justifying a reduced diacylglycerol (DAG) channeling into the GL pathway and the MGDG, DGDG and SQDG reduced content.

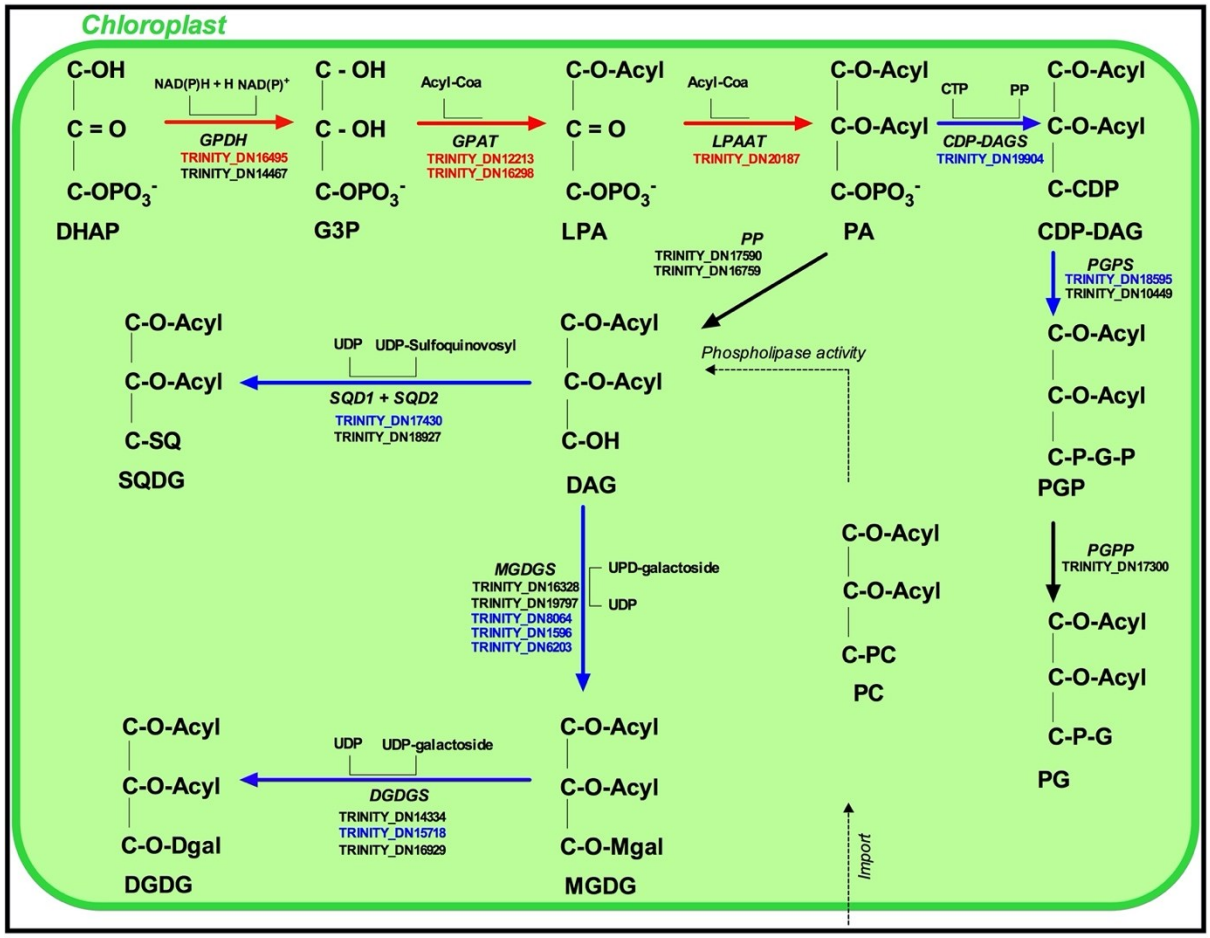

Figure 6.6 Reconstructed model pathway and expression analysis for chloroplastic PL and GL biosynthesis in *C. cryptica*. Genes up- and down-regulation are highlighted in red and blue, respectively; NDE genes or ≤ 1.5/- 1.5 fc are in black. Expression details and abbreviation legends for enzymes are in table 3. Substrate's abbreviations legend: Dihydroxyacetonephosphate (DHAP); glycerol 3-phosphate (G3P); lysophosphatidic acid (LPA); phosphatidic acid (PA), diacylglycerol (DAG), phosphatidylglycerol phosphate (PGP); phosphatidylglycerol (PG); monogalactosyldiacylglycerol (MGDG); digalactosyldiacylglycerol (DGDG); sulfoquinovosyldiacylglycerol (SQDG)

6.3.5 Heterotrophy induced TAG accumulation

TAGs profile appears to be substantially changed comparing heterotrophy and autotrophy (**Figure 6.7**). Five species were totally silenced (or drastically reduced) in heterotrophy namely TAG (18:4/14:2/16:1), TAG (18:4/14:1/16:1), TAG (18:4/14:0/16:1), TAG (18:4/14:0/14:0) and TAG (16:1/14:0/16:3). On the other hand, three different species were exclusively synthesized

upon heterotrophy: TAG (16:0/16:1/18:1) and TAG (16:1/18:1/20:5) and TAG (16:0/14:0/16:1). Intriguingly, the last represented one of the most biosynthesized TAGs upon heterotrophy together with TAG (16:1/16:1/20:5), TAG (16:1/16:1/20:5), TAG (16:1/14:0/16:1), TAG (16:0/16:1/20:5) and TAG (16:0/16:0/16:1). With the exception of dark overexpressed-TAG (16:0/16:1/20:5), the other species showed no significant differences between heterotrophy and autotrophy.

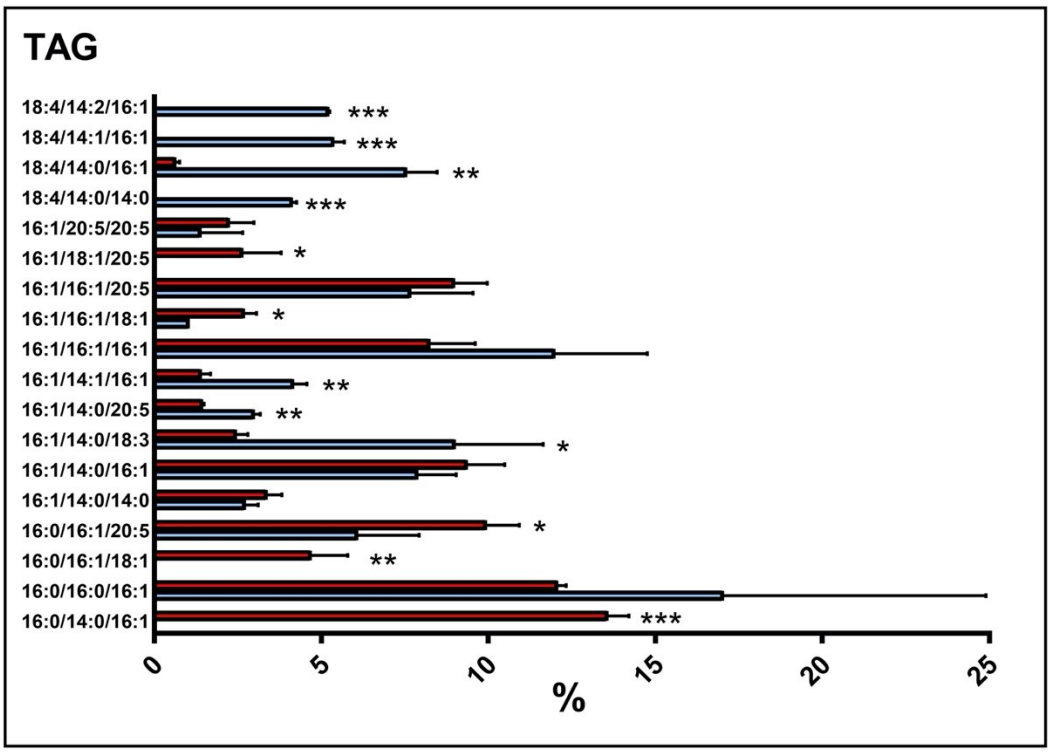

Figure 6.7 Profile of TAG species percentages from *C. cryptica* lipids/biomass cultivated upon autotrophic (blue bars) and heterotrophic (red bars) conditions after 7 days. Species included in the figures showed a percentage ≥ 2.5%. Asterisks indicate significantly different values in autotrophic and heterotrophic samples at $p \leq 0.05$ (*), $p \leq 0.005$ (**) and $p \leq 0.0005$ (***).

Considering the significant increase of TAG content (**Figure 6.2**), our results clearly indicated heterotrophy as suitable and effective systems to manage quantity and quality of TAG species.

Our results clearly indicated that heterotrophy is an unconventional condition leading to TAG accumulation for carbon storing as well as carbohydrates accumulation (**Figure 6.1**). FAs can be used as energy or carbon store in the form of TAGs [12,38]. This behavior puts heterotrophy on the same level of nutrients starvation, which is a well-accepted strategy to induce lipid accumulation in diatoms [18,20]. Up to now, the mechanisms used by diatoms to export FAs from

the plastid still remain unclear. It was proposed in higher plants a PC mediated transport, where acyl groups could leave the plastid to ER by membrane contact site [12]. Furthermore, two ABC transporters were reported by Li-Beisson et al. [37] as putative FA transporter in *Arabidopsis* At1g54350 and At4g39850. Putative orthologous of these was identified in our transcriptome (**Table 6.2** - TRINITY_DN18575). Diatoms showed two different TAG biosynthesis routes namely acyl-CoA dependent pathway and acyl-CoA independent pathway [12,47–49]. The final acylation steps inducing the synthesis of TAG in these two pathways were respectively catalyzed by acyl-CoA:DAG acyltransferase (DGAT) and Phospholipid:diacylglycerol acyltransferase (PDAT). The first incorporate the third acyl-CoA from DAG while the second uses PC as an acyl donor for the formation of TAG from DAG [12,50]. Our results reported up-regulations of different transcripts codifying for DGAT and PDAT thus justifying the enhanced content of TAG by molecular regulation (**Table 6.2, Figure 6.8**). Particularly, we clustered the DGATs from *C. cryptica* (**Figure 6.9**) identifying 3 type 1 DGAT (TRINITY_DN20217, TRINITY_DN11708, TRINITY_DN6303) and 2 type 2 DGAT (TRINITY_DN18843, TRINITY_DN12378). As reported for other diatoms [51], no DGAT3 were identified in our transcriptome. Both CcDGAT1-2 reported isoforms up-regulated by heterotrophy (**Table 6.2**). Diatom species showed different compositions of TAG. *P. tricornutum* showed TAGs composed by high levels of 16:0 and 16:1 while only trace of EPA were reported [12,52]. Contrarily, *T. pseudonana* is able to link both, DHA and EPA into TAGs at high level [53]. It is not clear if DGATs from different species showed substrate specificities or the composition of TAGs depends by substrate availability [12]. Our lipidomics results showed a number of TAG species containing 20:5 FA. This behavior would be related to specificity of *C.cryptica* DGATs because some of them were represented both in autotrophy and heterotrophy profiles but in addition heterotrophy further contributed to an increase of these TAG species. The exchange of FAs between the PL, DAG and TAG pools were recurrently demonstrated in diatoms [12,38,54]. Our transcriptome reported the presence of transcripts codifying for enzyme such as acyl-CoA:lysophosphatidylcholine acyltransferase (LPCAT), Phosphatidylcholine:diacylglycerolcholine phosphotransferase (PDCT) and PDAT. Their presence suggested the ability of *C. cryptica* to catalyze the exchange of FAs between the phospholipid and the DAG/TAG pools. Particularly, PDCT leading to the coexistence of neo-synthesized DAG or PC-derived DAG molecules with distinct FA molecular species at position

sn^{-1} and sn^{-2}. This process called acyl-editing was reported as major mechanism involved in the PUFA flux into TAG in Arabidopsis [55].

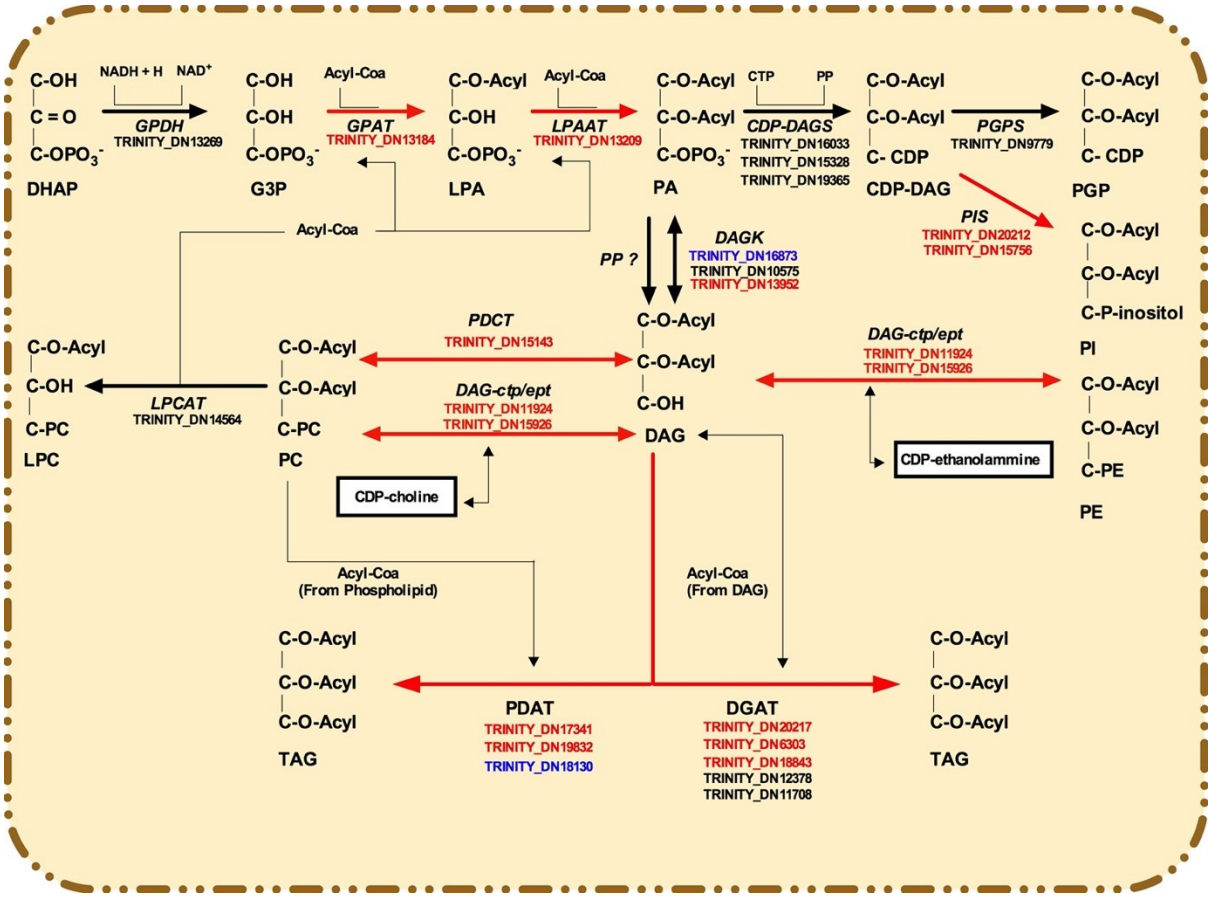

Figure 6.8 Reconstructed model pathway and expression analysis for PL and TAG biosynthesis in *C. cryptica*. Genes up- and down-regulation are highlighted in red and blue, respectively; NDE genes or ≤ 1.5/- 1.5 fc are in black. Expression details and abbreviation legends for enzymes are in table 3. Substrate's abbreviations legend: Dihydroxyacetonephosphate (DHAP); glycerol 3-phosphate (G3P); lysophosphatidic acid (LPA); phosphatidic acid (PA), diacylglycerol (DAG), phosphatidylglycerol phosphate (PGP); phosphatidylglycerol (PG); phosphatidylcholine (PC); phosphatidylethanolamine (PE); triacylglycerol (TAG).

6.3.6 FADs identification, characterization and differential expression analysis

Cyclotella transcriptome displayed the presence of 14 different expressed FADs (**Table 6.3**). Comparing heterotrophy and autotrophy 6 were up regulated, 2 were down regulated and 6 were non-differentially expressed. In order to cluster the different FADs, identify the enzymatic peculiarities and investigate their phylogenetic relationships, a comparison of the amino acidic putative sequences was performed by constructing an un-rooted phylogenetic tree (**Figure 6.9**). The previous characterization obtained using *P. tricornutum* FADs were used to predict similar functions in *C. cryptica* [56]. *C. cryptica* transcripts clustered with

corresponding *P. tricornutum* FADs while 3 transcripts (TRINITY_DN19657, TRINITY_DN18895 and TRINITY_DN10520) clustered far for any diatom FADs (**Figure 6.9**). Ambiguous results were only reported for *P. tricornutum* PHATRDRAFT_50443. Among the *P. tricornutum* FADs, 5 proteins namely PHATRDRAFT_25769, PHATRDRAFT_48830, PHATRDRAFT_29488, PHATRDRAFT_48423 and PHATRDRAFT_9316 were functionally characterized [57–60]. Phylogenetic analysis identified as *Cyclotella* orthologous TRINITY_DN20022, TRINITY_DN11256, TRINITY_DN15101, TRINITY_DN13156 and TRINITY_DN18100, respectively (**Table 6.3**). Furthermore, orthologous for other important diatoms namely *Fragilariopsis cylindrus* and *Thalassiosira pseudonana* were also identified (**Figure 6.9**). TRINITY_DN18100 was identified as CcSAD. This showed similarity with PHATRDRAFT_9316 namely chloroplastic localization, acting as Δ9 desaturase on ACP-16:0 or ACP-18:0 to synthesize 16:1 or 18:1 [56]. TRINITY_DN18100 showed an increased expression upon heterotrophy justifying the increase amount of 16:1 and 18:1 reported in **Table 6.1**. Intriguingly, TRINITY_DN10520 showed no similarities with *P. tricornutum* FADs but clustered near plants and green algae FAD4 (**Figure 6.9**). Particularly, AtFAD4 (At4g27030) encodes for a chloroplast fatty acid desaturase involved in the introduction of a Δ3 double bond on sn-2 palmitate of PG [61]. With the exception of SAD and of TRINITY_DN19760, the fatty acid desaturation chloroplastic route appeared to be scarcely influenced upon dark. This could be in part explaining the reduced amount of chloroplastic markers 16:2, 16:3 and 16:4 (**Table 6.1**). Usually, diatoms showed a major amount of unsaturated C16 FAs in chloroplast lipids supporting the idea that the main desaturation route is within this organelle [56].

On the other hand a number of ER FAD were functionally characterized in *P. tricornutum,* representing an alternative route to obtain polyunsaturated long and very long FAs [12,56,57,60]. The ERFAD2 (PHATRDRAFT_25769) able to catalyze Δ12 desaturation on 16:1 and 18:1 was identified in *P. tricornutum* [60]. Our phylogenetic analysis indicated TRINITY_DN20022 as putative orthologous. One Δ6 desaturase in ER was identified in *P. tricornutum* (PHATRDRAFT_29488) and called ERΔ6FAD [56,57]. The substrates of this enzyme were experimentally identified as $18:2^{\Delta 9,12}$ and $18:3^{\Delta 9,12,15}$ generating 18:3 and 18:4, respectively [60]. Our phylogenetic analysis indicated TRINITY_DN15101 as putative orthologous. Among the interesting PUFA produced by diatoms, eicosapentanoic acid (EPA, 20:5) represents a critical nutrient for human consumption and an appreciate product from diatoms [4]. Among the

possible routes producing EPA in diatom, experimental strategy suggested the elongation of 20:4 [62] and the activity of two Δ5 front-end desaturase, ERΔ5FAD.1 (PHATRDRAFT_46830) and ERΔ5FAD.2 (PHATRDRAFT_22459). By testing a subset of possible 20-carbon substrates, ERΔ5FAD.1 was shown to act on 20:1$^{\Delta 11}$, 20:2$^{\Delta 11,14}$, 20:3$^{\Delta 11,14,17}$, or 20:3$^{\Delta 8,11,14}$ thus indicating an high effective role of this enzyme in EPA biosynthesis [57]. Our phylogenetic analysis indicated putative role of TRINITY_DN11256 and TRINITY_DN18226 as ERΔ5FAD.1 and ERΔ5FAD.2, respectively. With the exception of TRINITY_DN11467, C. cryptica FADs localized in the ER showed an increased expression comparing heterotrophy *vs* autotrophy (**Table 3**).

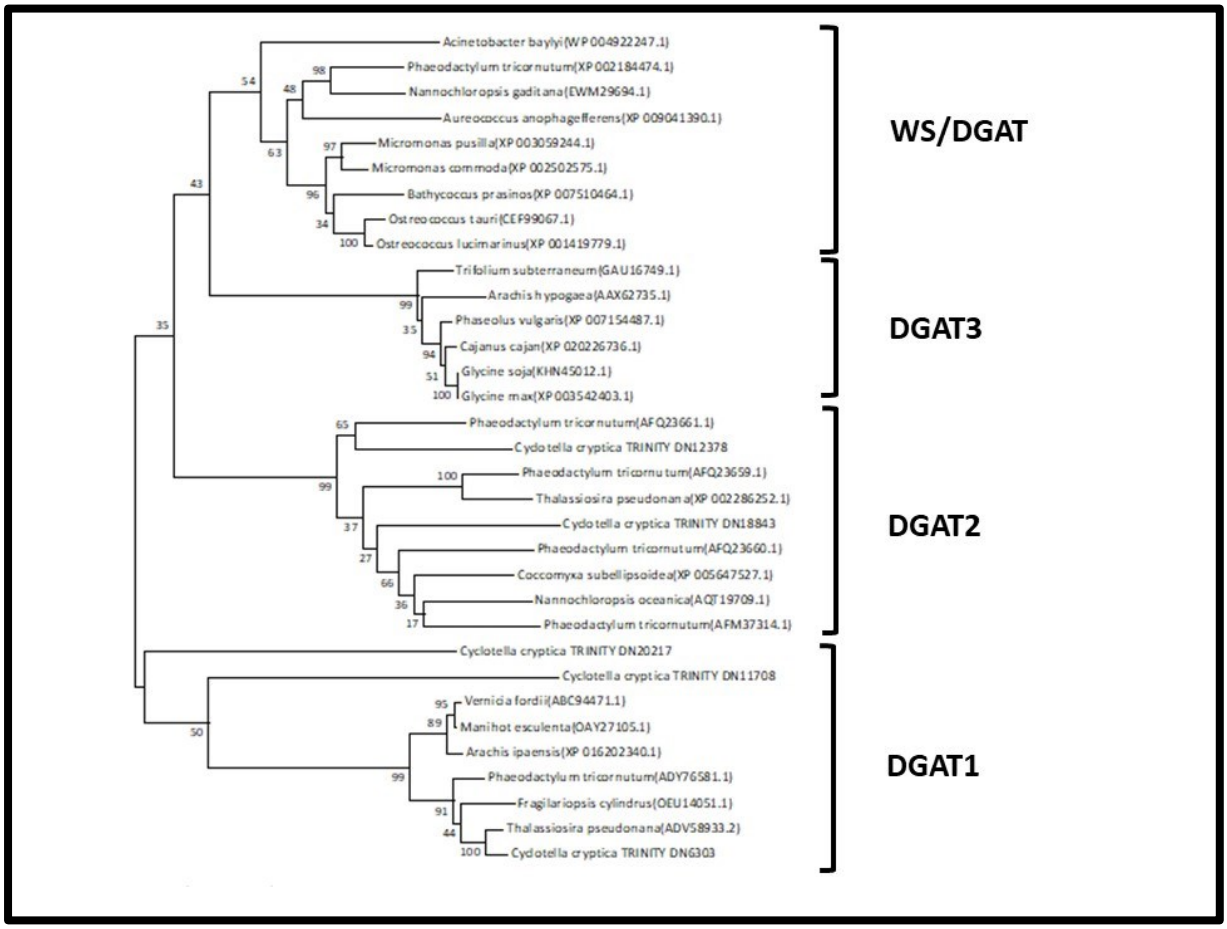

Figure 6.9 Un-rooted phylogenetic tree.

6.4 Conclusions

This study is the first to examine the lipidome and the transcriptome of a noticeable diatom in response to dark cultivation. The heterotrophic environment used in this study simulates condition and timing suitable for industrial applications. A limited number of microalgae and diatom species were identified as suitable for heterotrophic cultivation reporting interesting

results in lipids, PUFA, carotenoids and phycocyanin production [31,35,44,63,64]. Particularly, *C. cryptica* was previous identified as one of the wild type diatoms capable to grown upon dark condition [31,65]. Our results clearly reported no detrimental effects on *C. cryptica* heterotrophically growth. In fact, dark cultivated *Cyclotella* cells compared with light cultivated showed similar growth rates, increased biomass and cells dimension. The ability to positively respond to different light treatments (in variable time period) is a common and recognized ability of some of diatoms. Wild types *P. tricornutum* and *F. cylindrus* showed positive growing performances upon mixotrophic and heterotrophic conditions, respectively while improved ability to growth upon dark were obtained using *P. tricornutum* engineered strain [36,44,66].

C. cryptica showed the ability growth upon heterotrophic condition metabolizing the external glucose supplied as carbon source. This was used to biosynthesize both carbohydrates and lipids storage species. To the base of the modifications on fatty acids and lipids, genes involved in fatty acid synthase pathway were up regulated increasing the content of these compounds. Previous analysis on diatoms reported that single genes overexpression is not always sufficient to manipulate the lipid content [12]. For example the overexpression of Acetyl-CoA carboxylase in *C. cryptica* reported no differences in terms of lipid accumulation between wild type and engineering strain [67] thus highlighting the idea of a complex and overall molecular regulation as necessary requirement to manipulate lipid accumulation in diatoms. Heterotrophic cultivation of *C. cryptica* induced a drastic reduction of SQDG. This specie is usually synthesized in plastids from the UDP-glucose obtained from glucose 1-P and UTP using a plastidic UDP-glucose pyrophosphorylase. This is converted to UDP-sulfoquinovose (SQ) by the activity of UDP-SQ synthase (SQD1). The final step is catalysed by SQDG synthase (SQD2) transferring SQ from UDP-SQ to DAG [68]. Both SQD1 and SQD2 are codified by single loci in the *Arabidopsis* [37]. Our sequencing showed the presence of two transcripts codifying for SQD1 (TRINITY_DN17430) and SQD2 (TRINITY_DN18927). Particularly SQD1 showed a reduce expression upon heterotrophy. Marine microorganism showed modification in SQDG content upon nutrients starvations while positively regulation occurred upon high light illumination [69–71]. In our condition, it is not surprising the decreased content of SQDG, considering their crucial role in thylakoids structure, light harvesting complex (LHC) organization and in PSII and PSI functioning [68,72,73]. Compared with plants and other microalgae, diatoms showed an

enriched SQDG and PG content in thylakoid membranes thus making the anionic lipid SQDG the most abundant lipid in diatom thylakoids as well as MGDG [72].

Manipulation of TAG biosynthesis genes is an effective strategy to obtain diatom strains with increasing biomass, lipids and TAG yields. In this context, critical enzymes are GPDH, GPAT, LPAT and DGAT. GPDH plays the critical role in the conversion of dihydroxyacetone phosphate to Glycerol-3-phosphate (G3P) by the use of NADPH as reducing power [37]. Manipulated strain overexpressing GPDH showed a significant impact on numerous metabolic processes in diatom cells, including the biosynthesis of glycerol and neutral lipids [74]. Moreover, both GPAT1 and GPAT2 were overexpressed in *P. tricornutum* increasing the lipid content of about 2.9 and 2.3 fold change, respectively [75,76]. Interestingly, the artificial overexpression of GPAT2 regulates the natural expression of LPAT and DGAT inducing enhanced effects in terms of lipid content [76]. GPAT and LPAT play critical role in TAG biosynthesis catalysing the sequential addition of acyl-CoA to G3P. Similar results in term of TAG accumulation were obtained by the engineering of DGAT in *P. tricornutum,* which showed as main activity the esterification of DAG with acyl-CoA. [51,77,78]. Our transcriptomic data clearly reported the natural overexpression of GPDH GPAT, LPAT and DGAT upon heterotrophy. The overexpression of these genes increased the flux of carbons imported from the culture media into storage lipids and TAGs. Particularly, TAG species obtained during dark cultivation showed an increase amount of MUFA such as 16:1 and 18:1, which are appreciating feedstock for biofuel production [18]. On the contrary, high amounts of PUFA negatively affecting the oxidation stability of the biodiesel decreasing the quality [18]. Therefore, dark cultivation of *C. cryptica* appeared a successful approach to manipulate key genes of lipid and TAG biosynthetic pathways avoiding the genetic engineering or the use of OGM strains and overcoming the detrimental effects of nutrient starvation in term of PUFA percentages [18,20].

6.5 Materials and Methods

6.5.1 Strain and culture conditions

C. cryptica (CCMP 331) was purchased from National Center for Marine Algae and Microbiota (Bigelow Laboratory for Ocean Sciences, USA) and it has been grown both in autotrophic and heterotrophic culture conditions for 7 days. *C. cryptica* was grown at 20± 2°C in 2 L polycarbonate carboy in pre-filtered sterile (0.22 µm) F/2 medium [79]at an initial concentration of $1x10^4$ cells mL^{-1}. Cultures were gently bubbled with sterile air. In autotrophic conditions, diatoms were grown under artificial light (200 µmol photons m^{-2} s^{-1}), provided by day-light fluorescent tubes (OSRAM 965, Germany) with a 14:10-h light:dark photoperiod. In heterotrophic conditions, cultures were incubated in the dark and F/2 medium was supplemented with 2 pulses of 1g/L of glucose at day 0 and day 7. Cells growth was daily monitored by microscope observation (Axio VertA1, Carl Zeiss, magnification of 20X) using a Bürker counting chamber (depth 0.100 mm, Merck, Leuven, Belgium).

6.5.2 Biomass content

500 ml of heterotrophic and autotrophic cultures were taken at the end of the cultivation period ($7t^h$day) (exponential phase). Cells were centrifuged in a swing-out Allegra X-12R (Beckman Coulter Inc., Palo Alto, CA, USA) at 2.300 g for 10 min. Pellets were frozen at -80°C and lyophilized with a MicroModulyo 230 (Thermo Electron Corporation, Milford, MA, USA) freeze dryer to assess cell dry weight (mg L^{-1}).

6.5.3 Calculation

Growth rate of cultures µ, expressed as divisions day^{-1}, was calculated according to the equation 1:

1) $\mu = (\ln(N_2)-\ln(N_1))/t_2-t_1$

Where N_1 and N_2 are cell numbers (cells/ml) at time 1 (t_1) and time 2 (t_2) at the extremes of the linear phase. Doubling time t_d was calculated according to the equation 2:

2) $t_d = \ln_2/\mu$

Number of doublings (n) at a time interval t is determined by the relation t/td, where t_d is the doubling time or time required to achieve a doubling of the number of viable cells.

6.5.4 Lipid extraction

Lipid extraction was performed using MTBE method. Particularly, dry cell pellet (50 mg) was suspended with 400 µl of MeOH. After vortexing, 3 mL of MTBE were added to allow extraction at room temperature for 1 hour, at constant shaking. Then, 750 µl of water were added and samples were left for another 10 minutes at room temperature, under shaking. Organic extracts were recovered (upper phase), after centrifugation at 1000g for 10 min. The lower phase was re- extracted with 1 mL of MTBE and 750 µl of water, after centrifugation the upper phase was combined with the previous one. The extract was dried under nitrogen flow and weighed to estimate, gravimetrically, the lipid content (mg L^{-1}).

6.5.5 Fame analysis

The total fatty acid composition of organic extracts was determined by GC-MS on the corresponding fatty acid methyl esters (FAME) obtained after saponification of lipid extracts with Na_2CO_3 in methanol at 40°C for 4 hours. The reaction of transesterification was blocked by adding water (to dissolve completely Na_2CO_3) and adjusting to pH=7. The extraction was conducted with diethyl ether and water (1:1), the organic phase recovered and dried under nitrogen stream. FAME mixtures were dissolved in methanol (1 µg $µL^{-1}$) and analyzed by GC-MS equipped with an ion-trap on a 5% diphenyl column in EI (70 eV) and positive mode analyzer. Elution of free fatty acid methyl esters required an increasing gradient of temperature according to the following method: 160°C for 3 min then 3°C till 260°C followed by 7min at 310°C. FAME have been identified by retention time assigned after analysis of standard mixture FAME (Marine source analytical standards, Sigma Aldrich).

6.5.6 NMR analysis

Microalgae extracts were prepared according to MTBE method (as described above) after addition of the internal standard DHBP (4,4'-Dihydroxybenzophenone 1mg/mL) to measure extraction accuracy and ω-3 quantity assessment using ERETIC method for analysis of

microalgal extracts [79]. The diagnostic peaks at 2.35 ppm (methylene protons in α to carbonyl group) and at 0.9 ppm (methyl protons of ω-3 fatty acids) were integrated to assess the amount of Total Fatty Acids (TFA) and ω-3 fatty acids. ^{1}H-NMR spectra were recorded on Bruker DRX 600 spectrometer equipped with an inverse TCI CryoProbe. Peak integration, ERETIC measurements and spectrum calibration were obtained by the specific subroutines of Bruker Top-Spin 3.1 program. Spectra were acquired with 14 ppm of spectral width (8417.5 Hz), 32 K of time domain data points, 90°pulse, 32 K spectrum size, and processed with 0.6 Hz of line broadening for the exponential decay function[80].

6.5.7 LC-MS analysis

Lipid extraction using MTBE method, as described in the paragraph 6.5.4, was carried out on 8 mg of dried pellet of cultures harvested after day 7 of cultivation. Commercial standards purchased from Avanti polar lipids (https://avantilipids.com) (7 µg SQDG (16:0/18:3) , 3 µg MGDG (16:0/18:0), 1 µg PG (17:0/17:0), 5 µg PC (18:0/16:0), 5 µg TAG (17:0/17:0/17:0), 3 µg DGDG (18:3/18:3)and 3 µg MGDG (16:0/18:0) were added on pellets, before lipid extraction, for quantitative lipid analysis.

Chromatographic separations were achieved on Infinity 1290 UHPLC System (Agilent Technologies, Santa Clara, CA, USA), equipped with a Kinetex Biphenyl 2.6 µm, 150 × 2.1 mm column, (Phenomenex, Castel Maggiore, Bologna, Italy) at 28 °C. Eluent A: water and eluent B: MeOH. The elution program consisted of a gradient from 40 to 80% B in 2 min, then to 100%B in 13min, holding at 100%B for 7min. A post run equilibration step of 5 min was included prior to each analysis. Flow rate was 0.3 ml/min. The injection volume was 10 µl and the autosampler was maintained at 10 °C. MS analyses were carried out on Q-Exactive Hybrid Quadrupole- Orbitrap mass spectrometer (Thermo Scientific, San Jose, CA, USA) equipped with a HESI source. Source parameters were as follows: Spray voltage positive polarity 3.2 kV, negative polarity 3.0 kV, Capillary temperature 320 °C, S-lens RF level 55, Auxiliary gas temperature 350 ° C, Sheath gas flow rate 60, Auxiliary gas flow Rate 35. Full MS scans were acquired over the range 200–1800 with a mass resolution of 70,000. The target value (AGC) was 1e6 and the maximum allowed accumulation time (IT) was 100 ms. For the data dependent MS/MS (ddMS2) analyses a Top10 method was used. AGC was 2e5 with IT 75 ms and 17,500 mass resolution; injections were of 10 µl. For lipid identification and quantification

LC/MS/MS data for each sample were processed by Xcalibur 3.0.63 and LipidSearch 4.1.16 package (Thermo Scientific). Absolute quantitation was carried out by a calibration curve using the standards that represent all species included in the analysis. Data are reported relative abundance (% ± SD) related to the total amount per lipid class [81].

6.5.8 RNA extraction and sequencing

RNA extraction and the sequencing were performed on autotrophic and heterotrophic cultivations and was provided by Genomix4life S.R.L. (Baronissi, Salerno, Italy). Total RNA was extracted using the standard RNA extraction method with TRIzol (Invitrogen, Carlsbad, CA, USA). RNA concentration in each sample was assayed with a ND-1000 spectrophotometer (NanoDrop) and its quality assessed with the Agilent 2100 Bioanalyzer and the Agilent RNA 6000 nano kit (Agilent Technologies, Santa Clara, CA, USA). Transcriptome was sequenced in paired-ends (2x100bp) according to the protocol TruSeq RNA Illumina on a HiSeq2500.

6.5.9 RNA-seq bioinformatic analysis

RNA paired-end sequencing was performed on six samples. Quality check of the sequenced reads was performed using the FAST QC software (www.bioinformatics.babraham.ac.uk/fastqc). Then adapters and very short reads (<20) were removed using cutadapt bioinformatics tool [82]. The high quality reads from all the samples were joined and then used as input to obtain a *C. cryptica* exhaustive transcriptome using Trinity software[83]. This assembled transcriptome included ~ 60 Mbp in 77197 transcripts grouped in 64539 genes. The GC content mean was 45.61%. The average and median contigs length was 780 bp and 414 bp, respectively. The N50 was 1343 bp. To compute abundance estimation, the high quality reads were aligned to the Trinity transcriptome using TopHat v2.1.1 selecting the standard parameters for paired-end reads[84]. The quantification of transcripts expressed for each sequenced sample was performed using featureCount algorithm. In order to define the set of expressed genes, raw read counts were normalized using the TMM method (Trimmed mean). Differentially expressed genes (DEGs) were obtained using the DESeq2 package of R language [85] at a false discovery rate (FDR) ≤ 0.05. Expression value were showed as “Fold Change”, the ratio of the normalized expression value

in heterotrophy over autotrophy, where the values <1 are shown as (-1/FC) to display the negative behavior of the gene. The sequences of the assembled transcripts were translated into proteins with Transdecoder and the software Blast2GO was used to associate a function to identified transcripts. The bioinformatics analysis was provided by Genomix4life S.R.L. (Baronissi, Salerno, Italy). Sequencing and alignment stats were resumed in supplemental table 1. Gene ontology enrichment analysis (GOEA) was separately performed on up-regulated and down-regulated DEGs datasets using the GO categories assigned by Blast2GO using Hochberg hypergeometric (FDR ≤ 0.05) as statistical test method. The enrichment score for each GO category (assigned DEGs ≥ 4) was calculated comparing sample frequency *vs* background frequency. Localization predictions were performed using the tools at the Prot Comp9.0 server4 (http://linux1.softberry.com/berry.phtml) and Chloro-P prediction server (http://www.cbs.dtu.dk/service/ChloroP/).

6.5.10 Phylogenic analysis

Sequences of fatty acid desaturases (FADs) were found using TAIR database (https://www.arabidopsis.org) and uniprot database (https://www.uniprot.org/). Alignments and phylogenetic analyses were done using the software MEGA version 6[86]. Sequence alignments were obtained using the MUSCLE algorithm. Phylogenetic trees were created using the maximum likelihood method with the WAG substitution model, gamma distributed. The test of phylogeny was performed using the bootstrap method with a number of bootstrap replication equal to 100.

6.5.11 Statistics

Each experiment was made in at least three replicates. Values were expressed as mean ± standard error (SE). The statistical significance of cell numbers, biochemical analysis, GC-MS, NMR in heterotrophy and autotrophy was evaluated through Student's t-test ($p \leq 0.05$). Differentially expressed genes (DEGs) obtained using RNA sequencing were considered statistically significant at a false discovery rate (FDR) ≤ 0.05.

6.5.12 Data availability

The raw sequencing data from this study have been submitted to the NCBI SRA database (http://www.ncbi.nlm.nih.gov) under accession code PRJNA561910.

6.6 References

(1) De Jesus Raposo, M. F.; De Morais, R. M. S. C.; De Morais, A. M. M. B. Health Applications of Bioactive Compounds from Marine Microalgae. *Life Sciences*. 2013. https://doi.org/10.1016/j.lfs.2013.08.002.

(2) Yang, R.; Wei, D.; Xie, J. Diatoms as Cell Factories for High-Value Products: Chrysolaminarin, Eicosapentaenoic Acid, and Fucoxanthin. *Crit. Rev. Biotechnol.* **2020**, *40* (7), 993–1009. https://doi.org/10.1080/07388551.2020.1805402.

(3) Landi, S.; Esposito, S. Bioinformatic Characterization of Sulfotransferase Provides New Insights for the Exploitation of Sulfated Polysaccharides in Caulerpa. *Int. J. Mol. Sci.* **2020**, *21* (18). https://doi.org/10.3390/ijms21186681.

(4) Cupo, A.; Landi, S.; Morra, S.; Nuzzo, G.; Gallo, C.; Manzo, E.; Fontana, A.; Ippolito, G. Autotrophic vs . Heterotrophic Cultivation of the Marine Diatom *Cyclotella Cryptica* for EPA Production. **2021**, 1–11.

(5) Falkowski, P. G. The Role of Phytoplankton Photosynthesis in Global Biogeochemical Cycles. *Photosynthesis Research*. 1994. https://doi.org/10.1007/BF00014586.

(6) Armbrust, E. V. The Life of Diatoms in the World's Oceans. *Nature*. 2009. https://doi.org/10.1038/nature08057.

(7) Gallo, C.; D'Ippolito, G.; Nuzzo, G.; Sardo, A.; Fontana, A. Autoinhibitory Sterol Sulfates Mediate Programmed Cell Death in a Bloom-Forming Marine Diatom. *Nat. Commun.* **2017**, *8* (1). https://doi.org/10.1038/s41467-017-01300-1.

(8) Gallo, C.; Landi, S.; d'Ippolito, G.; Nuzzo, G.; Manzo, E.; Sardo, A.; Fontana, A. Diatoms Synthesize Sterols by Inclusion of Animal and Fungal Genes in the Plant Pathway. *Sci. Rep.* **2020**, *10* (1), 1–13. https://doi.org/10.1038/s41598-020-60993-5.

(9) Knig, S.; Eisenhut, M.; Brutigam, A.; Kurz, S.; Weber, A. P. M.; Bchel, C. The Influence of a Cryptochrome on the Gene Expression Profile in the Diatom *Phaeodactylum Tricornutum* under Blue Light and in Darkness. *Plant Cell Physiol.* **2017**, *58* (11). https://doi.org/10.1093/pcp/pcx127.

(10) Falkowski, P. G.; Barber, R. T.; Smetacek, V. Biogeochemical Controls and Feedbacks on Ocean Primary Production. *Science*. 1998. https://doi.org/10.1126/science.281.5374.200.

(11) Gügi, B.; Costaouec, T. Le; Burel, C.; Lerouge, P.; Helbert, W.; Bardor, M. Diatom-

Specific Oligosaccharide and Polysaccharide Structures Help to Unravel Biosynthetic Capabilities in Diatoms. *Marine Drugs*. 2015. https://doi.org/10.3390/md13095993.

(12) Zulu, N. N.; Zienkiewicz, K.; Vollheyde, K.; Feussner, I. Current Trends to Comprehend Lipid Metabolism in Diatoms. *Progress in Lipid Research*. 2018. https://doi.org/10.1016/j.plipres.2018.03.001.

(13) L. Rorrer, G.; Antonio Torres, J.; Durst, R.; Kelly, C.; Gale, D.; Maddux, B.; Ozkan, A. The Potential of a Diatom-Based Photosynthetic Biorefinery for Biofuels and Valued Co-Products. *Curr. Biotechnol.* **2016**, *5* (3). https://doi.org/10.2174/2211550105666160229223625.

(14) Rodolfi, L.; Zittelli, G. C.; Bassi, N.; Padovani, G.; Biondi, N.; Bonini, G.; Tredici, M. R. Microalgae for Oil: Strain Selection, Induction of Lipid Synthesis and Outdoor Mass Cultivation in a Low-Cost Photobioreactor. *Biotechnol. Bioeng.* **2009**, *102* (1), 100–112. https://doi.org/10.1002/bit.22033.

(15) Wang, J. K.; Seibert, M. Prospects for Commercial Production of Diatoms. *Biotechnology for Biofuels*. 2017. https://doi.org/10.1186/s13068-017-0699-y.

(16) Botte, P.; d'Ippolito, G.; Gallo, C.; Sardo, A.; Fontana, A. Combined Exploitation of CO_2 and Nutrient Replenishment for Increasing Biomass and Lipid Productivity of the Marine Diatoms *Thalassiosira Weissflogii* and *Cyclotella Cryptica*. *J. Appl. Phycol.* **2018**, *30* (1), 243–251. https://doi.org/10.1007/s10811-017-1221-4.

(17) Vella, F. M.; Sardo, A.; Gallo, C.; Landi, S.; Fontana, A.; d'Ippolito, G. Annual Outdoor Cultivation of the Diatom *Thalassiosira Weissflogii*: Productivity, Limits and Perspectives. *Algal Res.* **2019**, *42* (June 2018), 101553. https://doi.org/10.1016/j.algal.2019.101553.

(18) Andeden, E. E.; Ozturk, S.; Aslim, B. Evaluation of Thirty Microalgal Isolates as Biodiesel Feedstocks Based on Lipid Productivity and Triacylglycerol (TAG) Content. *Curr. Microbiol.* **2021**, *78* (2). https://doi.org/10.1007/s00284-020-02340-5.

(19) Adelfi, M. G.; Vitale, R. M.; d'Ippolito, G.; Nuzzo, G.; Gallo, C.; Amodeo, P.; Manzo, E.; Pagano, D.; Landi, S.; Picariello, G.; Ferrante, M. I.; Fontana, A. Patatin-like Lipolytic Acyl Hydrolases and Galactolipid Metabolism in Marine Diatoms of the Genus *Pseudo-Nitzschia*. *Biochim. Biophys. Acta - Mol. Cell Biol. Lipids* **2019**, *1864* (2), 181–190. https://doi.org/10.1016/j.bbalip.2018.11.008.

(20) Yang, Z.; Niu, Y.; Ma, Y.; Xue, J.; Zhang, M.; Yang, W.; Liu, J.; Lu, S.; Guan, Y.; Li, H. Molecular and Cellular Mechanisms of Neutral Lipid Accumulation in Diatom Following Nitrogen Deprivation. *Biotechnol. Biofuels* **2013**, *6* (1), 1. https://doi.org/10.1186/1754-6834-6-67.

(21) Zhang, S. F.; Yuan, C. J.; Chen, Y.; Chen, X. H.; Li, D. X.; Liu, J. L.; Lin, L.; Wang, D. Z. Comparative Transcriptomic Analysis Reveals Novel Insights into the Adaptive Response of *Skeletonema Costatum* to Changing Ambient Phosphorus. *Front. Microbiol.* **2016**, *7* (SEP). https://doi.org/10.3389/fmicb.2016.01476.

(22) Alipanah, L.; Winge, P.; Rohloff, J.; Najafi, J.; Brembu, T.; Bones, A. M. Molecular Adaptations to Phosphorus Deprivation and Comparison with Nitrogen Deprivation Responses in the Diatom *Phaeodactylum Tricornutum*. *PLoS One* **2018**, *13* (2). https://doi.org/10.1371/journal.pone.0193335.

(23) Remmers, I. M.; D'Adamo, S.; Martens, D. E.; de Vos, R. C. H.; Mumm, R.; America, A. H. P.; Cordewener, J. H. G.; Bakker, L. V.; Peters, S. A.; Wijffels, R. H.; Lamers, P. P. Orchestration of Transcriptome, Proteome and Metabolome in the Diatom *Phaeodactylum Tricornutum* during Nitrogen Limitation. *Algal Res.* **2018**, *35*. https://doi.org/10.1016/j.algal.2018.08.012.

(24) Wu, S.; Gu, W.; Huang, A.; Li, Y.; Kumar, M.; Lim, P. E.; Huan, L.; Gao, S.; Wang, G. Elevated CO_2 Improves Both Lipid Accumulation and Growth Rate in the Glucose-6-Phosphate Dehydrogenase Engineered *Phaeodactylum Tricornutum*. *Microb. Cell Fact.* **2019**, *18* (1). https://doi.org/10.1186/s12934-019-1214-x.

(25) D'Ippolito, G.; Sardo, A.; Paris, D.; Vella, F. M.; Adelfi, M. G.; Botte, P.; Gallo, C.; Fontana, A. Potential of Lipid Metabolism in Marine Diatoms for Biofuel Production. *Biotechnol. Biofuels* **2015**, *8* (1), 1–10. https://doi.org/10.1186/s13068-015-0212-4.

(26) Hu, Q.; Sommerfeld, M.; Jarvis, E.; Ghirardi, M.; Posewitz, M.; Seibert, M.; Darzins, A. Microalgal Triacylglycerols as Feedstocks for Biofuel Production: Perspectives and Advances. *Plant J.* **2008**, *54* (4), 621–639. https://doi.org/10.1111/j.1365-313X.2008.03492.x.

(27) Rene H.W., J. M. B. Perspective. An Outlook on Microalgal Biofuels. *Sci. \r* **2010**, *Vol. 329* (August), 796–799.

(28) Bumbak, F.; Cook, S.; Zachleder, V.; Hauser, S.; Kovar, K. Best Practices in Heterotrophic

High-Cell-Density Microalgal Processes: Achievements, Potential and Possible Limitations. *Appl. Microbiol. Biotechnol.* **2011**, *91* (1), 31–46. https://doi.org/10.1007/s00253-011-3311-6.

(29) Venkata Mohan, S.; Rohit, M. V.; Chiranjeevi, P.; Chandra, R.; Navaneeth, B. Heterotrophic Microalgae Cultivation to Synergize Biodiesel Production with Waste Remediation: Progress and Perspectives. *Bioresour. Technol.* **2015**, *184*, 169–178. https://doi.org/10.1016/j.biortech.2014.10.056.

(30) Borowitzka, M. A. Commercial Production of Microalgae : Ponds , Tanks , Tubes and Fermenters. **1999**, *70*, 313–321.

(31) Pahl, S. L.; Lewis, D. M.; Chen, F.; King, K. D. Heterotrophic Growth and Nutritional Aspects of the Diatom *Cyclotella Cryptica* (*Bacillariophyceae*): Effect of Some Environmental Factors. *J. Biosci. Bioeng.* **2010**, *109* (3). https://doi.org/10.1016/j.jbiosc.2009.08.480.

(32) Hamilton, M. L.; Powers, S.; Napier, J. A.; Sayanova, O. Heterotrophic Production of Omega-3 Long-Chain Polyunsaturated Fatty Acids by Trophically Converted Marine Diatom *Phaeodactylum Tricornutum*. *Mar. Drugs* **2016**, *14* (3). https://doi.org/10.3390/md14030053.

(33) Perez-Garcia, O.; Escalante, F. M. E.; de-Bashan, L. E.; Bashan, Y. Heterotrophic Cultures of Microalgae: Metabolism and Potential Products. *Water Res.* **2011**, *45* (1), 11–36. https://doi.org/10.1016/j.watres.2010.08.037.

(34) Pahl, S. L.; Lewis, D. M.; King, K. D.; Chen, F. Heterotrophic Production of the Microalgae *Cyclotella Cryptica* ; Fed for Aquaculture. *PhD Thesis Univ. Adelaide* **2010**, *24* (May), 235–239. https://doi.org/10.1016/j.jbiosc.2009.08.480.

(35) Sheehan, J. A Look Back at the U.S. Department of Energy's Aquatic Species Program—Biodiesel from Algae. *Program* **1998**, No. July.

(36) Kennedy, F.; Martin, A.; Bowman, J. P.; Wilson, R.; McMinn, A. Dark Metabolism: A Molecular Insight into How the Antarctic Sea-Ice Diatom *Fragilariopsis Cylindrus* Survives Long-Term Darkness. *New Phytol.* **2019**, *223* (2), 675–691. https://doi.org/10.1111/nph.15843.

(37) Li-Beisson, Y.; Shorrosh, B.; Beisson, F.; Andersson, M. X.; Arondel, V.; Bates, P. D.; Baud, S.; Bird, D.; DeBono, A.; Durrett, T. P.; Franke, R. B.; Graham, I. A.; Katayama, K.;

Kelly, A. A.; Larson, T.; Markham, J. E.; Miquel, M.; Molina, I.; Nishida, I.; Rowland, O.; Samuels, L.; Schmid, K. M.; Wada, H.; Welti, R.; Xu, C.; Zallot, R.; Ohlrogge, J. Acyl-Lipid Metabolism. *Arab. B.* **2013**, *11*, e0161. https://doi.org/10.1199/tab.0161.

(38) Li-Beisson, Y.; Thelen, J. J.; Fedosejevs, E.; Harwood, J. L. The Lipid Biochemistry of Eukaryotic Algae. *Progress in Lipid Research*. 2019. https://doi.org/10.1016/j.plipres.2019.01.003.

(39) Ma, Y. H.; Wang, X.; Niu, Y. F.; Yang, Z. K.; Zhang, M. H.; Wang, Z. M.; Yang, W. D.; Liu, J. S.; Li, H. Y. Antisense Knockdown of Pyruvate Dehydrogenase Kinase Promotes the Neutral Lipid Accumulation in the Diatom *Phaeodactylum Tricornutum*. *Microb. Cell Fact.* **2014**, *13* (1). https://doi.org/10.1186/s12934-014-0100-9.

(40) Dunahay, T. G.; Jarvis, E. E.; Dais, S. S.; Roessler, P. G. Manipulation of Microalgal Lipid Production Using Genetic Engineering. *Appl. Biochem. Biotechnol. - Part A Enzym. Eng. Biotechnol.* **1996**, *57–58*. https://doi.org/10.1007/BF02941703.

(41) Dolch, L. J.; Rak, C.; Perin, G.; Tourcier, G.; Broughton, R.; Leterrier, M.; Morosinotto, T.; Tellier, F.; Faure, J. D.; Falconet, D.; Jouhet, J.; Sayanova, O.; Beaudoin, F.; Maréchal, E. A Palmitic Acid Elongase Affects Eicosapentaenoic Acid and Plastidial Monogalactosyldiacylglycerol Levels in Nannochloropsis. *Plant Physiol.* **2017**, *173* (1). https://doi.org/10.1104/pp.16.01420.

(42) Petroutsos, D.; Amiar, S.; Abida, H.; Dolch, L. J.; Bastien, O.; Rébeillé, F.; Jouhet, J.; Falconet, D.; Block, M. A.; McFadden, G. I.; Bowler, C.; Botté, C.; Maréchal, E. Evolution of Galactoglycerolipid Biosynthetic Pathways - From Cyanobacteria to Primary Plastids and from Primary to Secondary Plastids. *Progress in Lipid Research*. 2014. https://doi.org/10.1016/j.plipres.2014.02.001.

(43) Bates, P. D.; Durrett, T. P.; Ohlrogge, J. B.; Pollard, M. Analysis of Acyl Fluxes through Multiple Pathways of Triacylglycerol Synthesis in Developing Soybean Embryos. *Plant Physiol.* **2009**, *150* (1). https://doi.org/10.1104/pp.109.137737.

(44) Hamilton, M. L.; Warwick, J.; Terry, A.; Allen, M. J.; Napier, A.; Sayanova, O. Towards the Industrial Production of Omega- 3 Long Chain Polyunsaturated Fatty Acids from a Genetically Modified Diatom *Phaeodactylum Tricornutum*. *PLoS One* **2015**, 1–15. https://doi.org/10.1371/journal.pone.0144054.

(45) Yang, Y. H.; Du, L.; Hosokawa, M.; Miyashita, K.; Kokubun, Y.; Arai, H.; Taroda, H. Fatty

Acid and Lipid Class Composition of the Microalga *Phaeodactylum Tricornutum*. *J. Oleo Sci.* **2017**, *66* (4). https://doi.org/10.5650/jos.ess16205.

(46) Jiang, H.; Gao, K. Effects of Lowering Temperature during Culture on the Production of Polyunsaturated Fatty Acids in the Marine Diatom *Phaeodactylum Tricornutum* (*Bacillariophyceae*). *J. Phycol.* **2004**, *40* (4). https://doi.org/10.1111/j.1529-8817.2004.03112.x.

(47) Cagliari, A.; Margis, R.; Dos Santos Maraschin, F.; Turchetto-Zolet, A. C.; Loss, G.; Margis-Pinheiro, M. Biosynthesis of Triacylglycerols (TAGs) in Plants and Algae. *Int. J. Plant Biol.* **2011**, *2* (1). https://doi.org/10.4081/pb.2011.e10.

(48) Du, Z. Y.; Benning, C. Triacylglycerol Accumulation in Photosynthetic Cells in Plants and Algae. *Subcell. Biochem.* **2016**, *86*. https://doi.org/10.1007/978-3-319-25979-6_8.

(49) Xu, C.; Andre, C.; Fan, J.; Shanklin, J. Cellular Organization of Triacylglycerol Biosynthesis in Microalgae. *Subcell. Biochem.* **2016**, *86*. https://doi.org/10.1007/978-3-319-25979-6_9.

(50) Liu, B.; Benning, C. Lipid Metabolism in Microalgae Distinguishes Itself. *Current Opinion in Biotechnology*. 2013. https://doi.org/10.1016/j.copbio.2012.08.008.

(51) Cui, Y.; Zhao, J.; Wang, Y.; Qin, S.; Lu, Y. Characterization and Engineering of a Dual-Function Diacylglycerol Acyltransferase in the Oleaginous Marine Diatom *Phaeodactylum Tricornutum*. *Biotechnol. Biofuels* **2018**, *11* (1), 1–13. https://doi.org/10.1186/s13068-018-1029-8.

(52) Hamilton, M. L.; Haslam, R. P.; Napier, J. A.; Sayanova, O. Metabolic Engineering of *Phaeodactylum Tricornutum* for the Enhanced Accumulation of Omega-3 Long Chain Polyunsaturated Fatty Acids $. *Metab. Eng.* **2014**, *22*, 3–9. https://doi.org/10.1016/j.ymben.2013.12.003.

(53) Tonon, T.; Harvey, D.; Larson, T. R.; Graham, I. A. Long Chain Polyunsaturated Fatty Acid Production and Partitioning to Triacylglycerols in Four Microalgae. *Phytochemistry* **2002**, *61* (1). https://doi.org/10.1016/S0031-9422(02)00201-7.

(54) Liang, Y.; Maeda, Y.; Yoshino, T.; Matsumoto, M.; Tanaka, T. Profiling of Fatty Acid Methyl Esters from the Oleaginous Diatom *Fistulifera Sp. Strain JPCC DA0580* under Nutrition-Sufficient and -Deficient Conditions. *J. Appl. Phycol.* **2014**, *26* (6). https://doi.org/10.1007/s10811-014-0265-y.

(55) Bates, P. D.; Fatihi, A.; Snapp, A. R.; Carlsson, A. S.; Browse, J.; Lu, C. Acyl Editing and Headgroup Exchange Are the Major Mechanisms That Direct Polyunsaturated Fatty Acid Flux into Triacylglycerols. *Plant Physiol.* **2012**, *160* (3). https://doi.org/10.1104/pp.112.204438.

(56) Dolch, L. J.; Maréchal, E. Inventory of Fatty Acid Desaturases in the Pennate Diatom *Phaeodactylum Tricornutum*. *Mar. Drugs* **2015**, *13* (3). https://doi.org/10.3390/md13031317.

(57) Domergue, F.; Lerchl, J.; Zähringer, U.; Heinz, E. Cloning and Functional Characterization of *Phaeodactylum Tricornutum* Front-End Desaturases Involved in Eicosapentaenoic Acid Biosynthesis. *Eur. J. Biochem.* **2002**, *269* (16). https://doi.org/10.1046/j.1432-1033.2002.03104.x.

(58) Liu, B.; Sun, Y.; Hang, W.; Wang, X.; Xue, J.; Ma, R.; Jia, X.; Li, R. Characterization of a Novel Acyl-ACP Δ9 Desaturase Gene Responsible for Palmitoleic Acid Accumulation in a Diatom *Phaeodactylum Tricornutum*. *Front. Microbiol.* **2020**, *11*. https://doi.org/10.3389/fmicb.2020.584589.

(59) Smith, R.; Jouhet, J.; Gandini, C.; Nekrasov, V.; Marechal, E.; Napier, J. A.; Sayanova, O. Plastidial Acyl Carrier Protein Δ9-Desaturase Modulates Eicosapentaenoic Acid Biosynthesis and Triacylglycerol Accumulation in *Phaeodactylum Tricornutum*. *Plant J.* **2021**. https://doi.org/10.1111/tpj.15231.

(60) Spiekermann, P.; Lerchl, J.; Beckmann, C.; Kilian, O.; Kroth, P. G.; Boland, W.; Za, U.; Heinz, E. New Insight into *Phaeodactylum Tricornutum* Fatty Acid Metabolism. Cloning and Functional Characterization of Plastidial and Microsomal Δ12-Fatty Acid Desaturases. *Plant Physiol.* **2003**, *131* (4), 1648–1660. https://doi.org/10.1104/pp.102.018317.color.

(61) Horn, P. J.; Smith, M. D.; Clark, T. R.; Froehlich, J. E.; Benning, C. PEROXIREDOXIN Q Stimulates the Activity of the Chloroplast 16:1Δ3trans FATTY ACID DESATURASE4. *Plant J.* **2020**, *102* (4). https://doi.org/10.1111/tpj.14657.

(62) Arao, T.; Yamada, M. Biosynthesis of Polyunsaturated Fatty Acids in the Marine Diatom, *Phaeodactylum Tricornutum*. *Phytochemistry* **1994**, *35* (5). https://doi.org/10.1016/S0031-9422(00)94817-9.

(63) Pérez-López, P.; González-García, S.; Allewaert, C.; Verween, A.; Murray, P.; Feijoo, G.;

Moreira, M. T. Environmental Evaluation of Eicosapentaenoic Acid Production by *Phaeodactylum Tricornutum*. *Sci. Total Environ.* **2014**, *466–467*, 991–1002. https://doi.org/10.1016/j.scitotenv.2013.07.105.

(64) Morales-Sánchez, D.; Martinez-Rodriguez, O. A.; Martinez, A. Heterotrophic Cultivation of Microalgae: Production of Metabolites of Commercial Interest. *J. Chem. Technol. Biotechnol.* **2017**, *92* (5), 925–936. https://doi.org/10.1002/jctb.5115.

(65) Pahl, S. L.; Lewis, D. M.; King, K. D.; Chen, F. Heterotrophic Growth and Nutritional Aspects of the Diatom *Cyclotella Cryptica (Bacillariophyceae)*: Effect of Nitrogen Source and Concentration. *J. Appl. Phycol.* **2012**, *24* (2), 301–307. https://doi.org/10.1007/s10811-011-9680-5.

(66) Villanova, V.; Fortunato, A. E.; Singh, D.; Bo, D. D.; Conte, M.; Obata, T.; Jouhet, J.; Fernie, A. R.; Marechal, E.; Falciatore, A.; Pagliardini, J.; Le Monnier, A.; Poolman, M.; Curien, G.; Petroutsos, D.; Finazzi, G. Investigating Mixotrophic Metabolism in the Model Diatom *Phaeodactylum Tricornutum*. *Philos. Trans. R. Soc. B Biol. Sci.* **2017**, *372* (1728). https://doi.org/10.1098/rstb.2016.0404.

(67) Roessler, P. G.; Ohlrogge, J. B. Cloning and Characterization of the Gene That Encodes Acetyl-Coenzyme A Carboxylase in the Alga *Cyclotella Cryptica*. *J. Biol. Chem.* **1993**, *268* (26). https://doi.org/10.1016/s0021-9258(19)36507-x.

(68) Kobayashi, K. Role of Membrane Glycerolipids in Photosynthesis, Thylakoid Biogenesis and Chloroplast Development. *J. Plant Res.* **2016**, *129* (4). https://doi.org/10.1007/s10265-016-0827-y.

(69) Sugimoto, K.; Tsuzuki, M.; Sato, N. Regulation of Synthesis and Degradation of a Sulfolipid under Sulfur-Starved Conditions and Its Physiological Significance in *Chlamydomonas Reinhardtii*. *New Phytol.* **2010**, *185* (3). https://doi.org/10.1111/j.1469-8137.2009.03115.x.

(70) Lepetit, B.; Goss, R.; Jakob, T.; Wilhelm, C. Molecular Dynamics of the Diatom Thylakoid Membrane under Different Light Conditions. *Photosynthesis Research*. 2012. https://doi.org/10.1007/s11120-011-9633-5.

(71) Endo, K.; Kobayashi, K.; Wada, H. Sulfoquinovosyldiacylglycerol Has an Essential Role in *Thermosynechococcus Elongatus BP-1* Under Phosphate-Deficient Conditions. *Plant Cell Physiol.* **2016**, *57* (12). https://doi.org/10.1093/pcp/pcw159.

(72) Schaller-Laudel, S.; Latowski, D.; Jemioła-Rzemińska, M.; Strzałka, K.; Daum, S.; Bacia, K.; Wilhelm, C.; Goss, R. Influence of Thylakoid Membrane Lipids on the Structure of Aggregated Light-Harvesting Complexes of the Diatom *Thalassiosira Pseudonana* and the Green Alga *Mantoniella Squamata*. *Physiol. Plant.* **2017**, *160* (3). https://doi.org/10.1111/ppl.12565.

(73) Nakajima, Y.; Umena, Y.; Nagao, R.; Endo, K.; Kobayashi, K.; Akita, F.; Suga, M.; Wada, H.; Noguchi, T.; Shen, J. R. Thylakoid Membrane Lipid Sulfoquinovosyl-Diacylglycerol (SQDG) Is Required for Full Functioning of Photosystem II in *Thermosynechococcus Elongatus*. *J. Biol. Chem.* **2018**, *293* (38). https://doi.org/10.1074/jbc.RA118.004304.

(74) Yao, Y.; Lu, Y.; Peng, K. T.; Huang, T.; Niu, Y. F.; Xie, W. H.; Yang, W. D.; Liu, J. S.; Li, H. Y. Glycerol and Neutral Lipid Production in the Oleaginous Marine Diatom *Phaeodactylum Tricornutum* Promoted by Overexpression of Glycerol-3-Phosphate Dehydrogenase. *Biotechnol. Biofuels* **2014**, *7* (1), 1–9. https://doi.org/10.1186/1754-6834-7-110.

(75) Wang, X.; Dong, H. P.; Wei, W.; Balamurugan, S.; Yang, W. D.; Liu, J. S.; Li, H. Y. Dual Expression of Plastidial GPAT1 and LPAT1 Regulates Triacylglycerol Production and the Fatty Acid Profile in *Phaeodactylum Tricornutum* 06 Biological Sciences 0601 Biochemistry and Cell Biology. *Biotechnol. Biofuels* **2018**, *11* (1), 1–14. https://doi.org/10.1186/s13068-018-1317-3.

(76) Wang, X.; Liu, S. F.; Li, R. Y.; Yang, W. D.; Liu, J. S.; Lin, C. S. K.; Balamurugan, S.; Li, H. Y. TAG Pathway Engineering via GPAT2 Concurrently Potentiates Abiotic Stress Tolerance and Oleaginicity in *Phaeodactylum Tricornutum*. *Biotechnol. Biofuels* **2020**, *13* (1). https://doi.org/10.1186/s13068-020-01799-5.

(77) Zulu, N. N.; Popko, J.; Zienkiewicz, K.; Tarazona, P.; Herrfurth, C.; Feussner, I. Heterologous Co-Expression of a Yeast Diacylglycerol Acyltransferase (ScDGA1) and a Plant Oleosin (AtOLEO3) as an Efficient Tool for Enhancing Triacylglycerol Accumulation in the Marine Diatom *Phaeodactylum Tricornutum*. *Biotechnol. Biofuels* **2017**, *10* (1). https://doi.org/10.1186/s13068-017-0874-1.

(78) Haslam, R. P.; Hamilton, M. L.; Economou, C. K.; Smith, R.; Hassall, K. L.; Napier, J. A.; Sayanova, O. Overexpression of an Endogenous Type 2 Diacylglycerol Acyltransferase in the Marine Diatom *Phaeodactylum Tricornutum* Enhances Lipid Production and Omega-3 Long-Chain Polyunsaturated Fatty Acid Content. *Biotechnol. Biofuels* **2020**, *13*

(1). https://doi.org/10.1186/s13068-020-01726-8.

(79) Guillard, R. R. L.; Ryther, J. H. Studies of Marine Planktonic Diatoms. I. *Cyclotella Nana Hustedt, and Detonula Confervacea* (CLEVE) . Canadian Journal of Microbiology 8:229-239. *Can. J. Microbiol.* **1962**, *8* (1140), 229–239.

(80) Nuzzo, G.; Gallo, C.; D'Ippolito, G.; Cutignano, A.; Sardo, A.; Fontana, A. Composition and Quantitation of Microalgal Lipids by ERETIC 1H NMR Method. *Mar. Drugs* **2013**, *11* (10), 3742–3753. https://doi.org/10.3390/md11103742.

(81) Cutignano, A.; Luongo, E.; Nuzzo, G.; Pagano, D.; Manzo, E.; Sardo, A.; Fontana, A. Profiling of Complex Lipids in Marine Microalgae by UHPLC/Tandem Mass Spectrometry. *Algal Res.* **2016**, *17*, 348–358. https://doi.org/10.1016/j.algal.2016.05.016.

(82) Martin, M. Cutadapt Removes Adapter Sequences from High-Throughput Sequencing Reads. *EMBnet.journal* **2011**, *17* (1). https://doi.org/10.14806/ej.17.1.200.

(83) Grabherr, M. G.; Haas, B. J.; Yassour, M.; Levin, J. Z.; Thompson, D. A.; Amit, I.; Adiconis, X.; Fan, L.; Raychowdhury, R.; Zeng, Q.; Chen, Z.; Mauceli, E.; Hacohen, N.; Gnirke, A.; Rhind, N.; Di Palma, F.; Birren, B. W.; Nusbaum, C.; Lindblad-Toh, K.; Friedman, N.; Regev, A. Trinity: Reconstructing a Full-Length Transcriptome without a Genome from RNA-Seq Data HHS Public Access. *Nat Biotechnol. Nat Biotechnol* **2011**, *29* (7).

(84) Kim, D.; Pertea, G.; Trapnell, C.; Pimentel, H.; Kelley, R.; Salzberg, S. L. TopHat2: Accurate Alignment of Transcriptomes in the Presence of Insertions, Deletions and Gene Fusions. *Genome Biol.* **2013**, *14* (4). https://doi.org/10.1186/gb-2013-14-4-r36.

(85) Love, M. I.; Huber, W.; Anders, S. Moderated Estimation of Fold Change and Dispersion for RNA-Seq Data with DESeq2. *Genome Biol.* **2014**, *15* (12), 1–21. https://doi.org/10.1186/s13059-014-0550-8.

(86) Tamura, K.; Stecher, G.; Peterson, D.; Filipski, A.; Kumar, S. MEGA6: Molecular Evolutionary Genetics Analysis Version 6.0. *Mol. Biol. Evol.* **2013**, *30* (12). https://doi.org/10.1093/molbev/mst197.

7. Molecular approach on Cyclotella cryptica to study key genes in lipid biosynthesis

This chapter reports the experimental activities carried out at “Institute de Biologie Physico-Chimique” (Paris), in the laboratory of Dr. Angela Falciatore

7.1 Introduction

The best developed diatom model species for molecular research are *P. tricornutum* and *T. pseudonana*. When the *T. pseudonana* CCMP1335 strain was chosen for the first sequencing experiment of a centric diatom, the ecological significance of *T. pseudonana* and its obligatory demand for silica were important factors to consider [1]; *P. tricornutum* Pt1.1 8.6 Bohlin (CCMP2561) was therefore designated as the pennate lineage's representative diatom [2].

In both species, the availability of multiple transcriptomic and proteomic data sets has considerably aided genome annotation efforts and, as a result, gene identification.

The following diatom genome sequences have recently become available: *F. cylindrus, T. oceanica, P. multistriata, P. multiseries, F. solaris, C. cryptica, and S. costatum.* The major efforts on diatom genome included the generation of large RNA-sequencing data sets as well as other "omics-data", acquired under a variety of growing circumstances relevant to the particular species. The availability of genetic data from *P. tricornutum* has allowed researchers to begin rebuilding diatom metabolic networks, as has been done in other green lineage models [3].

DiatomCyc (http://www.diatomcyc.org) and the Genome Scale Metabolic Model based on enhanced genome annotation and protein subcellular localization predictions are two diatom metabolism databases [4,5]. These tools are useful for tracking intracellular metabolic fluxes in diatoms growing under various energy sources, as well as for investigating the involvement of novel pathways or predicting the presence of new regulators of energy fluxes between organelles in connection to diatom acclimation.

The sequencing of wild phytoplankton populations is currently producing a large quantity of metagenomics and metatranscriptomics data. These data are valuable tools for learning more about the distribution of diatom genes and species [3].

The biolistic transfer of transgenes to *C. cryptica* and *Navicula saprophila* cells was the breakthrough that enabled reverse genetics in diatoms [6].

Electroporation can be used to transfer DNA to *P. tricornutum*, although the transformation efficiency is unpredictable. The transgene is randomly integrated into the genome, with numerous integration events, in both methods. Because of the physical pressures that cause double-strand breaks, which are repaired by non-homologous end joining, biolistic gene transfer has an impact on genome integrity [7].

To address these problems, new vectors encoding a yeast-derived sequence that can be reproduced as episomes in diatom cells have been developed [8]. Through bacterial conjugation with *Escherichia coli*, these episomes may be delivered to *P. tricornutum* and *T. pseudonana*. This transformation technique is more efficient than previously published strategies, but it is less stable, as episomes are lost when selection pressure is not applied. On the plus side, this property may be used to achieve temporary expression, which could be especially beneficial for transgenes that could be harmful. Vectors for expressing foreign genes in *P. tricornutum* plastids transformed by electroporation have also been developed. There is also evidence that homologous recombination plastid mutagenesis is possible in this species. Parallel to this, vectors for high-throughput protein tagging and promoter-reporter/target transgenes have been developed to investigate gene expression patterns and functions. The beta-glucuronidase gene for monitoring gene expression and GFP variants for protein subcellular localization are examples of reporter genes [3].

By producing antisense or inverted repeat sequences of target genes, downregulation of gene expression has been accomplished in *P. tricornutum* and *T. pseudonana*. The decrease of mRNA and protein levels is a common consequence of this technique [9], but how gene silencing occurs in diatoms is unknown.

The development of genome-editing technologies like as TALEN and CRISPR-Cas-9 in *P. tricornutum* and *T. pseudonana* was a recent important success [10].

Cas9/single guide RNA ribonucleoprotein complexes have recently been used to accomplish transgene-free genome editing in *P. tricornutum* [11].

Endogenous counter-selectable markers have been utilized with ribonucleoprotein administration to aid in the detection of mutant genes.

We were able to discover genes with substantial phenotypic effects that might be candidates for selection and therefore drive the evolution and adaptation of diatoms to their extremely varied environment through functional examinations of diatom model species. Because of the concrete potential to learn more about the processes driving phytoplanktonic communities and the capacity of marine ecosystems to endure, adapt to, and contribute to a changing climate, additional linkages between diatom ecology, genomics, and genetics will be strengthened in the future [3].

7.2 Results and discussion

7.2.1 General outline

In the laboratory of CNR-ICB, we discovered interesting variations in the lipid composition of *C. cryptica* grown under heterotrophy, both by analyzing the variations in gene expression (RNAseq), and by analyzing the lipid composition with spectroscopic (^{1}H-NMR) and mass spectrometric techniques (LC-MS, GC-MS), as extensively discussed in Chapter 6. Based on these findings, we have chosen some genes of interest, which are mentioned in the next paragraph, as candidates for approaching the current generation of recombinant DNA technologies, that allow to study a gene's function by knock-out or overexpression. Since there are few studies for microalgae that unequivocally demonstrate, experimentally, the functionality of a gene without parallels with other organisms, such as plants, it is critical to perform this step of linking chemical data (and thus phenotypic variations) and key genes that could determine them.

Dr. Angela Falciatore's group at the Institute of Physical-Chemical Biology, where I was hosted in Paris, is one of the major international experts in the study of diatom molecular biology.

The first task we faced during my time in Paris was to ensure that the sequences of the previously chosen genes were suitable for a knock-out. Diatoms are diploid microorganisms and variations in their gene sequences may hamper the complete shutdown of their functions. As a result, a control on the coding sequences was required. At the same time, I learned the techniques for the nuclear transformation of *C. cryptica*, both through biolistic and bacterial conjugation and essential step to introduce the CRISPR-Cas-9 vector. This chapter also illustrates the entire strategy that we intended to pursue to perform the knock-out of the genes. The strategy to be used for gene over-expression is also described, in order to have an additional molecular tool available to study the possible role of the selected genes.

7.2.2 Gene selection

The genes we selected based on their key role in lipid biosynthesis, and their modulation suggested by RNAseq and lipidomic approach are: UDP-sulfoquinovose synthase (SQD1), Lysophosphatidylcholine acyltransferase (LPCAT), Glycerol-3-phosphate acyltransferase

(GPAT), Lysophosphatidic acid acyltransferase (LPAAT), Sulfotransferase (SULT), Secretory phospholipase A2 (LAH), Phospholipid diacylglycerol acyltransferase (PDAT), Diacylglycerol acyltransferase (DGAT2), TAG lipase (TGL4).

UDP-sulfoquinovose synthase (SQD1) is involved in the biosynthesis of sulfolipids found in thylakoid membranes, it converts UDP-glucose and sulfite to the sulfolipid head group precursor UDP-sulfoquinovose (**Figure 7.1**).

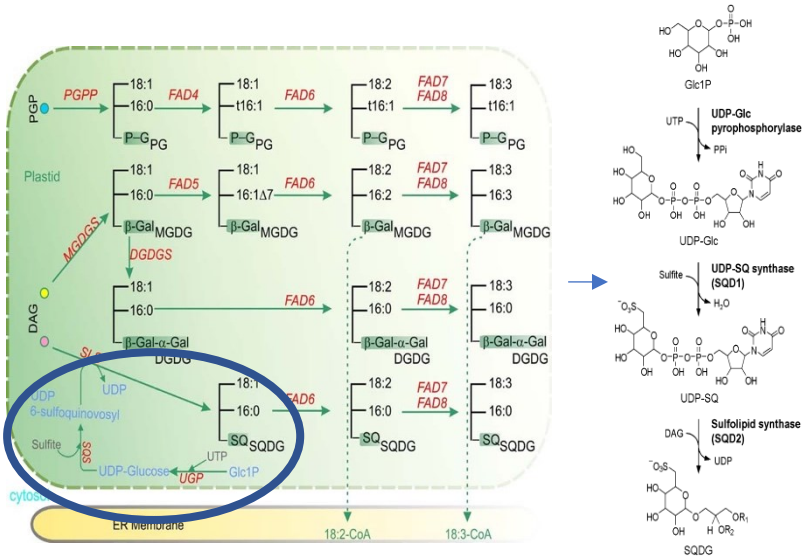

Figure 7.1 Pathway of glycolipid synthesis and reaction mediated by SQD1 in *Arabidopsis thaliana* [12].

SQD1 is a unique gene in *C. cryptica*, (Genome ID in *C. cryptica* CCMP332 is g9625.t1; transcriptome ID in *C. cryptica* 331 (our strain) is TRINITY_DN17430 and it is downregulated under heterotrophic condition.

Lysophosphatidylcholine acyltransferase (LPCAT) is an acetyltransferase which mediates the conversion of 1-acyl-sn-glycero-3-phosphocholine (LPC) into phosphatidylcholine (PC) (**Figure 7.2**).

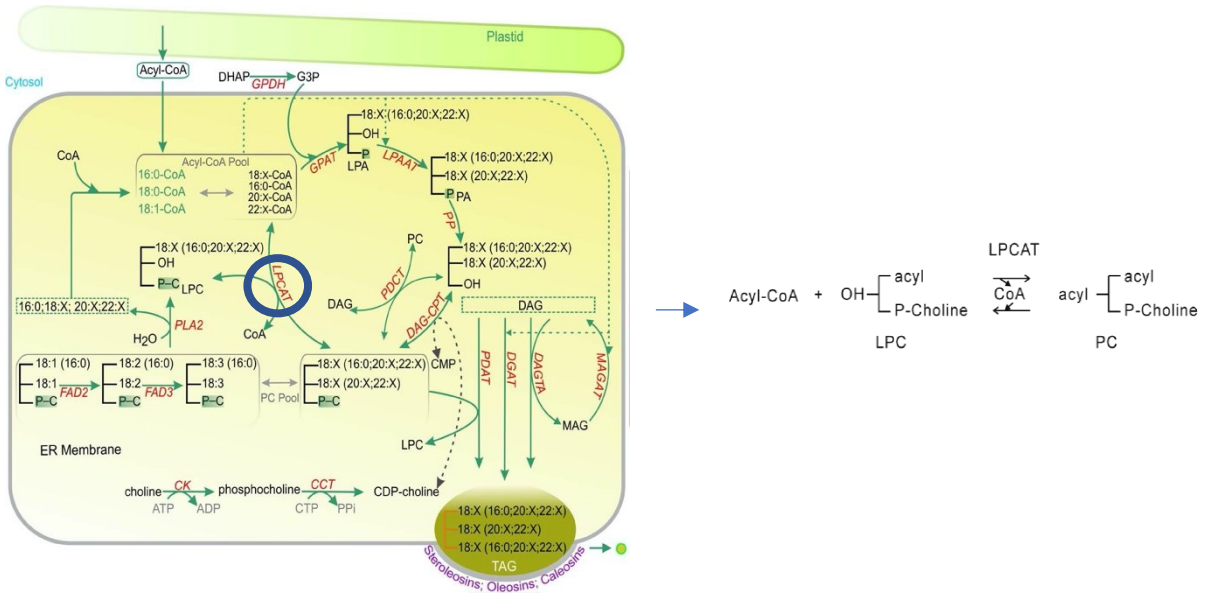

Figure 7.2 Triacylglycerol Synthesis in *Arabidopsis thaliana* and reaction mediated by LPCAT [12].

Also, LPCAT is a single gene in *C. cryptica* (Genome ID in *C. cryptica* CCMP332 is g6618.t1); transcriptome ID in *C. cryptica* 331 (our strain) is TRINITY_DN14564 and is it is not differentially expressed under heterotrophic condition.

Glycerol-3-phosphate acyltransferase (GPAT) esterifies acyl-group from acyl-ACP to the sn^{-1} position of glycerol-3-phosphate (**Figure 7.3**).

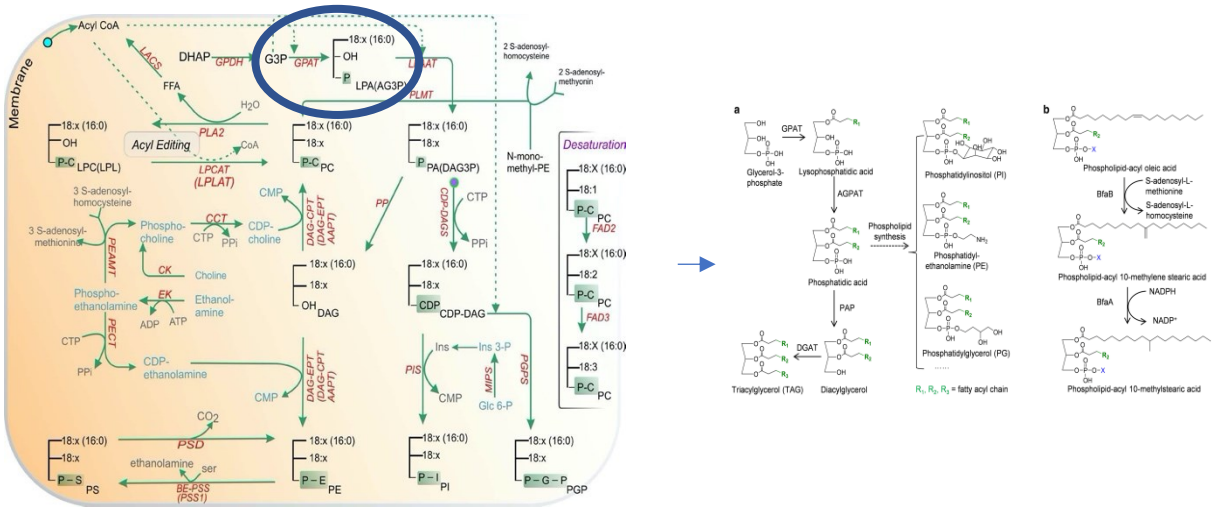

Figure 7.3 Eukaryotic Phospholipid Synthesis and Editing and reaction mediated by GPAT in *Arabidopsis thaliana* [12].

GPAT, like SQD1 and LPCAT is a single gene in *C. cryptica* (Genome ID in *C. cryptica* CCMP332 is g1933.t1; transcriptome ID in *C. cryptica* CCMP 331 (our strain) is TRINITY_DN12213 and it is upregulated under heterotrophic condition.

Lysophosphatidic acid acyltransferase (LPAAT) Catalyze the de novo formation of phosphatidic acid from lysophosphatidic acid (LPA) and a fatty acyl-CoA (**Figure7.4**).

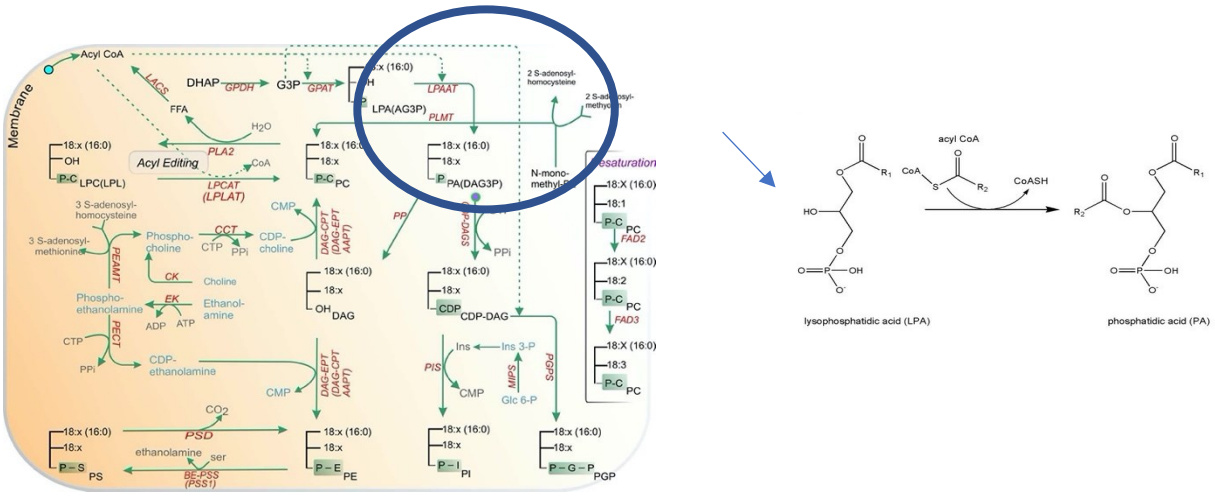

Figure 7.4 Eukaryotic Phospholipid Synthesis and Editing and reaction mediated by LPAAT [12].

For LPAAT gene there are probably two isoforms: once that encodes for a plastidial protein and the other for a cytosolic one. The cytosolic isoform is not annotated; therefore, we decided to study the sequence and try to silence the gene that codes for the plastidial protein (Genome ID in *C. cryptica* CCMP332 is g.11062; transcriptome ID in *C. cryptica* 331, our strain, is TRINITY_DN13209) and it is upregulated under heterotrophic condition.

Sulfotransferase (SULT) is a family of enzyme that transfer a sulfo-group or its anion form from the biochemical donor 30-phosphoadenosine-50-phosphosulfate (PAPS) to hydroxy or amine moieties of various substrates (**Figure 7.5**).

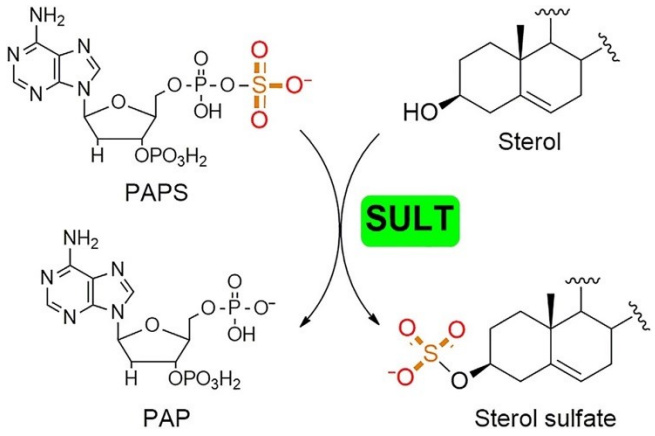

Figure 7.5 Sulfation reaction of sterols [13].

There are several genes that encode for proteins of SULT family. We decided to study g7621.t1 that encodes for a protein that is more similar to the human form and has higher affinity for cholesterol.

The lipolytic acyl hydrolases (**LAH**) are a large class of enzymes that recognize glycolipids (GL) and phospholipids (PL). It is suggested that the release of polyunsaturated fatty acids (PUFAs) from monogalactosyl diacylglycerols (MGDG) of diatoms is due to this enzyme class. PUFAs are direct precursors of lipoxygenase (LOX) products known as oxylipins (**Figure 7.6**), which serve intracellular and extracellular roles by acting as cell death and growth termination signals or as toxic chemicals that reduce the reproductive success of zooplankton grazers [14]. We decided to study this class of genes, since there is not a molecular characterization of the lipolytic enzymes in diatoms, in particular we planned a knockout of g1884.t, transcriptome ID TRINITY_DN18136, not differentially expressed in heterotrophy.

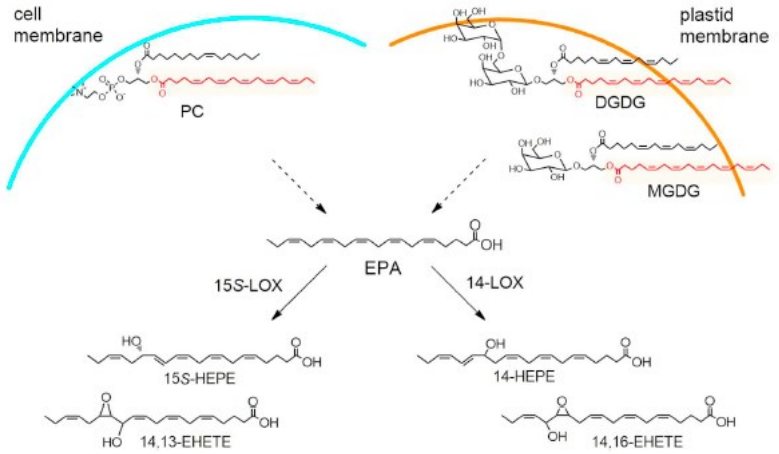

Figure 7.6 Biosynthesis of oxylipins from lipids of cell membranes and inner chloroplast membranes of *P. multistriata* and *P. arenysensis* [14].

Phospholipid: diacylglycerol acyltransferase (PDAT) involved in triacylglycerol formation by an acyl-CoA independent pathway. The enzyme preferentially transfers acyl groups from the sn-2 position of a phospholipid to diacylglycerol, thus forming an sn^{-1}-lysophospholipid (**Figure 7.7**).

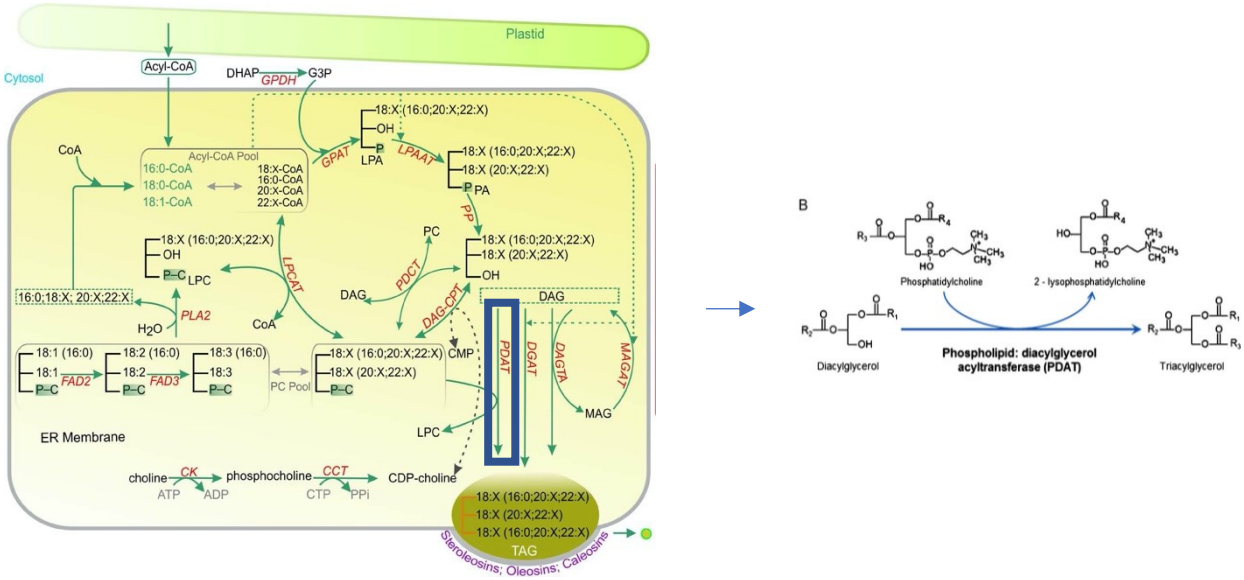

Figure 7.7 Triacylglycerol Synthesis in Arabidopsis, showing PDAT involvement [12].

In *C. cryptica* there are three genes that encodes for PDAT protein, two proteins have a plastidial localization and one is cytosolic (g718.t1). We decided to study the cytosolic form, that is not differentially expressed in heterotrophy (transcriptome ID: TRINITY_DN19832).

Diacylglycerol acyltransferase (DGAT2) gene encodes for a protein that catalyze the conversion of diacylglycerol and fatty acyl CoA to triacylglycerol (**Figure 7.8**).

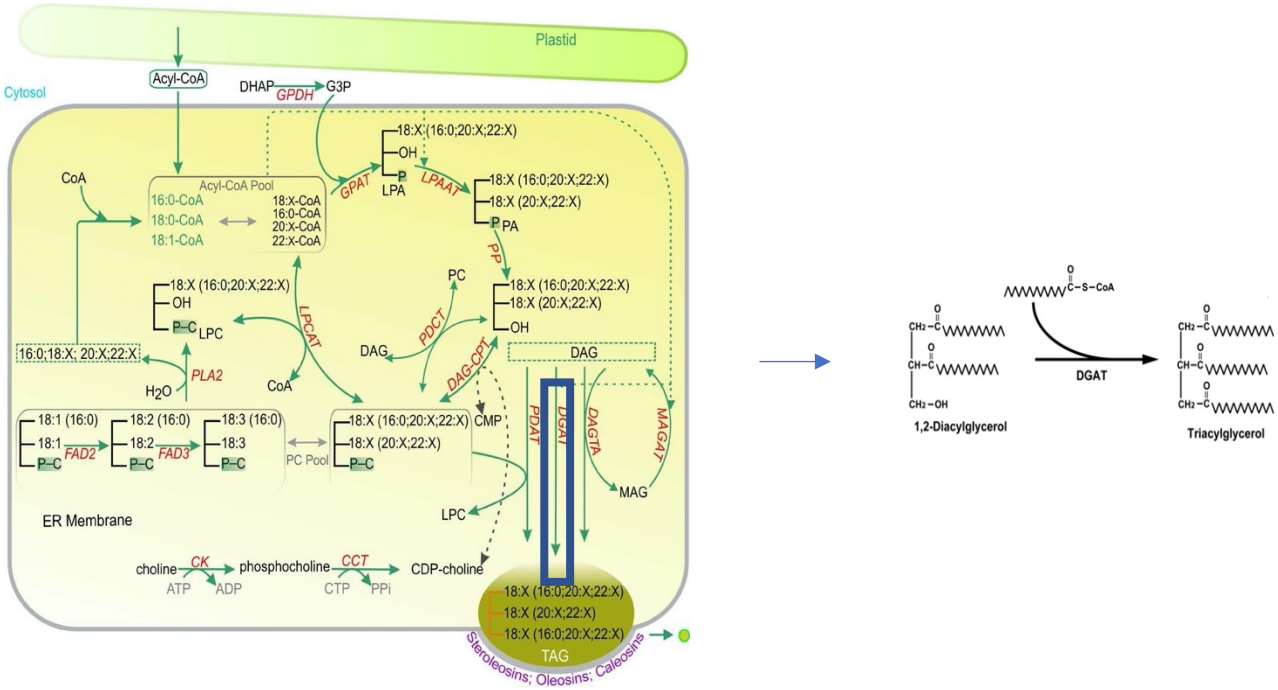

Figure 7.8 Triacylglycerol Synthesis in Arabidopsis, showing DGAT involvement [12].

There are three genes of DGAT1 family, 1 gene of DGAT2 family, 2 genes of DGAT3 family. We decided to investigate one gene belonging to family DGAT2 not differentially expressed under heterotrophy (g9591.t1, transcriptome ID: TRINITY_DN13615). In *C. cryptica* CCCMP332 there are three genes that potentially encode for **triacylglycerol lipases (TGL)**: g12179.t1; g18781.t1 g18865.t1. The correspondent proteins showed cytoplasmic localization.

An analysis of the functional domains revealed the presence of domains with lipase TGA activity IPR021771 https://www.ebi.ac.uk/interpro/entry/InterPro/IPR021771/ in all the proteins, and in proteins coded by g12179.t1 and g18781.t1 genes there is a patatin-like phospholipase domain IPR002641 https://www.ebi.ac.uk/interpro/entry/InterPro/IPR002641/, domains similar to those predicted for LAH. Proteins with similar bifunctional activity have been identified in yeasts encoded by TGL3, 4 and 5 genes.

Similar proteins (**Figure 7.9**) have also been analyzed in *Arabidopsis thaliana* (SDP1 gene) [12] and *Pheodactylum tricornutum* (TGL1 gene) [15] but the double TAG and PL lipase capacity has not been experimentally demonstrated.

In our transcriptome, g12179.t1 that corresponds to TRINITY_DN13324 is not differentially expressed, while g18781.t1 that is TRINITY_DN18955 is downregulated and we decided to study both simultaneously.

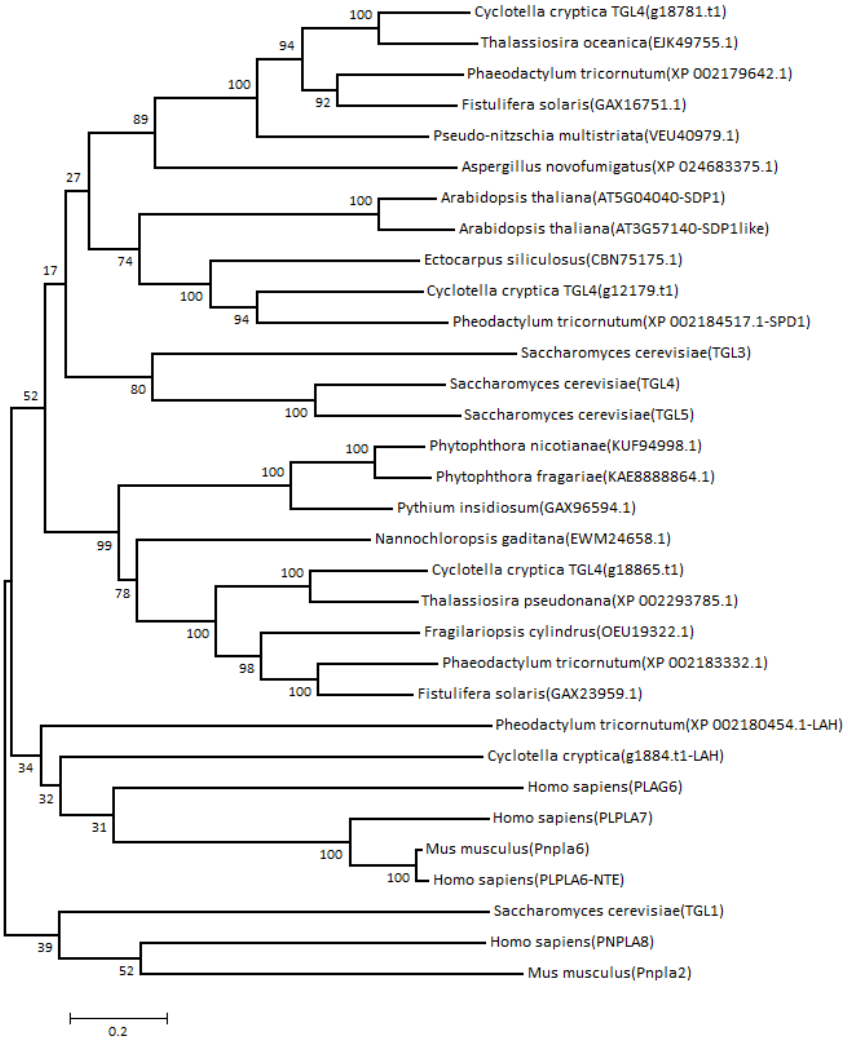

Figure 7.9. Phylogenetic tree.

7.2.3 Sequence validation

The first part of the work I conducted in Paris concerned the study of the genes selected previously, in Italy. Before planning an experiment of gene knock out, it is important to verify the presence of polymorphisms in the coding sequences. Otherwise, an incomplete switch-off of the gene function might occur.

To check the presence of polymorphism, I defined the exons, introns and splicing sites for each gene. I used SnapGene to map gene's sequence identified by the GOI.gff file, which allows the identification of *C. cryptica* CCMP332 gene sequence, starting from the ID of relative protein, defined by BLASTp approach through Geneious, from *Arabidopsis thaliana*. Subsequently, I designed primers on early exons for each gene with different tools as NCBI, Net primer, OligoCalc to check self- complementary, which causes self-dimerization and hairpin, making primer useless. Finally, I checked with Geneious the primer specificity for the coding sequence via alignment versus the whole genome of *C. cryptica*.

To test primer, I extracted DNA starting from the pellet of 5 ml of culture. I tested 3 different DNA concentrations: 1:5, 1:10, 1:20; as reported in **Figure 7.10** to find the better one. To be also sure of quality of DNA extraction I made a PCR both with primers of one gene, in this case SQD1, and with primer for gene of silicate transport (SIT), already available in the laboratory and tested previously for efficiency.

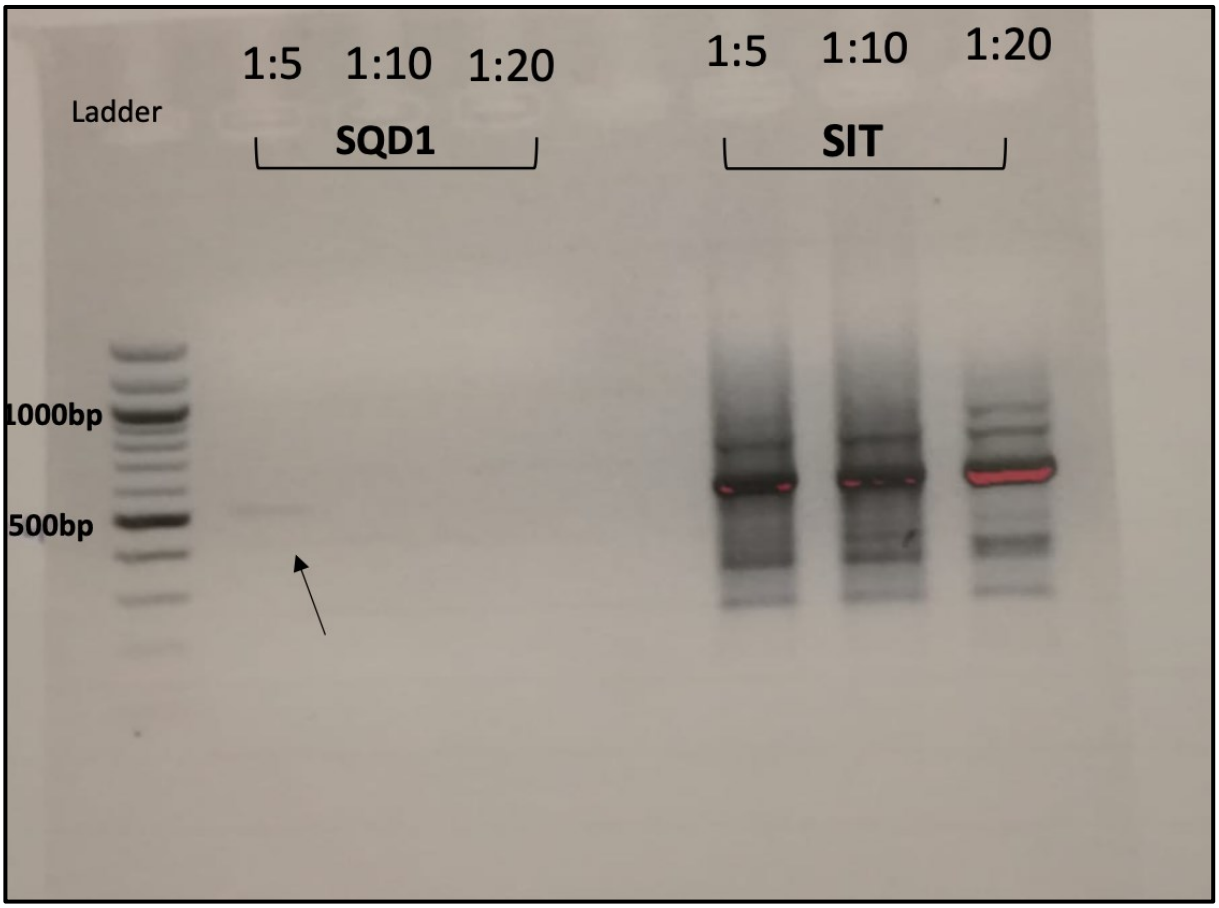

Figure 7.10 Different DNA concentration test with primers for SQD1 and SIT.

As shown in **Figure 7.10**, the DNA extraction was adequate to obtain visible PCR products and 1:5 was the best DNA dilution among those tested; I tried the same dilution also with the other primers, as reported **in Figure 7.11**. One band for each couple of primer granted me the correct design and functioning of the primers.

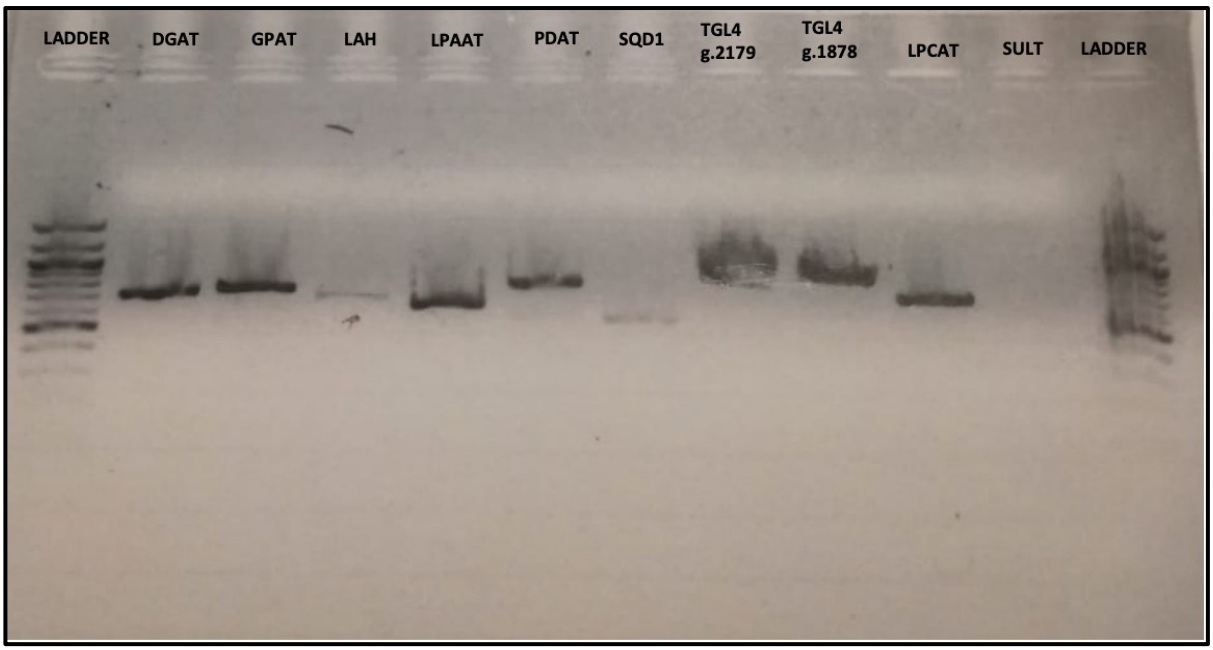

Figure 7.11 Primers test for DGAT, GPAT, LAH, LPAAT, PDAT, TGL4 g.2179, TGL4 g.1878, LPCAT, SULT genes.

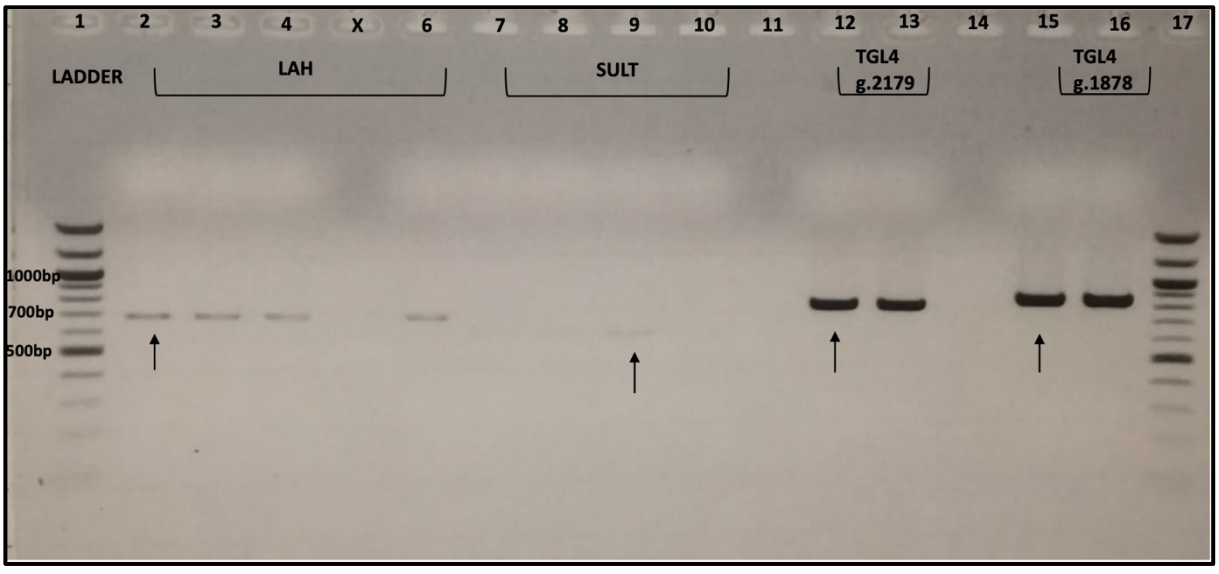

Figure 7.12 Experimental determination of annealing temperature for LAH, SULT, TGL4 g.2179, TGL4 g.1878.

For LAH, SULT and TGL4 gene I tried a gradient PCR which allows to find the better annealing temperature. **Figure 7.12** shows an agarose gel with the 12 samples that were loaded across

the block. The best condition is found in well 2 for LAH gene where the temperature was 50°C, in well 9 for SULT gene where temperature was 54°C, in well 12 for TGL4 g.2179 where temperature was 54°C and in well 15 for TGL4 g1878 where temperature was 54°C. After PCR, I purified DNA directly from Eppendorf with Qiagen kit to remove all residual PCR primers and unincorporated nucleotides, according to the protocol reported in 7.7.3.

I tested the DNA concentration with Nanodrop (Thermo scientific) and the amount of DNA obtained is reported in **Table 7.1**.

Table 7.1. Concentration of DNA expresses as ng/ µl

PCR product	**ng/ µl**
DGAT	16
GPAT	20.1
LPAAT	13.1
PDAT	14.2
SQD1	4.9
LPCAT	15.8
LAH	8.4
SULT	6.2
TGL4 g.2179	16.3
TGL4 g.1878	20.2

Subsequently, 17.5 µl of DNA plus 2.5 µl of Forward primer were sent to Eurofins to sequence. The result of the sequencing is displayed in the form of a chromatogram, which shows the fluorescence emissions that identify each of the 4 DNA bases. This results in a series of fluorescence peaks (at different frequencies), which can be well defined, as in the following chromatogram**, Figure 7.13**, free from background noise.

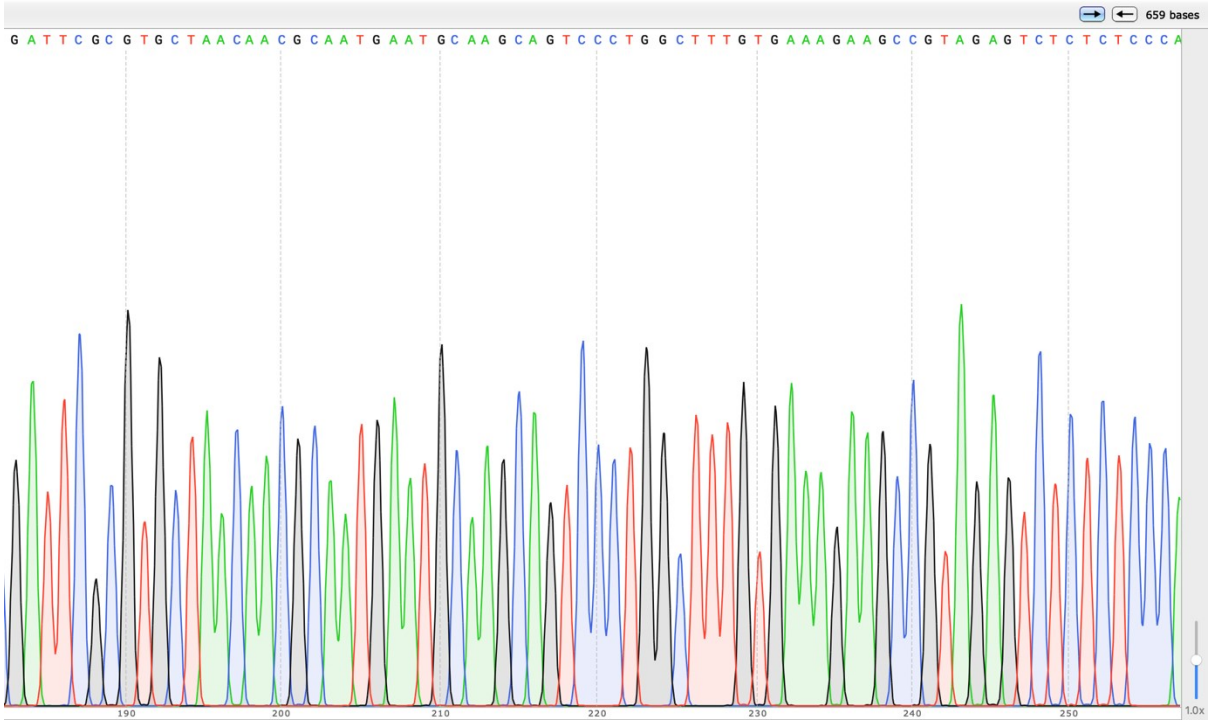

Figure 7.13 Example of Chromatogram obtained after PCR product sequencing.

7.2.4 Strategy for gene knockout

One of the goals of my period in the laboratory of dr. A. Falciatore was related to manage molecular tools in order to delete some of the putative genes implicated in the diatom lipid biosynthesis to assign them the unequivocal function.

The heterotrophic condition could have been a useful resource to screen the phenotypic behavior of cells after genome manipulation. As reported in this thesis, by lipidomic approach, we defined the typical pattern of *C. cryptica* lipid profile grown in heterotrophy.

We decided to use the genetic tool box CRISPR-Cas9 to produce gene-Knockouts.

CRISPR-Cas is a mechanism of defense used in nature by bacteria and archaea to protect them from virus infection. There are six types of CRISPR systems (I-VI), depending on the classification of CRISPR-cas loci. The most used in genetic engineering is CRISPR type II, constituted by a single endonuclease that is Cas9, with two different domains necessary for the double-strand cleavage: NHC and RUV. CRISPR (clustered regularly-interspaced short palindromic repeats) are DNA fragments containing short repeated-sequences. Each

sequence is flanked by DNA spacer. The DNA spacer consists in small fractions of phage or plasmid invading host.

Thus, during the immunization process, the foreign DNA is integrated into the CRISPR region as new spacers, acting as "memory" of the infection (**Figure 7.14A**).

A second infection from the same pathogen leads to a transcription of the CRISPR region with repeated and spacer sequences in a pre-CRISPR RNA transcript (**Figure 7.14B**).

The pre-CRISPR RNA transcript forms a complex with TracrRNA, Cas9 and RNase III which, by endonucleolytic cleavage, generates short mature CRISPR RNAs (crRNAs).

The resulting crRNA contains a spacer sequence at 5'end, complementary to the foreign genome and at 3'end a repeated sequence coming from the CRISPR array.

During the interference, mature crRNA and TracrRNA recruit Cas9 endonuclease leading it to the foreign genetic element, causing the cleavage of DNA that contains 20 nucleotides complementary to crRNA situated before PAM sequence (**Figure 7.14C**) [16].

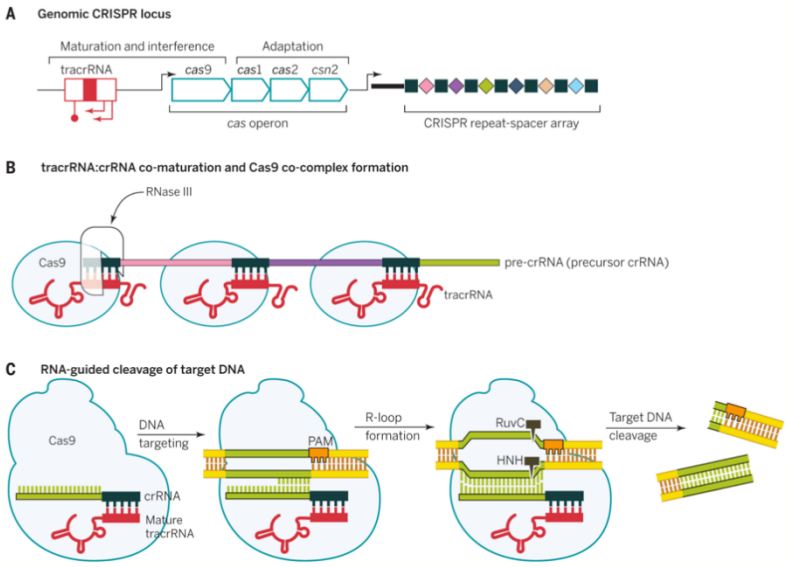

Figure 7.14 Biology of the type II-A CRISPR-Cas system [16].

Gene knockout is a consequence of repair mechanisms as non-homologous end joining (NHELJ) or homologous recombination (HR), introducing insertion or deletion in the first case and precise genome modification in the second one, to restore the double break on DNA strands.

In the Lab of Dr. Falciatore we designed a strategy to construct CRISPR-Cas9 vectors using Golden Gate cloning. This approach was explored by Hopes et al. for the editing of the urease gene in the diatom *Thalassiosira pseudonana* [17].

The principle of Golden Gate cloning is based on the special ability of type IIS restriction enzymes to cleave outside of their recognition site [18,19]. When these recognition sites are placed to the far 5' and 3' end of any DNA fragment in inverse orientation, they are removed in the cleavage process, allowing two DNA fragments flanked by compatible sequence overhangs to be ligated seamlessly.

As represented in **Figure 7.15** taken from the paper of Hopes, this strategy consists in two levels of assembly: level 1 and level 2.

Level 0 consisted of single modules created by PCR to add overhangs sequences and BsaI restriction enzyme sites, which are subsequently utilized in level 1 assembly. These modules (FCP promoter, FCP terminator, U6 promoter and Cas9 from Streptococcus pyogenes with an N-terminal SV40 NLS and a C-terminal YFP tag) were cloned into a pCR8/GW/TOPO vector (Thermo Fisher).

The final products of level 1 assembling are two vectors: vector one plCH47742:FCP:Cas9YFP containing the gene for Cas 9 under FCP promoter and terminator flanked by GCAA and ACTA sequences (to enable the correct assembling with the other vector of level 1) and sites for BpiI restriction enzyme.

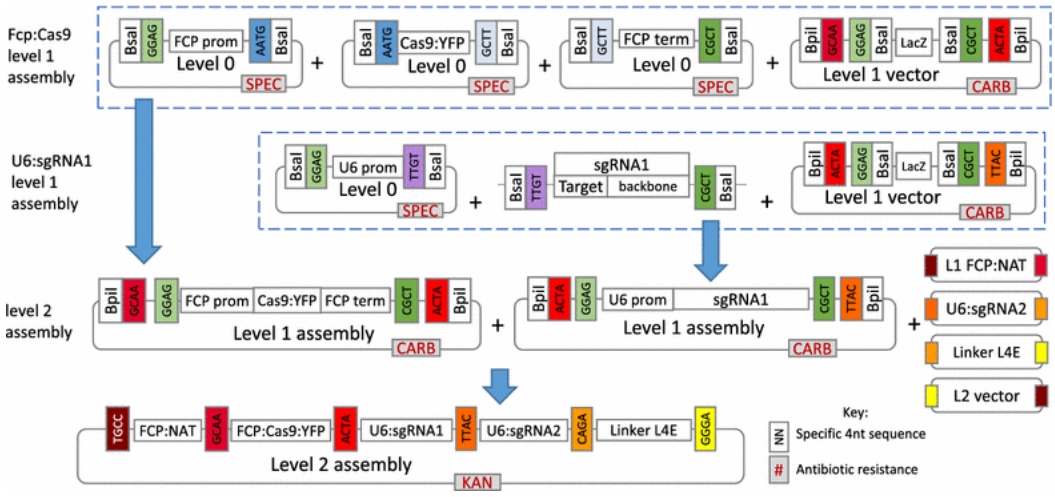

Figure 7.15 Overview of level 1 (L1) and level 2 (L2) Golden Gate cloning for assembly of the CRISPR-Cas construct pAGM4723[17].

The other vector plCH47751:U6:sgRNA1 and plCH47761:U6:sgRNA2 of level1 consisted of sgRNA under U6 promoter, flanked by ACTA and TTAC sequences and sites for BpiI restriction enzyme. Both promoters FCP and U6 are associated with high expression levels [17].

Using this modular cloning, it is possible to combine different vectors carrying different sgRNA in the final CRISPR vector to silence two genes, simultaneously.

By the way, we were intended to proceed one gene at time to study the phenotypic effect of the single gene deletion on lipid metabolism and for each selected gene we nonetheless created two vectors, containing two different sgRNA, to facilitate the screening (the resulting deletion will be easily visible by PCR) and to increase the chance that one of them will work.

Similarly with the mechanism of defense of Bacteria and Archaea, for engineered CRISPR systems two main components are required: a guide RNA (gRNA) and a CRISPR-associated endonuclease (Cas protein). The gRNA is a short synthetic RNA composed of a scaffold sequence necessary for Cas-binding and a custom-defined ~20 nucleotide spacer that defines the genomic target to be modified. There are several bioinformatic tools, I used Crispor (http://crispor.org), to identify the best 20 nucleotides for gRNA inside the coding sequence, predicting potential off targets in genome and on target activity [20]. As a matter of fact, the spacer of gRNA should be unique compared to the rest of genome and immediately adjacent to a PAM (Protospacer Adjacent Motif) sequence. PAM sequence is important for Cas binding and depends on type of Cas employed in the CRISPR system. We used Cas9 from *S. pyogenes* (SpCas9) and the related PAM sequence is NGG. The scaffold sequence is cloned in plasmid plCH86966 (figure 6.6), already available in the laboratory of Dr. Falciatore. The PCR products to be inserted in plCH47751 and in plCH47761 backbone are obtained setting up a PCR on plCH86966 vector, using as reverse primer one that is common to any single guide RNA we want to generate (GeneXsgRNA.Rv tggtctcaagcgtaatgccaactttgtacaag in the Figure 7.16) and a specific forward primer of each gene containing : BsaI site with the overhang sequence for cloning - 20 nucleotides designed for each gene - sequence annealing with the scaffold on the plCH86966 (GeneXsgRNA1.FW and GeneXsgRNA2.FW aggtctcattgt-N20-gttttagagctagaaatagcaag in the **Figure 7.16**).

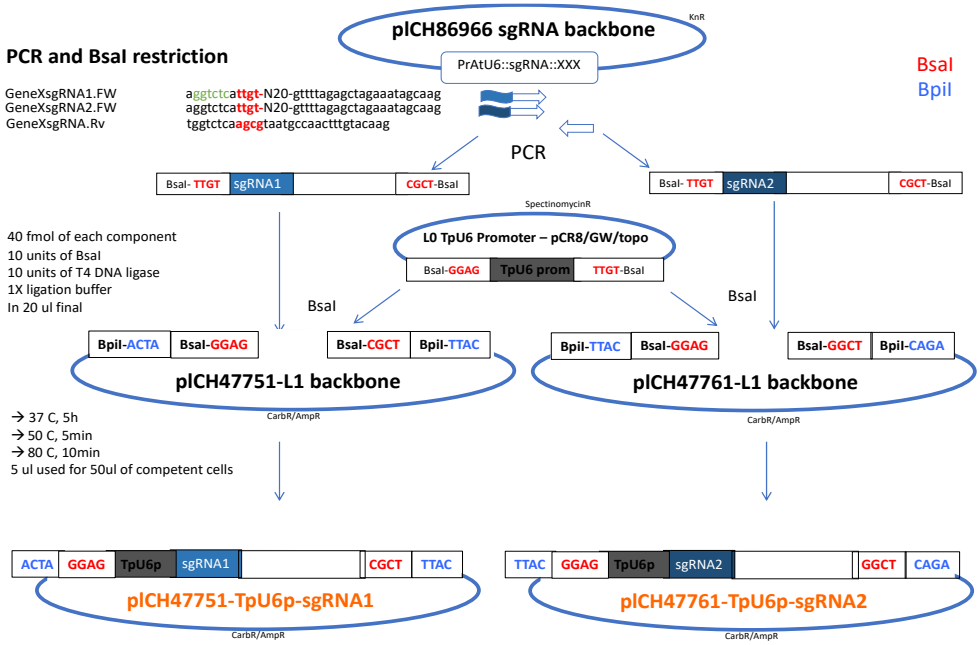

Figure 7.16 Focus on the strategy to produce vectors plCH47751-TpU6p-sgRNA1 and plCH7761-TpU6p-sgRNA2 for each selected gene.

Level 2 assembly, the last one, consists of assembling of plCH47742:FCP:Cas9YFP, plCH47751:U6:sgRNA, pl47751:FCP:NAT and L4E linker in the final CRISPR L2 vector PAGM4723.

7.2.5. Strategy for gene overexpression

In order to study the function of selected genes, we tried also to overexpress some of the genes, giving us another chance to succeed using a different molecular approach.
In particular we focused on SULT, SQD1, PDAT, LAH, TGL4 g.2179 and TGL4 g.1878 genes.
The design of overexpression strategy is based on Gibson cloning.
Gibson assembly, a sequence overlap-based method, was developed for the synthesis and assembly of Mycoplasma genomes [21,22] and enabled the assembly of DNAs of up to several hundred kilobases (kb) in one-pot isothermal reactions [23]. This method has been widely adopted by the synthetic biology community, being scar-free, versatile and relatively efficient. However, Gibson assembly generally relies on the use of oligonucleotides to perform in vitro amplification of DNA fragments, which can be error prone [24–26]. The method is also sensitive to sequence composition and repeats, and hence efforts have been made to standardize and

streamline Gibson assembly by including flanking unique nucleotide sequences (UNSs) that can be used as long overlaps for the cloning of transcription units (TUs) into larger constructs[27]. Perhaps because of the flexible nature of Gibson assembly, a standard for composing elemental parts into TUs has not been proposed to date [28].

The first step to proceed with overexpression is to identify the exons of each gene.

I used the bioinformatic tools SNAP gene, Expasy and GeneScan to locate start (ATG), stop codon (TAG) and splicing sites.

Subsequently, I designed primer to amplify the coding region of each gene from cDNA.

The primers should have sequences allowing the cloning by Gibson into the pL0 vector (green part in **Figure 7.17**), BsaI recognition enzyme sites, overhangs sequences (A/B/C/D) and ~18 nucleotides specific for each gene that should anneal on the first coding codon, after ATG.

I modified the original strategy of amplification by doing two PCR (Figure 6.8), because when planning to do many cloning, at the end it is cheaper to order specific primers with shorter UNS sequences and the other parts for a final length of ~50 nt, then doing a second PCR with UNS1FL.Fw and UNSXFL.Rv to have long enough UNS extremities for Gibson, rather than ordering ~70 nt long primer pairs for each gene to clone (**Figure 7.17**).

Table 7.2 showed primer sequences for each gene.

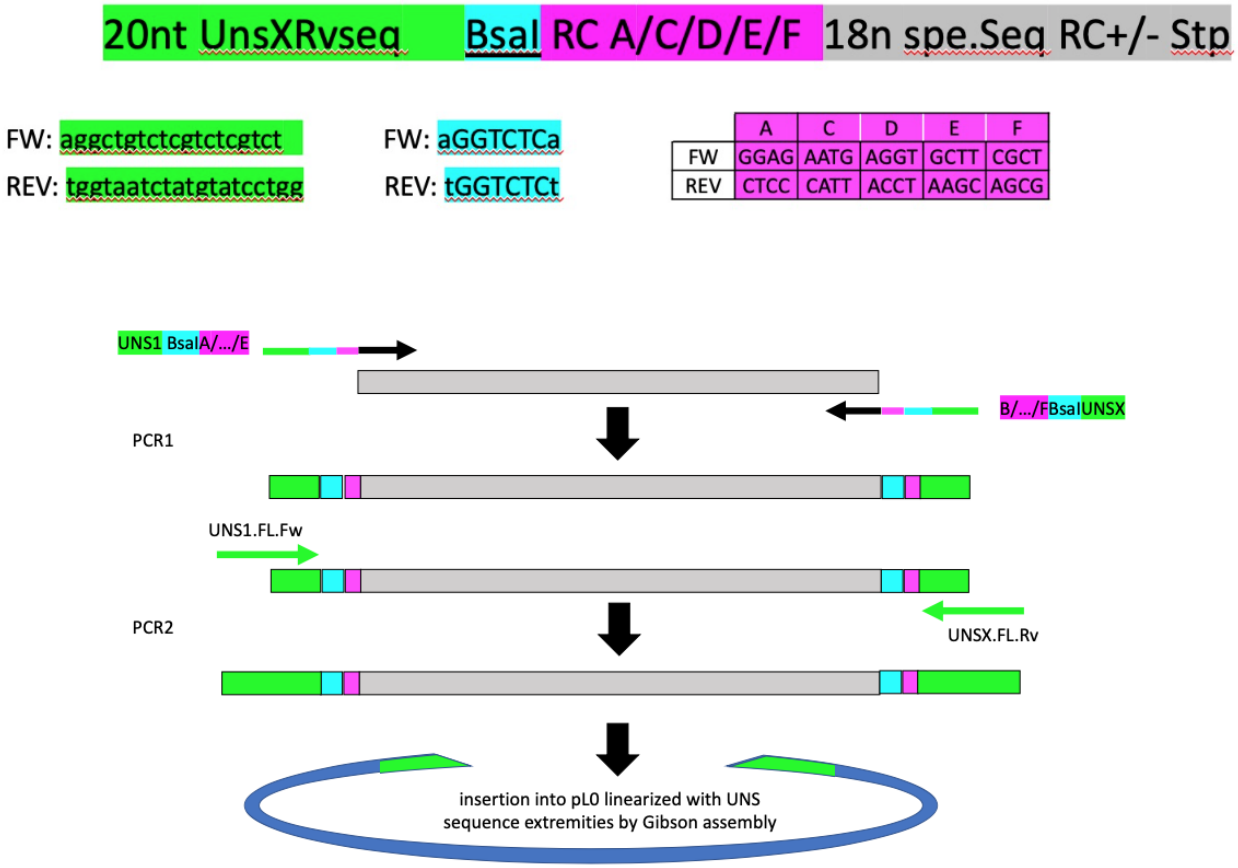

Figure 7.17 Elements required during primer design and insertion of coding sequence into PL-0 vector.

Table 7.2. Primer sequence design to allow Gibson assembly

SQD1 FW: aggctgtctcgtctcgtctcaGGTCTCaAATGAAATTCTATCTCTTTCTA REV: tggtaatctatgtatcctggtGGTCTCtACCTACGACCTTGACCTTCACACT
SULT FW: aggctgtctcgtctcgtctcaGGTCTCaAATGCTCCCAAAAACAAAA REV: tggtaatctatgtatcctggtGGTCTCtACCTATAGAGCTATCGACTACCCC
PDAT FW: aggctgtctcgtctcgtctcaGGTCTCaAATGAAGCGAAGAAACGCATC REV: tggtaatctatgtatcctggtGGTCTCtACCTATTTGAAATGCAGTTTTTAATC
TGL418781 FW: aggctgtctcgtctcgtctcaGGTCTCaAATGTCAGCAGCAGCCGCGCC REV: tggtaatctatgtatcctggtGGTCTCtACCTATGAAATCTACTGGAGAGGT
Tgl4 21179 FW: aggctgtctcgtctcgtctcaGGTCTCaAATGAAGGCAGACAAAATTGAT REV: tggtaatctatgtatcctggtGGTCTCtACCTATGTGTGATGTTGAACCTGT

As showed in **Figure 7.18** level 0 plasmids contained all the elements necessary to express the protein of interest: FCP promoter, FCP terminator, CDS and TAG sequence. TAG should be sequences for Venus or GFP, useful to localize protein expression. All the plasmids of level 0 contained BsaI sites, whose sequences were removed when assembled in plasmid of level 1 (PL1-2 in **Figure 7.18**) in the level 1 assembly. Flanking region A, C, D, E, F exposed after BsaI cut, allow the correct orientation in PL1-2 vector.

Level 2 assembly enable the cloning in the final vector PL2-1 of NAT cassette and PL1-2.

The cloning strategy is designed for 4 insertions at each level of assembly, thus to obtain a pL2 vector with all elements required for protein expression, 4 inserts coming from pL1-1, pL1-2, pL1-3, and pL1-4 needed; pL1-3 and pL1-4 are just used as linkers to allow the assembly (**Figure 7.18**).

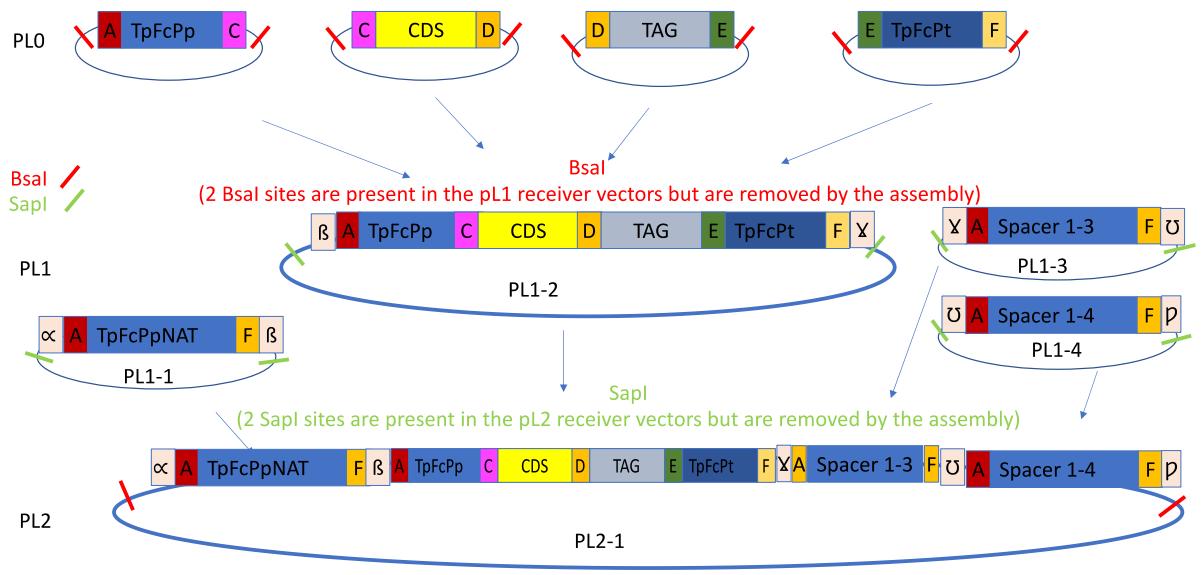

Figure 7.18 Gibson-based strategy cloning for gene overexpression.

Unfortunately, due to the global pandemic spread, I was unable to experimentally complete this interesting part of my PhD project in Paris.

The ICB-CNR laboratory is gearing up with the equipment necessary to approach molecular studies, with a view to a greater cross-cutting approach in research and soon these experiments will be carried out on-site.

7.3 Materials and methods

7.3.1 List of web resources mentioned in the text

- SnapGene https://www.snapgene.com
- Geneious https://www.geneious.com
- Net primer http://www.premierbiosoft.com/netprimer/
- OligoCalc http://biotools.nubic.northwestern.edu/OligoCalc.html
- Expasy https://www.expasy.org
- GenScan http://argonaute.mit.edu/GENSCAN.html
- Crispor http://crispor.tefor.net

7.3.2 DNA extraction

- Resuspend pellet (from 5ml of culture) in 20 µl of Lysis Buffer (1% Triton X100, EDTA pH8 2mM, Tris-HCl pH8 20mM)
- vortex 30 seconds

- incubation 15 min in ice
- boil 10 min at 95°

7.3.3 PCR parameters

For gradient PCR the following test parameters were selected:

45 cycles

- denaturation 95°C,30 s
- annealing 50°C -56.3°C, 30 s
- elongation 72°C, 45 s.

7.3.4 Purification of PCR products

- Add 5 volumes of Buffer PB to 1 volume of the PCR sample, and then mix.
- If pH Indicator I has been added to Buffer PB, check that the mixture's color is yellow.
- If the color of the mixture is orange or violet, add 10 µl of 3 M sodium acetate, pH 5.0, and mix. The color of the mixture will turn yellow.
- Place a QIAquick spin column in a provided 2 ml collection tube.
- To bind DNA, apply the sample to the QIAquick column and centrifuge for 30–60 s.
- Discard flow-through. Place the QIAquick column back into the same tube.
- Collection tubes are reused to reduce plastic waste.
- To wash, add 0.75 ml Buffer PE to the QIAquick column and centrifuge for 30–60 s.
- Discard flow-through and place the QIAquick column back into the same tube. Centrifuge the column for an additional 1 min.

IMPORTANT: Residual ethanol from Buffer PE will not be completely removed unless the flow-through is discarded before this additional centrifugation.

- Place QIAquick column in a clean 1.5 ml microcentrifuge tube.
- To elute DNA, add 50 µl Buffer EB (10 mM Tris-HCl, pH 8.5) or water (pH 7.0–8.5) to the center of the QIAquick membrane and centrifuge the column for 1 min.

Alternatively, for increased DNA concentration, add 30 µl elution buffer to the center of the QIAquick membrane, let the column stand for 1 min, and then centrifuge.

IMPORTANT: Ensure that the elution buffer is dispensed directly onto the QIAquick membrane for complete elution of bound DNA. The average eluate volumes are 48 µl from 50 µl elution buffer volume and 28 µl from 30 µl elution buffer.

7.3.5 Transformation

The first tests for *C. cryptica* transformation were performed through biolistic technique with the gene gun Bio-Rad PDS-1000/He microprojectile accelerator. The vector employed in the transformation has been prepared by the host laboratory prior to my arrival for the transformation of *T. pseudonana*. This vector was very similar to the ones employed in the first *C. cryptica* transformation documented [6], and carried the NTC resistance (NAT1) gene, *T. pseudonana* Fucoxanthin- chlorophyll a-c binding protein (TpLhcf9) promoter and TpLhcf9 terminator [17] .An antibiotic selection gene, ampicillin, was also present in the plasmid for the cloning in *Escherichia coli*. The DNA-coated tungsten particles were prepared adding 1.5 µg of plasmid, 50 µl of CaCl2 2.5 M and 3 µl of spermidine 0.1 M in this order to 30 mg of microparticles M17 (1.1 µm diameter). The transformation was performed starting from a culture of *C. cryptica* in exponential phase. Cells at the concentration of $3.6x10^5$ cells/ml were centrifuged in an Avanti® J-E centrifuge (Beckam Coulter) at a speed of 3000 rpm for 10 minutes. $7x10^7$ cells were spread on agar plates containing no antibiotics. Given that the average C. cryptica size observed in that culture was 0.01 mm x 0.01 mm and the area of the Petri dish is 7850 mm , if well distributed the cells could have formed a dense monolayer. The plates were let dry before inserting them in the microprojectile accelerator, afterwards one shot per plate was performed. The shoots were performed at a burst pressure of 1500 psi and at a vacuum of -0.84 bar. The entire 30 mg of DNA-coated microparticles were used for each transformation, divided in seven macrocarrier disks. After the shot, the diatoms were washed out from the plates with 1 mL of F/2 media and resuspended in 100 mL. The cultures were let to recover for two days before the selection of transformants. Four plates of $6x10^6$ cells of each shot culture were pored inside a 0,25% soft agar matrix supplemented with NTC 200 µg/ml. The remaining cells were kept in liquid selection with an NTC concentration of 200

µg/ml. Each liquid culture was diluted three times in the following period. The colonies grown in the solid selection were then resuspended in microwells for a second round of selection. The transformants able to grow were then diluted in larger volumes always supplemented with NTC.

7.4 References

(1) Armbrust, E. V.; Berges, J. A.; Bowler, C.; Green, B. R.; Martinez, D.; Putnam, N. H.; Zhou, S.; Allen, A. E.; Apt, K. E.; Bechner, M.; Brzezinski, M. A.; Chaal, B. K.; Chiovitti, A.; Davis, A. K.; Demarest, M. S.; Detter, J. C.; Glavina, T.; Goodstein, D.; Hadi, M. Z.; Hellsten, U.; Hildebrand, M.; Jenkins, B. D.; Jurka, J.; Kapitonov, V. V.; Kröger, N.; Lau, W. W. Y.; Lane, T. W.; Larimer, F. W.; Lippmeier, J. C.; Lucas, S.; Medina, M.; Montsant, A.; Obornik, M.; Parker, M. S.; Palenik, B.; Pazour, G. J.; Richardson, P. M.; Rynearson, T. A.; Saito, M. A.; Schwartz, D. C.; Thamatrakoln, K.; Valentin, K.; Vardi, A.; Wilkerson, F. P.; Rokhsar, D. S. The Genome of the Diatom *Thalassiosira Pseudonana*: Ecology, Evolution, and Metabolism. *Science.* **2004**, *306* (5693), 79–86. https://doi.org/10.1126/science.1101156.

(2) Bowler, C.; Allen, A. E.; Badger, J. H.; Grimwood, J.; Jabbari, K.; Kuo, A.; Maheswari, U.; Martens, C.; Maumus, F.; Otillar, R. P.; Rayko, E.; Salamov, A.; Vandepoele, K.; Beszteri, B.; Gruber, A.; Heijde, M.; Katinka, M.; Mock, T.; Valentin, K.; Verret, F.; Berges, J. A.; Brownlee, C.; Cadoret, J. P.; Chiovitti, A.; Choi, C. J.; Coesel, S.; De Martino, A.; Detter, J. C.; Durkin, C.; Falciatore, A.; Fournet, J.; Haruta, M.; Huysman, M. J. J.; Jenkins, B. D.; Jiroutova, K.; Jorgensen, R. E.; Joubert, Y.; Kaplan, A.; Kröger, N.; Kroth, P. G.; La Roche, J.; Lindquist, E.; Lommer, M.; Martin-Jézéquel, V.; Lopez, P. J.; Lucas, S.; Mangogna, M.; McGinnis, K.; Medlin, L. K.; Montsant, A.; Secq, M. P. O. Le; Napoli, C.; Obornik, M.; Parker, M. S.; Petit, J. L.; Porcel, B. M.; Poulsen, N.; Robison, M.; Rychlewski, L.; Rynearson, T. A.; Schmutz, J.; Shapiro, H.; Siaut, M.; Stanley, M.; Sussman, M. R.; Taylor, A. R.; Vardi, A.; Von Dassow, P.; Vyverman, W.; Willis, A.; Wyrwicz, L. S.; Rokhsar, D. S.; Weissenbach, J.; Armbrust, E. V.; Green, B. R.; Van De Peer, Y.; Grigoriev, I. V. The *Phaeodactylum* Genome Reveals the Evolutionary History of Diatom Genomes. *Nature* **2008**, *456* (7219), 239–244. https://doi.org/10.1038/nature07410.

(3) Falciatore, A.; Jaubert, M.; Bouly, J. P.; Bailleul, B.; Mock, T. Diatom Molecular Research Comes of Age: Model Species for Studying Phytoplankton Biology and Diversity. *Plant Cell* **2020**, *32* (3), 547–572. https://doi.org/10.1105/tpc.19.00158.

(4) Fabris, M.; Matthijs, M.; Rombauts, S.; Vyverman, W.; Goossens, A.; Baart, G. J. E. The Metabolic Blueprint of *Phaeodactylum Tricornutum* Reveals a Eukaryotic Entner-

Doudoroff Glycolytic Pathway. *Plant J.* **2012**, *70* (6), 1004–1014. https://doi.org/10.1111/j.1365-313X.2012.04941.x.

(5) Levering, J.; Broddrick, J.; Dupont, C. L.; Peers, G.; Beeri, K.; Mayers, J.; Gallina, A. A.; Allen, A. E.; Palsson, B. O.; Zengler, K. Genome-Scale Model Reveals Metabolic Basis of Biomass Partitioning in a Model Diatom. *PLoS One* **2016**, *11* (5), 1–22. https://doi.org/10.1371/journal.pone.0155038.

(6) Dunahay, T. G.; Jarvis, E. E.; Roessler, P. G. Genetic Transformation of the Diatoms *Cyclotella Cryptica* and *Navicula Saprophila*. *J. Phycol.* **1995**, *31* (6), 1004–1012. https://doi.org/10.1111/j.0022-3646.1995.01004.x.

(7) Liu, J.; Nannas, N. J.; Fu, F. F.; Shi, J.; Aspinwall, B.; Parrott, W. A.; Dawe, R. K. Genome-Scale Sequence Disruption Following Biolistic Transformation in Rice and Maize. *Plant Cell* **2019**, *31* (2), 368–383. https://doi.org/10.1105/tpc.18.00613.

(8) Karas, B. J.; Diner, R. E.; Lefebvre, S. C.; McQuaid, J.; Phillips, A. P. R.; Noddings, C. M.; Brunson, J. K.; Valas, R. E.; Deerinck, T. J.; Jablanovic, J.; Gillard, J. T. F.; Beeri, K.; Ellisman, M. H.; Glass, J. I.; Hutchison, C. A.; Smith, H. O.; Venter, J. C.; Allen, A. E.; Dupont, C. L.; Weyman, P. D. Designer Diatom Episomes Delivered by Bacterial Conjugation. *Nat. Commun.* **2015**, *6*, 1–10. https://doi.org/10.1038/ncomms7925.

(9) De Riso, V.; Raniello, R.; Maumus, F.; Rogato, A.; Bowler, C.; Falciatore, A. Gene Silencing in the Marine Diatom *Phaeodactylum Tricornutum*. *Nucleic Acids Res.* **2009**, *37* (14). https://doi.org/10.1093/nar/gkp448.

(10) Kroth, P. G.; Bones, A. M.; Daboussi, F.; Ferrante, M. I.; Jaubert, M.; Kolot, M.; Nymark, M.; Río Bártulos, C.; Ritter, A.; Russo, M. T.; Serif, M.; Winge, P.; Falciatore, A. Genome Editing in Diatoms: Achievements and Goals. *Plant Cell Rep.* **2018**, *37* (10), 1401–1408. https://doi.org/10.1007/s00299-018-2334-1.

(11) Serif, M.; Dubois, G.; Finoux, A. L.; Teste, M. A.; Jallet, D.; Daboussi, F. One-Step Generation of Multiple Gene Knock-Outs in the Diatom *Phaeodactylum Tricornutum* by DNA-Free Genome Editing. *Nat. Commun.* **2018**, *9* (1), 1–10. https://doi.org/10.1038/s41467-018-06378-9.

(12) Li-Beisson, Y.; Shorrosh, B.; Beisson, F.; Andersson, M. X.; Arondel, V.; Bates, P. D.; Baud, S.; Bird, D.; DeBono, A.; Durrett, T. P.; Franke, R. B.; Graham, I. A.; Katayama, K.; Kelly, A. A.; Larson, T.; Markham, J. E.; Miquel, M.; Molina, I.; Nishida, I.; Rowland, O.;

Samuels, L.; Schmid, K. M.; Wada, H.; Welti, R.; Xu, C.; Zallot, R.; Ohlrogge, J. Acyl-Lipid Metabolism. *Arab. B.* **2013**, *11*, e0161. https://doi.org/10.1199/tab.0161.

(13) Gallo, C.; Nuzzo, G.; d'Ippolito, G.; Manzo, E.; Sardo, A.; Fontana, A. Sterol Sulfates and Sulfotransferases in Marine Diatoms, 1st ed.; Elsevier Inc., 2018; Vol. 605. https://doi.org/10.1016/bs.mie.2018.03.003.

(14) Adelfi, M. G.; Vitale, R. M.; d'Ippolito, G.; Nuzzo, G.; Gallo, C.; Amodeo, P.; Manzo, E.; Pagano, D.; Landi, S.; Picariello, G.; Ferrante, M. I.; Fontana, A. Patatin-like Lipolytic Acyl Hydrolases and Galactolipid Metabolism in Marine Diatoms of the Genus *Pseudo-Nitzschia*. *Biochim. Biophys. Acta - Mol. Cell Biol. Lipids* **2019**, *1864* (2), 181–190. https://doi.org/10.1016/j.bbalip.2018.11.008.

(15) Barka, F.; Angstenberger, M.; Ahrendt, T.; Lorenzen, W.; Bode, H. B.; Büchel, C. Identification of a Triacylglycerol Lipase in the Diatom *Phaeodactylum Tricornutum*. *Biochim. Biophys. Acta - Mol. Cell Biol. Lipids* **2016**, *1861* (3), 239–248. https://doi.org/10.1016/j.bbalip.2015.12.023.

(16) Doudna, J. A.; Charpentier, E. The New Frontier of Genome Engineering with CRISPR-Cas9. *Science (80-.).* **2014**, *346* (6213). https://doi.org/10.1126/science.1258096.

(17) Hopes, A.; Nekrasov, V.; Kamoun, S.; Mock, T. Editing of the Urease Gene by CRISPR-Cas in the Diatom *Thalassiosira Pseudonana*. *Plant Methods* **2016**, *12* (1), 1–12. https://doi.org/10.1186/s13007-016-0148-0.

(18) Weber, E.; Engler, C.; Gruetzner, R.; Werner, S.; Marillonnet, S. A Modular Cloning System for Standardized Assembly of Multigene Constructs. *PLoS One* **2011**, *6* (2). https://doi.org/10.1371/journal.pone.0016765.

(19) Engler, C.; Kandzia, R.; Marillonnet, S. A One Pot, One Step, Precision Cloning Method with High Throughput Capability. *PLoS One* **2008**, *3* (11). https://doi.org/10.1371/journal.pone.0003647.

(20) Concordet, J. P.; Haeussler, M. CRISPOR: Intuitive Guide Selection for CRISPR/Cas9 Genome Editing Experiments and Screens. *Nucleic Acids Res.* **2018**, *46* (W1), W242–W245. https://doi.org/10.1093/nar/gky354.

(21) Gibson, D. G.; Benders, G. A.; Andrews-Pfannkoch, C.; Denisova, E. A.; Baden-Tillson, H.; Zaveri, J.; Stockwell, T. B.; Brownley, A.; Thomas, D. W.; Algire, M. A.; Merryman, C.; Young, L.; Noskov, V. N.; Glass, J. I.; Venter, J. C.; Hutchison, C. A.; Smith, H. O. Complete

Chemical Synthesis, Assembly, and Cloning of a Mycoplasma Genitalium Genome. *Science* . **2008**, *319* (5867), 1215–1220. https://doi.org/10.1126/science.1151721.

(22) Gibson, D. G.; Glass, J. I.; Lartigue, C.; Noskov, V. N.; Chuang, R. Y.; Algire, M. A.; Benders, G. A.; Montague, M. G.; Ma, L.; Moodie, M. M.; Merryman, C.; Vashee, S.; Krishnakumar, R.; Assad-Garcia, N.; Andrews-Pfannkoch, C.; Denisova, E. A.; Young, L.; Qi, Z. N.; Segall-Shapiro, T. H.; Calvey, C. H.; Parmar, P. P.; Hutchison, C. A.; Smith, H. O.; Venter, J. C. Creation of a Bacterial Cell Controlled by a Chemically Synthesized Genome. *Science* . **2010**, *329* (5987), 52–56. https://doi.org/10.1126/science.1190719.

(23) Gibson, D. G.; Young, L.; Chuang, R. Y.; Venter, J. C.; Hutchison, C. A.; Smith, H. O. Enzymatic Assembly of DNA Molecules up to Several Hundred Kilobases. *Nat. Methods* **2009**, *6* (5), 343–345. https://doi.org/10.1038/nmeth.1318.

(24) Keohavong, P.; Thilly, W. G. Fidelity of DNA Polymerases in DNA Amplification. *Proc. Natl. Acad. Sci. U. S. A.* **1989**, *86* (23), 9253–9257. https://doi.org/10.1073/pnas.86.23.9253.

(25) Gibson, D. G.; Smith, H. O.; Hutchison, C. A.; Venter, J. C.; Merryman, C. Chemical Synthesis of the Mouse Mitochondrial Genome. *Nat. Methods* **2010**, *7* (11), 901–903. https://doi.org/10.1038/nmeth.1515.

(26) Potapov, V.; Ong, J. L. Examining Sources of Error in PCR by Single-Molecule Sequencing. *PLoS One* **2017**, *12* (1), 1–19. https://doi.org/10.1371/journal.pone.0169774.

(27) Torella, J. P.; Lienert, F.; Boehm, C. R.; Chen, J.-H.; Way, J. C.; Silver, P. A. Unique Nucleotide Sequence–Guided Assembly of Repetitive DNA Parts for Synthetic Biology Applications. *Nat. Protoc.* **2014**, *9* (9), 2075–2089. https://doi.org/10.1038/nprot.2014.145.

(28) Pollak, B.; Cerda, A.; Delmans, M.; Álamos, S.; Moyano, T.; West, A.; Gutiérrez, R. A.; Patron, N. J.; Federici, F.; Haseloff, J. Loop Assembly: A Simple and Open System for Recursive Fabrication of DNA Circuits. *New Phytol.* **2019**, *222* (1), 628–640. https://doi.org/10.1111/nph.15625.

8. Conclusions and future perspectives

This PhD thesis was mainly carried out at the Institute of Biomolecular Chemistry (CNR, Pozzuoli), where I explored the heterotrophic development of the marine diatom *C. cryptica* CCCMP 331, as well as the chemical and biochemical characterization of biomass and added-value products.

Heterotrophy is highly attractive from an industrial point of view for the growth of microorganisms from which it is possible to obtain valuable products, taking advantage of the well-established fermenter technology, widely exploited in both pharmaceutical and food sectors.

The first result obtained was the setting-up of heterotrophic cultivation conditions in flask and carboy, using glucose as organic carbon source, in order to have robust small-scale systems (200ml-10L) to investigate phenotypical and biochemical differences of heterotrophic in comparison to autotrophic conditions. Under these experimental conditions, cells of *C. cryptica* grow well in the dark, both in artificial sea water and natural sea water, and without using antibiotics during cultivation. These are important aspects for the industrial scale-up of the process.

The growth of *C. cryptica* was evaluated on various substrates such as sucrose, starch, lactose, thinking about the reuse of waste substances to reduce production costs. At the moment, glucose at a concentration of 2 g/L was the optimal carbon source, yielding 809.33 mg/L of lyophilic biomass in 10 days. Further study will be necessary to test other polysaccharides as feed of heterotrophic process with the prospective of valorizing sugar-based by-products.

Spectrophotometric assays, mass spectrometry techniques (GC-MS/LC-MS), and spectroscopic techniques (^{1}H-NMR) have been used to characterize produced biomass and components.

After 7 days of growth in the dark, the biomass of *C. cryptica* is well balanced in terms of gross chemical composition, with 32.6% of proteins, 21.7% of lipids, and 18.0% of carbohydrates. Under adequate nutrition regimes, repeated growth cycles do not significantly alter cellular composition, but impact on the overall productivity of the system.

Glycerolipid distribution assessed by ^{1}H-NMR revealed a significant decrease of SQDG and DGDG under heterotrophy offering the potential of addressing the role of these lipidic pools in the switch form autotrophy to heterotrophy.

The fatty acid pattern evaluated in GC-MS shows a simplified picture in heterotrophy, with a reduction or absence of some polyunsaturated fatty acids.

Palmitic acid (C16: 0), palmitoleic acid (C16: 1), and EPA (C20:5) are the main fatty acids synthesized under both culture conditions, as predicted. Interestingly, after 7 days of dark C16:1 and C18:1 exhibited an increase in content, but the key plastidial diatom markers C16:3 and C16:4 showed a substantial decrease in content under heterotrophy.

Interesting insights have been obtained from the assessment of glycerolipid profile in LCMS. It was possible to establish the variation of acyl chain and distribution in different pool of glycerolipids, such as MGDG, DGDG, SQDG, phospholipids and triglycerides, to obtain key information about lipid assembly induced by dark.

The molecular basis of lipid rearrangement and the mechanisms regulated by the auto-heterotrophy switch were investigated using RNA sequencing technique. We identified 12327 differential expressed genes (DEGs), comparing heterotrophic *vs* autotrophic conditions. To mine the *C. cryptica* transcriptome assembled in this study, we used the well-known *Arabidopsis thaliana* and diatom understandings about enzyme sequences and pathways to evaluate the entire lipid biosynthesis pathway of *C. cryptica*. A total of 97 lipid related transcripts were identified. Among these, 33 were up regulated and 21 were down-regulated comparing heterotrophy *vs* autotrophy.

In order to unequivocally assign a function to some selected genes involved in lipid metabolism, we have planned a cloning strategy using CRISPR-Cas-9 technology.

This part of the project, which began last year in Paris at the “Institut de Biologie Physico-Chimique” in partnership with Dr. Falciatore, has not yet been finished experimentally due to the spread of SARS-CoV-2 virus.

During my research period at I.GI., a vegetable oil refinery, we have successfully increased the growth volumes from few ml of culture in flask up to 60 liters of culture in polypropylene carboys, setting up a repeated-batch process for heterotrophic cultivation of marine diatoms *C. cryptica*. The marine diatom is cultured under optimized heterotrophic conditions in 6 bioreactors of 10 L each, using glucose as carbon source, harvesting every 7 days 9/10 of the

culture, and using 1/10 as seed culture for the next cycle. Results indicated that it's possible to sustain diatom growth in heterotrophic conditions for at least 6 cycles for a total of 42 days, without using antibiotics. The process led to an average dry biomass production of 1.5 ±0.12 g L^{-1} and a lipid production of 290 ± 36 mg L^{-1}, containing 60% triglycerides, 20% phospholipids and 20% glycolipids, as assessed by ^{1}H-NMR. Main fatty acids in biooil were C16:0 (55%), C16:1 ω-7 (25%) and C20:5 ω-3 (14%), distributed in specific modality as acyl chains in glycerolipids.

In conclusion, this PhD thesis acts as a milestone for the understanding of adaptive mechanisms of photosynthetic diatoms to the dark, in particular for the response in terms of lipid biosynthesis and remodeling. In addition, the thesis reports first data on the potential biotechnological applications of diatom products obtainable by exploiting low-cost fermenter technology, such as flour for food and feed applications, EPA and biofuels.